Analysis of midgut regeneration in lepidopteran pest, *Achaea janata* upon Cry toxication

To be submitted for the award of degree of
Doctor of Philosophy in Animal Biology
by

Narender
15LAPH10

Submitted to

Department of Animal Biology
School of Life Sciences
University of Hyderabad
Hyderabad-500046
India

October, 2019

Ph.D. Thesis

(A Central University established in 1974 by an Act of Parliament)

DECLARATION

I, **Narender** hereby declare that this thesis entitled **"Analysis of midgut regeneration in lepidopteran pest, *Achaea janata* upon Cry toxication"** submitted by me under the supervision of Prof. Aparna Dutta Gupta is a bonafide research work which is also free from plagiarism. I also declare that it has not been submitted previously in part or in full to this University or any other University or Institution for the award of any degree or diploma.

Date:

Narender
15LAPH10

(A Central University established in 1974 by an Act of Parliament)

CERTIFICATE

This is to certify that this thesis entitled **"Analysis of midgut regeneration in lepidopteran pest, *Achaea janata* upon Cry toxication"** submitted by **Narender, 15LAPH10** in partial fulfillment of the requirements for award of Doctor of Philosophy in the **Department of Animal Biology, School of Life Sciences** is a bonafide work carried out by him, under our supervision and guidance.

This thesis is free from plagiarism and has not been submitted previously in part or in full to this or any other University or Institution for the award of any degree or diploma.

Parts of this thesis:

A. Published in the following publications-

i. **Narender K. Dhania**, Vinod K. Chauhan, R.K. Chaitanya and Aparna Dutta-Gupta; RNA-Seq analysis and *de novo* transcriptome assembly of Cry toxin susceptible and tolerant *Achaea janata* larvae. Scientific Data, 2019, 6:159,1-6, s41597-019-0160-0.

ii. **Narender K. Dhania**, Vinod K. Chauhan, R.K. Chaitanya and Aparna Dutta-Gupta; Midgut *de novo* transcriptome analysis and gene expression profiling of *Achaea janata* larvae exposed with *Bacillus thuringiensis* (Bt)-based biopesticide formulation. Comparative Biochemistry and Physiology – Proteomics and Genomics, 2019, 31, 81-90.

iii. Vinod K. Chauhan*, **Narender K. Dhania***, R. K. Chaitanya, Balasubramanian Senthilkumaran and Aparna Dutta-Gupta; Larval midgut responses to sub-lethal dose of Cry toxin in lepidopteran pest *Achaea janata*. Frontiers in Physiology, 2017, 8:662,1-12. (*Equal contribution).

B. Presented in the following conferences-

iv. **Narender K. Dhania** and Aparna Dutta-Gupta; Gut regeneration in lepidopteran pest, *Achaea janata* upon Cry intoxication. Oral presentation. International Conference of Molecular Signaling, University of Hyderanbad, Hyderabad, 2018.

v. **Narender K. Dhania** and Aparna Dutta-Gupta; Proliferative/mitogenic effects of arylphorin in midgut regeneration upon Cry toxin intoxication in a Lepidopteran pest. International Symposium on Recent Advances In Comparative Endocrinology, MCC, Chennai, 2017.

vi. **Narender K. Dhania**, Vinod K. Chauhan, and Aparna Dutta-Gupta; Evaluation of gut regenerative response upon Sub-lethal Cry toxin intoxication in a Lepidopteran pest *Achaea janata*. Bio Quest 2015, (P-34) University of Hyderabad, Hyderabad, 2015.

Further, the student has passed the following courses towards partial fulfillment of Ph.D. submission.

S. No.	CourseCode	Name	Credits	Pass/Fail
1	AS 801	Analytical Techniques	4	Pass
2	AS 802	Research Ethics, Data Analysis and biostatistics	3	Pass
3	AS 803	Lab Work & Seminar	5	Pass

Supervisor **Cosupervisor**

Head of the Department **Dean of the School**

This thesis is dedicated to
my mother…

Acknowledgments

The process of earning a Ph.D. is a long and arduous endeavor that is certainly not an individual experience; rather it takes place in a collective context and includes many people, whom I would like to thank sincerely. Gratitude is an emotion least expressible in words. Withstanding, however, this limitation, I would like the reader to know that the following words are sincere feelings which I shall cherish for a lifetime.

First and foremost I would like to express my profound gratitude to my supervisor **Prof. Aparna Dutta Gupta** for her admirable and unique guidance, constant encouragement, precious suggestions and enthusiasm throughout my Ph.D. I am indebted for her expertise, keen interest and for giving me complete freedom to design and execute my doctoral work. The joy and enthusiasm she has for research was contagious and motivational for me, even during tough times in the Ph.D. pursuit. Needless to say that none of this would have been possible without her dedicated mentorship and drive. I thank her for always pushing me a wee bit further.

I am grateful to **Prof. S. Dayananda** Dean, School of Life Sciences, and former Deans **Prof. K.V.A Ramaiah,** and **Prof. P. Reddanna**, for providing all the facilities at the school.

I thank **Prof. Anita Jagota**, Head, Dept. of Animal Biology, and former Head **Prof. Jagan Pongubala** for providing the necessary facilities in the department to carry out my research work.

I thank my doctoral committee members **Prof. Srinivasalu Kurkuti** and **Prof. G. Ravi Kumar** for their critical comments and valuable suggestions.

I would like to extend my sincere thanks to **Prof. B. Senthilkumaran, Dr. K. Arun Kumar, Dr. Y. Suresh, Dr. Vivek, Dr. Bindu Madhava Reddy, Prof. Mrinal Kanti Bhattacharyya (SLS Faculty)** and **Prof. S.C. Lakhotia (BHU), Prof. Murlidhar, Dr. Shourya Dutta-Gupta (IIT-H)** for sharing their facilities and for their critical suggestions in carrying out the work.

I am thankful to **Dr. Chaitanya, Dr. Venkat Rao, Dr. Surendra** and **Dr. Pavani** for their encouragement and support during my entire Ph. D. duration.

Huge thanks to my lab mates **Dr. Vinod K. Chauhan** and **Meenakshi** for providing an intellectually inspiring and friendly environment to work in. Special thanks to my friends **Yugantak, Sandeep, Sushmita, Harshita, Gungun, Nikita, Abdul, Deepak Shiristi, Debo, Eshwar** and others (**SLS-UoH cricket team**) for their support and happy stay in University of Hyderabad.

I would like to thank all the lab members of **Prof. B. Senthilkumaran, Prof. S. Dayananda, Dr. Suresh Yenugu,** and **Dr. Kota Arun Kumar** for their timely help.

I am thankful to **Mrs. Leena Bhashyam** for all her support whenever I needed at the Genomics Facility.

I would also like to thank all the **Faculty** and **Research scholars** of the School of Life Sciences. I am grateful to all **my teachers**, who taught me and are instrumental in shaping up my life.

I would also like to thank all the **Faculty-in charge** and **Scientific officers** of all common instrumentation facilities of the School of Life Sciences, for providing wonderful technical and instrumentation support.

I thank **Mr. Mallesh** and **Mr. Laxman** for their assistance. I would also like to thank the non-teaching staff **Mr. Jagan, Mr. Gopi,** and **Mr. Pandu** for their assistance in using common facilities., thanks to all the administrative staff of Dept. of Animal Biology, especially **Mrs. Vijayalaxami, Mr. Rangaswamy, Mr. Nikhil** and **Mr. Srinivas**. The help and cooperation of the non-teaching staff of the School of Life Sciences are highly acknowledged.

I'm very thankful for the sources that have supported our laboratory financially- funding from the **CSIR, DST, UGC, UGC-BSR** and **DBT-CREBB** and **DST** to School, **DST-FIST** and **UPE-II** to Department. Fellowship by **UGC** is greatly acknowledged.

I wish to express my deepest gratitude and reverence to my parents **Sh. Balbir Singh, Smt. Darshana Devi** and my siblings **Dr. Sonia, Vikram** and **Nitika** who have sacrificed comforts of their life to give a better life to me and for their epitome of patience in allowing me to choose the career of my interest.

Narender

Table of contents

Abbreviations

ºC	Degree centigrade/Celsius
ABCC2	ATP-binding cassette transporter subfamily C2
ACP	Acid phosphatase
ALP	Alkaline phosphatase
ANOVA	Analysis of variance
APN	Aminopeptidase N
BBMVs	Brush border membrane vesicles
BCIP	Bromo-4-chloro-3-indolyl phosphate
BLAST	Basic Local Alignment Search Tool
BrdU	5-Bromo-2'-deoxyuridine
Bt	*Bacillus thuringiensis*
BSA	Bovine serum albumin
cDNA	Complementary DNA
cAMP	Cyclic adenosine monophosphate
DNA	Deoxyribonucleic acid
DEPC	Diethyl pyrocarbonate
dNTPs	Deoxy ribonucleoside triphosphates
DTT	1, 4-Dithiothreitol
EDTA	Ethylenediaminetetraacetic acid
EGTA	Ethylene glycol-bis (2-aminoethylether- N,N,N',N'-tetra acetic acid
HRP	Horseradish peroxidase
IgG	γ Immunoglobulin
kDa	Kilo Dalton
LB	Luria-Bert
LD	Light:Dark
mg	Milligram
mM	Millimolar
mRNA	Messenger ribonucleic acid
NaCl	Sodium chloride

NBT	Nitrotetrazolium blue
NCBI	National Centre for Biotechnology Information
ng	Nanogram
nM	Nanomolar
OCT	Optimal cutting temperature
PAGE	Polyacrylamide gel electrophoresis
PBS	Phosphate buffered saline
PCR	Polymerase chain reaction
PDB	Protein Data Bank
pmol	Picomole (10^{-12} moles)
pH	Negative logarithm (base 10) of the molar concentration of dissolved hydrogen ions (H+)
PKA	Protein kinase A
PMSF	Phenylmethylsulfonyl fluoride
PP	Prepupa
RH	Relative humidity
RT	Room temperature
RNA	Ribonucleic acid
rpm	Revolutions per minute
SDS	Sodium dodecyl sulphate
SNK	Student-Newman-Keuls
TAE	Tris-acetate EDTA
TBS	Tris buffered saline
TBST	Tris buffered saline Tween-20
TE	Tris-EDTA
TEMED	N,N,N',N', tetramethylethylenediamine
v/v	volume/volume
w/v	weight/volume
µg	Microgram
µM	Micromolar

General Introduction

Insects

Insects are categorized under Phylum Arthropoda, Class Insecta and constitute around 80 percent (3/4 of animal species) of all living organisms and are incredibly abundant. Among the all insect orders Coleoptera, Lepidoptera, Hymenoptera, and Diptera comprise of fairly large numbers of pest species. The insects have exceptional adaptability and are distributed widely in different habitats. They play an important role in maintaining food chain and are important component of ecological system. Some of them, have high commercial importance such as honey bees, silkworms etc. A large number insects are known to cause heavy loss in agricultural practice and are serious pest of crops as well as stored grains. They not only destroy the crop, by feeding directly on the plant parts (leaf, stem, roots, fruits etc.), but also act as vector and transmit the bacterial, viral or fungal infections from infected to healthy plants. Furthermore, Lepidoptera, Diptera and Coleoptera are three major orders, which make major component of agricultural and stored grain pests. The current study is focused on a lepidopteran pest which causes serious loss of castor planataiton in various parts of India.

Control for pest based crop damage

Majority of pest management practices used today either rely on changing/modifying the environmental conditions and/or application of various chemical formulations. Based on their source the insecticdes are classified into different types (Fig. 1). Continous attempt to develop effective insecticide for the control of crop pests has not only lead to the presence of lot of these toxic compound in the environment but also promotes the generation of resistant variety of pest. Therefore there is an increasing demand for natural/biological pesticides. Recent pesticide usage trend also reveals that there is a shift towards the usage of envioronmetnal friendly biological control agents, which are primarly derived from bacteria, fungi, viruses and plants.

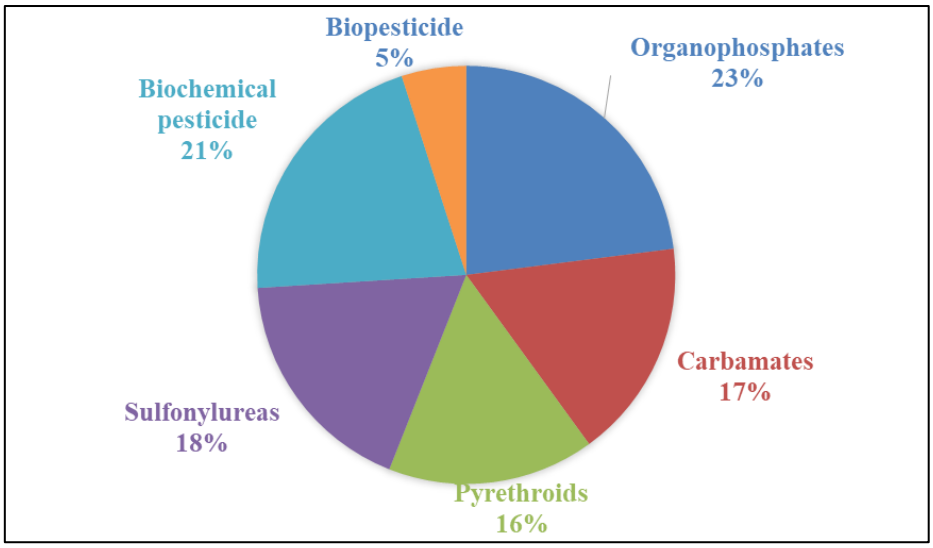

Fig. 1 The above venn diagram represents the usage ratio of different kinds of insecticides for the management of insect pests (adopted from Encyclopedia Britannica).

A comprehensive report from US, Canada, Japan, Europe, Asia-Pacific, Latin America, and rest of world reveals that there is a 4,580 thousand US$ worldwide market for Biopesticides (https://www.reportlinker.com/p02284883 press releases PR Newswire, 2018) which is expected to rise in the span of next five years. Rising demand for biopesticides is associated with increased awareness towards the side effects of toxic chemical pesticides and demand for organic food. United States Environmental Protection Agency reported that 299 biopesticides were registered till April 2016 (https://www.epa.gov/ingredients-used-pesticide-products/what-are-biopesticides). *Bacillus thuringiensis* (Bt) based biopesticides are extensively used for controlling the lepidopteran pests, either in the form of Bt transgenic plants or in form of Bt formulations. Among Bt based biopesticides, Crystalline (Cry) toxin is the one which has been maximally exploited during past 30 years. In the present study, we have carried out an study with a Cry toxin based formulation (DOR-Bt1) using a lepidopteran pest *Achaea janata.*

Bacillus thuringiensis

Bacillus thuringiensis a gram positive bacteria, during growth and sporulation produce variety of toxins which exhibit toxicity against various insect orders. Three different kinds of

toxins produced are classified as i) Crystal (Cry), ii) Vegetative insecticidal proteins (Vip), and iii) Cytolytic (Cyt) toxins. As these toxins are fairly species specific or order specific hence they have been used for the management of specific insect pests (Fig. 2). Being in non-pathogenic categories for humans, Bt based insecticides are the most successful and are being used for the pest management.

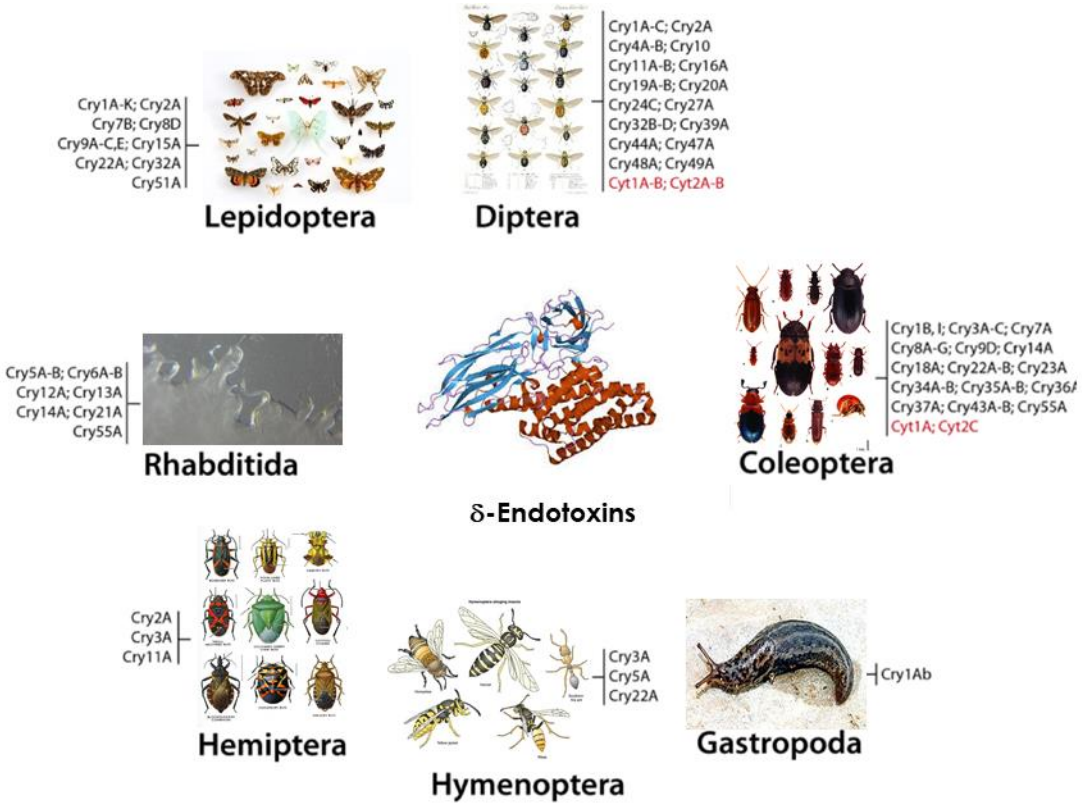

Fig. 2 Bt δ-endotoxins activity against various insect order, summarized view showing recognised host spectrum (picture adopted from Palma et al., 2014).

As mentioned in above section current work is based on Cry toxin (δ-endotoxins, produced during sporulation) based Bt formulation which was prepared from local strain of Bt (i.e. DOR-Bt1) isolated by Indian Oil Seed Reserch Institute, Hydreabad, India. Cry toxins are known to be effective against lepidopteran, coleopteran, dipteran and hymenopteran order of insects (Schnepf et al., 1998). Further being species specific and entomopathogenic in nature they do not have deleterious effect on other organisms. This also makes Bt genes (primarily *cry* genes) to serve as a reservoir for the generation of transgenic crops which are insect

resistant. Few genetically modified crops have already been approved for cultivation such as *Bt* cotton, *Bt* corn, *Bt* maize, *Bt* brinjal etc. in differenet countries including India where Bt cotton is being successfully farmed (Report by Michael Specter in "The New Yorker", 2014). Presently usage of Bt based spray formulations of spores and crystal and Bt transgenic plant is very popular among farmers.

Mechanism of Cry toxin insecticidal action

More than 500 different forms of Cry toxins have been reported so far (Crickmore et al., 2005, 2008, 2016). These toxins have specific mode of action in various Cry susceptible larvae and exhibit a specific mode of action. Effective Cry intoxication in larvae leads to midgut cell death. Various models have been prepared to understand the Cry toxin effects on larval physiology (Schenepf et al., 1998; de Maagd et al., 2001, 2003; Vacher et al., 2003; Bravo et al., 2004, 2007; Zhang et al., 2006; Gonzalez et al., 2008; Feil et al., 2010; Pardo-Lopez et al., 2012; Adang et al., 2014).

It has been shown that, 130 kDa δ-endotoxins (protoxin) upon ingestion, under alkaline pH gets solubilised in the midgut lumen. Reducing alkaline condition in the gut lumen facilitates proteases to cleave protoxin in into ~ 65 kDa active toxin (Schnepf et al., 1998). This active toxin now binds to specific receptor present at midgut brush border towards apical side of the epithelium (Vadlamudi et al., 1993; Gómez et al., 2001, 2002). After cleavage of α helix from domain I of active toxin, it binds to Cadherin like receptor, present at brush border gives rise to oligomeric form of toxin (Nagamatsu et al., 2003 Gómez et al., 2002). Additionaly Peng et al., (2010) suggested that active toxin molecules interact among themselves to generate effective form of toxin. The oligomeric form of toxin now binds to species specific receptor such as GPI-anchored receptors like aminopeptidase N (APNs) in *Manduca sexta* or alkaline phosphatase (ALPs) in *Heliothis virescences* (Agrawal et al., 2002; McNall and Adang, 2003; Bravo et al., 2004; Jurat-Fuentes and Adang, 2004; Angelucci et al., 2008; Pacheco et al.,

2009). Midgut Cry toxin binding/receptor proteins are unique in different insectan orders such as Cadherin, P252, APN and ALP in Lepidoptera; Cadherin, APN, ALP and alpha-glucosidase in Diptera and Cadherin, ADAM 3 metalloprotease and ALP in Coleoptera (Rajmohan et al., 1998; Nakanishi et al., 2002; Wang et al., 2005; Baxter et al., 2008; Bravo et al., 2013). Apart from these, ATP-binding cassette transporter subfamily C member 2 (ABCC2) is also shown to be Cry toxin receptor in *Bombyx mori, Helicoverpa armigera, Plutella xylostella* and *Spodoptera exigua* (Tanaka et al., 2013, 2016; Zhao et al., 2016; Endo et al., 2017; Pinos et al., 2019). Altogether binding of oligomeric active form of Cry toxin to epithelial brush border receptors, leads to its cellular insertion as a result Cry toxins are termed as pore-forming toxin (PFT). Pore formation in midgut epithelial cell alters its osmotic behavior followed by septicemia and cell death (de Maagd et al., 2003; Whalon and Wingerd, 2003; Bravo et al., 2004; Soberon et al., 2009).

Zhang et al., (2006) proposed an additional hypothesis where the pore formation in epithelial cells by Cry toxin was suggested to be associated with Mg^{2+} dependent signal cascade pathway. *In vitro* experiment using Cry toxin receptor transfected ovarian cell (*Trichoplusia ni*) showed that active oligomeric form of toxin bound to guanine nucleotide-binding protein (G-protein). This unique binding lead to adenylyl cyclase activation and production of intracellular cyclic adenosine monophosphate (cAMP). Increased cAMP caused activation of protein kinase A (PKA) which facilitated intracellular downstream pathway leading to cell death. Overall effects of Cry toxins are purely based upon unique receptor identity of a given pest species and varies significantly from one to another larvae even in same order.

The impact of Cry toxin application

The alteration, as well as adaptation in midgut cells, was carefully analysed in various insect pests during Cry intoxication (Baines et al., 1997; Loeb et al., 2001; Knaak and Fiuza.,

2005). *In vitro* and *in vivo* experiments using *Lymantria monacha* showed rupture of microvilli and cytoplasmic vacuolisation upon Cry toxicity (Rausel et al., 2000). Loeb et al., (2001) demonstrated that Bt-AA 1-9 and HD-73 intoxication in *Heliothis virescens* caused a reduction in number of columnar and globular midgut cells.

In India there is a continuous increase in usage and more than five percent of pesticides used presently are of biological origin. There is increasing evidences that continuous usage of the same formulation and/or toxin also leads to the development of resistance to Bt based biopesticide. As mentioned above pest insects demonstrate enormous adaptive capabilities which supports them to survive during adverse conditions, and develop tolerance/resistance against *Bt* based formulation. In India, the pink bollworm was shown to become resistant to Monsanto 1st generation, Bt toxin (Cry1Ac) transgenic plant (Bagla, 2010; http://www.monsanto.com/newsviews/Pages/india-pink-bollworm.aspx). Which was followed by release of 2nd generation of cotton seeds with multiple Cry genes. Resistance in bollworm was also reported in China, Spain, Australia and America (Just, 2006; Lu et al., 2010; Tabashnik et al., 2013, 2014). In addition, Indian meal moth was also reported to be resistant against *B. thuringiensis* based biopesticide (Candas et al., 2003; Baxter et al., 2011), suggesting that lepidopteran pests have tendncy to become Cry toxin tolerat.

Its nearly two decaded since plantaion of Bt crops is being used in various countries including India. The uncontrolled widespread use of biopesticides seems to be the major reason for development of tolerance and resistance in insect pest. Alteration/mutation in midgut binding/receptor sites is one of the major reason which causes development of resistance (Pigott and Ellar, 2007; Guo et al., 2015). Extensive studies report mutation in different Cry toxin receptors, Cadherin, APN, ALP and ABCC2 which contribute to the development of Cry toxin resistance in various insects (Gomez et al., 2002; Xie at l., 2005; Fabrick et al., 2009; Zhang et al., 2006, 2008; Khajuria et al., 2011; Likitvivatanavong et al., 2011, Pardo-Lopez et

al., 2013; Bravo et al., 2013; Endo et al., 2017; Nakaishi et al, 2018; Martínez-Solís et al., 2018; Liu et al., 2018; Pino et al., 2019). In addition other physiological responses which are primarily based on non-receptor mediated mechanisms also facilitate the development of Cry toxin resistance. Enhanced midgut regeneration was observed during Cry intoxication as well as in Cry resistant larvae. In lepidopteran larvae recovery during Cry toxin exposure was supported by midgut epithelial regeneration (Dulmage et. al., 1978; Spies and Spence, 1985; Martinez-Ramirez et al., 1999; Loeb et al., 2001; Tanaka et al., 2012; Castagnola and Jurat-Fuentes 2016). Evolution of Cry ressitance is definitely an important facet in optimal usage of biopesticide and needs a proper attention for its judicious application in long term.

Castor plant and its uses

The cu rrent study was carried out using a lepidopteran insect model *Achaea janata* which is a major pest of castor plant (*Riccinus communis*). Castor is non-edible oilseed crop and is grown extensively in Gujarat, followed by Rajasthan, Andhra Pradesh and Telangana. According to 'The Economic Times' a total production of castor plant was estimated to 11.26 lakhs tonnes in 2018-19 and 14.16 lakhs in 2017-2018 (https://economictimes.indiatimes.com/news/economy/agriculture/). At present (2018-2019) in Indian agriculture scenario castor average yield is estimated around 1520 Kg/Ha. Castor oil has a worldwide demand and United States, Japan, China and Thailand are the major importers of it (https://www.castoroilworld.com/). The growing demand for Castor bean oil is associated with its high viscosity and presence of ricinoleic acid (mono-unsaturated fatty acid). This is of great economic importance and used for in due trial applications such as lubricants in aviation, industrial paints and varnishes, synthetic polymers, resins, fabric dyeing, leather manufacturing etc. It is a powerful laxative and natural moisturizer. It also exhibits countless medicinal properties which promote wound healing and represent anti-inflammatory, anti-fungal, antimicrobial, hydration cleansing properties

(https://www.medicalnewstoday.com/articles/319844.php). Being a major source of ricinoleic acid with other fatty acids, castor oil is a powerful medicinal product, particularly for derma care.

***Achaea janata* Linn.**

Achaea janata (Castor semilooper) is a holometabolus insect and a major pest of castor plant (https://www.krishisewa.com/articles/disease-management/64-castor-pests.html). It belongs to Noctudidae family and order Lepidoptera. *A. janata* larvae cause extensive damage to castor foliation and it is widely spread in tropical and sub-tropical agricultural region of the world. Its larvae primarily damage/feed on fresh castor leaves and completely defoliate it which leads to complete devastation. Along with *Ricinus communis*, castor semilooper occasionally feeds on Euphorbiaceae, Brassica and Ficus species in the absence of priamary host plant. Gaikwad and Bilapte (1992) reported that during July-September (monsoon season) *A. janata* larvae are responsible for 50-70% loss of castor crop in various parts of India.

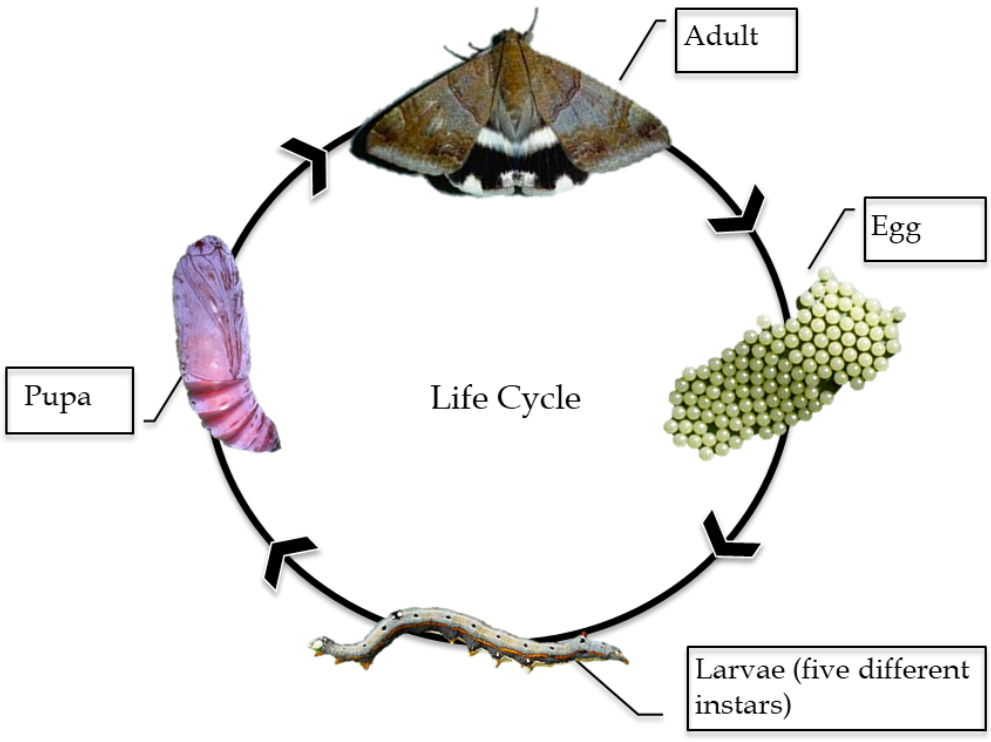

Fig. 3 Life cycle of *A. janata* larvae showing egg, larva, pupa and adult stages.

Holometabolous insect complete their life cycle in four different stages i.e. adult, egg, larvae and pupa (Fig. 3). *A. janata* completes its life cycle in 45-50 days under favorable condition (Karmawati and Tobing, 1988). The larval stges consist of five different instars which are voracious feeders and defoliator. From one instar to another instar larva takes 3-5 days. Before pupation it attains the size up to ~6 cm. Pupation normally takes place in moisturised soil and during unfavorable condition it remians as pupa for longer times i.e. called diapause. Environmental temperature and humidity have direct influence on pupal metamorphosis.

Various larval organs of *A. janata*:

i) **Gut**: The larval gut, is majorly associated with the digestion and absorption of food. It is subdivided into foregut, midgut and hindgut. From lumen side, gut is continuously protected by peritrophic matrix membrane which also acts as first-line defense against various pathogens. Arrangement of gut in larvae allows the uptake of nutrient and ion as well as removal of excess water is associated with defensive behaviour (Lehane and Billingsley, 1996, Terra et al., 1996; Grant, 2007). The outer periphery of gut is also supported by basal muscular layer, which has rich supply of trachea/ tracheoles and nerves.

In gut, midgut plays an important role in enzyme secretion, food digestion and absorption (Chapman, 2013; Nation, 2015). It consists of different cell types which are commonly known as columnar cells (containing dense microvilli and basal foldings), entero-endocrine cells, Goblet cells and midgut stem cells. Lepidopteran midgut is not only involved in food digestion but also plays role in immune response. The columnar epithelial cells possess microvillar apical brush border (microvilli increases surface area), which helps in enzyme secretion and digested nutrient absorption (Cavalcante and Cruz-Landim, 1999).

ii) **Fat body**: Fat body is a primary larval metabolic organ which is important for macromolecular synthesis as well as nutrient storage in insect (Law and Wells, 1989). It is majorly composed of adipocytes, oenocytes, urocytes and bacteriocytes (Arrese and Soulages, 2010). Fat body is multifunctional organ which synthesizes and stores various insect proteins. It co-ordinates hormonal and nutritional signals that regulate insect development as well as metamorphosis. During pupal adult development fat body is known to be associated with synthesis of vitellogenin and regulates ovarian development (Colombani et al., 2005).

iii) **Malpighian tubules**: In insect larvae, Malpighian tubules are attached at the junction of midgut and hindgut. Malpighian tubule is primary excretory and osmoregulatory organ in insect larvae. Larval metabolic waste from gut is collected by the Malpighian tubules through gut specific valve. Furhtermore, Malpighian tubules also collect secretory wastes or toxic content from the haemolymph, followed by release of collected waste/toxic content into exterior side through hindgut and rectum.

iv) **Salivary gland**: Salivary glands are specialized tubular structure in lepidopteran larvae majorly associated with mouth part. They play important role during metamorphosis because they are specialized to secrete silk as well as other salivary enzymes. Salivary glands are associated with different mouth parts i.e. mandibular, maxillary, hypopharyngeal, and labial. Each of them have unique function in different species and at different stages of development. In present study it was the labial gland which commonly known as silk gland was used for the study.

v) **Haemolymph**: In insect haemocoelic cavity is filled with a circulatory fluid which is called as haemolymph. It is a connective tissue which primarily consist of plasma and haemocytes. Larval haemolymph shows presence of large number of storage proteins such as hexamerins. It is rich in macro and micro molecules which are needed for the development and growth of

insects. Hexamerin constitute more than 70-80% of insoluble protein during the final larval instar which are synthesised by fat body and released into the haemolymph during active feeding phase (Telfer and Kunkel, 1991; Zhao and Kanost, 1996; Burmester, 1999; Wheeler et al., 2000).

Midgut cell types

Insect larval midgut represents the association of internal and external surrounding as discussed above. It consists of four cell types i.e. columnar cell, entero-endocrine cell, Goblet cell and midgut stem cell (Dow, 1987).

i) **Columnar cells**: Columnar cells are the primary midgut cell type, which is responsible for digestion and absorption (Nation, 2015). These cells are commonly involved in transport of solutes, ions etc. Moreover microvilli present in these cells increase the surface area which is responsible for nutrient absorption. The innser laminal brush border of these cells possses large number of molecules such as cadherin, aminopeptidases and alkaline phosphatase, which play important role in gut biology. These cells are also responsible for various signalling network and crucial for larval development and metamorphosis. It is interesting to note that the common molecules present at the brush border (cadherin, APNs, ALPs etc.) also interact with Cry toxins and act as their receptors.

ii) **Entero-endocrine cell**: Similar to columnar cells, entero-endocrine cells are also distributed throughout the epithelium. These cells are secretory in nature and release bioactive humoral molecules into the lumen. These cells are also responsible for hormonal regulation as well as tissue homeostasis. Song et al., (2014) demonstrated that quality of ingested nutrient can be assessed using humoral secretion. Further few other reports suggest that stem cell proliferation linked peptide is also released by entero-endocrine cells (O'Brien et al., 2011; Amcheslavsky et al., 2014).

iii) **Goblet cells**: Among all the cell type Goblet cells exhibit unique characteristics, they are characterised by large cavity with the presence of extreme pH condition (Terra et al., 1996). They are exclusively present in larval midgut epithelium and scattered in between entero-endocrine and columnar cells. They possess large cavity but lined by dense microvilli from internal cytoplasmic side (Caccia et al., 2019). Goblet cell nucleus is positioned towards lateral side because of thin cytoplasmic layer cannot harbour large dense nucleus (Gomes et al., 2013).

iv) **Midgut stem cell**: Apart from digestion, absorption, ionic regulation etc. midgut epithelium additionally maintains itself or repairs itself during development or any other adverse/impaired condition. The overall integrity of the midgut is maintained by these midgut stem cells. They are present primarily at the base of midgut epithelium and exist in form of scattered cells (Lepidoptera and Diptera) or organised in cluster/nidi (Orthoptera and Odonata) or lie inside regenerative crypts/pouches (Coleoptera) (Lehane and Billingsley, 1996). They are characterised with dense cytoplasm containing lipid droplets and glycogen granules (Tettamanti et al., 2007, Chajec et al., 2012; Franzetti et al., 2015). Midgut stem cells demonstrate remarkable division capacity which is fundamental to ensure larval growth. Franzetti et al., (2015) reported that in larvae, midgut epithelium was completely replaced by new one during metamorphosis. There is dearth of knowledge in lepidopteran larval midgut stem cell regulation however ecdysteroids, α-arylphorin and bombyxin were reported to promote midgut stem cell proliferation (Hakim et al., 2010). Source of midgut stem cell regulating factor is not yet clear, however in current study we made an attempt to see the midgut stem cell regulation in lepidopteran pest *A. janata.*

Objective

Earlier studies from our laboratory in various lepidopteran insects have revealed alteration in midgut luminal protease profile, presence of Cry toxin receptor, altered

development, histopathological changes in gut, fat body, Malpighian tubule and salivary gland, occurence of necrotic cell death, alteration in aminopeptidase profile upon Cry toxin application (Budhata et al., 2007, 2008; Ningshen et al., 2017; Chauhan et al., 2017). In current study taking preliminary background from afore mentioned reports, research was carried out to check the impact of long term field application of DOR-Bt1 formulation and find out whether or not castor semilooper also becomes toxin tolerant? In an earlier study we reported that actively dividing cells are primarily located in basal region of midgut epithelium (Chauhan et al., 2017). In this present study an attempt was made to analyse, how these proliferative cells support repair of larval midgut epithelium and what mediates it? Keeping this in mind following objectives were framed to evaluate the effect of sublethal Cry toxins exposure-

1. Cry toxin induced cellular changes in the larval midgut of *Achaea janata*.
2. *De novo* transcriptome analysis and gene expression profiling of larval midgut.
3. Analysis of regeneration:

   a) Evaluating the role of arylphorins in regeneration and repair of midgut epithelium

   b) Analysis of epithelial alteration in APN profile of Cry toxin susceptible and tolerant larvae.

General Materials and Methods

Insect rearing

Achaea janata eggs were collected from the fields of the Indian Institute of Oil Seed Research, Hyderabad, Telangana, India. The collection was carried out from the fields which were never sprayed with pesticides and hence, the collected eggs were free from their exposure. Further, immediately after hatching, the neonates were fed on fresh castor leaves and maintained for a total life cycle of five generations at the insectary of School of Life Sciences, University of Hyderabad, Hyderabad, Telangana, India. Susequently for each generation larvae were maintained on fresh castor leaves collected from university open field where castor plantation was grown free of pesticides/herbicides and maintained throughout the year. The larvae were maintained under 14h light and 10h dark period with 70 ± 5% relative humidity and 27 ± 2℃ temperature until pupation. The larval instars (from 1^{st}- 5^{th}) were maintained in plastic troughs till pupation. Pupae were collected from the plastic trough and transferred on the sterilized moist sand. Soon after the emergence, the adult male and female moths were collected and transferred to wooden breeding cages and maintained at room temperature (RT). The adults were fed with 10% honey solution in breeding cages, where female moths laid eggs on castor leaves. Once again eggs were collected, sterilized and used for maintenance of continuous cultures. They hatched in 6-7 days and neonates larvae were collected and transferred into plastic troughs containing fresh castor leaves. The cycle was maintained throughout the study and several generations of these insects were used.

RNA isolation

Larvae were narcotized by placing them on ice. The required tissue was dissected in insect Ringer solution under cold condition and transferred to TRI reagent TM (Sigma Aldrich, USA). For total RNA isolation, 100 mg tissue was homogenized using all glass microhomogeniser. To the homogenate gently 200 µl chloroform was added and left for 10

min at room temperature followed by centrifugation at 15,000 rpm at 4℃ for 15 min. After centrifugation separated aqueous layer was carefully collected with a pipette and transferred into a fresh Eppendorf tube. To it, two volumes of iso-propanol was added, gently mixed and kept for 1 h at -20℃ for precipitation. The precipitated RNA was pelleted by the centrifugation (15000 rpm at 4℃ for 15 min). The centrifuged pellet was washed thrice with 70% DEPC (diethylpyrocarbonate) treated ethanol and air dried. The RNA pellet was dissolved in DEPC treated nuclease free water and quantity as well as quality was evaluated using Nanodrop (Thermo Scientific, USA). Further integrity of isolated RNA was checked by performing 1% agarose gel electrophoresis (Sambrook et al., 1989). For obtaining DNA free RNA, DNase treatment was carried out by incubating 2 µg of RNA with 1 µl of DNase1 enzyme (1 U/µl) (Invitrogen, Life Technologies, USA) in DNase1 reaction buffer at 37℃ for 20 min.

Complementary DNA (cDNA) synthesis

DNA free RNA prepared using the above protocol was used for first strand cDNA synthesis using SuperScript™ III First-Strand synthesis kit, protocol was followed as prescribed by the manufacturer (Invitrogen, Life Technologies, USA). For synthesis of cDNA, reaction mixture was prepared by adding 1 µl RNA solution containing 1 µg RNA, 2 µl of dNTP mix, 1 µl of oligo dT primers and 16 µl nuclease free water in a final volume of 20 µl in PCR tube. The reaction mixture was incubated at 65ºC for 5 min. After this cDNA synthesis mix was prepared by adding 4 µl of reaction buffer (5X), 1 µl of RT enhancer and 1 µl of reverse transcriptase enzyme (200 U/µl) to the pre-incubated reaction mixture. Finally to carry out first strand cDNA synthesis, total mixture was incubated at 42ºC for 60 min followed by reaction termination by heating at 85℃ using thermocycler for 5 min. The freshly synthesized cDNA was kept on ice to chill and for long term storage it was further stored at -20℃.

Primer designing of short oligos

As for the model organism (*Achaea janata*) midgut transcriptome assembly (GHGZ00000000.1) was generated and submitted at NCBI database, so most of the primers used in the present study were gene specific primers. However few of the gene sequences from other tissues were not available, so the degenerate primer based strategy was adopted using the gene sequences of closely related lepidopteran species available in NCBI database (https://www.ncbi.nlm.nih.gov/) (Dieffenbach and Dveksler, 2003). For the nucleotide/ amino acid multiple sequence similarity analyses, MAFFT version 7 was used (https://mafft.cbrc.jp/alignment/). Designing of the primer was constrained with parameters of primer length (15-30 bp), GC content (~ 50%), annealing temperature (~ 55-60℃) and other features like hairpin, homodimer and heterodimer formation etc. Oligoanalyzer tool 3.1 (Integrated DNA Technologies Inc., USA) was used to check the final primer parameters.

Polymerase chain reaction (PCR)

PCR was carried using 10 µl reaction mixture containing 5 µl master mix (2X) (Clonetech, USA), 0.5 µl each of forward and reverse primers (10 pmol each), 0.5 µl cDNA template (1:10 dilution) and 3.5 µl nuclease free water. The reaction was carried out for initial denaturation at 94℃ for 2 min followed by 30-35 cycles of denaturation-annealing-amplification (94℃ for 30 sec → ~55-60℃ for 30 sec → 72℃ for 30-90 sec) respectively and final amplification at 72℃ for 10 min. Finally, the thermocycler was adjusted at 4℃ until the PCR product was taken out from the blocks.

Agarose gel electrophoresis

Separation of nucleic acids was carried out using 0.5~1.2 % agarose gel electrophoresis. It was used for total RNA, PCR product, plasmid DNA, digested fragments separation etc. It was prepared using TAE buffer (Tris base (40 mM), acetic acid (20 mM) and 0.5 M EDTA (2 mM)). Solid 1g agarose (Lonza, USA) was mixed in 100 ml of TAE buffer. The suspension was

boiled for 2 min 10 sec using microwave and further allowed to cool down at room temperature. Ethidium bromide (10 mg/ml) was added to this solution before pouring the solution into casting boat. The casting boat was sealed using plastic adhesive tape and required size comb was positioned. The agarose solution with EtBr was poured into it and left at room temperature for solidification. For separation, the nucleic acid sample was mixed with loading dye containing 0.25% (w/v) bromophenol blue, 30% (v/v) glycerol and 0.25% (w/v) xylene cyanol. Each gel was also loaded with appropriate DNA marker such as 100 bp (SM0241), 1 Kb (SM0312) ladders (Thermo Scientific, USA). After loading the samples (total RNA, PCR product, plasmid DNA or digested fragments) the gel boat was submerged into the electrophoretic tank containing TAE buffer and electrophoresed at 100 V for 30~40 min. After completion, the nucleic acid fragments were visualized using UV illuminator or documented using gel documentation apparatus (Bio-Rad, USA).

PCR product elution

Once the required PCR product obtained was confirmed with gel electrophoresis, it was either eluted using PureLink™ PCR purification kit (Invitrogen, Life Technologies, USA) or extracted using gel extraction kit (Thermo Scientific, USA). The steps were followed as per the manufacture's protocol. For purifying the PCR product, binding buffer with isopropanol was added to the sample and mixed gently. Sample was loaded onto a clean-up spin column and centrifuged at 12000 rpm for 1 min. In clean-up, flow-through was discarded and column was placed back into the wash tube. Then wash buffer with ethanol was added in the column and centrifuged at 12000 rpm for 1 min. This centrifugation step was once again repeated for the removal of excess ethanol. Following which 20-30 µl elution buffer or nuclease free water was added to the column and was kept for 8~10 min at room temperature. Column was reinserted into the collection tube, for the collection of elute by centrifugation at 12000 rpm for 1 min. Purified DNA sample was checked for quantity/quality using Nanodrop. However, for

the gel extraction based DNA purification, required gel slices were chopped and dispersed into the L3 buffer (PureLink™ Gel Extraction Kit (Invitrogen, Life Technologies, USA)). For this, the tube containing dispersed DNA containing agarose sample was incubated at 50℃ for 10 min and inverted thrice in-between for better dissolving. All other steps followed were the same as for the purification of PCR products.

Recombinant vector construction

The amplified DNA product (desired nucleotide fragment) was inserted into a cloning vector pTZ57R/T (Thermo Fisher Scientific, USA) for sequencing and storage. For protein expression, pET-28a(+) expression vector (Novagen, USA) was used. Insert and vector ratio was maintained at 3:1 or 5:1 as suggested in the manufacturer's protocol. In a complete ligation reaction mixture, 4 µl reaction buffer (5X), 2 µl pTZ57R/T (55 ng)/ pET-28a(+) vector, 1 µl T4 DNA ligase, PCR product (variable volumes) and 10-13 µl nuclease free water were added to make up the final volume 20 µl. The ligation reaction mixture was mixed gently by shaking the tube and centrifuged briefly followed but incubation at 4℃ for 12-16 h.

Competent cells preparation

Competent *E. coli* bacterial cells either of DH5α or BL21 strain were prepared. For this, cells from the glycerol stock was first streaked on LB (Luria-Bertani) agar plate, followed by incubation for 12-16 h at 37℃ for optimal growth. Once bacterial colonies appeared on the agar plate, carefully a single colony was picked up by sterile toothpick and inoculated in 10 ml of LB broth for 12-16 h at 37℃ with 200 rpm shaking. A small inoculum of prepared culture (0.1 ml in 10 ml) was further used for the inoculation of fresh LB broth and grown for 2~3 h till the growth reached 0.5-0.6 optical density. This actively growing culture suspension was placed on ice for 30 min and later centrifuged at 6000 rpm for 10 min at 4℃. The supernatant was discarded and leftover bacterial pellet was suspended in 0.1M $CaCl_2$ (10 ml) on ice and

incubated for 60-90 min. After cold treatment the cell suspension was centrifuged at 4℃ for 6000 rpm. The upper supernatant layer was carefully discarded so that the pellet remained suspended in 1 ml solution. The prepared cell pellet was dispersed and sample was aliquoted (100 µl) and used, or stored at 4℃ for later use.

Transformation

For ligation reaction, vectors pTZ57R/T and pET-28a were used and transformation was carried out. Ligation mixture containing plasmid (50-100 ng) was added to DH5α or BL21 *E. coli* competent cells and incubated on ice for 30 min. Immediately after cold treatment, the reaction was subjected to heat shock at 42℃ for 90 sec followed by incubation in ice for 5 min. Then, 1 ml of LB broth was added to transformed cells and incubated at 37℃ for 1 h with continuous shaking at 200 rpm. This actively grown suspended culture was centrifuged for 5 min at 3000 rpm, the supernatant was gently removed leaving 200 µl in the tube. To this 200 µl of cell culture, 10 µl of IPTG (1M) and 20 µl of X-gal (40 mg/ml) was added for blue white colony screening. This mixed cell culture was plated on LB plate containing antibiotics. Desired antibiotics was used in LB plate for the growth and selection of specific transformed cells. The plates were incubated at 37℃ for 12 h to 14 h, till the colonies appeared.

Plasmid isolation

Overnight grown bacterial cell culture was used for the plasmid isolation using Plasmid DNA Miniprep Kit (Thermo Scientific, USA). Steps were followed as mentioned in manufacturer's manual, firstly the suspended cell culture was centrifuged at 6000 rpm for 5 min at RT. The centrifuged pellet was suspended in resuspension buffer with RNase A by gently inverting the tube for 6-7 times. To this 400 µl lysis buffer was added and incubated at room temperature for 4-5 min, until clear solution was visible. Immediately after that precipitation buffer was added and tube was gently inverted until the mixture became

homogenous. This lysate suspension was centrifuged at 12000 rpm for 10 min at room temperature. Prepared cell lysate was loaded on to the equilibrated column and washed twice with wash buffer given in the kit using gravity flow.

The flow-through was discarded and the plasmid was eluted with elution buffer or TE buffer into a sterile micro-centrifuge tubes. The quality and concentration of plasmid was assessed using Nanodrop. Plasmid was either sequenced commercially or stored at -20℃ for further usage.

Real time PCR for gene expression analysis

Quantitative expression analysis was carried out using real time PCR analysis, SYBR® Premix Ex Taq™ II (Takara, USA) master mix based 10 µl reaction. The total reaction mixture was prepared by adding SYBR master mix (5 µl), PCR gene specific forward primer (0.5 µl), reverse primer (0.5 µl), template (1 µl) and nuclease free water (3 µl). The primer was custom designed to attain amplicon size of 180-200 bp for various genes. A standard PCR protocol was used for the reaction which was performed in 3 steps; i) holding stage (95 ℃ for 10 min), ii) cycling stage (95 ℃ for 5 sec followed by 60℃ for 30 sec) /40 cycles and iii) melt curve stage (fluorescent signal was monitored as the gradual increase of temperature from 59℃ to 68℃). After the completion of PCR reaction, amplification and melting curves were checked. Cycle threshold (Ct) value for each reaction was obtained and expression was calculated using $2^{-\Delta Ct}$ method (Livak and Schmittgen, 2001).

Heterologous expression and recombinant protein purification

Desired cDNA sequence (open reading frame) without any cleavage site for the restriction enzyme was inserted into expression vector pET-28a(+) (Novagen, USA). The restriction sites were checked with Nebcutter version 2.0 (http://www.labtools.us/nebcutter-v2-0/), based on that expression primers were used. Transformed vector was sequenced and cross checked with 5' to 3’ end protein expression as well as restriction site sequences. The

desired cDNA overhangs with sticky ends were maintained. The recombinant vector thus generated was used for the transformation of BL21 *E. coli* expression host cells. The transformed cells were plated on the agar plate and a single positive colony was used for inoculating in 10 ml of LB broth with required antibiotics. This culture was allowed to grow at 37℃ for 12-14 h. After optimal growth the culture was induced with IPTG (100 µl of 0.5 M) and allowed to grow for another 3-4 h at same temperature. Finally, it was centrifuged at 6000 rpm for 10 min and the pellet thus obtained, was washed thrice with phosphate buffered saline (PBS; 1.8 mM KH_2PO_4, 137 mM NaCl, 10 mM Na_2HPO_4 and 2.7 mM KCl, pH 7.4).

The His-tagged recombinant protein was expressed and purified using Nickel-NTA column. IPTG induced recombinant protein was suspended in Tris-imidazole equilibration buffer (pH 7.4) containing 50 mM Tris, 10 mM imidazole and 250 mM NaCl. To this lysozyme (10 mg/ml) was added for bacterial cell lysing; after 10 min the samples were sonicated with 31% amplitude, 10 sec on and 30 sec off. During sonication, the samples were maintained on ice. The lysate obtained was constantly kept on ice. Further, the bacterial cell lysate was centrifuged at 4℃ for 30 min at 10000 rpm. The supernatant was collected and loaded onto equilibrated Ni-NTA column (Qiagen, Gemany). It was further washed extensively with wash buffer (50 mM Tris, 40 mM imidazole and 250 mM NaCl; pH 7.4). After washing, the bound His-tagged recombinant protein was eluted using elution buffer (50 mM Tris, 250 mM imidazole and 250 mM NaCl; pH 7.4). Eluted 1 ml fraction was collected in tube and purity of the protein was assessed using SDS-PAGE.

Protein estimation

Bradford colorimetric assay was used for estimation of protein in the required sample (Bradford et al., 1976). Bovine serum albumin (BSA) 10 mg/ml was used for the preparation of standard solution. For each sample, small aliquot (~ 10 µl) was taken and it was made to 100 µl by adding 10 mM Tris-HCl (pH 7.4). To this, 900 µl of Bradford reagent (Bio-Rad,

USA) was added. The tubes were incubated for 10 min in the dark at room temperature and the absorbance was measured at 595 nm using spectrophotometer (Shimadzu, Japan). A BSA standard curve was used to assess the protein sample concentration.

Protein profiling

Sodium dodecyl sulphate-polyacrylamide gel electrophoresis (SDS-PAGE)

SDS-PAGE was carried out for protein profiling using well established protocol of Laemmli (1970). Stacking and resolving gels were prepared in Tris-HCl buffer using acrylamide, ammonium per sulphate and TEMED. In a solution, proteins were normally folded with positive and negative charges, hence β–mecaptoethanol and SDS were added to reduce the disulfide bonds and linearize it with negative charge. For the preparation of SDS based gel matrix, stacking gel with a lower pH (6.8) and resolving gel with a higher pH (8.8) was used. For 10% resolving gel (3/4th of the complete gel matrix), 1.83 ml of 1.5 M Tris-HCl (pH 8.8), 2.43 ml of 30% acrylamide mix, 150 µl of freshly prepared 10% APS, 3.5 ml double distilled water and 10 µl of TEMED was added. The solutions were quickly mixed and poured into casting unit which was sealed with agarose solution. Solidification of resolving gel was followed by preparation of stacking gel which was 1/4th of the complete gel matrix. For this 625 µl of 0.5 M Tris-HCl (pH 6.8), 400 µl of 30% acrylamide mix, 25 µl of 10% APS, 1.44 ml double distilled water and 10 µl of TEMED were added. After quick addition of TEMED, stacking gel was poured on the top of resolving gel in casting unit and desired volume sized plastic comb was inserted before its polymerization. The casted gel was assembled in the electrophoretic unit with the help of binder clips and buffer tanks were filled with running buffer containing Tris-base (25 mM), glycine (192 mM) and SDS (10%). The protein samples were mixed with loading buffer containing 10% β-mercaptoethanol, 4% SDS, 20% glycerol in 0.125 M Tris-HCl (pH 6.8) with tracking dye (0.02% w/v bromophenol blue). Initially the electrophoresis was carried out at 60 V and once the samples crossed the stacking matrix area,

the voltage was increased to 100 V for the separation of proteins in the resolving gel. Once the run was completed, the gel was taken out carefully and stained for visualizing the protein/peptide.

Visualization of separated peptide fragments using Coomassie staining

The electrophoresed gel with proteins/ peptides was stained with Coomassie brilliant blue stain by following protocol of Wilson et al., (1979). A 0.025% solution of Brilliant Blue-R 250 was prepared in 40% methanol containing 7% acetic acid. The gel was submerged in staining solution at room temperature for 12-14 h with continuous gentle shaking on rocker. To avoid overstaining or to perform destaining; destaining solution containing 40% methanol with 12% glacial acetic acid was used. Once the gel background was clear and bands were clearly visible it was documented with the scanner.

Silver nitrate staining

Silver nitrate staining method was primarily used to visualize the proteins/ peptides of lower concentrations in the sample after SDS-PAGE separation (Blum et al., 1987). This method has higher sensitivity when compared with Coomassie staining. This staining method involved five sequential steps: i) fixation: the gel with separated proteins/ peptides was incubated with 50% methanol, 12% acetic acid and 0.05% formaldehyde solution for 3 h, it was followed three times washing by in 50% ethanol, ii) sensitization: gel was soaked in sodium thiosulphate hypo-solution (0.02%) and washed thrice with distilled water (1 min each), iii) staining: 0.2% silver nitrate in 0.076% formaldehyde solution was used for staining the peptides/proteins in gel matrix (20-30 min incubation on slow moving rocker), iv) development of color: after staining the gel was washed with distilled water and submerged in 6% sodium carbonate containing 0.05% formaldehyde solution till the bands were clearly visible and v) stopping: to avoid over-staining and to obtain clear background, the stained gel was transferred to 12 % acetic acid and documentation was carried out using scanner.

Generation of polyclonal antibodies

Model organism used in this study was *A. janata*, which is a local pest therefore specific antibodies against required proteins were not commercially available. Hence BALB/c mice based antibody was generated against *A. janata* midgut arylphorin. For generation of polyclonal antibody six month old mice were used using standard protocol (Leenaars and Hendriksen, 2005) after obtaining approval from Institutional Animal Ethics Committee, UH (reg. no. 154/RO/C1999/CPCSEA). Recombinant arylphorin protein (100 µl) was emulsified with 500 µl of complete Freund's adjuvant and injected subcutaneously in mice. Before injection, tail vein of mice was bled to collect pre-immune sera. Successively after two weeks 2nd booster was given to mice with 50 µg of recombinant protein emulsified with incomplete Freund's adjuvant. Mice was monitored daily after immunization and after 12-15 days of 2nd booster dose, blood was collected from mice. Collected blood was kept 12-14 h at 4℃ for clotting, followed by centrifugation at 6000 rpm for 20 min for collection of sera which was processed for antibody purification.

Antibody purification

Protein-A agarose column (Amersham, Germany) based affinity chromatography was performed to purify mouse IgG fraction. Binding/wash buffer containing 20 mM sodium phosphate, (pH 7.4) in 150 mM NaCl solution was added to the serum protein (1:1 ratio). Diluted sera was loaded onto equilibrated column and gently washed 5-10 times with wash buffer till the eluted solution absorbance matched with the absorbance of wash buffer at 280 nm. The acidic elution buffer containing 100 mM glycine-HCl, (pH 3.0) was used to elute the purified IgG fraction and recovered in several collected fractions. The eluted fractions were pooled and neutralization was carried out using 1 M Tris HCl (pH 9.0). The purified IgG fraction was aliquoted in several tubes and for long term storage it was lyophilized and kept at -20°C.

Western blot analysis

SDS-PAGE gel matrix based electrophoresed protein/peptides were transferred to charged nitrocellulose membrane following the steps discussed in Towbin et al., (1979). Before setting up the transfer the membrane and SDS gel was immersed in Towbin buffer contains 25 mM Tris, 192 mM glycine in 20% methanol for 10-15 min. Gel with seprated protein along with membrane was stacked into a cassette containing filter paper, which was placed gently in the transfer unit and filled with Towbin buffer, followed by transfer of peptides/proteins at 25 V with 250 mA current for 14 h. After the complete transfer of proteins/peptides, the nitrocellulose membrane was stained with Ponceau S stain (0.1% (w/v)) in acetic acid (5%) to confirm the transfer of proteins/peptides.

The nitrocellulose blot containing proteins/peptides was processed for washing with Tris buffered saline (TBS) containing 10 mM Tris-HCl (pH 7.4) in 150 mM NaCl solution. The following incubation steps were carried out on rocker with gentle shaking. The membrane was washed thrice for 15 min and then submerged in blocking solution (5% bovine serum albumin solution in 0.1% Tween-20 containing TBS) to avoid non-specific binding. After 3 h of blocking the blot was washed thrice with TBS, TBST and TBS, 15 min each, followed by incubation with desired/specific primary antibody with 1:1000 dilution (diluted in 2% BSA) at 4℃ for 12-14 h. Further, primary antibody was collected in 50 ml tube and blot was washed again with TBS-TBST-TBS, 15min each to remove excess antibody. Incubation of blot was carried out with secondary mouse IgG conjugated with alkaline phosphatase. The secondary antibody was diluted using 2% BSA (1:4000) and blot was soaked for 3-4 h. The excess unbound antibody was removed from blot by washing with TBS-TBST-TBS and processed for color development using BCIP/NBT (G-Biosciences, USA). Developed blot was immediately documented with Kodak Photo Imager.

Histological analysis

Histological analysis included several steps from tissue dissection to microscopic analysis. Detailed steps used in the experiments are mentioned below:

i) Tissue dissection and fixation: Firstly, insect larvae were narcotized by placing them on ice for 15-20 min, followed by dissection in insect Ringer solution. Specific tissue (midgut, fat body and ovary) was taken out carefully after cutting open the larval skin and transferred to Bouin's fixative (water saturated picric acid: formaldehyde: glacial acetic acid 15:5:1) for 12-14 h at room temperature.

ii) Dehydration and clearance: Before wax embedding the tissue was dehydrated by using series of ethanol. In first step tissue was immersed in 70% ethanol for 1 h and repeated thrice with different tubes containing 70% ethanol. Tissue dehydration was further continued by transferring the tissue to 90% ethanol for 1 h followed by two changes of absolute ethanol for 1 h each. Finally the dehydrated tissue was processed through xylene for clearance (2-5 min).

iii) Paraffin embedding: The cleared tissue was and immediately transferred to the mixture of xylene and molted paraplast (1:1) for 5-8 min at 60°C. Tissue was infiltrated with molted paraffin at 60°C and three changes were performed each for 30 min. After three successive changes, the tissue was finally embedded in semi molted paraffin wax at room temperature in paper or L-shaped blocks and allowed to solidify.

iii) Trimming and sectioning: Prepared wax block was trimmed in square shape for sectioning using clean knife/blade. The block was fixed on small wooden box (2 cm^3) with the help of molted wax and placed on block holder of rotary microtome (Leica Microsystems, Germany). The blocks were sectioned and 3-5 µm thick tissues sections were cut. The strips were placed on a clean glass slide. For attachment and flattering of the wax strip, slide was pre-coated with Mayer's albumin few drops of water was poured and kept on hot plate at 40°C. Once the wax

strips was flattened, water was gently drained and slides were kept at 37℃ for 12-14 h for drying.

iv) Staining, mounting and visualization: Slides containing dried tissue section was cross checked for the tissue presence and later processed for staining. Most of stains used in laboratory were water soluble therefore the sections were first de-paraffinized by immersing them in xylene filled coupling jar. Followed by rehydrating using ethanol series; 100%-100%-90%-70%-50%-30% ethanol and water for 5 min each. Immediately after rehydration, water soluble stain (Methylene blue) was over flowed on the sections and kept for 10-12 min at room temperature. The overstaining of section and slide background was cleared by water immersion. Stained section was again dehydrated using gradient ethanol series 30%-50%-70%-90%-100%-100% for 5 min and cleared using xylene (2 changes for 5 min each). Finally the section was mounted using DPX mountant (Sigma-Aldrich, USA) and left at RT for 3-4 h for polymerization. The slides were visualized using compound microscope (Leica Microsystems) and documented using attached CMOS camera.

Statistical analysis

Calculation and raw data presented in the current thesis was validated using various statistical analysis. Most of the experiments were performed in triplicates, therefore the average value was calculated and standard deviation was plotted against it (n=3). Statistical significance between comparative values was calculated using Sigma Plot v14. For One-Way ANOVA (Analysis of Variance) followed by SNK (Student-Newman-Keuls) post confirmatory test was performed for pairwise comparative analysis. Significant p values were calculated for each comparison.

Chapter 1

Cry toxin induced cellular changes in the larval midgut of *Achaea janata*.

1. Introduction

The insecticidal *Bacillus thuringiensis* (Bt) based Crystalline (Cry) toxins are being used to manage *Achaea janata* larvae, which exhibit a specific mode of action leading to cell death as discussed in General Introduction. Various models have been prepared to understand the Cry toxin effects on larval physiology (Zhang et al., 2006; Pardo-Lopez et al., 2012; Adang et al., 2014). Extensive studies in lepidopteran species represented several structural changes after Cry toxin application such as elongation or rupture of intestinal lumen microvilosities, vacuolisation of cytoplasm, cell hypertrophy and degradation of peritrophic membrane (Griego et al., 1980; Mathavan et al., 1989; Bravo et al., 1992; Baines et al., 1997; Loeb et al., 2001; Knaak and Fiuza., 2005; Knaak et al., 2010; Caccia et al., 2019). Alteration in intestinal epithelium was also observed when intoxicated with nuclear polyhedrosis virus (Knaak and Fiuza, 2005). *Bacillus thuringiensis* AA 1-9 and HD-73 toxication were also reported to reduce columnar and globular midgut cell number in *Heliothis virescens* (Loeb et al., 2001). Cry toxin exposed caterpillars had ruptured microvilli and vacuolisation of the cytoplasm in *Lymantria monacha* (Linnaeus) as well as *in vitro* test of the same also revealed the disorganisation and hypertrophy of the midgut cells (Rausel et al., 2000). Baines et al. (1997), tested Cry1A toxins in lepidopteran species and demonstrated a collapse in the electrochemical gradient of midgut epithelium which lead to insect mortality. *In vitro* reports using *Lymantria dispar* membrane also showed irreversible depolarisation when treated with Cry1Aa proteins (Peyronnet et al., 1997).

Interestingly, additional physiological responses revealed that when lepidopteran larvae were exposed to Cry toxin, they recovered after initial toxin induced damage (Dulmage and Martinez, 1973). As discussed earlier, toxin damage induced several other physiological alterations which also lead to death of an organism. However, there are always descriptive alternatives leading to physiological responsiveness which support animal survival during

toxication. At present various insect pests have been reported to be resistant variety against Bt toxin, which includes; *Spodoptera frugiperda*, *Pectinophora gossypiella*, *Busseola fusca*, *Diabrotica virgifera*, *Helicoverpa armigera*, *Chilo suppressalis*, *Tribolium castaneum*, *Ostrinia nubilalis* and *Ostrinia furnacalis* (Storer et al., 2010; Zhao et al., 2010; Carmona et al., 2011; Dhurua and Gujar, 2011; Kruger et al., 2011; Zhang et al., 2011; Kliot and Ghanim, 2012; Jakka et al., 2015; Pereira et al., 2015; Xu et al., 2015; Shabbir et al., 2018; Yu et al., 2018). Alterations in toxin receptor profile was observed in Cry resistant larvae of *Trichoplusia ni* (Tiewsiri and Wang, 2011), which exhibited modulated expression of aminopeptidase-N (APN) for insect survival. Affected intracellular protein trafficking was also observed during Cry toxication, which was associated with alteration of midgut epithelial cadherin receptor and supported cotton bollworm survival (Wang et al., 2018). Pink bollworm resistance was also reported to be associated with alteration in cadherin alleles (Morin et al., 2003), while mutation of cadherin gene was associated with resistance of Asian Corn borer (Jin et al., 2014). Changes in receptor profile leads to alterations in several physiological properties which helps in insect survival during toxication. Other than mutation/alteration in receptors, midgut epithelial cells also facilitated repair and epithelial regeneration (Spies and Spence, 1985; Forcada et al., 1999). Enhanced midgut regeneration in *Heliothis virescens* indicated midgut healing response to facilitate recovery after Cry toxin damage (Martinez-Ramirez et al., 1999, Castagnola and Jurat-Fuentes, 2009). In an earlier report, we presented histological analysis which revealed cell death during early Cry toxin exposure recovered by active cell proliferation (Chauhan et al., 2017). The current study further unravels the basis of larval survival upon Cry toxicity.

For Bt based biological control of insect pests, more than 400 formulations are available and are used as sprays (Ahmedani et al., 2008; Ali et al., 2010; Sanahuja, et al., 2011). One of the largely used biopesticides for controlling *Achaea janata* in Andhra Pradesh and Telangana is Cry toxin based DOR Bt-1 formulation (Directorate of Oil Seed Research) which is proven

successful against this castor pest (Vimaladevi et al., 2006). DOR Bt-1 formulation with high potential insecticidal activity was formulated as powder/granules for field application similar to other Bt formulations and named Wnock WP (DOR Bt-1). It was released by the Indian Institute of Oil Seed Research (IIOR) in 2006. So far this formulation was given to farmers and used in fields of Telangana and Andhra Pradesh and till now there is no reported resistance against this particular Cry toxin formulation (Lakshminarayana and Raoof, 2005). This formulation contains Cry1 (Cry1Aa, Cry1Ab, and Cry1Ac) and Cry2 (Cry2Aa and Cry2Ab) genes. As discussed in General Introduction part, Cry toxins have host specificity and its delta-endotoxin protein inclusion caused insect cell death (de Maagd et al., 2003; Bravo et al., 2004; Patel et al., 2009).

The most common practice of pesticide application on castor plant in India is spray based, using mechanical sprayers, in which dry formulation is mixed with water or any other liquid carrier and their emulsions are sprayed on plant. But spraying pesticide also has applicative inefficiencies due to deposition, spray drift, leaching, seepage, precipitation, evaporation, dry deposition etc. followed by loss of toxicity from degradation by UV light, wash-off by rain, drying, temperature etc. (Pinnock et al., 1975; Leong et al., 1980; Beckwith and Stelzer, 1987; VanFrankenhuyzen and Nystrom, 1989). All these are possible reasons for sublethal or harmless toxin exposure on pest under previously mentioned conditions. Foliar spray of Bt formulation often results in the loss of toxin effectively under afore mentioned conditions, so there is always possibility of sublethal toxin exposure. Therefore, in the present study we have aimed to understand the effect of sublethal DOR Bt-1 formulation on larvae of castor semilooper. In the present study physiologically relevant sublethal toxin effects were analysed during larval intoxication and survival.

Toxin exposure leads to physical impairment and damage of several tissues in an organism including insects. However, some tissues or organs have the capacity to self-repair

such as epithelial tissue in insect larvae, liver in human, tail regeneration in lizards etc. Hydra is a well known regeneration model, repair in Hydra was reported through cell differentiation to replace the damaged tissue during injury (Frank et al., 2009; Gold et al., 2013). Similarly most of the species related to metazoans demonstrate restricted regenerative capabilities (Fig. 1) (Alvarado and Tsonis, 2006; Bely and Nyberg; 2010; Li et al., 2015) and these species have functional capacity to repair themselves. Innate immunity dependent pathogen defense which maintains physiological balance and promotes tissue regeneration is well reported in mosquitoes (Hilyer et al., 2010; Sim et al., 2014). Various kinds of stress inducers were also reported to promote tissue damage in *Drosophila melanogaster*, specifically gut epithelium based cellular damage recovered through intestinal stem cell proliferation (Micchelli and Perrimon, 2006; Ohlstein and Spradling, 2006; Nazzai et al., 2015).

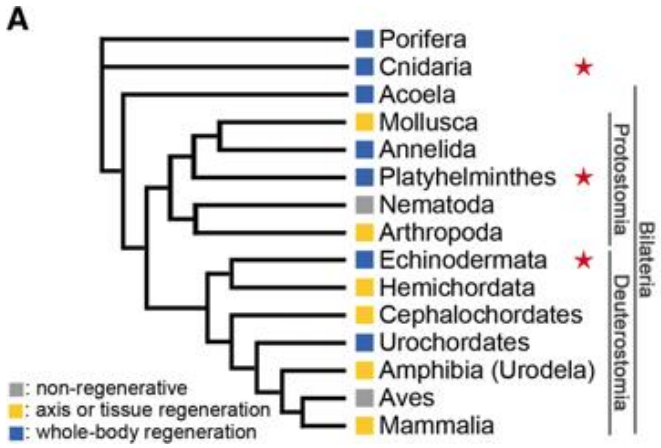

Fig. 1. Phylogenetic distribution of regeneration capacity seen in various animal taxa. Please note that Arthropoda which include insect shows axis or tissue regeneration (adopted from Cary et al., 2019).

As discussed in General Introduction the lepidopteran larval midgut is composed of four different cell type i.e. entero-endocrine cells, columnar cells, Goblet cells and regenerative/stem cells (Lehane and Billingsley, 1996). These cells are responsible for exclusive/limited functions such as secretion, digestion, homeostasis, absorption etc. In gut epithelium scattered midgut stem cells are present, which helps in midgut extension, cellular

distribution, tissue remodelling etc. (Cioffi 1979, Santos et al. 1984, Lehane and Billingsley 1996, Cristofoletti et al. 2000, Pinheiro et al., 2008).

Insect epithelium has multiple cells but each one performs its own function to maintain cellular homeostasis (Huang et al., 2015). Enterocyte endoreplication promotes polyploidy which contributes to cell size (Lee et al., 2009). Lepidopteran epithelial stem cells are the only gut cells which help in homeostasis and regeneration, their division is the only source of repair and growth which can increase the epithelial area upto 200-folds during larval development (Baldwin and Hakim, 1991). *Drosophila* adult gut is well characterised for stem cell differentiation and asymmetric intestinal stem cell division which facilitates in maintaining the same number of intestinal stem cells. Symmetric division assists in growth under response of various nutrients (O'Brien et al., 2011). However, no intestinal stem cell regenerates after complete ablation of progenitor cell. Further, once the stem cell differentiates it will not dedifferentiate (Lu and Li, 2015). In *Manduca sexta*, Nardi et al., (2011) reported that tracheal stem cell regulates midgut epithelial regeneration, which increased the amount of tracheal support during moulting and support muscle layer with epithelial division and differentiation. Intestinal stem cells also restore the epithelial integrity during moulting in any kind of biotic and abiotic stress. In some cases, it represented additional growth distinct from stem cell proliferation such as DNA duplication which was detected during gastrointestinal perforation followed by repair (Hung et al., 2016). *Corcyra cephalonica* and *M. sexta* midgut were shown to regenerate upon Bt infection and same was also reported for *in vitro* culture of *Heliothis virescens* larvae (Spies and Spence, 1985; Chiang et al., 1986; Loeb et al., 2001).

Morgan (1901) suggested that injury, loss of part will sharply lead to physiological regeneration to repair. Moulting is a part of insect life cycle where insect renew or grow their size by cellular regeneration and progressive increase in number of nuclei and cell cytoplasm of gut epithelium is prominent. Followed by histogenesis during postembryonic development,

migration of small nuclear cell (stem cell) from basal membrane to lumen side accompanies new differentiated cell or the cells containing brush border membrane at the apical side (Kellogg, 1906). Kellogg also described a phenomena called "complete metamorphosis" i.e. larvae emerged from eggs are radically different from defined adults and this was achieved by extraordinary dual process of degeneration and regeneration during postembryonic life (moulting and metamorphosis). Metamorphosis in insect is regulated by an interplay of two hormones, 20-hydroxyecdysone and juvenile hormone. Ecdysteroids coordinate moulting by switching gene expression (Riddiford, 1996). All through moulting insect stem cells not only divide but also differentiate and migrate from origin to precise functional position, which is an essential step during larval development.

Tissue damage/injury is repaired by proliferation, differentiation and migration of stem cells as well as progenitor cells. Cell migration is controlled by cytoskeleton elements and cell-substrate adhesion sites, where front driving force is provided by actin cytoskeleton and microtubule coordinates rear retraction (Wehrle-Haller and Imhof, 2003). Cross-talk of actin and tubulin network is proposed well for the mechanistic movement of cell from one place to other in tissue remodelling. The role of actin and tubulin is cell type specific but dynamic in nature to support complex cytoskeleton environment. Recently actin-tubulin microenvironment was reported to facilitate niche establishment of stem cell and differentiated cell (Ambriz et al., 2018). Extracellular matrix environment was also shown to be associated with inner structures of cell such as nucleus and regulated migration (Sen et al., 2015, 2017), suggesting that the organization of tissue was initiated inside the cell. A complex scaffold of cytoskeleton elements is required for division, differentiation, migration, tissue reorganization and also to support the rigidity and structure of tissue (Janmey, 1998; Fletcher and Mullins, 2010). As discussed in earlier section that during Bt toxin exposure, larval gut tissue undergoes damage and later it is repaired by gut healing process. This involves midgut stem cell division,

differentiation and migration. In this study, we examined the role of actin and tubulin and tried to decipher its function in midgut stem cell migration from basal border to lumen side of epithelium.

Lepidopteran larvae were shown to recover from damage of Bt toxin exposure by midgut epithelial regeneration (Spies and Spence, 1985; Forcada et al., 1999). In this chapter, a detailed histological study has been carried out to analyse the major cellular changes induced during sublethal Bt toxin exposure. Further, the study also revealed that how the midgut stem cells repaired the epithelial damage in *A. janata* larvae during sublethal Cry toxin exposure.

2. Materials and Methods

2.1 DOR *Bt*-1 bacterial formulation

Bacillus thuringiensis DOR Bt-1 formulation was obtained from Indian Institute of Oilseeds Research, Hyderabad previously known as Directorate of Oil Seed Research. This formulation was proven to exhibit insecticidal activity against larval forms of castor semilooper (Vimala Devi et al., 2006; Budatha et al., 2007; Ningshen et al., 2013, 2017; Chauhan et al., 2017). The formulation was obtained in powder form and dissolved in distilled water. Suspended toxin formulation in water was used for the treatment application on castor plant leaves. Larval feeding bioassay was also performed using castor semilooper neonates.

2.2 *Bt* toxin activity evaluation and selection of sublethal dosage

Bioassays and other experiments were performed using 3rd instar larvae of *A. janata.* Fresh castor leaf was collected from green house castor plantation area of University of Hyderabad. The castor leaf was coated with suspended toxin formulation in water and kept for air drying. This was followed by keeping the larvae with toxin coated leaves at different concentrations (2-20 ng/cm^2) of Cry toxin in a round plastic troughs. Control for each

experiment was maintained on fresh castor leaf without any toxin coating. DOR Bt-1 formulation was used for the experiment and for LC_{50} calculation Probit algorithm was used as suggested by Finney, (1978).

2.3 Tissue isolation

For tissue damage analysis, 3rd instar larvae were used and dissected after Cry toxin exposure. The larvae were collected at 24 h, 36 h, 48 h, 60 h and 72 h time frame after Cry toxin exposure. Prior to dissection, the larvae were narcotized by keeping them for 15-20 min on ice. Followed by pinning them carefully on head and in the last abdominal segment on wax plate using dissection pin. During dissection, these larvae were submerged in insect Ringer solution containing 130 mM NaCl, 0.5 mM KCl and 0.1 mM $CaCl_2$ to sustain physiological conditions. Through abdominal region, a gentle cut was made and continued along the length of the body. The larvae were now opened and dissected to collect the required tissue such as gut, fat body, salivary gland etc. Most of the experiments in current study was performed on midgut therefore midgut was carefully excised excluding foregut (anteriorly to gastric caeca) and hindgut (extended below from Malpighian tubules) region. Further, the larval tissues collected were used for histological analysis.

2.4 Histological analysis of midgut

Larvae exposed to sublethal (2.5 $\mu g/cm^2$) Cry toxin were carefully dissected and fixed overnight with Bouin's fixative as described in detail in General Materials and Methods section. Isolated larval tissue was dehydrated using alcohol series and embedded in hot molten paraplast (Sigma-Aldrich, USA) in glycerine coated square paper boat or steel container. Paraplast embedded tissue was trimmed carefully with sharp blade and fixed on wooden blocks for sectioning. Leica RM2255 rotatory microtome was used for cutting sections. Four micron thick sections were cut and mounted on a clean glass slide coated with Mayer's albumin. The sections on the slide were floated with water on hot plate to remove the wrinkles and then dried

overnight by keeping them in a dust free cabinet. Following it, the slides were de-paraffinizatied- rehydrated- stained- dehydrated and cleared. The stained slides were mounted using DPX mount solution and visualized under microscope. The sections were photographed using Leica stereomicroscope.

2.5 Epoxy embedding

Dissected larval midgut was also embedded in Epoxy medium for detailed cytological analysis, as it has comparatively lower viscosity than other resins or araldite based polymers. Epoxy mixture was prepared as described in product information booklet (Epoxy-Embedding Kit, 45359, Sigma-Aldrich, USA). To begin with, small midgut pieces (3 mm thickness) were dehydrated using acetone gradient series 30%-50%-70%-90%-100%-100%-100% for 10 min each. Epoxy embedding blend was prepared as per the instruction provided in the manual-

A: Epoxy embedding medium 5 ml and DDSA 8 ml (2-Dodecenylsuccinic anhydride) was thoroughly mixed.

B: Epoxy embedding medium 8 ml, NMA 7 ml (Methylnadic anhydride) and DPM-30 [2,4,6-Tris (dimethylaminomethyl) phenol] 1.5 %) were mixed together gently with a sterile wooden stick till a homogenous solution was obtained.

After dehydration, the tissue was submerged in 50 % acetone + 50 % epoxy embedding blend for 30 min followed by 25 % acetone + 75 % epoxy embedding blend for next 30 min. Finally tissue pieces were embedded in Epoxy embedding blend and kept for polymerization at 45°C for 12 h into pre-dried gelatin mould. After initial polymerization, the same block was kept for 24 hours at 60°C for hardening.

2.6 Ultramicrotomy

The Epoxy embedded larval midgut tissue was sectioned into thin section of 80 nm which is normally referred as semithin section. For this, Epoxy embedded tissue block was

trimmed under Leica EM UC7 Ultramicrotome (Leica Microsystem) attached with microscope using sharp razor blade and trapezium shape was obtained in the end. Trimmed Epoxy block was attached with specimen holder in the segment arc of ultramicrotome and tightened. The angle was adjusted to 0° angle. Under the specimen, glass knife was inserted in the knife block and knife angle was adjusted to 45° with reference to epoxy block. Before rotation, clearance angle and knife holder angle was set accordingly and manually adjusted towards the sample. Viewing angle was adjusted for ergonomic posture and knife centre as well as orientation was adjusted to approach the optimum accuracy. After focusing the knife edge, backlight was turned and by visualizing the "light-gap", the knife alignment and distance was adjusted. Cutting window was set by moving the sample above and below the knife followed by switching on the top light and plastic trough (attached with glass knife), which was filled with double distilled water. Before proceeding to specimen sectioning, water level was adjusted until it became silvery. Feed was set at 80 nm and speed to 8 mm/sec, once the specimen section started coming in the water boat, speed was reduced to 3-4 mm/sec. After obtaining the ribbon, they were adjusted to place under circular ribbon, ribbon size was selected and carefully picked with loop. Ribbon was placed on clean glass slide with a drop of water. Later water was drained and sections were stained with methylene blue (0.1% in water). The stained tissue sections were photographed using Leica stereomicroscope.

2.7 Differential interference contrast microscopy

The Cry toxin exposed larval midgut transverse sections were screened under Carl Zeiss LSM 880 confocal microscope for better topographical visualization. DIC images were acquired with higher contrast gradient. Unstained midgut tissue section was captured and documented using attached high resolution camera. Topologically resolved micrographs were visualized for cellular damage, cytoskeletal changes and brush border formation.

2.8 Cytoskeleton staining

The active involvement of cytoskeleton during midgut damage and repair was tracked using α-actin and β-tubulin labelling. Paraffin embedded section was deparaffinised using xylene followed by rehydration using alcohol series gradient. For immunocytochemistry tissue slide was rinsed twice with phosphate buffer saline (pH 7.4) for 10 min. Tissue blocking was done using 5% BSA dissolved in PBST (0.1% Tween 20). After blocking, slide was over flowed with primary antibody of either α-actin or β-tubulin (1:500, dissolved in 2% BSA) and kept for 12-14 h at 4°C. Slide was re-washed using PBST solution and antibody detection was carried out using anti-mouse IgG secondary antibody (tagged either with Alexa Flour 555 or with Alexa Flour 633). Visualization of stained slide was carried out using confocal microscope at specific wavelength.

3. Results

3.1 Toxicity and selection of sublethal dosage

The larval feeding bioassay was carried out using neonates and compared with DOR Bt-4, DOR Bt-5 and Kurstaki HD1 formulation (Table 1). For neonates the calculated LC_{50} obtained was 4.01 µg/cm^2, which matched with the previously reported one (Chauhan et al., 2017). DOR1 showed high insecticidal activity and it lacked exotoxin activity. The higher toxicity of this strain is known to be associated with the presence of multiple Cry toxins (Vimala Devi et al., 2006).

Local toxins	Feeding bioassay LC_{50} (µg/cm^2 Leaf surface)	Exotoxins activity	Reference
DOR *Bt-1*	4.01	NO	Chauhan et al., 2017
DOR *Bt-4*	33.40	YES	Budatha et al., 2007
DOR *Bt-5*	4.90	YES	Ningshen et al., 2013
Kurstaki HD1	50.09	NO	Monsanto

Table 1. Insecticidal activity of local Bt strain against Castor semilooper larvae. For the above experiment neonate larvae were used.

Histological and other experiments were carried out using 3rd instar larvae therefore feeding bioassay was performed using the samee. The result obtained showed that 2.50 µg/cm^2, DOR *Bt*-1 formulation feeding lead to 2-5% mortality and around 80% pupal-adult emergence (Table 2).

DOR Bt-1 formulation dosage (µg/cm2)	Percentage of larval mortality (3rd instar)	Percentage of pupal-adult emergence
Nil (control)	1-2 %	95-98%
15 µg	40-46%	10%
10 µg	20-24%	25-28%
5 µg	4-6%	50-55%
2.5 µg	2-5%	80%

Table 2. Evaluation of insecticidal activity by DOR Bt-1 formulation using the 3rd instar larvae of *A. janata.*

3.2 Feeding behaviour and effect of sublethal Cry toxin exposure

Differential feeding behaviour was observed at different dosages (Table 2) of toxin exposure. At higher dosages (15-10 µg/cm^2) of Cry toxin application 3rd instar larvae stopped feeding, however at lower dosages (5-2.5 µg/cm^2) larvae kept feeding on toxin coated leaves (Fig. 2)

Fig. 2. Differential feeding behaviour was seen upon Bt toxin exposure. Please note that in higher dosage coated leaves insect stops feeding.

Upon sublethal (2.5 µg/cm^2) Cry toxin exposure, retarded larval growth and defective development was observed (Fig. 3a). Further, this was associated with larval mortality. Morphological changes were observed when toxin exposed larvae were dissected for pathological analysis. Cry toxin exposed larval gut was shrunken when compared with control

larvae and the fat body volume was reduced. The Malpighian tubules appeared opaque and thinner and the salivary glands were also fairly thin in appearance. (Fig. 3b).

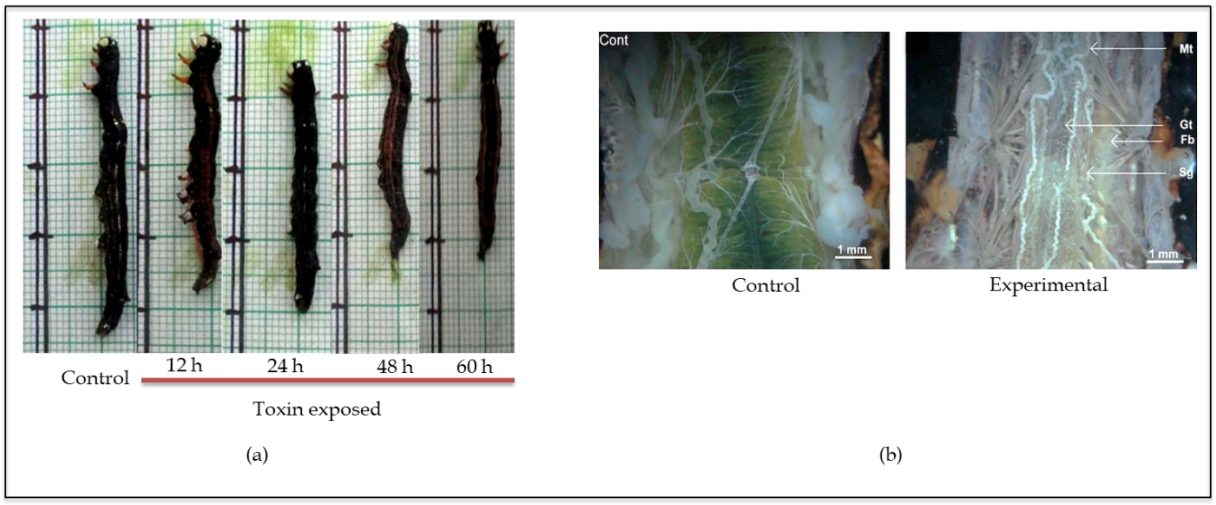

Fig. 3. Morphological alterations seen in larval tissue upon Cry toxin exposure. a) Comparison in size of larval body length when 3rd instar larvae was exposed to sublethal dosages of toxin. b) Internal larval tissue after dissection in control and Cry toxin exposed larvae, please note the changes seen in various tissue. Scale bar, 1 mm.

3.3 Cry toxin induced histological alterations in midgut epithelium

After morphological changes, cellular alterations were analysed using histological approach. To analyse the damage associated with sublethal Cry toxin feeding, 4 micron thick transverse tissue sections were stained with methylene blue, from the midgut tissue obtained from different time points of toxin exposures (24, 36, 48, 60 and 72 h) and the results are presented in figure 4. The following changes were observed in midgut epithelium; (a) during early toxin exposure time point's significant damage was seen in epithelial cells and their brush border which was associated with swelling of cells, (b) the cells show condensed nucleus, large number of vacuoles associated with low cytoplasmic content, (c) it was interesting to note that the damage and repair of the brush border at apical end towards the luminal side was a fairly dynamic process, during continuous sublethal toxin exposure. While analysis of sections, we observed that the relatively large number of small size cells were intact even during the maximum damage seen at 24 h toxin exposure (Fig. 5), suggesting the possibility of the

presence of regenerative/putative midgut stem cell. This was confirmed by identifying the active and dividing cells towards the basal side of the midgut epithelium.

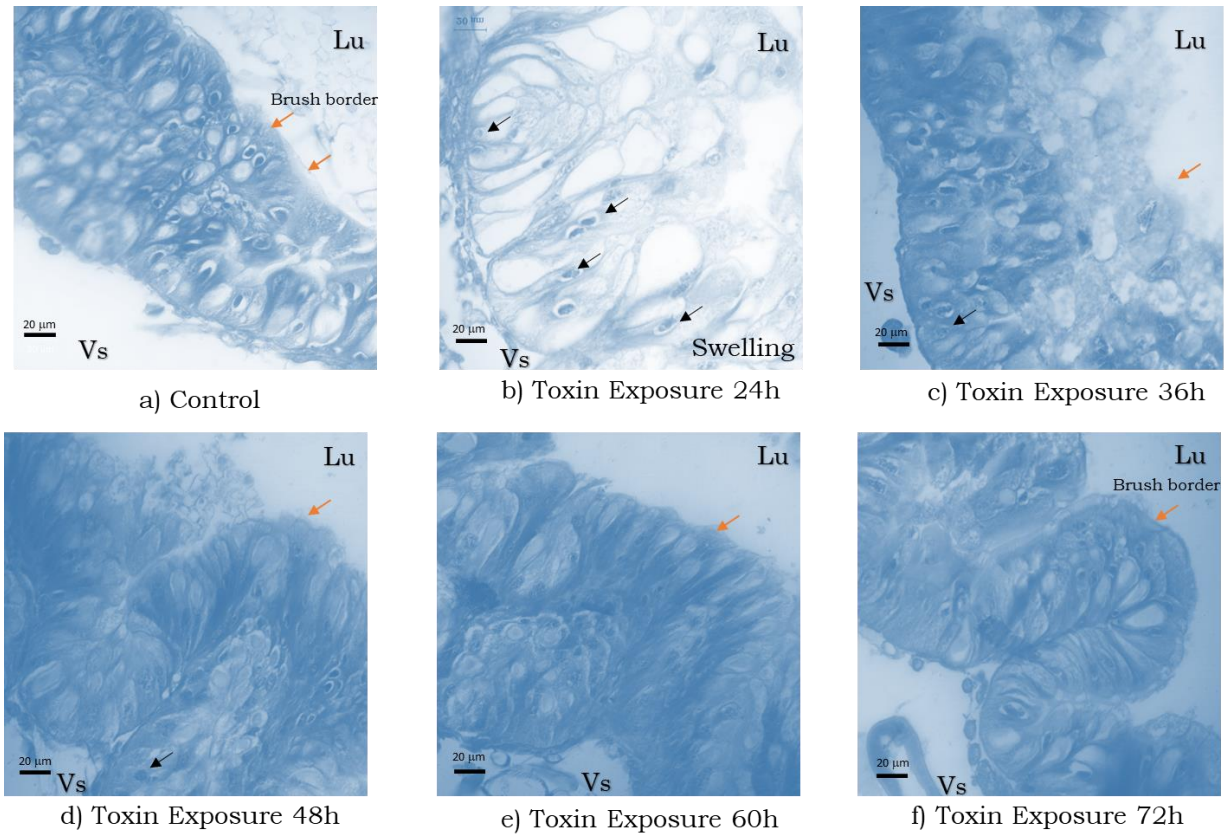

Fig. 4 Damage and repair of midgut epithelium upon Cry toxin exposure. Maximum damage was observed during early toxin exposure (24 h), followed by recovery till 72 h. At 24 h, 36 h and 48 h, the damage or absence of brush border was observed, which was regenerated and repaired at 60 h and 72 h even after continuous sublethal toxin exposure (orange arrow, →). Interestingly, midgut stem cell was clearly visible at 24 h time point (black arrow, →). Scale bar, 20 µm.

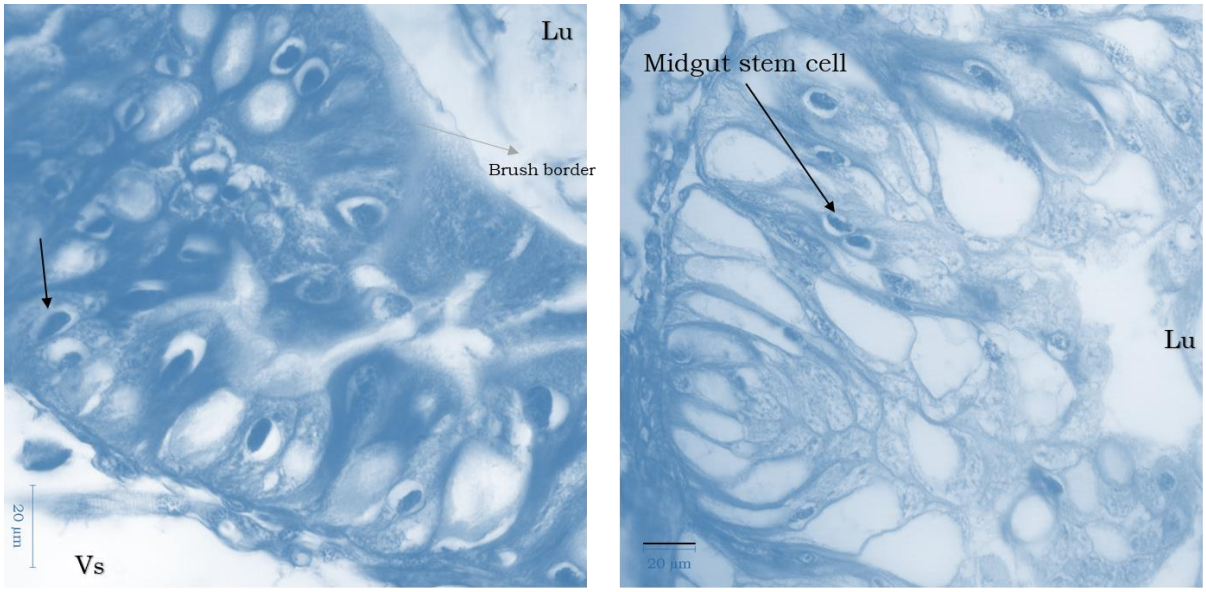

a) Control b) Toxin Exposure 24h

Fig. 5 Midgut transverse section of control larvae represents all cell types with continuous brush border at apical end, whereas 24 h toxin exposed midgut section showed alteration in cellular structure, damage of brush border along with cellular swelling. However, intact midgut stem cells were still present (black arrow, →). Scale bar, 20 µm.

3.4 Identification of various cell types in midgut epithelium

Although, midgut is an important part in lepidopteran larvae, to the best of our knowledge as well as literature survey did not show the cellular map of any lepidopteran species. Hence, detailed analysis using semithin section was carried out. Epoxy embedded midgut tissue was cut in 80 nm thin transverse sections and stained with methylene blue. Midgut epithelium showed the presence of columnar cell, entero-endocrine cell; which are primarily responsible for absorption and secretion (Fig. 6). Midgut of *A. janata* larvae showed large number of Goblet cells (Fig. 6) which are known to be responsible for potassium ion secretion. These cells could be identified easily because of large central cavity. The overall growth, repair and regeneration of midgut is known to be associated with midgut stem cell. The midgut sections of *A. janata* revealed the presence of a large number of compact, actively dividing cells primarily towards the basal border of the epithelium, which possess a fairly condensed chromatin (Fig. 6).

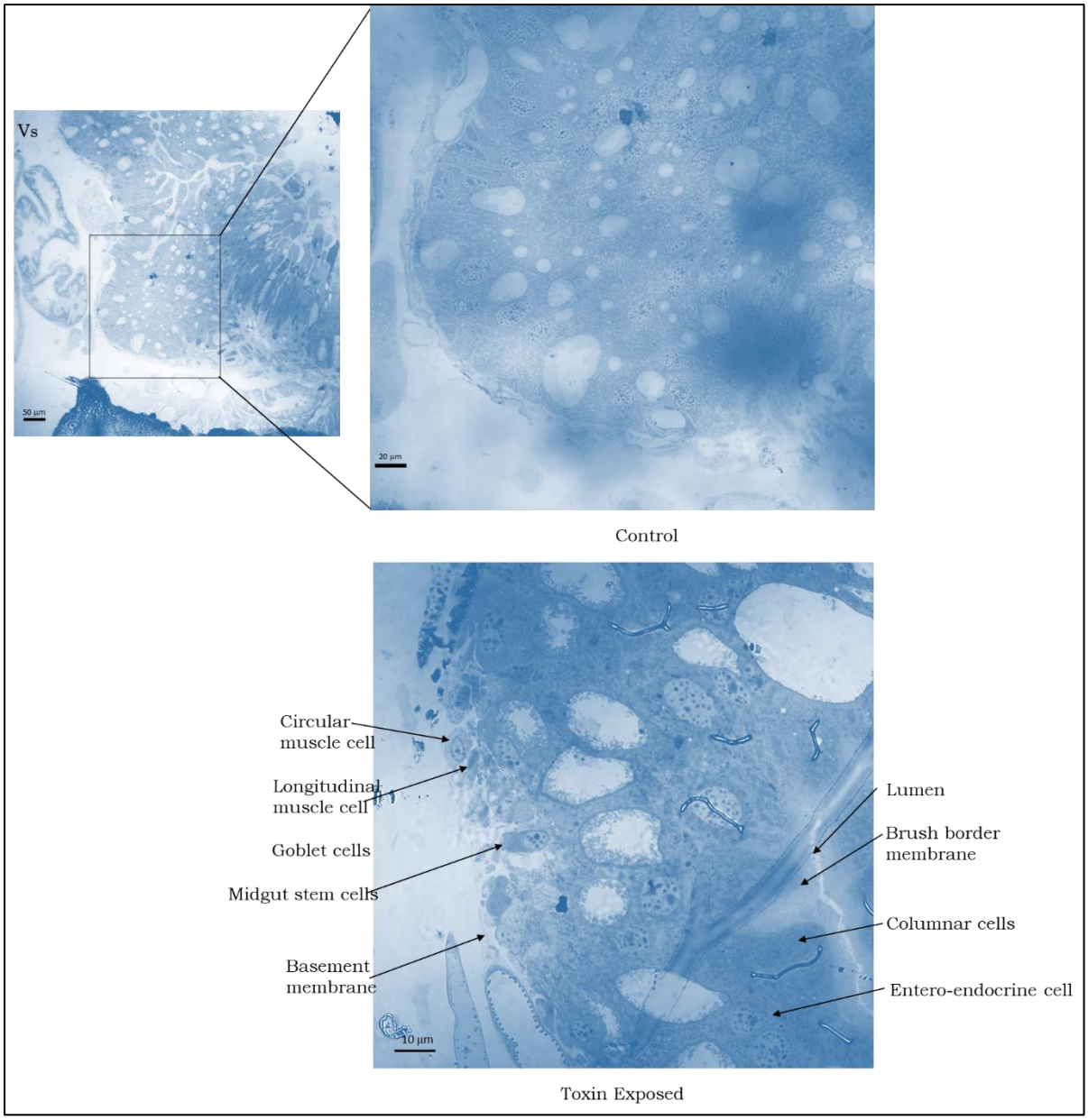

Fig. 6 Micrograph showing details of the midgut epithelium from control and toxin exposed larvae. Please note the presence of various types of cells and their specific localization in the epithelium. Scale bar, 10 µm, 20 µm, 50 µm.

3.5 Topographical analysis of midgut epithelium

The larvae were fed with Cry toxin coated leaves and midgut tissue was isolated and processed for detailed structural analysis to monitor the topographical changes at different time points of exposure and this was observed by differential interference contrast microscopy. Intercellular structural variation observed during 36-48 h of toxin exposure (Fig.7), clearly

revealed extensive damage of epithelium primarily towards the luminal side of the gut epithelium. It is interesting to note that the brush border, which underwent extensive damage during initial toxin exposure of 24-48 h (Fig. 7 b and c) got regenerated and distinct microvillar border once again developed with longer exposure times of 60-72 h (Fig.7 e and f). This clearly suggested a progressive repair of midgut epithelium towards the luminal side even during the continuous Cry toxin exposure.

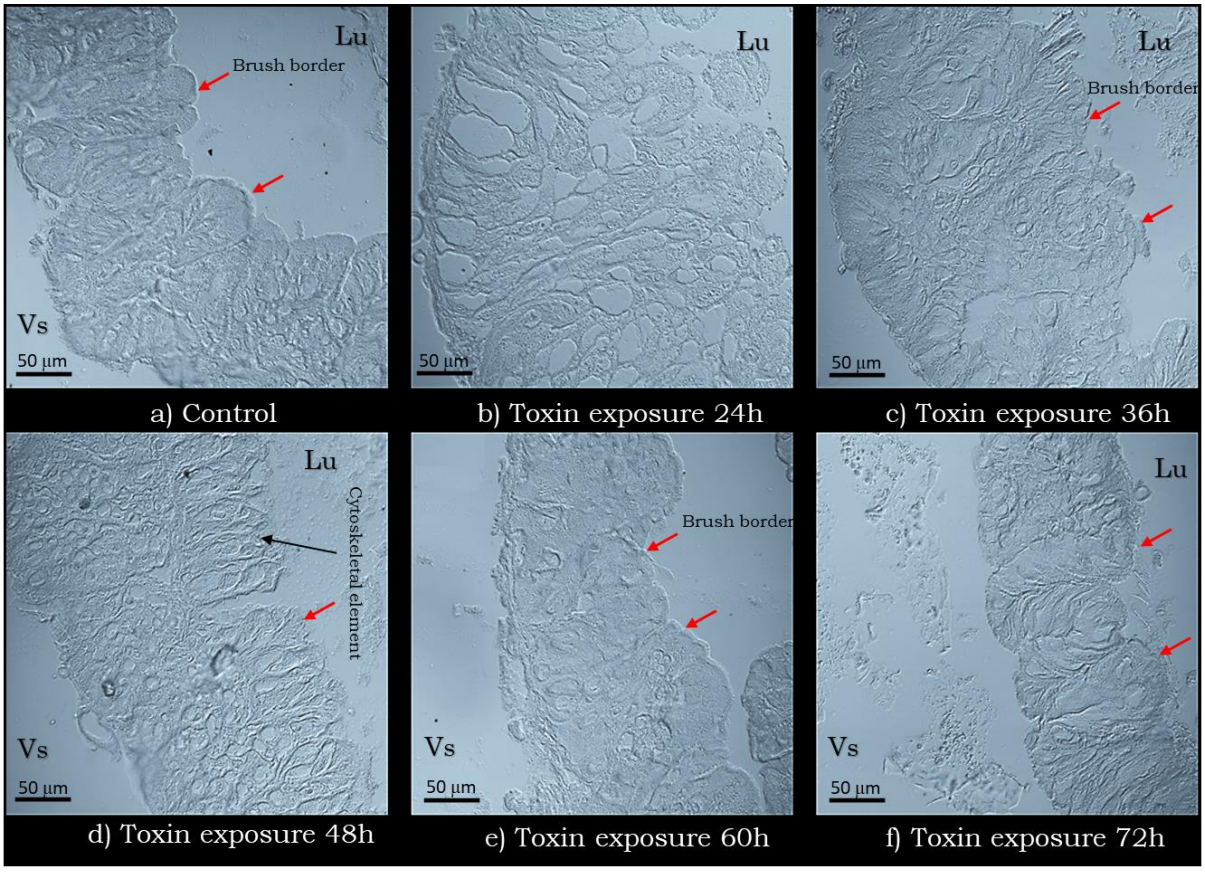

Fig. 7 Micrograph obtained using Differential Interference Contrast Imaging Microscopy from Cry toxin fed larval midgut samples at different time points (24-72 h). Stem cell migration, differentiation and formation of brush border was clearly visible in differential interference topographical images. Please note the damaged microvillar border (red arrow, →) at early sublethal Cry toxin exposure (24-48 h) which got repaired during 60-72 h. Topographical visualisation of cytoskeleton elements was observed in 36-48 h time point micrograph (black arrow, →). Scale bar, 50 µm.

3.6 Role of cytoskeletal elements in cell migration during midgut repair

Topographical visualisation of cytoskeletal elements using Differential Interference Contrast imaging revealed the involvement of these elements in midgut cellular regeneration. A detailed immuno-localization analysis of midgut epithelium using primary antibody against mouse β-tubulin protein was carried out, which was detected using Alexa Flour 633 tagged secondary anti-mouse antibody. It revealed β-tubulin distribution at different time points of Cry toxin exposure (Fig. 8). Similarly Alexa Flour 488 tagged secondary anti-mouse was employed to visualize for α-actin distribution in midgut epithelium (Fig. 9). Results obtained clearly show that tubulin played an important role during the regeneration of midgut epithelium. This is clearly visualized in figure 8, where tubulin got polymerized and formed microtubules which were present in form of stack during 36-60 h Cry toxin exposure (Fig. 8 c and d). The intensity of staining was fairly reduced at 72 h where the epithelium already regenerated (Fig 8 e and f). Although, active cross reactivity persisted in the epithelium, it was more dispersed.

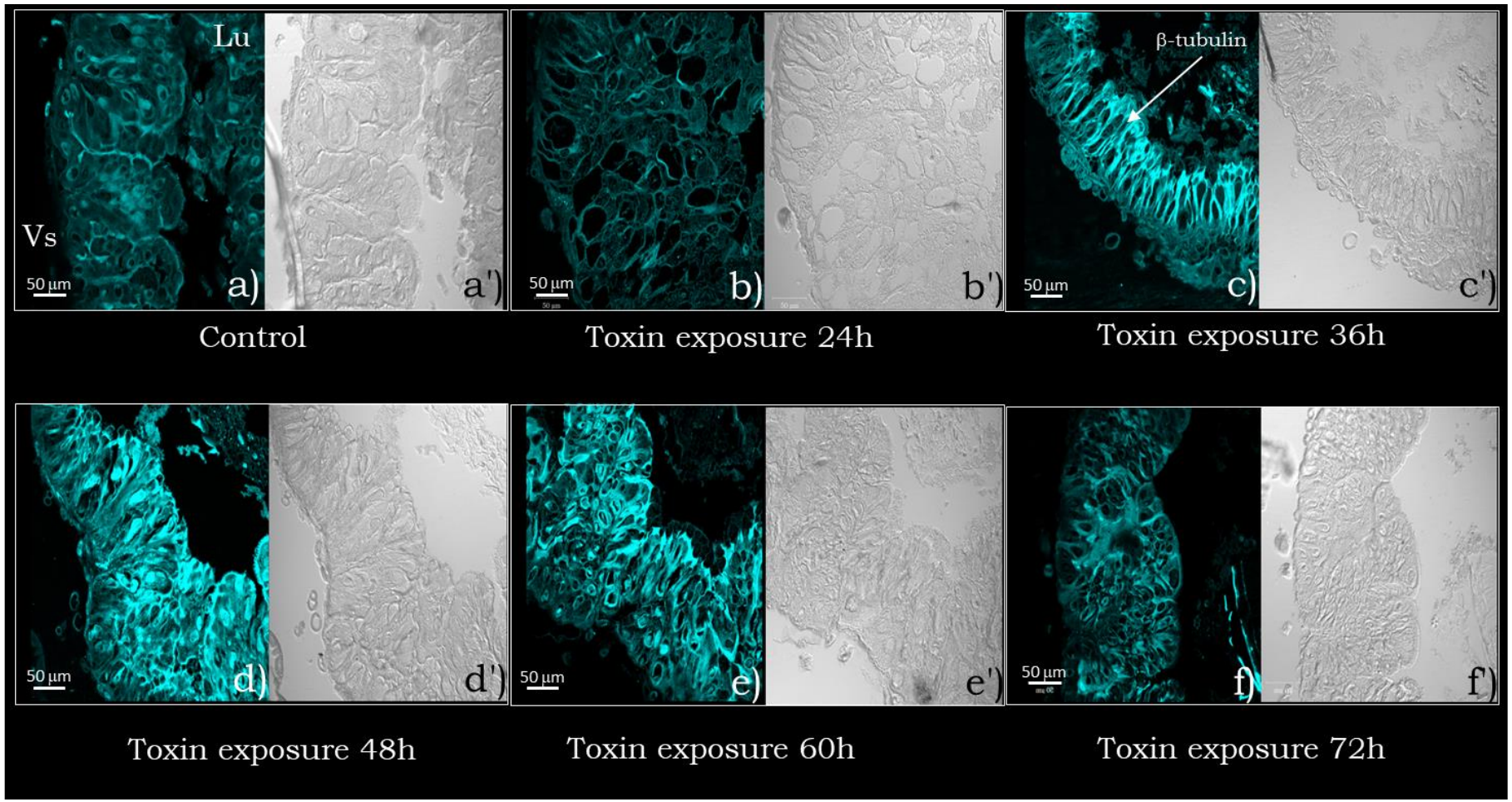

Fig. 8 Immunofluorescent staining of β-tubulin at different time points of toxin exposure. β-tubulin localization in the midgut epithelium was carried out using Alexa Flour 633 tagged anti- mouse IgG secondary antibody against primary mouse antibody. Fluorescent blue green staining indicates the presence of β-tubulin. Maximum labelled β-tubulin was observed at 36 h and 48 h of toxin exposure. (a) control, b) toxin exposure 24h, c) toxin exposure 36h, d) toxin exposure 48h, e) toxin exposure 60h, f) toxin exposure 72h). Comparative Differential Interference Contrast micrographs (a' to b'). Scale bar, 50 µm.

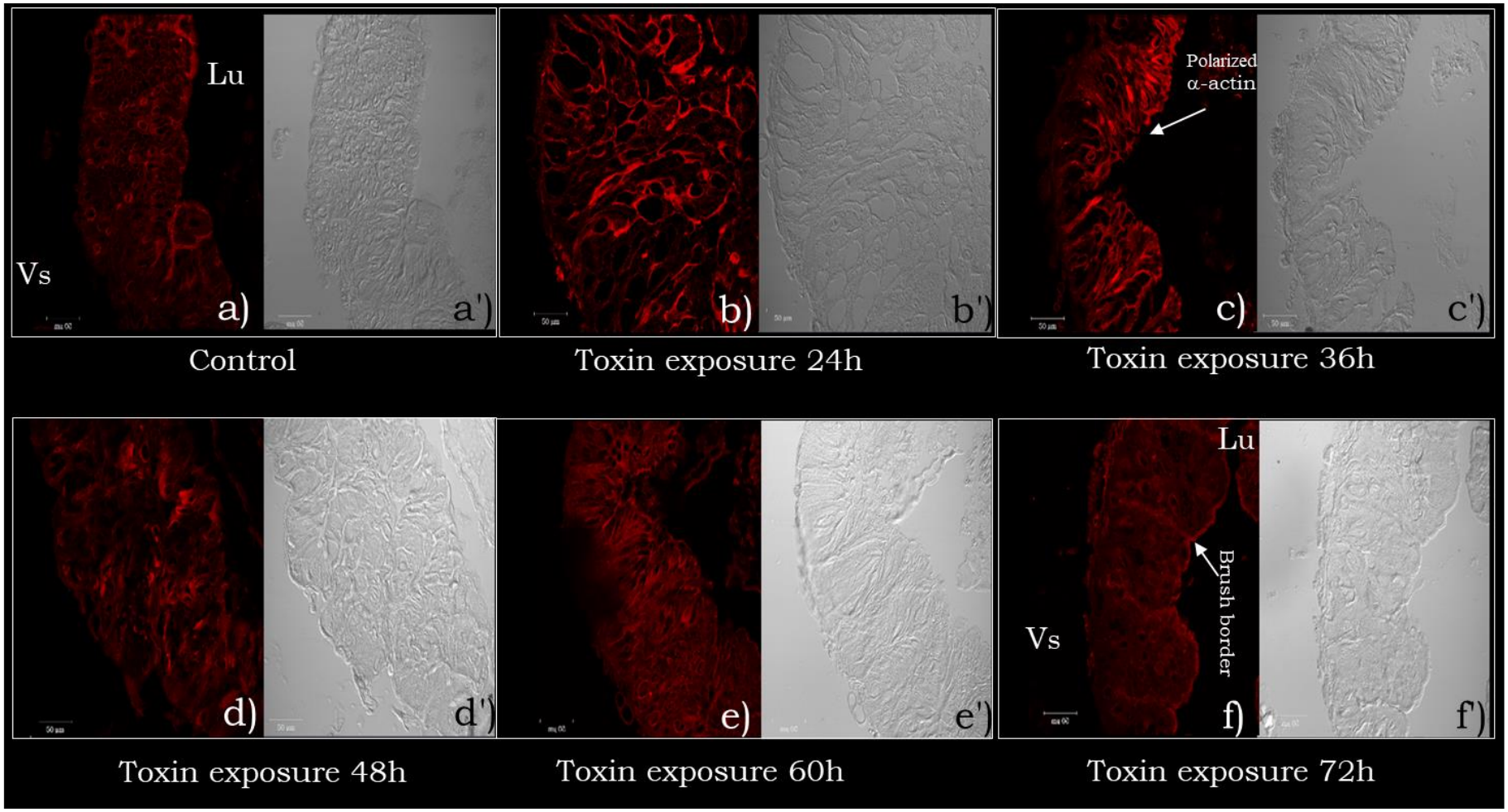

Fig. 9 Immunofluorescent staining of α-actin during different time point of toxin exposure. α-actin localization in midgut epithelium was done using Alexa Flour 633 tagged anti- mouse IgG secondary antibody against primary α- actin antibody. Fluorescent red staining indicates the presence of polymerized α-actin. Higher level of polymerized α-actin was observed at 24 h to 36 h of toxin exposure. Brush border of midgut from control as well as toxin exposed (72 h) showed higher presence fluorescent staining which indicated the presence of abundant polymerized α-actin at brush border. Comparative Differential Interference Contrast micrographs (a' to b'). Scale bar, 50 µm.

4. Discussion

The work presented in this chapter clearly demonstrates the cellular changes after sublethal dosage of Cry toxin exposure. Effect of Cry toxin on midgut epithelium of *A. janata* larvae was assessed at different time points of exposure. As mentioned in the earlier section of this chapter, multiple Cry toxin based DOR Bt-1 formulation was used for this analysis and was formulated by the Indian institute of Oilseeds Research, Hyderabad and released as Knock WP in 2006 for the management of *A. janata* in the castor fields of Telangana/ Andhra Pradesh. Reddy et al., (2012) described the presence of *cry1Aa*, *cry1Ab*, *cry1Ac*, *cry2Aa* and *cry2Ab* genes in this formulation and demonstrated high toxicity against lepidopteran and dipteran larvae. However, there are many evidences which suggest that, foliar spray of Bt toxin based formulation (proteinaceous in nature) on leaves leads to dis-similar amount of toxins on various parts of plants. Moreover, in canopy plants the leaves in upper whorl gets exposed to higher concentrations of spray from the one in the lower whorl. In addition, the reasons for afore mentioned toxicity loss could be degradation due to ultraviolet light, rain wash-off, heat dryness, soil chemistry/properties and environment at temperature which once again varies from upper to lower parts of the canopy plants and castor belongs to the same group (Leong et al., 1980; Beckwith et al., 1987; Van Frankenhuyzen and Nystrom 1989). Hence, the possibility of sublethal toxin exposure to field pest including lepidopteran insects is fairly common. Hence in the present study, we tried to replicate the field possibilities of sublethal toxin exposure for shorter and longer periods. Vimala Devi et al., (2006) reported 247.52 µg/ml as lethal dosage for 3rd instar old, *A. janata* larvae. In the present study 2.5 µg/cm^2 dosage was used for coating castor leaf surface. The toxicity of DOR Bt-1 formulation was reassessed and found to be same as previously obtained by other workers of our laboratory. This further signifies the stability of Cry toxins in the DOR Bt-1 formulation even after longer storage period which was primarily at 6-8^{o}C.

For the effective pest management of lepidopteran larvae, Bt based formulations are sprayed in the field when 2nd and 3rd instar larvae are observed. The results obtained from the present study clearly demonstrated retarded larval growth and defective development which was associated with larval mortality. It was interesting to note that several morphological changes occur in larval tissues upon sublethal toxin exposure. The results obtained in the present study substantiate various earlier reports from other lepidopteran pests where Cry toxin exposure was associated with reduced body weight, low digestive activities and retarded larval growth (Eizaguirre et al., 2005; Hussein et al., 2006; Lomate et al., 2013; Palma et al., 2014; Chauhan et al., 2017; Guo et al., 2019).

The larval midgut tissue of castor semilooper was further analysed after sublethal toxin exposure. For that, 3rd instar larvae were exposed to DOR Bt-1 sublethal toxin coated leaves in a closed aerated plastic chamber and allowed to feed by their choice. After 24 h, 36 h, 48 h, 60 h and 72 h time frame larvae were collected and the midgut tissue was dissected and processed for histological analysis. Notable feature in the present study was extensive damage of midgut epithelium during early exposure to even sublethal dosages of toxin at 24 h time point. However, it was interesting to note that the damaged epithelium started regenerating and got repaired after longer duration of toxin exposure (60-70 h). Few other reports also demonstrated similar phenomena in other lepidopteran species, where repair of injured midgut epithelium lead to recovery of larvae during sublethal toxin exposure (Spies and Spence 1985; Loeb et al., 2001). However, high dosages of Bt toxin caused persistent and irreparable damage followed by larval mortality (Tabashnik et al., 2013). In the current study, Cry toxin induced histological alterations observed in transverse section of midgut epithelium revealed significant changes in gut epithelium which included damage of cellular organisation of midgut epithelium associated with swelling of epithelial cells, condensation of nucleus and the appearance of a large number of vacuoles which was associated with low cytoplasmic content. The damaged epithelium also

revealed destruction of brush borders at initial time points (24 h-36 h) which slowly got repaired upon continuous sublethal toxin exposure (48 h-72 h). These findings clearly suggest that at initial toxin exposure, the larvae feed and later they reduce feeding on toxin coated leaves, during which the damaged epithelium, starts getting repaired and gets regenerated.

Similar to many other tissue damage, the midgut epithelium repair is also associated with regenerative cells. This kind of recovery/repair is known to be supported by the presence of regenerative/proliferative cells present in a given tissue; *Plasmodium falciparum* ookinete invasion in *Anopheles stephensi* midgut was followed by proliferative regeneration of epithelium (Baton and Ranford-Cartwright, 2007). In *Aedes albopictus* damage, induced cell regeneration was seen (Janeh et al., 2017), while in *Culex quinquefasciatus* also the midgut recovered by cell proliferation after damage (Okuda et al., 2007). *Drosophila*, a widely studied model for damaged based tissue regeneration, clearly revealed the presence of regenerative cells (Lucchetta and Ohlstein, 2012, Tettamanti et al., 2019). Coleopteran beetle *Epilachna cf nylanderi* showed recovery of midgut epithelium using cellular regeneration (Rost-Roszkowska et al., 2010). During postembryonic development degeneration and regeneration were shown to occur together in the midgut of *Podisus nigrispinus* (das Dores Teixeira et al., 2013). Regenerative cells were the only population of cell which was reported to be capable of division, differentiation and supported the damaged tissue in all the above lepidopteran species. Epithelial cell regeneration was also demonstrated in lepidopteran larvae which replaced the damaged epithelium (Martinez-Ramirez et al., 1999; Castagnola and Jurat-Fuentes, 2009, 2016). Present semithin section analysis clearly confirms the presence of regenerative/ putative midgut stem cell in *A. janata*, which resides towards the basal side of midgut epithelium. Cell mapping analysis using ultrathin sections clearly showed the presence of lumen followed by brush border membrane, columnar cells, entero-endocrine cells, Goblet cells, midgut stem cells, basement membrane supported externally by longitudinal and circular muscle cells.

Midgut stem cells were found to be located at the basal part of epithelium responsible for repair/regeneration of midgut epithelium.

Cell migration is an important phenomenon in organ/ tissue formation during embryonic as well as postembryonic development of lepidopteran insects. As discussed, midgut stem cells reside at the basal side of epithelium, but during repair process these cells undergo active division and differentiate into various cell types as well as give rise to regenerated epithelium with a defined brush border at the luminal side of the midgut. This definitely generates an interesting question that how these undifferentiated cells replace damaged differentiated cells, localized far away from the regenerative nidi.

This is only possible if these cells (midgut stem cells) divide, migrate and undergo differentiation in the required location. Migration is a well-known phenomenon associated with the involvement of cytoskeletal elements. Polarization of cytoskeleton elements is known to initiate the movement of cell where cross-talk between actin and tubulin network is well known to drive the mechanistic movement. During cell migration, it has been reported that cytoskeleton elements bind to the substrate adhesion sites followed by movement providing the driving force to the actin cytoskeleton and microtubule coordinated rear retraction (Wehrle-Haller and Imhof, 2003), followed by development of cytoskeletal niche around differentiated cell (Ambriz et al., 2018). Motility in cell was initiated by an actin-dependent protrusion of the cell towards leading edge, which provided cellular architecture (Mattila et al., 2008). Similarly microtubules get polarized to build α- and β-tubulin heterodimers which helped in protrusion followed by movement of the cell to a given direction and location (Desai and Mitchison, 1997).

To understand the involvement of actin and tubulin in midgut epithelium regeneration of *A. janata* larvae, α-actin and β-tubulin were localized in the transverse section of midgut

epithelium. Immunohistochemical analysis proved that at 36 h toxin exposure, most of the epithelial cell got labelled with β-tubulin primary antibody followed by 48 h. The intensity of the fluorescence was reduced gradually at 60 h to 72 h time points. Interestingly, these results corroborated well with differential interface contrast imaging where maximum cytoskeleton movement or protrusion was visualized during 36 h to 48 h time points. These time points are crucial for larval survival where at early toxin exposure (24 h) midgut epithelium showed maximum overall damage which was gradually reduced as well as repaired during 36 h to 72 h time points. However, cytoskeleton labelling of α-actin was comparatively lower than β-tubulin, except those time points when brush border was completely repaired (72 h). The results obtained in the present study suggested that overexpression of β-tubulin plays an important role in cell migration while α-actin expression primarily support brush border filament formation. Further, these cytoskeletal elements facilitated midgut stem cell migration, differentiation and formation of brush border towards lumen side of the epithelium.

Findings from this part of study clearly suggested that during sublethal Cry toxin (DOR Bt-1 formulation) exposure, there is an early damage of gut epithelial cells including brush border associated with deleterious effects of Cry toxin. Midgut epithelium underwent significant amount of swelling and midgut cells showed condensed nuclei and a large number of vacuoles in the cells related with low cytoplasmic content. This confirmed that Cry toxin induced histological alterations in midgut epithelium. Cell mapping and histological analysis proved the presence of midgut proliferative cells even during maximum toxin damage upon sublethal exposure. With longer duration of toxin exposure- division, migration and differentiation of midgut proliferative cells in the epithelium promoted and facilitated the regeneration of midgut which supported larval survival upon sublethal Cry toxin exposure.

Chapter 2

De novo transcriptome analysis and gene expression profiling of larval midgut.

1. Introduction

In earlier chapter, the changes during sublethal Cry toxin (DOR Bt-1 formulation) exposure have been recorded. The findings suggest that early exposure of Cry toxin is associated with gut epithelial cell damage followed by stem cell division, migration of newly generated cells and their migration and differentiation for the recovery/repair of epithelium. This promotes and facilitates the survival of larvae to sublethal dose of Cry toxin exposure. Further, whenever the repair of epithelium takes place, it involves the regulation of various factor which includes transcriptional factor as well as regulatory molecules. Detailed characterisation of RNA profile would facilitate the understanding of larval biology during sublethal Cry toxin exposure. RNA sequencing based transcriptome analysis would further help to understand/characterize expression profile of various genes associated with this distinct biological event. RNA-Seq analyses provides a wide range of data for temporal patterns of mRNA expression at a given stage in specific tissue. It is especially useful for generating data for non-model organisms such as *Achaea janata* (castor semilooper), which is of great agricultural importance. Further, the literature survey revealed a total lack of genome or transcriptome sequence information. Hence, RNA sequencing was employed to obtain the transcriptomic data for *A. janata* larvae which causes severe loss of castor plantation in state of Telanagana and other Indian states too. In earlier studies, various platform was used for analysing mRNA expression data for other insect pests and the information obtained was proved as a useful resource to gain insight in various properties of susceptible and resistant pest larva (Li et al., 2013; Yin et al., 2014; Perera et al., 2015; Zhou et al., 2018; Pavlidi et al., 2018). The role of RNA especially mRNA is well recognised in molecular biology as genomics and proteomics intermediary and has become a standard part of research toolkit. Various RNA-Seq data type presently used includes mRNA profiling, small RNA profiling, miRNA-Seq,

ChIP-Seq, HiC-Seq, methyl-Seq, bisulfite-Seq etc. In the current study, mRNA profiling was employed to obtain the required information.

Before discussing the type of sequencing platform, we would like to mention that in the present study three different experiments were performed, at three time intervals with two different NGS platforms. In the initial phase of study (March 2015), *de novo* transcriptome analysis was carried out using Illumina Next Seq 500 platform with only two samples of control (larvae without toxin exposure) and treated (larvae exposed to 24 h of sublethal toxin exposure). As we found that the data has serious experiment shortenings, we expanded the study in December 2016 and complete analysis was carried out. Large scale microarray analysis was carried out using the Agilent's Quick-Amp labelling Kit with microarray slides: Castor semilooper_GXP_8X60K AMADID: 84278. This microarray was performed using the transcript information obtained from afore mentioned NGS data of control and treated samples. This included control, 12 h, 24 h, 36 h, 48 h, and 60 h time points of Cry toxin exposure. However, once again detailed microarray analysis revealed few more loopholes such as microarray gene expression data was based primarily on transcript information obtained from control and 24 h toxin exposed larvae. Hence transcripts expression which were specific for various other time points such as 36 h, 48 h and 60 h were completely missing. Keeping this lacuna again in December 2018, we carried out an additional sequencing analysis using control, starved and toxin exposed larva midgut samples of different time points of Cry toxin exposure using Illumina HiSeq 2500 system. Further, during this duration laboratory based toxin tolerant larval population were generated by feeding the larvae on toxin coated leaves for several generations. Finally, transcripts generated from toxin tolerant population were compared with control, starved and toxin exposed larval samples.

For *A. janata* based damage control, various strategies of pest management are being adopted. Till a decade back, Castor semilooper was highly susceptible to *Bacillus thuringiensis*

based bio pesticides in Andhra Pradesh and Telangana (Vimala Devi and Sudhakar, 2006). However, like other lepidopteran larvae there is always a possibility of generation of Cry toxin resistant population of *A. janata* after continuous application of Bt based crops and Bt based formulation (Tabashnik et al., 2013, 2019; Badran et al., 2016; Melo et al., 2016). Due to long term application of Bt various resistance insect species have emerged which including *Spodoptera frugiperda, Pectinophora gossypiella, Plutella xylostella, Busseola fusca, Diabrotica virgifera, Helicoverpa armigera, Chilo suppressalis, Tribolium castaneum, Ostrinia nubilalis* and *Ostrinia furnacalis* (Sayyed et al., 2004; Storer et al., 2010; Dhurua and Gujar, 2011; Kruger et al., 2011; Zhang et al., 2011; Kliot and Ghanim, 2012; Jakka et al., 2015; Pereira et al., 2015; Xu et al., 2015; Shabbir et al., 2018; Yu et al., 2018). The major reasons reported for the development of resistant behaviour such as alteration in proteolytic cleavage (Candas et al., 2003) and reduction in Cry toxin binding to epithelial receptors (Ferre and Van Rie, 2002; Tabashnik et al., 2013). Apart from defective proteolytic cleavage and altered receptor binding, several other epithelial changes were shown to be responsible for the development of resistance (Zhao et al., 2010; Bretschneider et al., 2016; Carrière et al., 2016; Jurat-Fuentes and Crickmore, 2017).

Recent studies from our laboratory have also recorded several changes at the cellular and molecular level in midgut epithelium of *A. janata* when exposed to Cry toxin sublethal dosages (Ningshen et al., 2017; Chauhan et al., 2017), few of them have already been addressed in Chapter 1. To the best of our knowledge no report has been published mentioning about development of Bt resistance in *A. janata.* Keeping this in view, as the insect is an important local pest of castor we made an attempt to generate laboratory based Cry toxin tolerant larval population. This was done to primarily demonstrate various mechanism which might be responsible for making Bt based biopesticide strategy less or not effective specifically for this lepidopteran pest. In our laboratory, we have also tried to understand the biology of *A. janata*

epithelium during Cry toxication. As *A. janata* is a local pest and non-model insect we needed to generate our own genomics/ transcriptomics or proteomics dataset. Hence, in the present study we employed next generation transcriptome analysis to characterize the gene expression profile of *A. janata* larvae midgut epithelium during Cry toxication. Transcriptome sequencing was one of the well proven strategies which provide useful resources to investigate various characteristics of pest control methods, especially for non-model organisms which are agriculturaly important (Paris et al., 2012; Wolf, 2013; Li et al., 2013; Lei et al., 2014; Perera et al., 2015; Tassone et al., 2016; Song et al., 2016; Yao et al., 2017; Zhou et al., 2018; Pavlidi et al., 2018). Transcriptomic repertoire obtained in the present study would provide a basic platform to understand molecular basis of larval midgut responses during Cry toxin exposure. Further, this transcriptomic profile of larval midgut responses would provide an insight of the mechanisms which slowly evolve during generation wise development and facilitate Cry toxin tolerance in the pest. This is used to obtain the basic information which could be use in designing appropriate long term strategies for the field management of given pest.

In the first transcriptome profiling data obtained using Illumina Next Seq 500 platform, in control and toxin exposed larval midgut sample a total of 34,612 and 41,109 transcripts were identified respectively. The total annotated transcript was 18,836 in control and 21,046 in toxin exposed samples. These genes were further monitored for expression pattern at distinctive time points of toxin exposure using microarray data analysis. mRNA expression data during Cry toxin exposure revealed several upregulated as well as downregulated genes. Validation of afore mentioned data was carried out using qRT-PCR with randomly selected upregulated and downregulated transcripts. In our recent transcriptomic data, we have performed a detailed Sequencing of control, starved and toxin exposed larval midgut samples using Illumina HiSeq 2500 system. In absence of adequate genomic and transcriptomic information available for the pest, this study would help in unravelling the molecular mechanisms of altered physiological

responses of Bt exposed tolerant and susceptible insect strains. Furthermore, this biochemical biological and molecular research information obtained for given pest species, would not only facilitate us to find basic interaction but would provide a robust platform for extensive *in silico* analysis. This could be employed for targeting the biopesticide at appropriate stage of development/ timeframe as well as use them with other controlling agents in the practice of IPM (Integrated pest management). This is useful for the present day demand of chemical pesticide free ecofriendly insect pest controlling approach. In this chapter we report midgut *de novo* transcriptome assembly and clustering of Cry toxin exposed susceptible and tolerant *A. janata* larvae.

Note:

For this chapter commercial raw database (NGS; Illumina Seq 500 & Microarray) was generated by Genotypic Pvt. Ltd., under Genotypic Project No: SO_5975 and SO_4020 and detailed analysis was carried out us in our laboratory using various bioinformatics tools and platform. Later (NGS; Illumina Seq 2500) by Xcelris Labs Limited with project ID: NGS_931 was obtained and further detailed analysis was carried out using appropriate bioinformatics tools.

2. Materials and Methods

2.1 *A. janata* collection and rearing

As discussed in General Materials and Methods, the *A. janata* larvae were collected from the field of IIOR, Hyderabad, India (maintained for castor rearing only). These collection fields were maintained without any exposure to chemical and biological pesticides. To carry out further experimentation, larvae were reared and maintained on fresh castor leaves (cultivated in University of Hyderabad plant culture facility without any chemical or biological pesticides). Field collected fresh eggs were used and sterilized for laboratory breeding. The larvae were maintained at 27 ± 2 ºC, 14:10 h (light:dark) photoperiod with 60-70% RH for three successive generations at the insect culture facility of School of Life Sciences, University of Hyderabad, India and a homogeneous population was obtained.

2.2 Larval sample processing for NGS library preparation

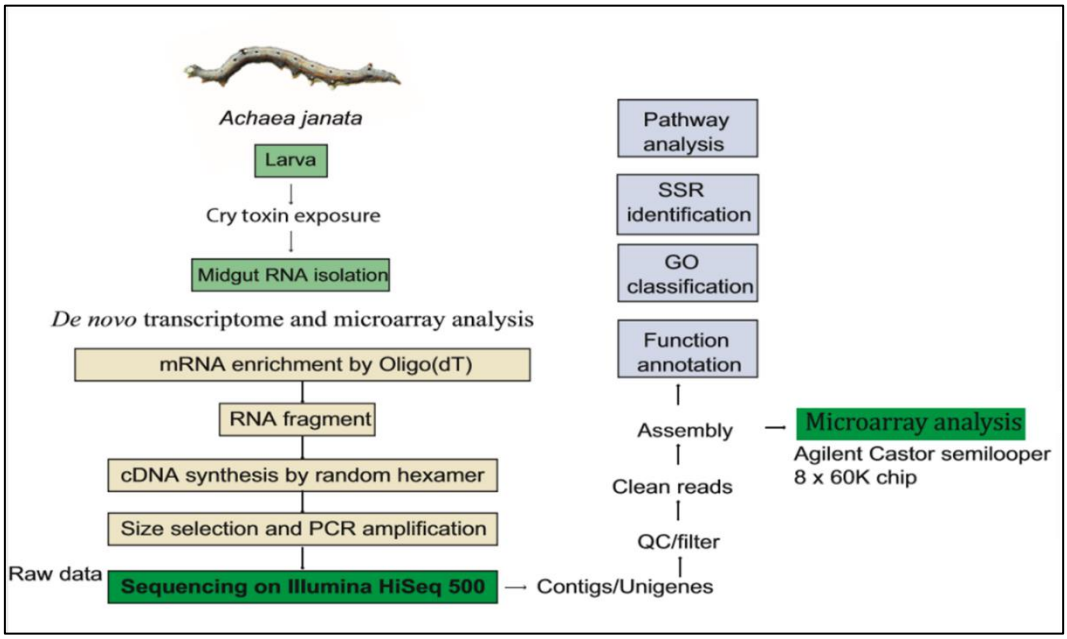

Fig. 1 Flow chart showing summary of *de novo* transcriptome analysis and microarray gene expression profiling of *A. janata* larval midgut.

For the present transcriptome and microarray analysis, 3rd instar larvae of *A. janata* were used. Larvae were fed with DOR Bt-1 toxin coated leaves and it was uniformly done

using a glass spreader. For initial transcriptome sequencing, 2.5 μg/cm^2 toxin was coated on fresh castor leaves and two groups of 30 larvae were kept in closed chamber. They were collected from a homogenous batch of larval population. For toxin treatment, one group of larvae was exposed to Cry toxin coated leaves and in the same experiment another group of larvae was exposed to water coated leaves as control sample (Fig. 1). Fifteen larvae were randomly selected for midgut isolation and subSequently processed for the experiment.

For microarray analysis, a batch of 150 larvae was exposed to Cry toxin and fifteen larvae were collected for tissue isolation after each successive 12 h time frame till 60 h (Fig. 1). Same experiment was repeated and sample was used for RNA isolation for validation, and qRT-PCR analysis was carried out from the isolated RNA sample. Finally, an updated sequence transcriptome was generated using four different groups of *A, janata* larval midgut samples. The sample list includes:

Group (i)	susceptible larvae exposed to medium (water)
Group (ii)	susceptible larvae exposed to 1/10 of LD50 dosage of DOR Bt-1 formulation
Group (iii)	susceptible larvae subjected to starvation
Group (iv)	tolerant larvae exposed to LD50 dosage of DOR Bt-1 formulation (reared for 15 generations)

For all afore mentioned Sequencing, larval midgut was dissected using routine method followed in laboratory (Fig. 2). The larvae were narcotized by placing them on ice flakes followed by the dissection in ice-cold insect Ringer solution (0.5 mM KCl, 0.1 mM $CaCl_2$ and 130 mM NaCl). TRIzol® method (Thermo Fischer Scientific, USA) was used for total RNA isolation. Quantity and purity of isolated RNA was checked using NanoDrop™ 8000 spectrophotometer and sample were only processed if the assessed number was above standards and satisfactory.

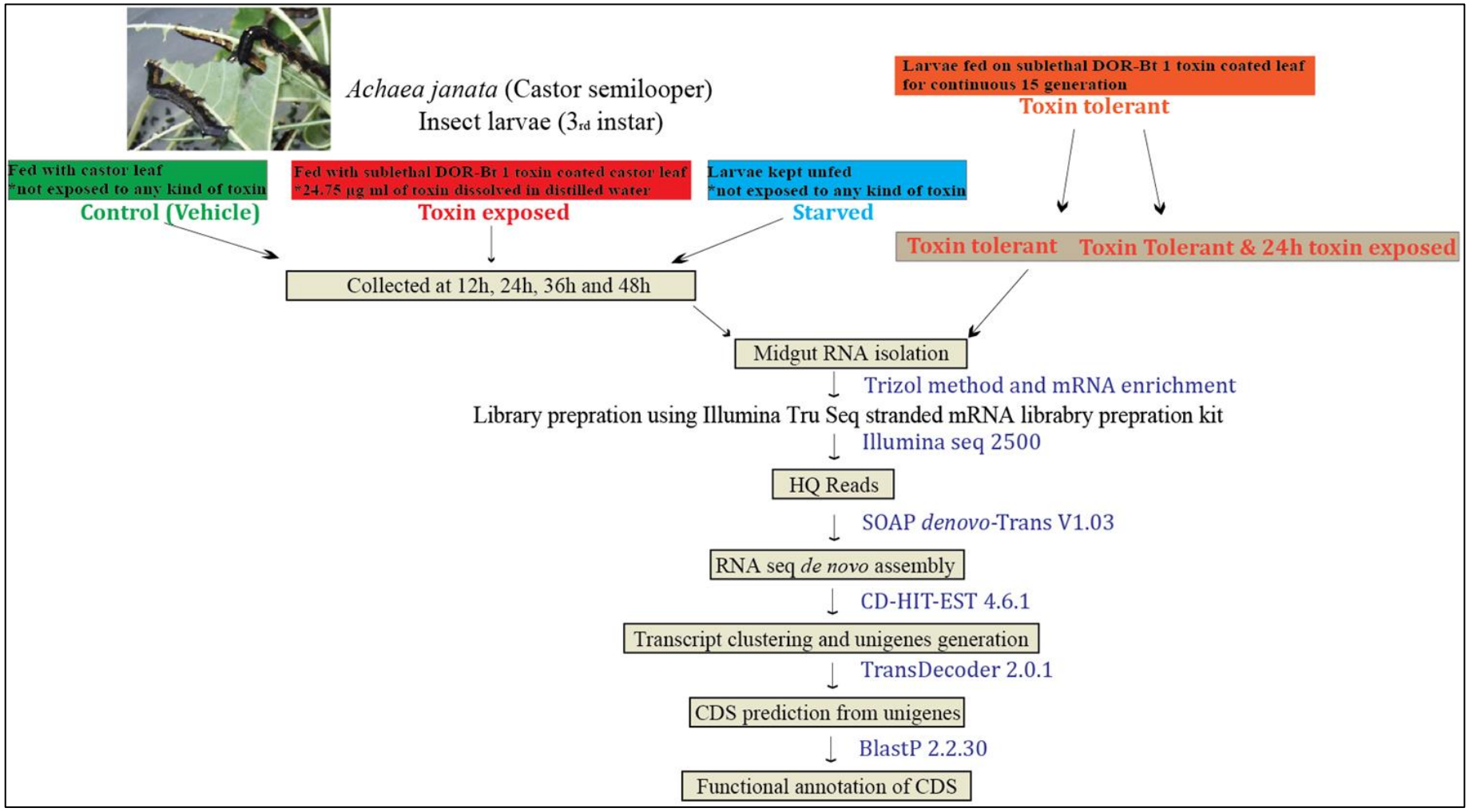

Fig. 2 Flow chart showing the summary of Illumina Seq 2500 sequencing, protocol and detailed assembly as well as gene expression analysis.

2.3 Library preparation and Illumina sequencing

For both the next generation sequencing used in present analysis, Illumina 2 x 150 pair end library was prepared. In pair end library, template can be sequenced in both the forward and reverse directions. During Illumina Seq500 library preparation, Sure Select Strand-Specific RNA Library Prep Kit (Agilent Technologies, USA, Cat #5500-0116, #5190-6410) was used and initial control and toxin exposed midgut libraries were prepared. Enrichment of mRNA was carried out using oligo (dT) magnetic beads and poly $(A)^+$ mRNA was isolated. Using RNA-Seq fragmentation mix purified mRNA was chemically fragmented to 150 bp with a raised temperature of 94ºC for 8 min. Using RNA-Seq First Strand master mix first-strand cDNA was synthesized and Actinomycin D (120 ng/µL) was added into the reaction mixture to maintain specificity. Before processing for the second strand cDNA synthesis and reaction mixture was cleaned up using AMPure XP beads followed by synthesis of second-strand cDNA using RNA-Seq Second Strand mix. Again, AMPure XP beads were used for cleaning up the cDNA followed by end repair using RNA-Seq dA tailing based adapter ligation. Later, the adaptor ligated purified cDNA was enriched and indexed by using 12 cycles of PCR. Final cDNA library was quality checked by DNA High Sensitivity Assay Kit (Agilent Technologies, USA) followed by sequencing using Illumina Next Seq 500, which was commercially done.

In Illumina Seq 2500 library preparation was carried out as suggested in manufactures protocol and paired-end sequencing was generated. Illumina Seq 2500 library preparation was carried out using TruSeq Stranded Total RNA Library Preparation Kit (Illumina Inc. USA, Cat # RS-122-2201). TruSeq Stranded Total RNA Library prep workflow includes: Depletion and fragmentation of RNA (RNA clean XP beads) → Synthesis of first-strand cDNA → Synthesis second-strand cDNA → Adenylation of 3’ ends → Ligatation of RNA adapters (AMPure XP beads©) → Enrichment of DNA fragments (AMPure XP beads©) → Nomalization and pooling libraries.

2.4 Transcriptome assembly and annotation of Illumina Seq libraries

Before assembly in both sequencing, Illumina Seq raw reads were subjected for quality check. In Illumina Seq 500, raw reads were trimmed at 5'- and 3'-ends with in house script followed by quality check using FASTA QC software. In Illumina Seq 500 samples (control and toxin exposed), clean reads were pooled and assembly were done separately for each sample using Grabherr et al., (2011) suggested Trinity software.

Clustering was done using CD-HIT-EST (Cluster Database at High Identity with Tolerance) fast program (http://www.bioinformatics.org/cd-hit). Redundancy was avoided in the final assembly of nucleotide sequence and threshold identity was maintained at 95% in comparing sets (Li and Godzik, 2006). As the pair-end sequence was generated, alignment was carried out using paired end alignment mode of Bowtie2 software (http://bowtie-bio.sourceforge.net/bowtie2) (Langmead and Salzberg, 2012). Annotation was done using BLASTx uniprot and sequence similarity was performed with transcripts of >300 bp length. After obtaining similar sequences, identified protein sequence was annotated with putative function (http://www.uniprot.org/). For comparing the sequence NCBI BLAST [2.2.29] and animal TF database were used for homology search and transcription factor identification (http://www.bioguo.org/AnimalTFDB/). MIcroSAtellite (MISA) Perl script database was used for simple sequence reads (SSRs) identification (http://pgrc.ipk-gatersleben.de/misa/). KEGG Automatic Annotation Server (KAAS) database was used for pathway analysis (http://www.genome.jp/tools/kaas/) (Moriya et al., 2007). For pathway analysis, reference sequence of *Nasonia vitripennis, Apis mellifera, Drosophila melanogaster, Anopheles gambiae, and Acyrthosiphon pisum* were used in KAAS database. Analysis of gene expression was carried done in between control and toxin exposed sample using DESeq software (https://www.huber.embl.de/users/anders/DESeq/) (Anders and Huber, 2010).

In Illumina Seq 2500, 28 samples raw reads were processed and (phred40) was assessed for sequence quality. Trimmomatic (v.0.36) was used for quality assessment followed by removing adaptor sequence and filtered by quality score (ILLUMINACLIP:adapter.fasta:2:30:8 MINLEN:40) (Bolger et al., 2014) followed by trimming at 5'- and 3'-ends with in house script. Trimmed sequence was also quality checked with FASTA QC software. Processed 28 sample raw reads were pooled together and *denovo* assembly was carried out using "SOAP-*denovo*-Trans (v1.03)" assembler (Xie et al., 2014). Assembled transcript was clustered using CD-HIT package (Fu et al., 2014) and redundancy was removed using CD-HIT-EST v4.6.1 with 100% coverage and 90% identity followed by designated non-redundant clustered transcripts as unigenes. Transdecoder with default parameter were used to predict unigene sequences as CDS (coding sequences) and identified CDS were subjected for annotation. NCBI's non-redundant (nr) database "BLASTP algorithm" was used for similarity analysis of predicted CDS. NR, UniProt, KOG and Pfam databases were used and e-value threshold was maintained at $1e^{-5}$.

2.5 Microarray hybridization and analysis

Gene expression analysis was carried out using microarray expression analysis. One colour based microarray gene expression analysis was done with 12 h, 24 h, 36 h, 48 h and 60 h toxin exposed larval midgut sample. Agilent's Quick-Amp labelling Kit was used for cyanine-3 (Cy3) labelling of complementary RNA of control and toxin exposed larvae sample as suggested in manufacturer's protocol. RNeasy mini column purification kit was used for purifying Cy3-labeled cRNA (Qiagen, USA) followed by quality check of labelled cRNA using NanoDrop spectrophotometer. As per manufacturer's instructions, labelled cRNA (specific activity >10 pmol of Cy3) was fragmented at 60°C for 30 min in 1x fragmentation buffer (Agilent©) and 2x blocking agent (Agilent©).

Agilent's hybridization buffer was used for cRNA hybridization to Agilent© customised made Castor semilooper 8 x 60K (AMADID: 84278) chip at 65°C in spinning oven for 17-18 h and washed with Gene Expression buffer. During post hybridisation, the slide was rewashed and dried. For the image quality control, the images were manually verified and found to be devoid of uneven hybridization, streaks, blobs and other artifacts. Hybridization across the slide was clear based on their number of features that includes "g is PosAndSignif" which symbolises whether it is positive and significantly above background. The normalization has been done using GeneSpring GX Software (https://www.agilent.com/en/products/software-informatics/life-sciences-informatics/genespring-gx). Intra-array normalization deals with variability within a single array, "dye normalized background-subtracted signal intensity, gProcessed signal" was log-transformed, following which each of the 75th percentile array value was calculated separately and intensity values of each sample was log transformed. For obtaining the expression values of each probe, obtained value was subtracted by calculated 75^{th} percentile value of the respective array.

2.6 cDNA synthesis and qRT-PCR validation

Illumina Seq d*e novo* transcriptome and microarray data validation of was carried out using real time PCR analysis. For the gene expression analysis ribosomal gene S7 (rS7) was taken as internal reference control. As described in General Materials and Methods, larval midgut RNA was isolated for respective time points using TRIzol methods followed by cDNA synthesis. SuperScript™ III First-Strand Synthesis System kit (Invitrogen, Life Technologies, USA) was used for the cDNA synthesis. Isolated RNA was dissolved in diethyl pyro carbonate (DEPC) treated ddH_2O (1 µg/µl). For cDNA synthesis RNA, oligo dT primer, dNTPs (10 µl) was added to a PCR tube and incubated for denaturation at 65°C for 5 min later placed on later placed on ice for 1-2 min. Kit based cDNA synthesis mix (10 µl) was added in the afore mentioned tube and for annealing it was kept at 50°C for 50 min followed by termination of

the reaction by adjusting the thermocycler at 85°C for 5 min. The residual RNA was eliminated by adding 1 µl of RNase H and incubating the reaction tube at 37°C for 20 min.

Gene specific primer factors for qPCR analysis, after manually designing the primers were analysed using Oligo analyzer tool 3 (Table 1) (https://eu.idtdna.com/pages/tools/oligoanalyzer) (Integrated DNA Technologies Inc, USA). Each primer was individually checked for oligonucleotide properties such as melting temperature, hairpins, dimers, mismatches etc. Primers were commercially ordered from Integrated DNA Technologies Inc, USA following the minimum standard. Before proceeding to the qPCR each primer set was checked using regular PCR followed by agarose gel electrophoresis. After primer confirmation qPCR reaction was carried out, in each 10 µl reaction mixture 1 µl of sample cDNA, 1 µl of reverse and forward primer (10 µM), 10 µl of SYBR® Green Master Mix was added. The reaction mixture was programmed in Step-One Plus qRT-PCR system (Thermo Fisher Scientific, USA). The qPCR thermocycling parameters were programmed as follows: 95°C for 10 min → 40 cycles of 95°C for 30 s and 60°C for 30 s, followed by melting curve generation from 59 to 68°C. Each qPCR reaction was performed thrice for biological replicate and each time three technical replicates was used in the reaction. Cycle threshold was obtained for each reaction and comparative Ct was calculated using Schmittgen and Livak, (2008) method. Calculation of change ($2^{-\Delta\Delta CT}$) in Ct value with respect control was carried out using Microsoft Excel and the obtained value was statistically analyzed using Sigma Plot v14.0 software (https://systatsoftware.com). To check the significance of $2^{-\Delta\Delta CT}$ value, One-Way ANOVA analysis was carried out followed by SNK test. Multiple comparisons between each set of experiments was plotted as P value for each set of experiments.

S.No.	Sequence Name	Sequence (5'-3')
1	DUF233 FP	TCTTAGCAGTCGGCATTCCTGA
2	DUF 233 RP	TATGATCACCACCTGCTTCGCT
3	SERINE PROTIASE I FP	ACAGCGAGAATCACGACCTTGA
4	SERINE PROTIASE I RP	TAGAGCGACGTCAACCTCTGTG
5	Unknown +8.0 FP	GGACACGGGCACTATGAAGTGG
6	Unknown +8.0 RP	TCCAGTATACTTATCACGGAAAGGCC
7	GST EPSILON FP	CCACGGAGAAGAACATCGAGGA
8	GST EPSILON RP	CGTGAGACCCACTCAGTGGTAC
9	Cocoonae 8.0 FP	TTGCAAGGGAGATTATGGAGGTCC
10	Cocoonae 8.0 RP	GGGCTAAAGCTAGTCGTGGATCA
11	Unknown -10.25 FP	CGTGCCAATATGCGAAAGGACTTG
12	Unknown -10.25 RP	ACGTCACTAGGAACACACCTTCCA
13	Chymotrypsin FP	GGCCGACAAGATACGTAAGGCT
14	Chymotrypsin RP	GAACTTCTCCGTCGAACCAGCA
15	Niemann FP	ACTACGCTGGACCTCTTCCAAC
16	Niemann RP	GGACTTTTCGCCCAAGTTGTAGG
17	Trypsin FP	AGCTTGCCGTCATCATCTCGTA
18	Trypsin RP	GTAGGTCCACCCTGCAAAACAGT
19	Unknown -9.0 FP	CAACGCATGTAGCAATAGCCAGC
20	Unknown -9.0 RP	CGCAGTCACCTTGTCATCAACG
21	Cytochrome P450 FP	CGGGAACGTTTACCAACAGTCGA
22	Cytochrome P450 RP	GCAGTTGATGAGCGGGATGACT
23	Defense Protein FP	GGCAGAAATGCTGTGCAGACTG
24	Defense Protein RP	ATCACAGTCGAAGGCTCAGGTAAC
25	60S ribosomal FP	CAGGAAAGTTAGGCGTACCGAAGT
26	60S ribosomal RP	ACGAGTGGGCTTCTTCATGTGG
27	Apoptosis linked FP	AGAGACAACTCGGGCAACATTGA
28	Apoptosis linked RP	GCCGGAATGCAGAAGTCAGAGTA
29	Cecropin FP	CCGCTTCAGGTTGAATACTCGCTT
30	Cecropin RP	CGAATGTTGCGACCCACTTTCTC
31	rS7 FP	ACGTGGACGGTTCACAACTCATCA
32	rS7 RP	TTCGCGGCCTGTTAGCTTCTTGTA

Table 1. List of primers used for real time PCR, expression analysis in control and toxin exposed larval RNA sample for the validation of DESeq and microarray analysis.

2.7 Data Records

Illumina Seq *de novo* transcriptome raw sequencing data was submitted to NCBI-SRA database (National Center for Biotechnology Information Sequence Read Archive). Illumina Seq 500 raw data was deposited to NCBI SRA database with accession number SRX4119388 (https://www.ncbi.nlm.nih.gov/sra/SRX4119388[accn]). The microarray raw data was submitted to Gene expression omnibus (GEO-NCBI) database with accession number GSE114934 (https://www.ncbi.nlm.nih.gov/geo).

Illumina Seq 2500 raw data was deposited to NCBI-SRA database (https://identifiers.org/insdc.sra:SRP186750). The raw data of 28 samples was submitted with accession numbers SRR8617834, SRR8617835, SRR8617836, SRR8617837, SRR8617838, SRR8617839, SRR8617840, SRR8617841, SRR8617842, SRR8617843, SRR8617844, SRR8617845, SRR8617846, SRR8617847, SRR8617848, SRR8617849, SRR8617850, SRR8617851, SRR8617852, SRR8617853, SRR8617854, SRR8617855, SRR8617856, SRR8617857, SRR8617858, SRR8617859, SRR8617860 and SRR8617861.

Followed by submission of assembled transcript in TSA–NCBI (Transcriptome Shotgun Assembly Sequence Database) with accession number GHGZ00000000.1 (https://identifiers.org/ncbi/insdc:GHGZ00000000.1). The associated BioProject and BioSample was submitted to NCBI database with accession number PRJNA523326 and SAMN09241884 respectively.

3. Results

3.1 Illumina Seq analysis and *de novo* assembly

Illumina Seq based *de novo* transcriptome assembly was carried using Trinity assembler (https://omictools.com/trinity-tool) and SOAP-*denovo*-Trans assembler (https://omictools.com/soapdenovo-trans-tool) for Illumina Seq 500 and Illumina Seq 2500 respectively. Before processing the raw data for assembly, integrity of data transfer was checked using MD5 checksum for Illumina sequencer and lab system. Detailed and technical validation of present data is mentioned in Fig. 8. Illumina Seq 500 sequencing, resulted in 1,68,50,105 and 2,05,01,613 raw reads in control and toxin exposed larval samples, which yielded a total of 37 million reads. After trimming in control and toxin exposed samples, 1,57,10,416 and 1,90,81,749 clean reads were obtained. In both the samples 44% GC content

was calculated in the clean reads. Using Trinity assembler total 34,612 and 41,109 transcripts were generated and 39.55 and 49.11 Megabytes length was obtained in control and toxin exposed samples respectively. In control and toxin exposed samples, 1,772 and 1,992 transcripts showed N50 assembly quality in terms of contiguity. In both control and toxin exposed samples, 200 and 500 bp length transcripts were obtained in maximun number. All afore mentioned points are summarised in Table 2.

Sample	Control	Toxin exposed
Raw reads	1,68,50,105	2,05,01,613
Clean reads	1,57,10,416	1,90,81,749
Transcripts generated	34,612	41,109
Total transcripts length	3,95,54,452	4,91,15,238
Maximum transcripts length	17,216	26,151
Minimum transcripts length	301	301
Average transcript length	1,142.8	1,194.76
Sequences >=300-500 bp	12,085	14,524
Sequences >=500-1 Kbp	9,876	11,085
Sequences >=1-5 Kbp	12,141	14,696
Sequences >=5-10 Kbp	491	779
Sequences >=10 Kb-1 Mbp	19	25
N-50 Value	1,772	1,922
CD-HIT Clustering identity	95%	95%
GC %	44	44

Table 2. Details of reads and assembly statistics of Illumina Seq 500 *de novo* transcriptome data obtained from control and toxin exposed larval midgut RNA samples.

Using Illumina Seq 2500, 28 libraries were sequenced and ~ 3.05 GB high quality data was generated for each larval midgut sample (Table 3). Finally, from all the samples an average of 19 million clean reads were obtained. High quality reads, base counts and data size statistics are presented in Table 3. For assembly, all the 28 samples were pooled together to generate one single transcriptome. Assembled transcript statistics and length distribution is summarised in table 3. Finally, a total of 1,74,066 transcripts were generated using 28 raw sample clean reads. SOAP-denovo-Trans assembler was used for master assembly and transcriptome length of 10,02,47,510 bps was generated. An average of 575 bps transcript length was obtained in master assembly (Table 4).

Sample Id	Reads	Total reads	Bases	Total bases	Data in Gb
Contorl_12h_R1.fq	10028942	20057884	1494397342	2988787694	3
Contorl_12h_R2.fq	10028942		1494390352		
Contorl_12h_replicate_R1.fq	8628916	17257832	1290865585	2581697738	2.6
Contorl_12h_replicate_R2.fq	8628916		1290832153		
Contorl_24h_R1.fq	8034841	16069682	1200570075	2401166556	2.4
Contorl_24h_R2.fq	8034841		1200596481		
Contorl_24h_replicate_R1.fq	6983555	13967110	1041173358	2082342736	2.1
Contorl_24h_replicate_R2.fq	6983555		1041169378		
Contorl_36h_R1.fq	8192427	16384854	1225981812	2451900622	2.5
Contorl_36h_R2.fq	8192427		1225918810		
Contorl_36h_replicate_R1.fq	15482277	30964554	2300666804	4601406035	4.6
Contorl_36h_replicate_R2.fq	15482277		2300739231		
Contorl_48h_R1.fq	8122611	16245222	1215439428	2430731536	2.4
Contorl_48h_R2.fq	8122611		1215292108		
Contorl_48h_replicate_R1.fq	9181499	18362998	1368283592	2736491403	2.7
Contorl_48h_replicate_R2.fq	9181499		1368207811		
Starved_12h_R1.fq	9799368	19598736	1436448890	2872654806	2.9
Starved_12h_R2.fq	9799368		1436205916		
Starved_12h_replicate_R1.fq	11031631	22063262	1644880206	3289737316	3.3
Starved_12h_replicate_R2.fq	11031631		1644857110		
Starved_24h_R1.fq	7656143	15312286	1147275767	2294330772	2.3
Starved_24h_R2.fq	7656143		1147055005		
Starved_24h_replicate_R1.fq	10655240	21310480	1590345218	3180759227	3.2
Starved_24h_replicate_R2.fq	10655240		1590414009		
Starved_36h_R1.fq	9079024	18158048	1355319182	2710650819	2.7
Starved_36h_R2.fq	9079024		1355331637		
Starved_36h_replicate_R1.fq	9110626	18221252	1356931776	2713884186	2.7
Starved_36h_replicate_R2.fq	9110626		1356952410		
Starved_48h_R1.fq	10697833	21395666	1597804024	3195502905	3.2
Starved_48h_R2.fq	10697833		1597698881		
Starved_48h_replicate_R1.fq	7723461	15446922	1148556771	2296940516	2.3
Starved_48h_replicate_R2.fq	7723461		1148383745		
Toxin_exposed_12h_R1.fq	16730802	33461604	2493020155	4986040101	5
Toxin_exposed_12h_R2.fq	16730802		2493019946		
Toxin_exposed_12h_replicate_R1.fq	10576431	21152862	1579145784	3158259574	3.1
Toxin_exposed_12h_replicate_R2.fq	10576431		1579113790		
Toxin_exposed_24h_R1.fq	10730932	21461864	1594011699	3188078513	3.2
Toxin_exposed_24h_R2.fq	10730932		1594066814		
Toxin_exposed_24h_replicate_R1.fq	10807754	21615508	1612408105	3224781975	3.2
Toxin_exposed_24h_replicate_R2.fq	10807754		1612373870		
Toxin_exposed_36h_R1.fq	10061786	20123572	1500281280	3000456189	3
Toxin_exposed_36h_R2.fq	10061786		1500174909		
Toxin_exposed_36h_replicate_R1.fq	10027587	20055174	1490013434	2979780038	3
Toxin_exposed_36h_replicate_R2.fq	10027587		1489766604		
Toxin_exposed_48h_R1.fq	9080458	18160916	1332234024	2664384624	2.7
Toxin_exposed_48h_R2.fq	9080458		1332150600		
Toxin_exposed_48h_replicate_R1.fq	6058585	12117170	900542510	1800917863	1.8
Toxin_exposed_48h_replicate_R2.fq	6058585		900375353		
Toxin_tolerant_R1.fq	10917204	21834408	1616926175	3233853623	3.2
Toxin_tolerant_R2.fq	10917204		1616927448		
Toxin_tolerant_replicate_R1.fq	14952551	29905102	2225358452	4450657173	4.5
Toxin_tolerant_replicate_R2.fq	14952551		2225298721		
Toxin_tolerant_24h_exposed_R1.fq	7372799	14745598	1094370604	2188784068	2.2
Toxin_tolerant_24h_exposed_R2.fq	7372799		1094413464		
Toxin_tolerant_24h_exposed_replicate_R1.fq	18861211	37722422	2813649674	5627188694	5.6
Toxin_tolerant_24h_exposed_replicate_R2.fq	18861211		2813539020		

Table 3. Presents statistics of high-quality data obtained from midgut RNA samples of *A. janata* larva, under different experimental conditions.

Description	Master Assembly
Total number of transcripts	1,74,066
Total transcriptome length in bps	100,247,510
Average transcript length in bps	575
N50	421
Maximum transcript length in bps	25,338
Minimum transcript length in bps	200
Metrics	Master Assembly
Length >= 200 & <= 300	85429
Length > 300 & <= 400	32056
Length > 400 & <= 500	13439
Length > 500 & <= 600	8124
Length > 600 & <= 700	5796
Length > 700 & <= 800	4098
Length > 800 & <= 900	3028
Length > 900 & <= 1000	2444
Length > 1000 & <=5000	18383
Length >5000	1269

Table. 4 Illumina Seq 2500 statistics of assembled transcripts and length distribution, of different Sequence.

3.2 Annotation

Illumina Seq 500 assembly reads were annotated using BLASTx algorithm against NCBI's non-redundant (nr) database. A total of 18,836 and 21,046 transcripts were annotated. However, in control and toxin exposed larval samples, a total of 34,612 and 41,109 transcripts were obtained. In this transcriptome analysis, *A. janata* sequence showed a close matching with *Bombyx mori* (35.66%), followed by *Danaus plexippus* (32.63%), *Parargea egeria* (10.22%), and the same is summarised in pie chart (Fig. 3a). Transcripts were classified into three major groups, on the basis of gene ontology i.e. cellular component, molecular function and biological processes; respectively subcategories in 11 types (Fig. 3b). In biological process category, the maximum number of transcripts in both the samples were associated with serine/threonine kinase activity. However, the maximum number of transcripts in the cellular component category were found to be associated with the integral membrane components followed by

nucleus. Subsequently, ATP and Zinc-ion binding factor transcripts were primarily represented in the molecular function category (Fig. 3b).

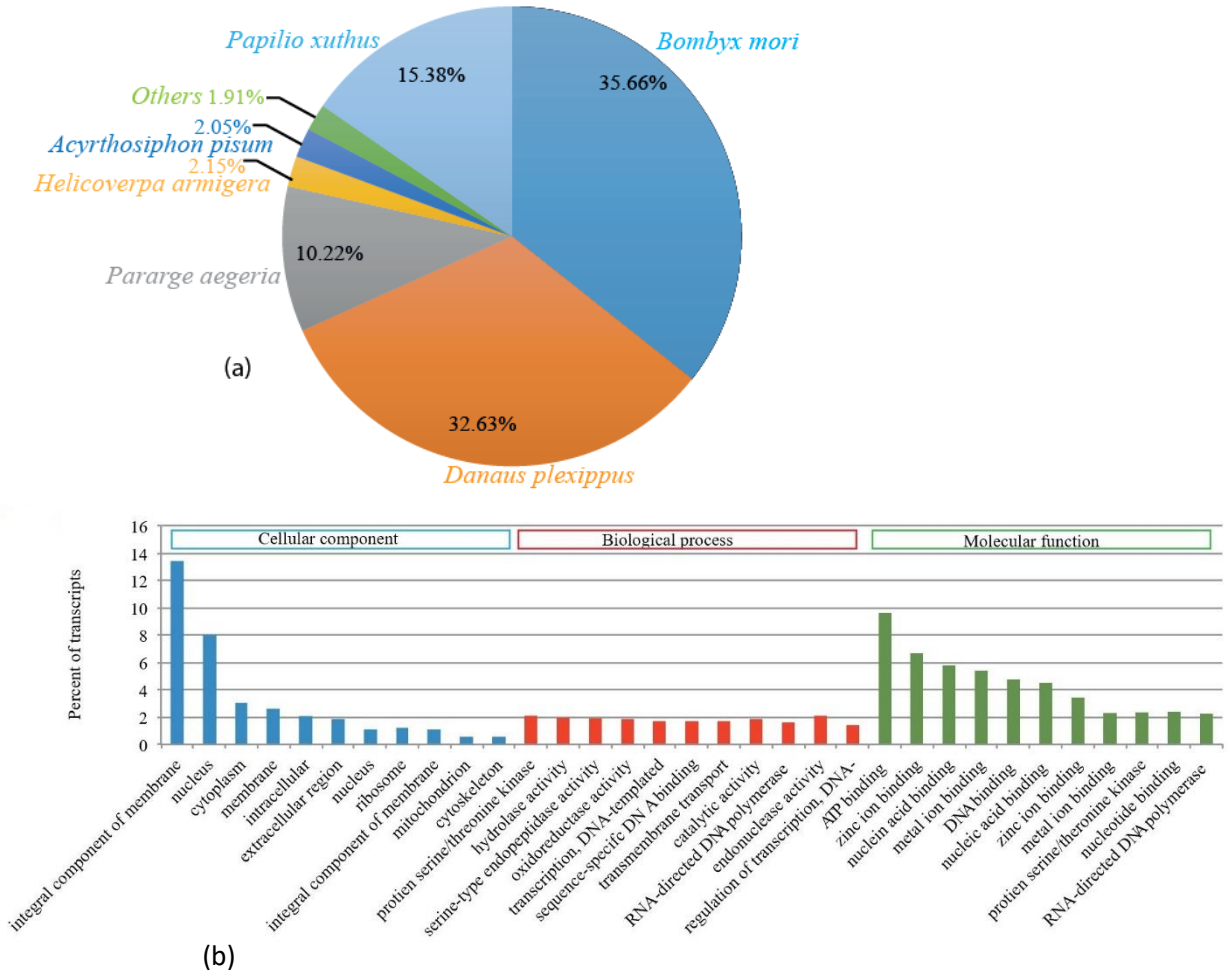

Fig. 3. This figure represents Illumina Seq 500 transcriptome analysis of control and toxin exposed larvae. (a) Pie chart showing species percentage distribution of most closely related insect species resulting from annotation, (b) Gene ontology classification based on cellular component, biological process, and molecular function, (y-axis: percentage of transcript in each category).

Illumina Seq 2500 annotation was carried out with NCBI's nr database (non-redundant) using the BLASTP algorithm. From 1,74,066 transcripts, a total of 35,559 proteins were reported and 32,561 proteins were captured with hits and 2,998 with no hits. In this transcriptome analysis data, *A. janata* sequence closely matched with *Spodoptera litura* (23%) followed by *Helicoverpa armigera* (23%) and *Heliothis virescens* (22%) (Fig. 4). In parallel to this NR, UniProt, KOG and Pfam database were also used for sequence similarity search and

alignment was carried out using BLASTP algorithm with $1e^{-5}$ e-value threshold. The inclusive BLAST result of four databases is presented in figure 5.

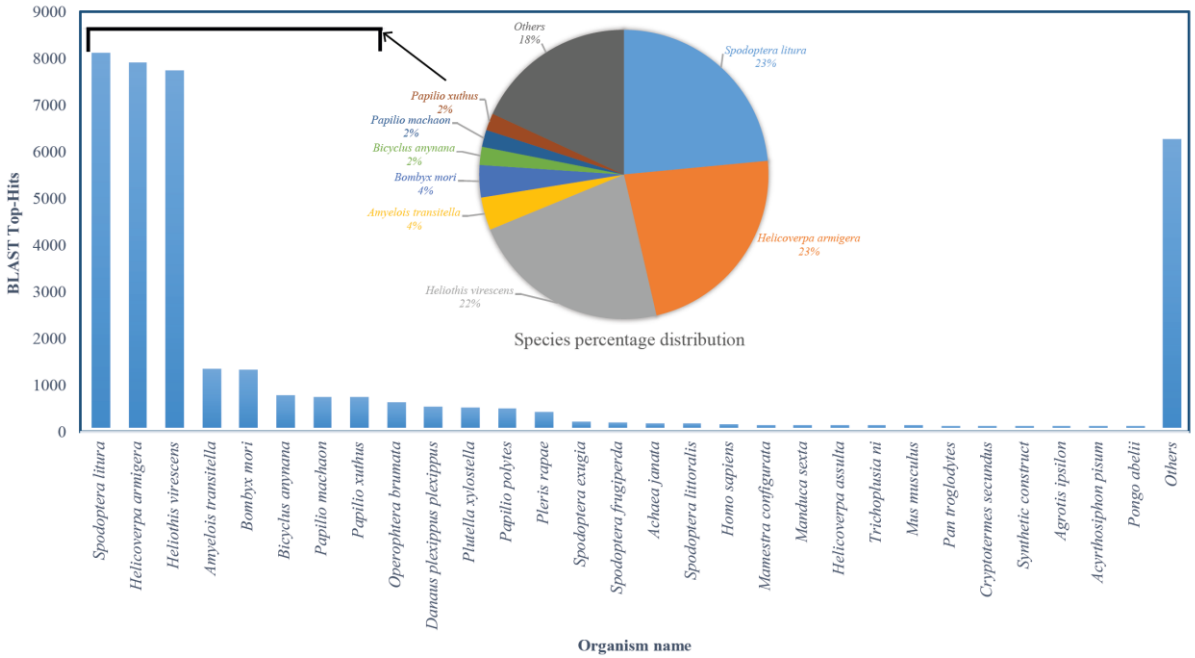

Fig. 4 Pie chart showing species percentage distribution of transcriptome of most closely related insect species resulted from annotation.

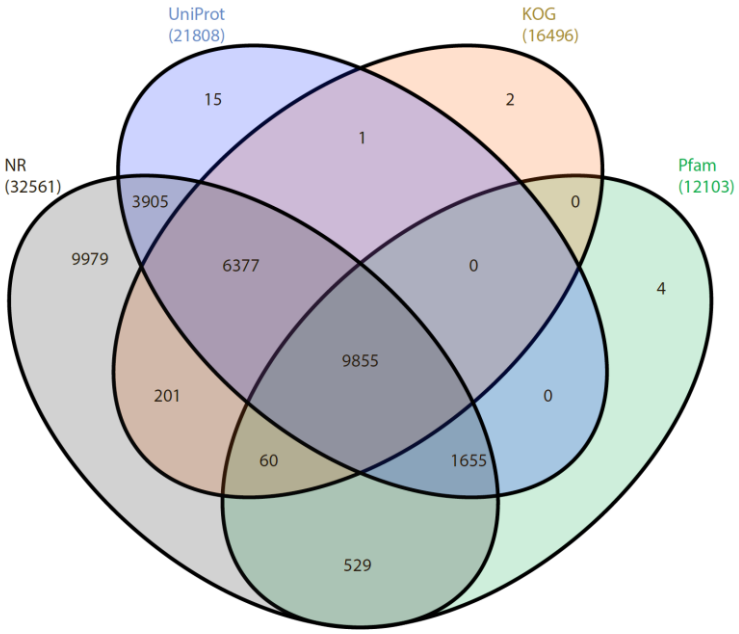

Fig. 5 Venn diagram representation of annotated proteins obtained using different protein databases (NR, UniProt, KOG and Pfam).

3.3 Differential gene expression analysis

With Illumina Seq 500 sequencing data, differential gene expression (DGE) analysis was carried out between control and toxin exposed samples. FPKM (Fragments Per Kilobase of exon per Million reads) count based volcano plot was constructed using log2fold change obtained from transcriptome analysis (Fig. 6). For this current analysis, 2-fold capping was kept for log2 fold-change in determining upregulated and downregulated genes (Fig. 6). A total of 41,224 transcripts were obtained out of which 16,670 transcripts were differentially expressed. In these 16,670 transcripts, 8,033 and 8,637 were upregulated and downregulated respectively. On the other hand in both samples 24,574 transcripts were impartially regulated. In addition, a total of 1,701 in control and 5,002 transcripts in toxin exposed samples were uniquely present (Table 5).

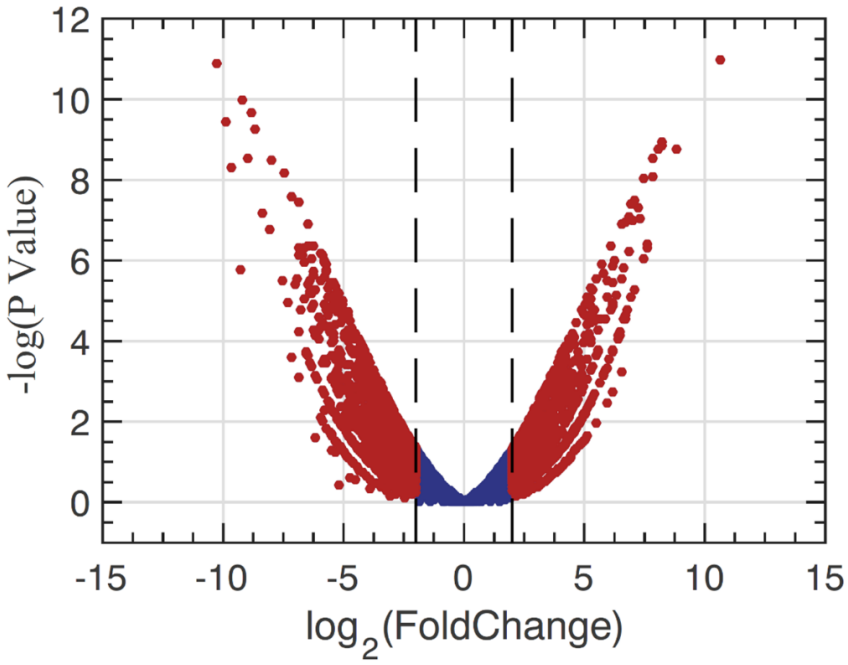

Fig. 6 Volcano plot analysis of differentially regulated genes in control and toxin exposed samples. DeSeq was used for determining upregulation and downregulation of genes based upon relative FPKM counts (x-axis: log2fold change; y-axis: -log, P value) plot was generated using RStudio Version 1.1.453© 2009–2018.

DGE Statistics				
Total Unigene available	**47959**			
No. of transcript in each category	**Total**	**Up**	**Down**	**Neutral**
No. of transcript expressed in both samples	41244	8033	8637	24574
No. of transcript expressed only in Control	1707	--	--	--
No. of transcript expressed only in Treated	5002	--	--	--
No. of P-significant transcript	1611	701	910	--
No. of Q-significant transcript	280	115	165	--
Software used for carrying out DGE	DeSeq			

Table 5. Shows the result obtained from differential gene expression statistics of transcriptome analysis of the Illumina Seq 500. P (probability of the occurrence of a given event) and Q (probability of any single false positive) significant transcripts were obtained after normality expression of data.

Once again the data obtained from Illumina Seq 2500 was analysed for differential gene expression. In this analysis we compared the control and Cry toxin tolerant larval transcript profile using map reads obtained in the differential expression analysis. Analysis of count data was carried out using DESeq.2 in RStudio platform. A significant difference was noticed in the tolerant larval population. In this DESeq analysis a total of 35,559 CDS were analysed and 320 CDS showed significant variation, with padj < 0.05 (Fig. 7). Few of the genes like (i) gi|1131919362| Ca2+-binding protein, RTX toxin-related, (ii) gi|1199381583| superoxide dismutase [Cu-Zn] 2-like, (iii) gi|315139350| serine protease 63, (iv) gi|1274141826| trypsin, alkaline C-like and (v) gi|1274136486| apolipophorins isoform X2 were shown to be upregulated, while (i) gi|123995301| ribosomal protein SA, (ii) gi|744619941| predicted: 60 S ribosomal protein L8, (iii) gi|45219787| ribosomal protein S3A, (iv) gi|1344818460| alanine aminotransferase 1-like and (v) gi|501300966| ubiquitin were downregulated.

(Data available at figshare, https://springernature.figshare.com/articles/Differential_expression_analysis_of_susceptible_and_tolerant_larval_population/8255996).

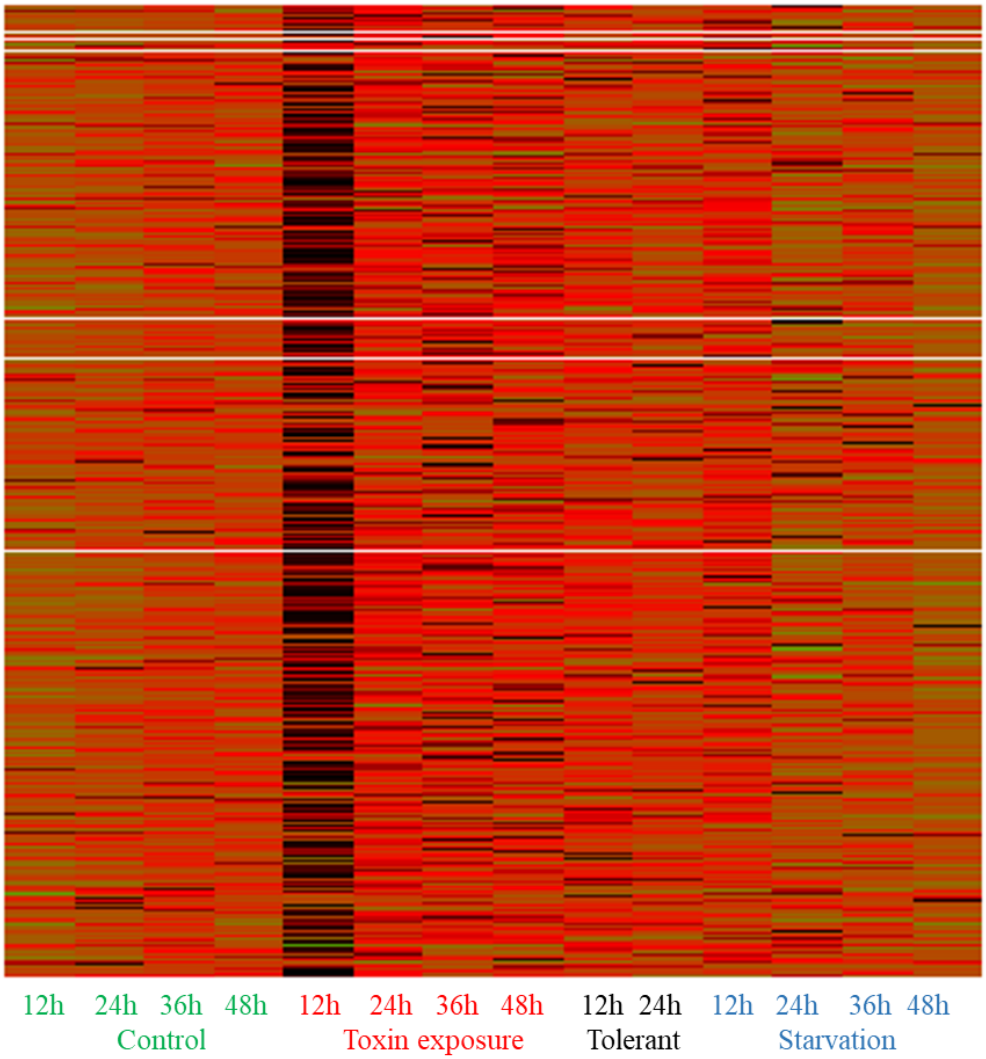

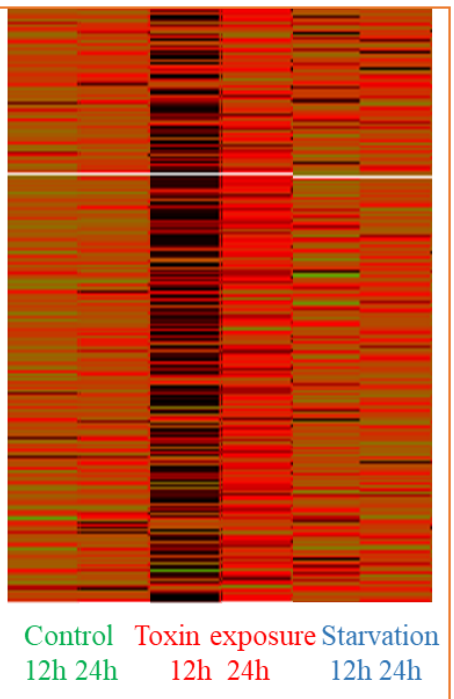

Fig. 7 Differentially regulated genes in control, toxin exposed, starved and tolerant samples. FPKM counts were used for determining upregulation and downregulation of genes, heat plot was generated using RStudio Version 1.1.453© 2009–2018. "Inset represents the difference in toxin exposed and starved sample gene expression."

$$FPKM_i = \frac{q_i}{\frac{l_i}{10^3} * \frac{\sum_j q_j}{10^6}} = \frac{q_i}{l_i * \sum_j q_j} * 10^9$$

3.4 Prediction of transcription factor and metabolic pathways

Using *D. melanogaster* as reference, a total of 1,052 and 1,221 transcription factors in control and toxin exposed samples were respectively annotated using the transcription factor database (http://www.bioguo.org/AnimalTFDB/). Zinc-finger family-Cys2His2, ZBTB and homeobox transcription factors family were showed 401, 69 and 64 hits in control sample as compared to 475, 66 and 63 hits in toxin exposed (Fig. 8a). *A. janata* metabolic pathways prediction was carried out using KEGG pathway analysis, figure 8b repersents percentage division of control and toxin exposed sample. These results revealed transcripts associated with translation, signal transduction followed by folding, sorting and degradation are maximum is both larval midgut samples (Fig. 8b).

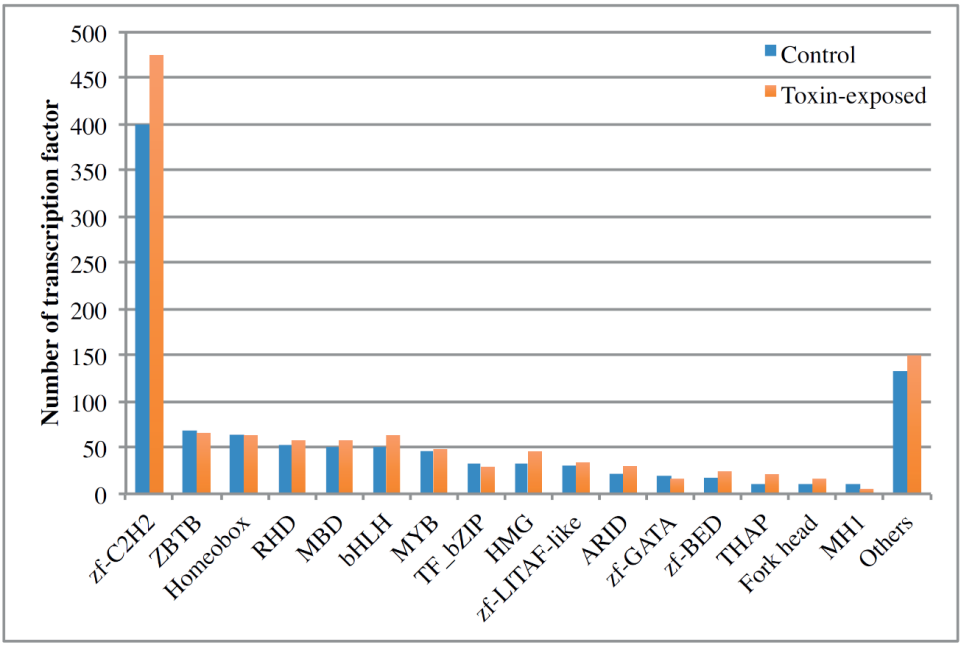

Fig. 8a. Transcription factor annotation with TFDB showing number of transcripts in each transcript family, Distribution of transcript in control & toxin exposed samples.

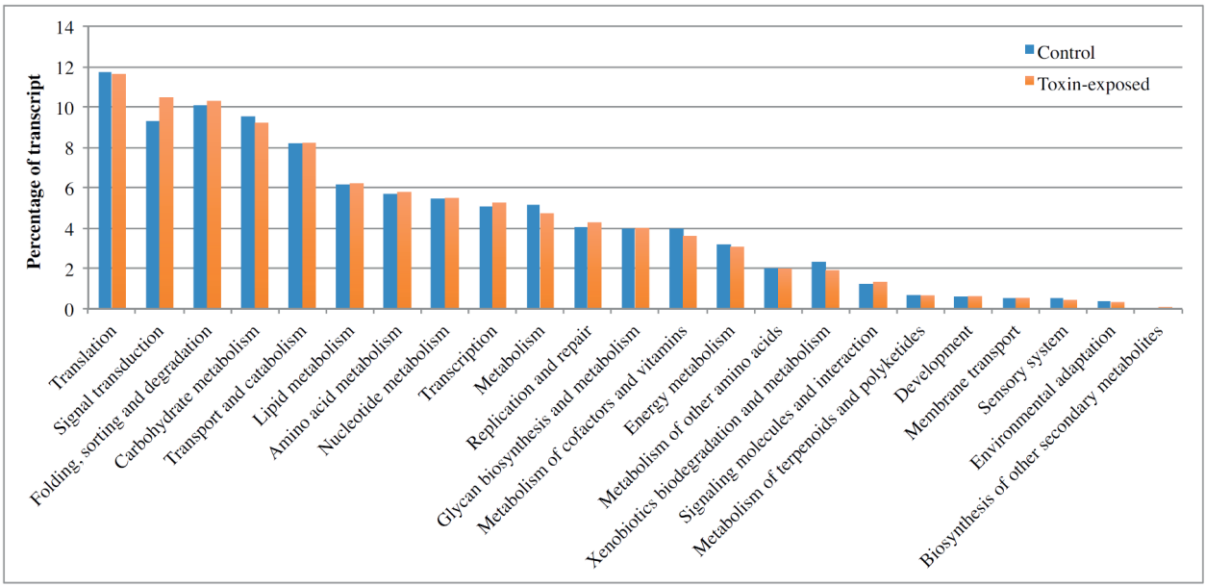

Fig. 8b. Prediction of metabolic pathways of *A. janata* midgut obtained using KEGG pathway analysis. The histogram shows percentage distribution of various transcript distribution in control and toxin exposed samples.

3.5 Identification of Single Sequence Repeats (SSR)

MISA Perl script was used for single sequence repeat identification and analysis. A total of 3,947 and 5,043 transcripts were identified that harboured SSR motifs, which includes SSRs prediction, 4,770 and 6,115 respectively in control and toxin exposed samples. SSR analysis revaled that mono-nucleotide (72.41%) followed by di-nucleotide (13.12%) and tri-nucleotide (12.64%) repeats were present in control samples. However, mono-nucleotide (72.51%), tri-nucleotide (13.01%) and di-nucleotide (12.72%) repeats were present in treated samples (Fig. 9).

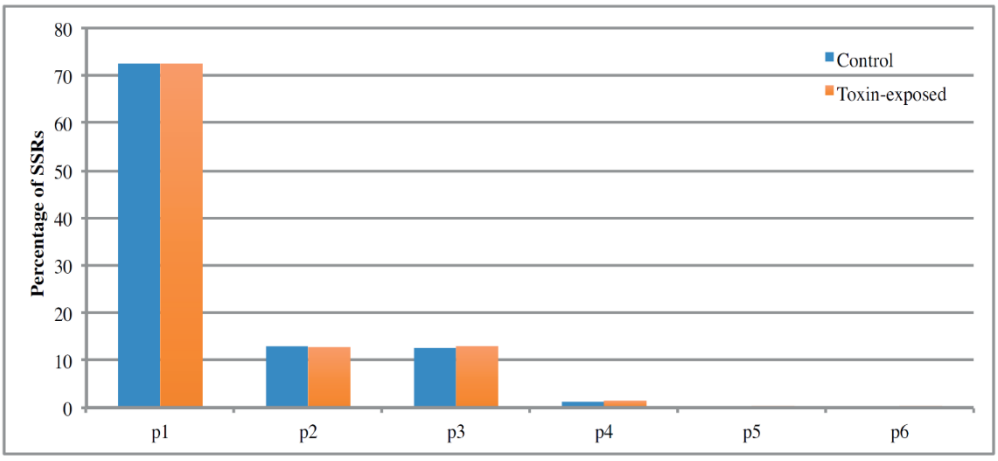

Fig. 9. Identification of SSR using MISA perl script, for total SSRs prediction in control and toxin exposed samples, (p1 = mono-nucleotide, p2 = di-nucleotide, p3 = tri-nucleotide, p4 = tetra-nucleotide, p5 = penta-nucleotide and p6 = hexa-nucleotide).

3.6 Microarray analysis

The microarray based expression analysis clearly revealed differential gene expression values of toxin exposed time-series samples (12, 24, 36, 48 and 60 h) when compared to control sample (Fig. 10). Labelled cRNA spectrophotometric testing of cRNA showed 260/280 ratio of samples >2.29 with specific activity varying from 6.71 to 9.61. A total of 954 genes were differentially regulated in all the samples where 375 genes were upregulated and 579 were downregulated. In toxin exposed samples of 12 h, 24 h, 36 h, 48 h and 60 h; 192, 111, 187, 156 and 106 mRNAs were uniquely upregulated (Fig. 11, i) in contrast 97, 85, 108, 104 and 69 mRNAs were uniquely downregulated (Fig. 11, ii) (Transcript details is available in Dhania et al., 2019a; Supplementary File 1, 2). For the present study, heat maps were generated for visualisation of differential gene expression achieved from the microarray data.

3.7 qRT-PCR validation

The qRT-PCR analysis was performed to validate the results of microarray gene expression with fifteen selective differentially expressed genes. “DUFF233, Serine protease inhibitor, Serpin 1a, GST-epsilon, Cocoonase, Chymotrypsin, Niemann-Pick type C2 protein, Trypsin-like proteinase T23, Cytochrome P450, Defense protein 1, 60S ribosomal protein L18,

Apoptosis-linked protein 2, Cecropin and three uncharacterized proteins" were checked in this study (Fig. 12). The qRT-PCR and microarray gene expression data synchronised equally well with the respective results. Associated Pearson's correlation coefficient 0.5866864 was calculated for microarray and qRT-PCR dataset, this indicates a noble correlation.

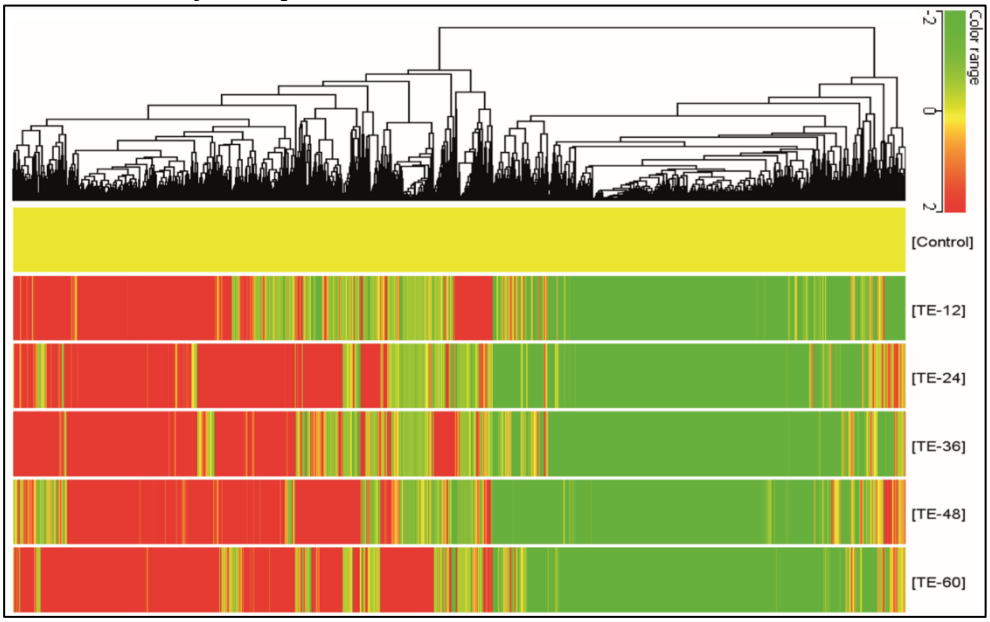

Fig. 10. Differential gene expression analysis upon continuous toxin exposure using microarray. The overall cluster of differentially regulated genes obtained through microarray analysis. The red colour indicates high, green indicates low and yellow indicates neutral gene expression levels (fold change expression is provided as log2).

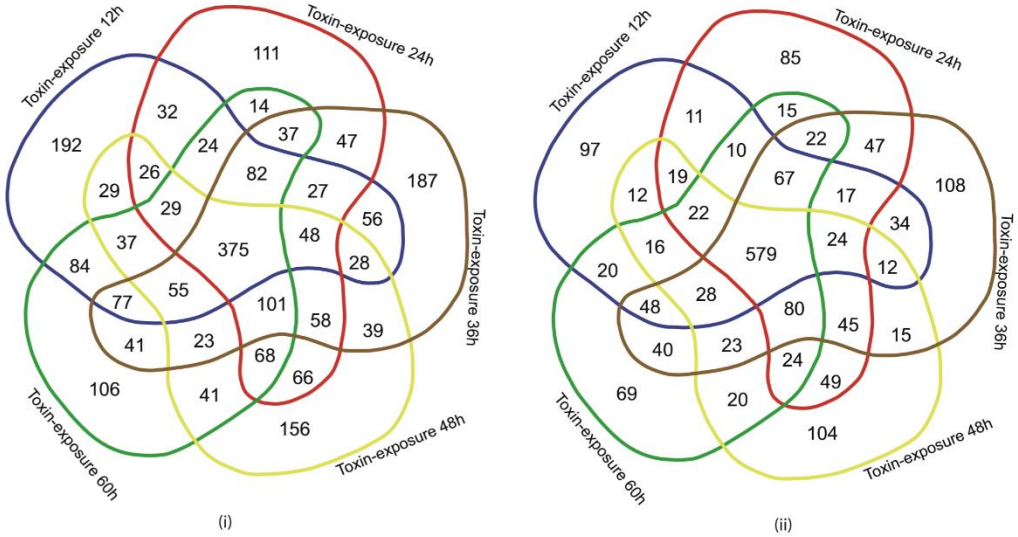

Fig. 11. Venn diagram depicting the number of larval midgut transcripts at various toxin exposure time points. (i) Commonly upregulated transcripts at the various time point of toxin exposure, (ii) commonly downregulated transcripts at various time points of toxin exposure.

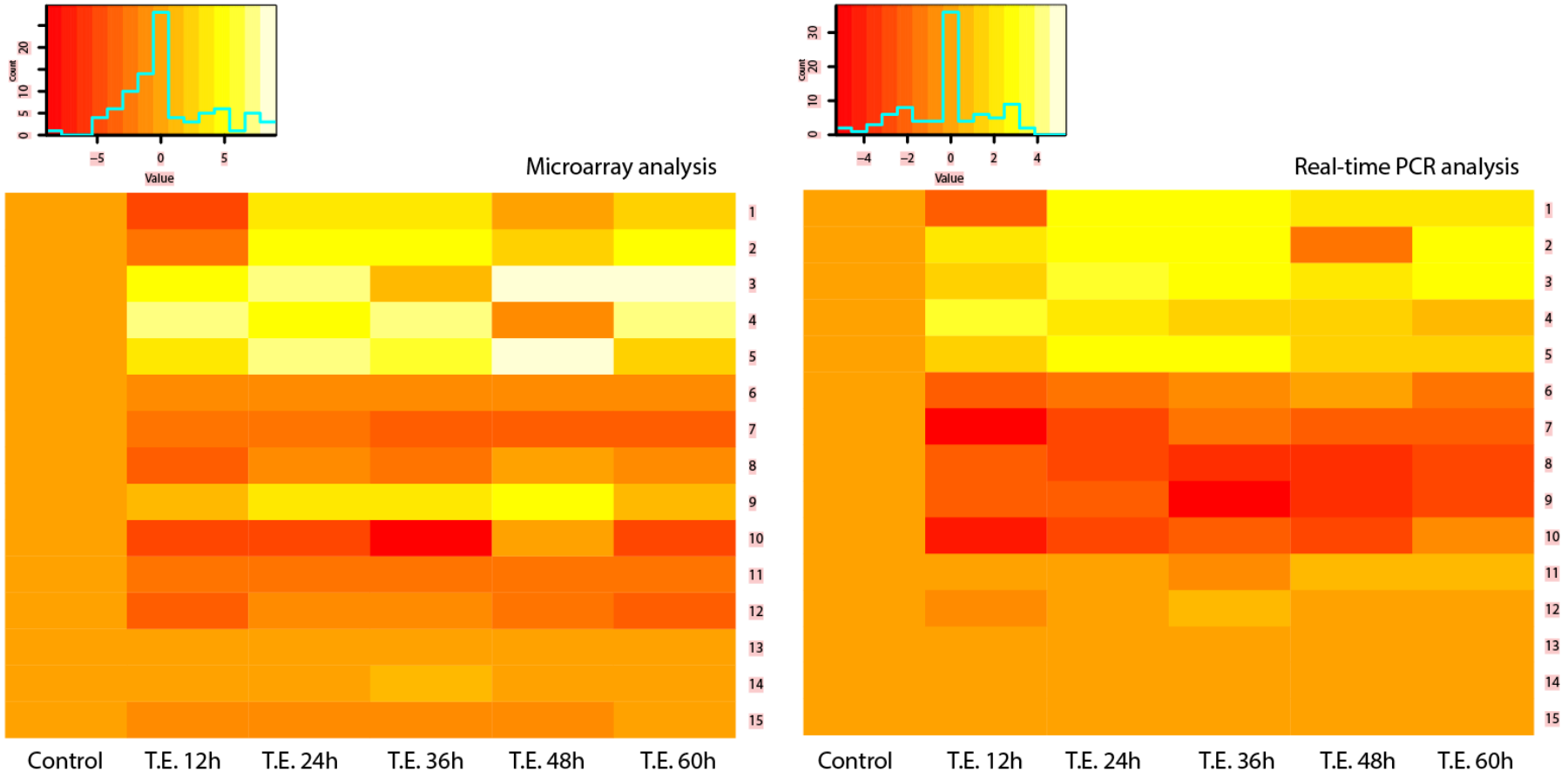

Fig. 12. Validation of the RNA-Seq and microarray data using qRT-PCR analysis, data was normalised with rS7 as reference gene. The transcripts validated were (1) DUFF233, (2) Serine protease inhibitor, Serpin 1a, (3) Unknown +8 fold upregulated, (4) Glutathione S-transferase epsilon, (5) Cocoonase, (6) Unknown −10 fold downregulated, (7) Chymotrypsin, (8) Niemann-Pick type C2 protein, (9) Trypsin-like proteinase T23, (10) Unknown −9 fold downregulated, (11) Cytochrome P450, (12) Defense protein, (13) 60S ribosomal protein L18, (14) Apoptosis-linked protein 2 and (15) Cecropin. Microarray analysis heat plot were generated using value obtained from RNA-Seq and microarray data, Real time PCR heat plot were generated using value obtained from qRT-PCR analysis. Plots were generated using RStudio Version 1.1.453–© 2009–2018. Statistical significance for qRT-PCR data was calculated using Sigma plot ($P < 0.005$, between experimental groups ($n = 3$)). Pearson's correlation coefficient was 0.5866864 between microarray data and qRT-PCR analyses calculated from RStudio.

3.8 Expression of Cry toxin receptors

In this study Cry toxin receptor's gene expression was monitored (Pigott and Ellar, 2007; Tabashnik et al., 2013). These results revealed downregulation of "protocadherin-like protein, DE-cadherin, cadherin, alkaline phosphatases 1, 2, and 3, aminopeptidases N (APN1, APN6, APN7, APN9, APN8 and APN11), fat body APN and amino peptidase P-like protein". In correlation to the above "mutant cadherin and midgut class 2 aminopeptidase N" mRNAs revealed significant upregulation upon toxin exposure (Fig. 13).

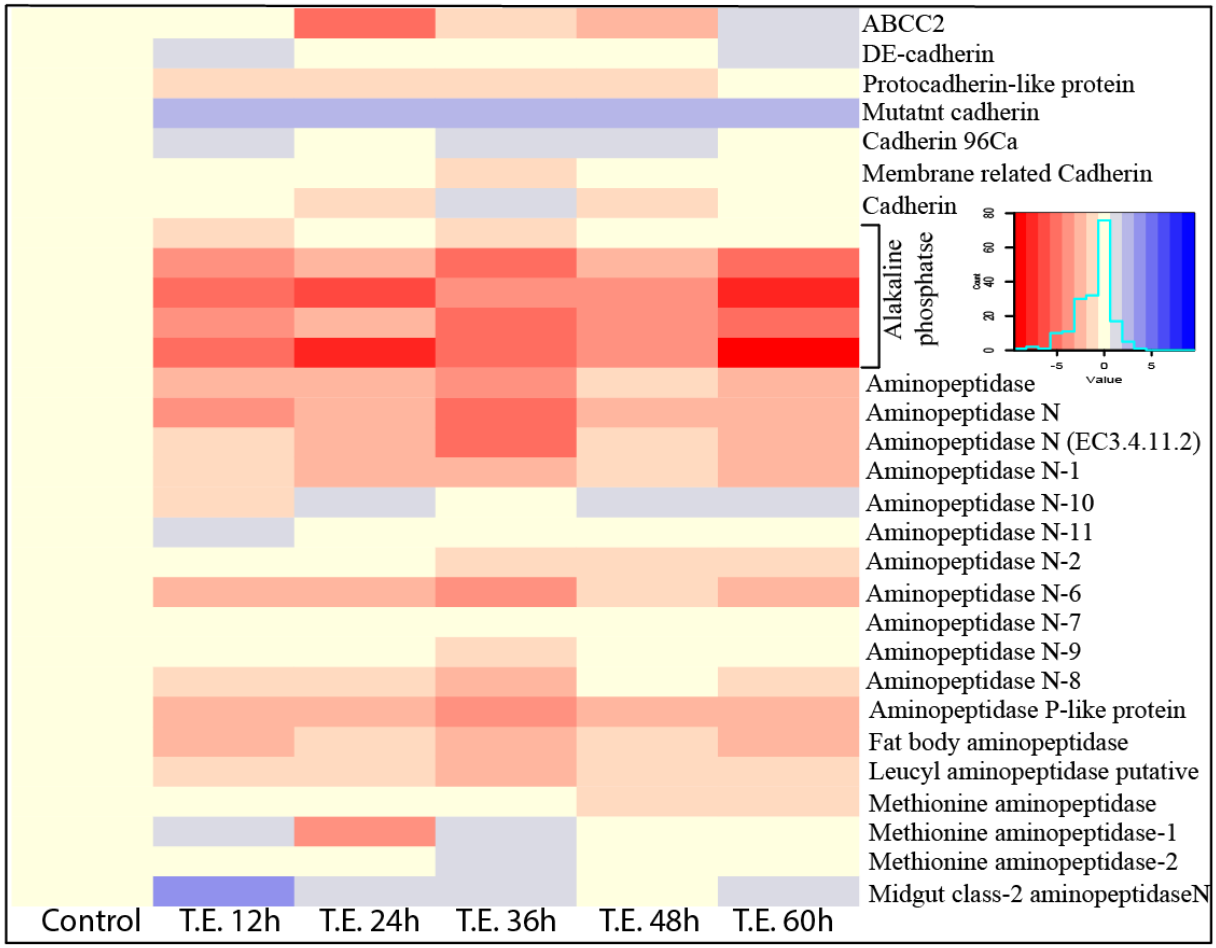

Fig. 13. Expression analysis of transcripts of Cry toxin receptors at various time points of toxin exposure.

3.9 Arylphorin and REPATs (pathogen-response gene) expression

Bt toxin damaged based regeneration associated midgut responsive genes such as arylphorins and REPATs were monitored (Burmester, 2015; Castagnola and Jurat-Fuentes,

2016; Chauhan et al., 2017). Results revealed that arylphorin was initially downregulated upon Cry toxin exposure (24 h) insects but it was upregulated during 36 h and 48 h time period. Several REPAT mRNAs showed differential responses to Cry toxin exposure. In this study, REPAT 32, REPAT 38 were upregulated and REPAT 30, REPAT 34 transcripts were shown downregulated (Fig. 14).

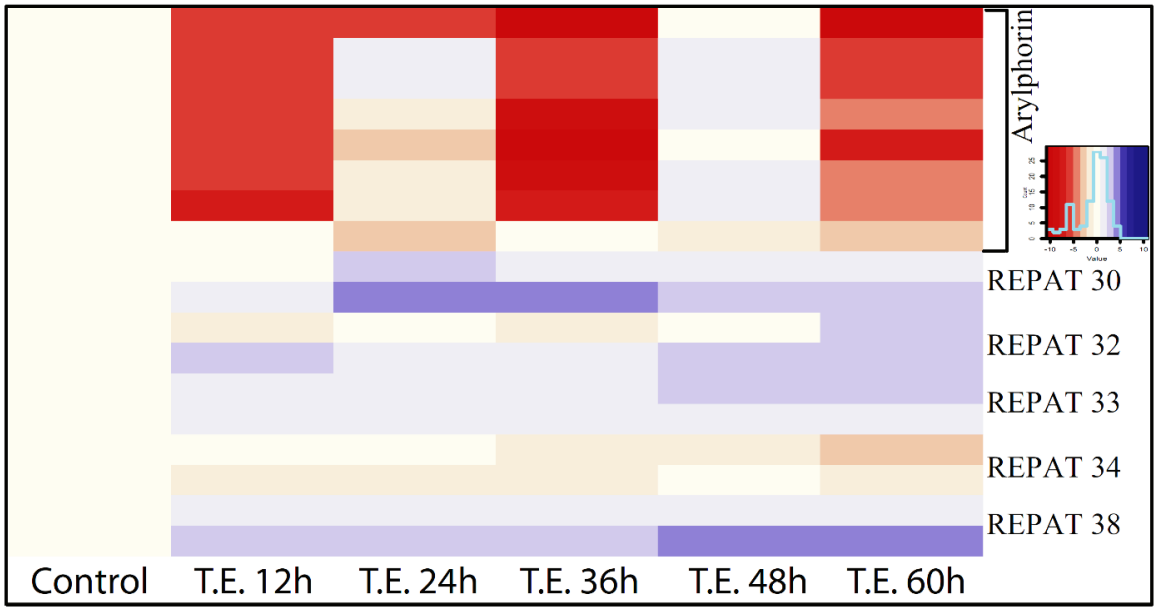

Fig. 14. Shows the profile of arylphorin and REPATs transcript expression during Cry toxin exposure.

3.10 Expression of gut proteases

Bt toxin activation in larval gut lumen is associated with gut proteases which are initial determining steps for Bt toxicity after ingestion. In current study primarily serine proteases constituted large group of differentially expressed transcripts in toxin exposed sample. "Trypsin, trypsin-like proteins, chymotrypsins (C3, C6, C7 and C14)" encoded transcripts were downregulated. However, chymotrypsin (2) and chymotrypsin like-protein transcripts were selectively upregulated at some time points. Expression of protease inhibitors including "serine protease inhibitor 1, 2 and 3 and serpin 1a" transcript was upregulated. It is interesting to note that transcript expression of "26s protease, endoproteases, ATP-dependent Clp proteases, protease M1, zinc metalloprotease and endopeptidases" reamined unaffected (Fig. 15).

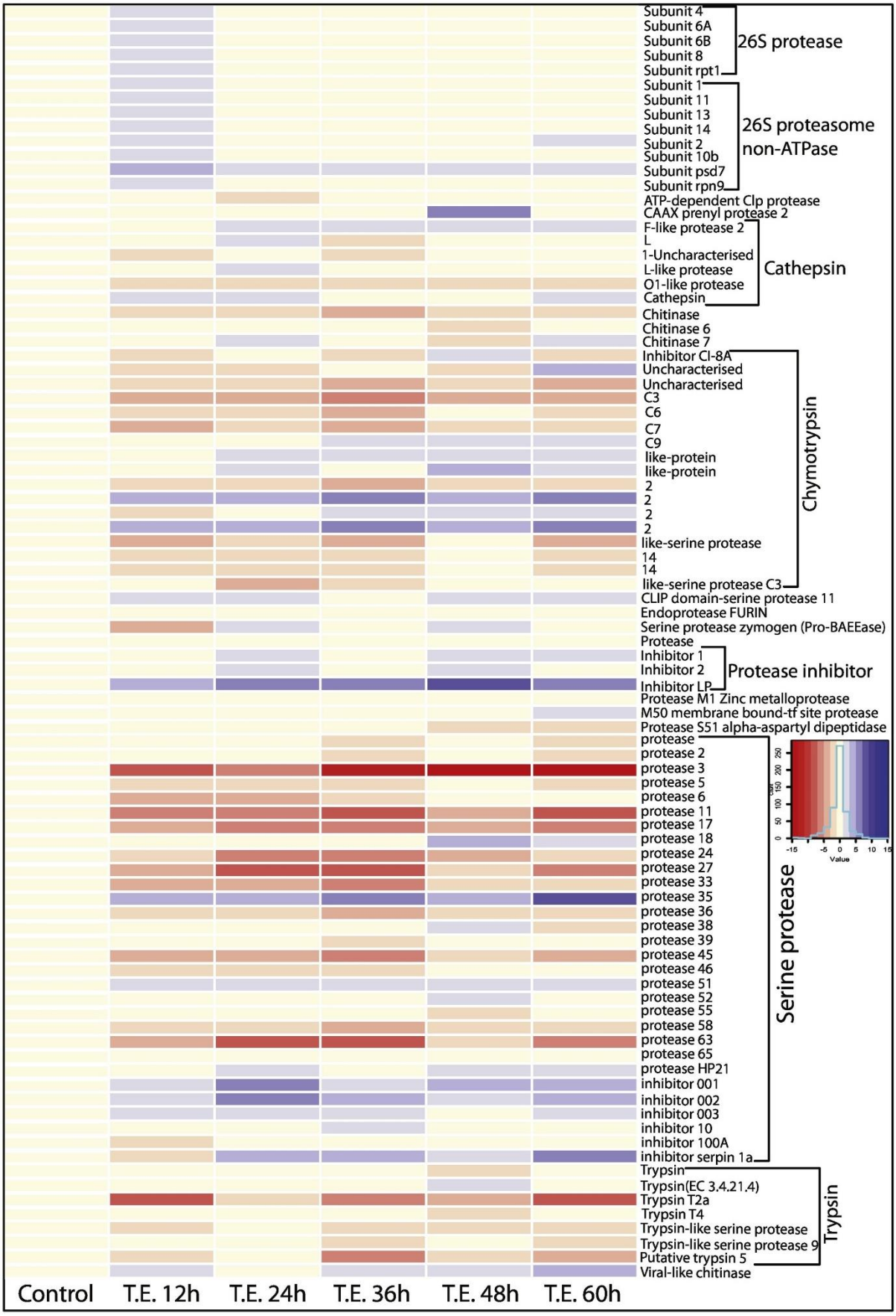

Fig. 15. Shows the transcripts analysis of various gut proteases during Cry toxin exposure in the larval midgut of *A. janata.*

3.11 Expression of detoxification enzymes

The detoxifying enzyme-mediated endogenous anti-oxidative activity was well reported in the counterbalance of toxin-induced oxidative damage in susceptible larvae (Rodríguez-Cabrera et al., 2008; Gullipalli et al., 2010; Lei et al., 2014, Pavani et al., 2015). Various glutathione S-transferases (GSTs) transcripts belonging to various super-families were identified in *A. janata* transcriptome analysis. In the present study, "GST-delta 4, GST-epsilon, Cytochrome p450 and Cu-Zn superoxide dismutase" expression was significantly upregulated however GSTs including "GST-omega,-sigma, -zeta and -theta" was marginally downregulated or unaffected (Fig. 16).

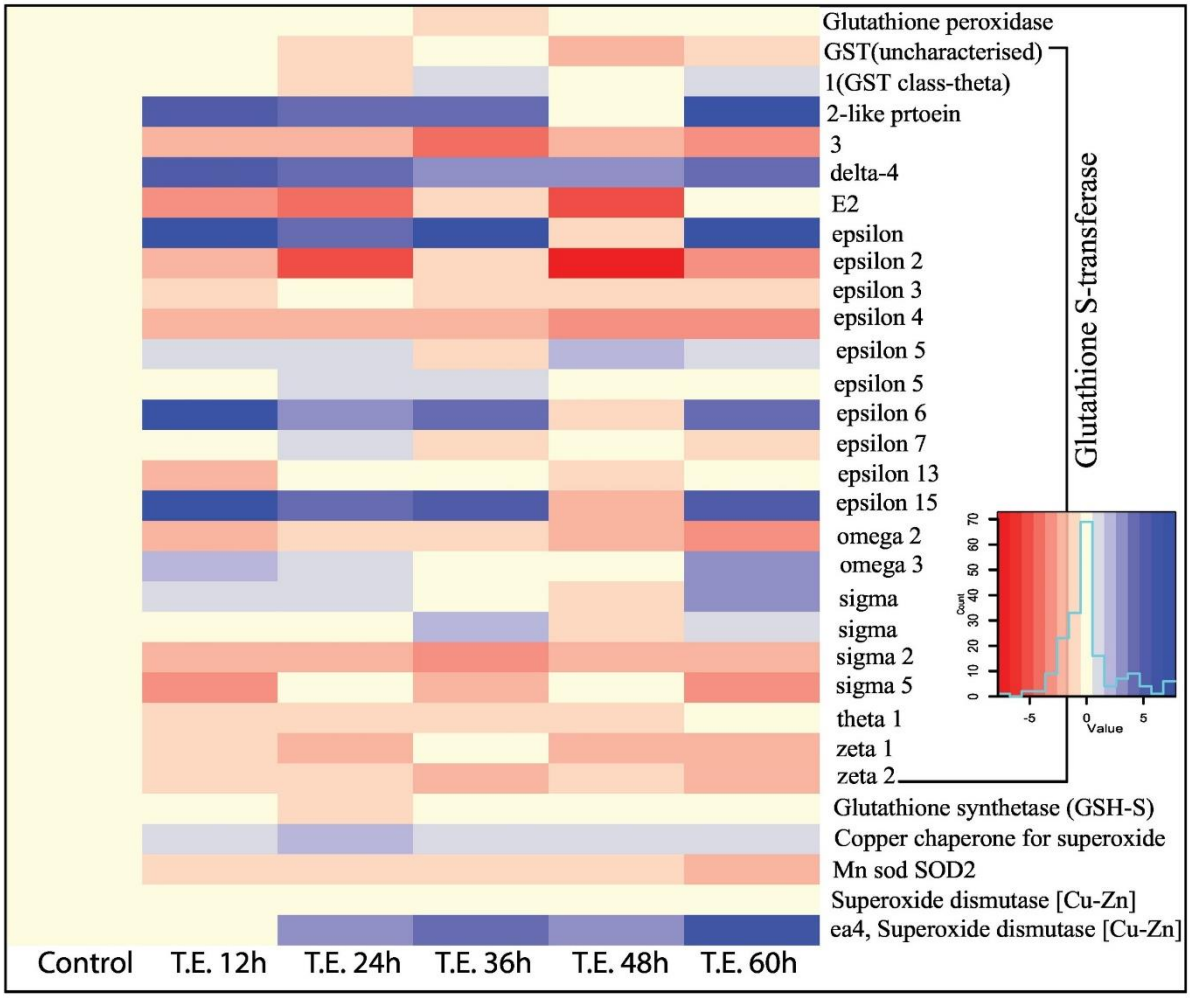

Fig. 16. Expression analysis of detoxification enzyme transcripts at various time point of Cry toxin exposure.

3.12 Expression of aquaporins

Aqua-glyceroporin and aquaporin transcripts (Aquaporin-1 and Aquaporin-Gra2) were identified in the present larval midgut transcriptome. Notably, transcript expression of both "integral gut membrane water-transport" proteins was seen to be downregulated during toxin exposure (Fig. 17).

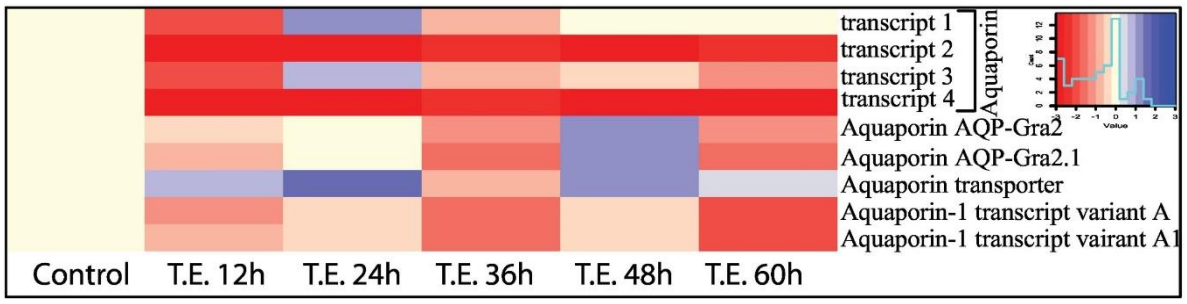

Fig. 17. Profile of aquaporin and aqua glyceroporin transcripts expression during Cry toxin exposure.

4. Discussion

In the current study RNA sequencing was carried out using Illumina platforms that account for large data size, precision and ease. Sequence assembly was done using Trinity which is one such efficient tool for a robust *de novo* assembly of transcriptomes particularly of species without a reference genome (Yin et al., 2014; Song et al., 2016). Trinity revealed the presence of large number of genes which was reported in *A. janata* transcriptome. Further a detail analysis was carried out using the transcripts associated with five important classes' viz., "Cry toxin receptors, gut proteases, arylphorins & REPATs, detoxification enzymes and aquaporins" to evaluate their role during Cry toxicity.

Description of Bt insecticidal proteins relation with their hosts is crucial for understanding the molecular basis of Bt specificity and its insecticidal activity. Various studies demonstrated that APNs and cadherins are the functional Cry toxin receptors in large number

of lepidopteran speices including *A. janata* (Xu et al., 2005; Pigott and Ellar, 2007; Chauhan, 2017). However so far eight different classes of aminopeptidaseN have been characterised in lepidopteran insects (Crava et al., 2010, 2013; Lin et al., 2014). APNs differential expression and its subsequent binding to Cry toxin proteins was shown to determine insect's susceptibility or tolerance to the toxin (Pigott and Ellar, 2007; Tiewsiri and Wang, 2011; Qiu et al., 2017; Chauhan, 2017). Pacheco et al., (2009) proposed "ping-pong" binding mechanism, where in initially APNs bind to the Cry toxin, promote toxin localization at the brush border and facilitate its successive binding to cadherin. Following which the toxin binds to aminopeptidase(s) with a higher affinity for post oligomerization. Moreover, cadherin gene mutation has been reported to be associated with the generation of Cry toxin resistance (Xu et al., 2005; Zhao et al., 2010; Pardo-Lopez et al., 2013; Fritz et al., 2019). In present study, upregulation of APN2 transcripts and mutant cadherin was observed to implicates their role in Cry toxication.

The lepidopteran larvae require a repertoire of "proteolytic enzymes including trypsins, chymotrypsins, aminopeptidases, carboxypeptidases, elastases and cathepsin-like proteases" for protein digestion. In lepidopteran larvae, protein-digestion primarily depends on trypsin, chymotrypsin and serine protease active sites. Budatha et al., (2007) reported multiple isoforms of trypsin and chymotrypsin in *A. janata*, as well as in other lepidopteran insect species the same was reported in associtation to "naturally occurring antagonistic biomolecules" and/or "adaptation to their different food sources" (Zhu-Salzman and Zeng, 2015). Bravo et al., (2007) and Budatha et al., (2007) showed activation of protoxin which is mediated by midgut proteases, particularly trypsin and chymotrypsin. In present study, the reduced transcript levels of trypsin, chymotrypsin and elevated levels of serine protease inhibitors were shown during sublethal exposure of Bt toxin. Reduced activities of trypsin and chymotrypsin were correlated to decreased conversion of protoxin which activates Cry toxin, a well established phenomena

(Oppert et al., 1997; Pardo-Lopez et al., 2013; Adang et al., 2014). Further the involvement of altered trypsin, chymotrypsin and proteinase/protease activity has been shown in the context of Bt resistance among several lepidopteran insects (Li et al., 2004; Zhu et al., 2011). It was demonstrated in a recent study that trypsin gene downregulation is correlated with the development of Bt toxin resistance (Yao et al., 2017). In contrast, the present study demonstrates high expression of serine protease inhibitor transcripts which successively reduce gut protease activities and thereby prevent any further gut tissue damage and induce Cry toxin tolerance.

In current study, arylphorin expression was upregulated during 36-48 h time span of Cry toxin exposure from "log2 value of -7 fold to 1.6 fold". This coincides with active cell proliferation phase which was demonstrated by BrdU labeling in *A. janata* larvae (Chauhan et al., 2017). In *H. virescens* mitogenic effect of arylphorin was reported to play a significant role in midgut regeneration during Cry induced damage (Castagnola and Jurat-Fuentes, 2011; 2016). In addition to that REPAT "low molecular weight proteins" gene expression was shown to be associated with midgut cells. Under the αREPAT and βREPAT groups, forty six REPAT proteins have been characterised. In *Spodoptera* larvae REPAT genes differential expression was reported upon Cry toxin exposure (Navarro-Cerrillo et al., 2013). In Cry1Ca treated *Spodoptera* larvae, upregulation of REPATs 4, 21, 32, and 42 transcript expression was observed in midgut stem cells, whereas REPAT 39 and 44 were shown to be downregulated (Navarro-Cerrillo et al., 2013). Genes are modulated upon toxin exposure in species specific manner and REPATs differential response seen in the present study upon Cry toxin exposure corroborates well with previous findings and suggests the same.

Variety of insecticides are used for the management of insect that infests agricultural crops. Insect's are known to detoxify them using various metabolic pathways. In general insecticide detoxification happens in two phases- "phase I enzymes", include cytochrome P450

proteins (P450s) which participate in metabolism of xenobiotics. These enzymes are divided in four groups; CYP2 (Cytochrome P family), CYP3, CYP4, and mitochondrial (Feyereisen, 2006). “Phase II enzymes”; include GSTs, which transform allelo-chemicals into water-soluble compounds for excretion. In insect’s GSTs are classified into seven major classes: “sigma, zeta, omega, theta, microsomal, delta, and epsilon” (Friedman, 2011). In present transcriptomic analysis, GST sigma, omega, delta, and epsilon classes of genes are shown to be present in *A. janata*. Among them, only GST-delta 4 was upregulated upon Cry toxin exposure. In addition, Cu-Zn superoxide dismutase expression was also upregulated in *A. janata*. These findings corroborated well with the report of higher enzymic activity seen in the larval forms of *S. litura* fed on Cry1Ab transgenic crop (Yinghua et al., 2017).

Like other animals, the osmotic balance in insect is also regulated by aquaporins (Spring et al., 2009). Cohen, (2012) suggested that aquaporins also plays a vital role in developing cold tolerance as well as evolving resistance against desiccation. Only few aqua-glyceroporins have been characterised in insects up till now (Campbell et al., 2008; Ishibashi et al., 2017). A recent report on hemipteran white-backed planthopper, *Sogatella furcifera* demonstrated altered mRNA levels of aquaporin upon insecticide exposure (Zhou et al., 2018). Moreover in *Aedes aegypti* mosquito larvae, enhanced desiccation resistance was shown to associate with downregulation of aquaporins (Drake et al., 2015). In current study we reported downregulation of aquaporins and aqua-glyceroporin transcript during Cry toxin exposure. However, the exact significance of them has to be looked in and further studies need to be carried out to elucidate their exact role during Cry toxicity.

Using 15 selective gene, qRT-PCR analysis was carried out to validate *in silico* (NGS and microarray) differential expression of transcripts. Results of transcriptome and microarray analyses were found to be in agreement with the expression pattern of the genes. The findings of the present study revealed that a repertoire of differentially expressed transcripts are

involved in Cry toxin induced responses in *A. janata* larvae. Current RNA-Seq analysis provides first step towards unraveling the molecular mechanisms at transcriptomic level. Results from this chapter potentially aid to develop strategies against toxin resistance in Bt-exposed insect larvae. In near future, studies will be carried out to investigate that whether the reported DEGs in this study are truly associated with Cry toxication in *A. janata* larvae and aimed to provide a basis for their functional role in pest management and Bt toxin tolerance/resistance.

The lack of adequate information about insect pest genome and transcriptome limit our ability to determine the molecular mechanisms of altered physiological responses in Bt-exposed susceptible and tolerant insect strains. The present study reports midgut *de novo* transcriptome assembly and clustering of susceptible Cry toxin exposed and Cry toxin tolerant *A. janata* larvae with appropriate age-matched and starved controls as well. This will facilitate us for more efficient biocontrol of *A. janata.*

It is now possible to characterize complete repertoire of transcripts under different conditions with the advent of next generation sequencing technology, further one can also predict pathways with their molecular mechanisms. The RNA Sequencing data presented here is the first *de novo* transcriptome assembly of castor semilooper larvae. The work has been recently published in two different research article (Dhania et al., 2019a; 2019b). Further a comparison of gene expression signatures between toxin exposed susceptible and tolerant larvae provides the primary basis for Cry tolerance in the pest, which could be utilized for designing the safe pest management strategies of economically important lepidopteran pest castor semilooper that causes serious loss of castor crop in Indian continent.

Chapter 3

Analysis of regeneration:

a) Evaluating the role of arylphorins in regeneration and repair of midgut epithelium.

b) Analysis of epithelial alteration in APN profile of Cry toxin susceptible and tolerant larvae.

1. Introduction

Insect midgut epithelium symbolises border involving external and internal environment in the insect body cavity. This unique tissue supports various functions such as food uptake, enzyme secretion, digestion, absorption, transport of ions and nutrient as well as others functions such as the first line of defence against various infectious microorganisms. Release of signalling molecules including various hormones that regulate general physiology of insect is also one of the important characteristics. As discussed in "General Introduction" and demonstrated in Chapter 1, the larval epithelium consists of columnar cells, epithelial cells, Goblet cells and stem cells. Furthermore, these various cell types are located at a specific site in epithelium such as the stem cells are primarily present at the basal side of epithelium, while the differentiated and mature secretory/absorptive cells with microvillar border are present at the apical end, towards the luminal side. During the evolution, insects are known to undergo enormous changes in various parts of alimentary canal, reflected by variety of adaptations, primarily to meet the adverse conditions (Terra 1988). Larval midgut represents a specific section that is derived from the endoderm during embryonic development which acts as an effective defense barrier for entrance of the pathogens in haemocoel where majority of other visceral tissues are localized (Ryu et al., 2010; Huang et al., 2015). A complex regionalization was also seen in the midgut where, the anterior, middle, and the posterior regions could be characterized with specialized features, such as columnar cell morphology, region specific gene expression, presence of atypical cell types, secretion of different digestive enzymes, altered luminal pH, differential microbiota load and varied cellular architectural arrangement (Lemos and Terra 1991; Buchon et al., 2013; Broderick et al., 2014; Buchon and Osman 2015; Pimentel et al., 2018; Bruno et al., 2019; Casartelli et al., 2019). Due to such uniqueness, the midgut is emerging as a fascinating tissue for investigation of regeneration and recovery after toxin damage (Loeb et al., 2001; Castagnola and Jurat-Fuentes 2016; Janeh et al., 2017). *Drosophila*

melanogaster has been well studied and the presence of midgut stem cells, their involvement in active regeneration of tissue upon variety of damages induced by various factors/ physiological reasons is being widely investigated (Bonfini et al., 2016; Jiang et al., 2016). In lepidopteran larvae, midgut tissue remodelling has also been analysed during metamorphosis as well as during complete renewal of alimentary canal (Morgan, 1901; Hakim et al. 2010; Romanelli et al. 2016; Tettamanti and Casartelli 2019; Tettamanti et al. 2019). The total cell number increased during each larval instar and was supported by repetitive stem cell proliferation (Baldwin and Hakim, 1999; Hakim et al., 2007). However in *Drosophila*, the larval epithelium showed constant number of intestinal stem cells, which underwent symmetrical division in response to enriched nutrients (O'Brien et al., 2011). In addition, once stem cell differentiated they were incapable of division (Lu and Li, 2015).

To the best of our knowledge and the search of literature survey revealed that the lepidopteran insect larvae have not been investigated well for stem cell proliferation. However, they serve to be an ideal model to elucidate regeneration because cells in the epithelium, divided and differentiated during molting (Sadruddin et al., 1994). In addition, majority of the existing reports on regeneration were carried out using the primary midgut cell culture (Loeb et al., 2001, Castangnola and Jurat-Fuentes., 2011). Further, these cultures were transient in nature and were not stable cell cultures. During the initial period of work, we also tried establishing *A. janata* midgut primary cell culture but were not able to successively propagate them due to high levels of contamination which was primarily associated with the luminal food content. However, few reports in lepidopteran species do claim the isolation of *Drosophila* type intestinal stem cells which undergo asymmetric cell division during growth and repair (Inaba and Yamashita, 2012). Loeb (2010) demonstrated the division of lepidopteran intestinal stem cells by adding midgut differentiation factors called MDFs. Later, in *Heliothis virescens* larvae, midgut stem cells were cultured by adding fetal bovine serum in media and in the same study

active cell proliferation was demonstrated to be induced by Albumax II (Castangnola and Jurat-Fuentes., 2011). Hakim et al., (2010) also discussed several other mitogens for cultured stem cell systems which were identified from conditioned media as well as from the larval hemolymph of various insects (Hakim et al, 2010).

Midgut differentiation factor (MDF) was identified as a peptide with 30 amino acid which exhibited high similarity to fetuin towards C-terminus end (Loeb at al., 1999). This fetuin like peptide was also reported to promote cell division and cell attachment in mammalian cell cultures (Nie, 1992). However midgut cell culture of *H. virescens* was reported to be unaffected when supplemented with undigested fetuin but proliferation was promoted after addiction of tryptic digested fetuin peptide supplementation and was termed as midgut differentiating factor 2 (Loeb at al., 1999). This was followed up by identification of several other midgut differentiating factors and named MDF3 and MDF4. Both of these were obtained after chymotryptic digestion of MDF extracted from *Lymantria dispar* haemolymph (Loeb and Jaffe, 2002). Though midgut differentiating factors were shown to promote the differentiation but never with 100% efficiency, which suggested that there might be several other molecules that were responsible and played a synergistic role in midgut cell proliferation as well as differentiation. Factors/molecules like ecdysone (Boudjelida et al., 2005), α-arylphorin (Blackburn et al., 2004) and insulin-related Bombyxin (Goto et al., 2005) were also demonstrated to promote midgut cell differentiation when supplemented in culture media.

Amongst afore mentioned factors, α-arylphorin was reported to be a major differentiating factor in *in vitro* midgut cell cultures as well as under *in vivo* conditions, and it was proposed as a mitogen for midgut mitogenic activity (Blackburn et al., 2004; Hakim et al., 2007; Castangnola et al., 2017). Earlier this aromatic amino acid (phenylalanine, tryptophan, tyrosine, histidine) rich protein commonly known as hexamerin (arylphorin) was reported to present in very high level in the haemolymph during the growth of last larval instar, where the

larvae attained maximum size during postembryonic development (Kramer et al., 1980; Willott, 1988; Ismail et al., 1993). Same was reported again with *in vivo* effect, when the 4th instar larvae were fed with arylphorin supplemented diet, larvae showed increased in weight gain after feeding (Hakim et al., 2007). Other than intestinal stem cell regeneration, lepidopteran cell proliferation was also reported to regulate by tracheal regeneration. Nardi et al., (2011) demonstrated that in *Manduca* tracheal epithelial stem cell increased number during larval molting were supported by muscle layer present beneath the basal epithelium.

In lepidoptera, during molting extensive intestinal stem cell proliferation reported is known to restore epithelial integrity (Baldwin and Hakim, 1991). Further similar restoration of lepidopteran larval epithelium was also reported during abiotic and biotic stress or injuries (Huang et al., 2016). This healing responses not only involved, intestinal stem proliferation but also other additional processes, as an example after physical perforation of gut in *Bombyx mori*, recruitment of hemocytes followed by production of melanized scab and repair of damaged epithelium associated with stem cell proliferation was detected by DNA synthesis (Huang et al., 2016). Furthermore, *Bacillus thuringiensis* infection based damage was also shown to be repaired by midgut regenerative response (Spies and Spence, 1985; Chiang et al., 1986). This suggested that Cry toxin promoted damage and facilitated stem cell proliferation in midgut stem cell cultures (Loeb et al., 2001). Hernández-Martínez et al., (2010) reported up regulation of arylphorin and other gene transcripts during Bt pesticide intoxication. As mentioned above that insects represent exceptional variety of morpho-functional adaptations when they were fed with Cry toxin containing food, the larvae continuously replaced the damaged cells which is invariably associated with midgut stem cell proliferation and mediated by MDF-1 (Loeb, 2010). Replaced epithelium upon continuous exposure showed alteration in cellular properties such as changes in cell surface profile which also lead to the development of resistance in insects (Spies and Spence, 1985; Martinez-Ramirez et al., 1999; Castagnola and Jurat-Fuentes,

2016). Lehane, (1997) suggested that insect evolution was driven by nutritional quality, food texture, type (solid, liquid) and other factors which facilitated the specialization of various cell's in gut.

Additionally larval midgut arrangement allowed contact of the anterior and posterior parts of alimentary canal which facilitated removal of excess water and concentration of ions as well as nutrients (Hubert et al. 1989; Lehane and Billingsley, 1996; Le Caherec et al. 1997; Shanbhag and Tripathi, 2009). As discussed earlier in General Introduction, Bt toxication primarily damaged the midgut section of alimentary canal, in current chapter we have evaluated and discussed about the role of arylphorins during sublethal Bt toxin exposure. Earlier mentioned reports from Blackburn et al., (2004); Hakim et al., (2007); Castangnola et al., (2017) suggested arylphorin to be the major differentiating factor in midgut and termed this as mitogen. This arylphorin protein primarily a hexamerin is a well known storage protein with multiple functions. Hexamerins are synthesized by fat body and released into the haemolymph during active feeding phase of larvae. They are hexameric in nature which could be either a homomers or heteromers with a subunit size of 70-90 kDa (Telfer and Kunkel, 1991; Burmester, 1996, 1998, 1999; Hathaway et al., 2009). Hexamerins constitute 70-85% of haemolymph protein in final instar and based on their chemical composition. The subunits are divided into i) arylphorin, ii) methionine rich and iii) riboflavin binding proteins. Receptor mediated sequestration of these proteins by different visceral tissues are well demonstrated (Ismail et al., 1991; 1993; KiranKumar et al., 1997; Pan et al., 2001; Chandrasekar et al., 2008; Budatha et al., 2011; Martins et al., 2011). During amino acids requirement, these stored proteins in the fat body get hydrolysed and become accessible to support the insect's metabolic needs. Telfer and Kunkel, (1991) and Burmester, (1999) initially proposed hexamerins act solely as storage proteins that provide amino acids and energy during non-feeding periods. Effect of fat body extract (synthesis and storage site of hexamerins) was also demonstrated to

be associated with midgut cell proliferation, a purified protein from fat body extract showed growth in larval midgut cell (Smagghe et al., 2003). Presence of exogenous arylphorin is significantly high in midgut regenerative cells suggesting that it might play an important role in cell proliferation. In this chapter we discuss about two different types of arylphorin (i) exogenous and (ii) endogenous arylphorins and evaluate their role in midgut regeneration. Confirmation of endogenous arylphorin was carried out using real time PCR and *in-situ* hybridization. Further the involvement of Cyclin B, which is known as hallmark for cellular proliferation was also checked for midgut stem cell proliferation/ regeneration in the midgut of castor semilooper.

As discussed in Chapter 2, we had generated laboratory based tolerant larval population subjected to sublethal dose of DOR Bt-1 formulation exposure and reared for following 15 generations. Aminopeptidase N are well known Cry toxin receptors, in lepidopteran insect and has already been reviewed in General Introduction. In this chapter we carried out a detailed analysis of epithelial alteration if any in APN profile using Cry toxin susceptible and tolerant larvae. The study in this chapter was primarily aimed to carry out an comprehensive analysis of susceptible and tolerant larval midgut at the cellular level. Along with cell morphology, development of altered epithelium in sublethal toxin exposed tolerant larval population of *A. janata* in a fifteen generation analysis is being reported in current study.

2. Materials and Methods

2.1 Sequence analysis

Arylphorin sequences were pooled out from transcriptomic sequence data, presented in Chapter 2, and were analysed using Basic Alignment Search Tool based algorithm. Homology of these sequences were checked using sequence database available on NCBI web portal. Obtained sequences from NCBI database and Illumina seq result was aligned based on CLUSTAL format alignment by MAFFT (v7.427). MAFFT based L-INS-I result was obtained. Fat body arylphorin (named as exogenous arylphorin in the present study) and midgut arylphorin (endogenous arylphorin) were analysed using open Rost Lab software (https://rostlab.org/).

2.2. Haemolymph collection

For the current experiment 4th instar larvae were narcotised (Fig. 1). After ensuring numbing of larvae, larval prolegs was carefully excised using sharp scissors which were sterlized. Larvae was bled directly into 1.5 ml Eppendorf tube, pre-coated with 0.1% of phenylthiourea. Phenylthiourea was added to stop the melanisation and tyrosine kinase activity in the haemolymph. Before processing the haemolymph sample was centrifuged for 2 min at 4000 rpm. Centrifugation was carried out at 4℃ to sediment the haemocytes. Collected supernatant, which contained hexamerins and was used for sequestration analysis.

Fig. 1 Showing larvae narcotisation using ice based cold shock therapy. This helped in maintaining the insects in immobilized state for collection of haemolymph.

2.3 Alexa Flour labelling of haemolymph protein

Our group has already demonstrated the sequestration of hexamerins (Arylphorin; confirmed with sequence similarity) by the fat body, salivary gland, male accessory reproductive glands and ovary (Ismail et al., 1991; 1993; KiranKumar et al., 1997; Damara et al., 2010; Budatha et al., 2011). With this prior knowledge and that arylphorin is large sized (~75 kDa) protein, the isolated haemolymph was concentrated using sucrose bed dialysis (Fig. 2). Diluted haemolymph was transferred to dialysis membrane bag with 50K MWCO, which retained the all proteins with at least size of 50 kDa. The bag was sealed with plastic clips and placed on dry sucrose bed, which allowed excess of fluid to get drained out.

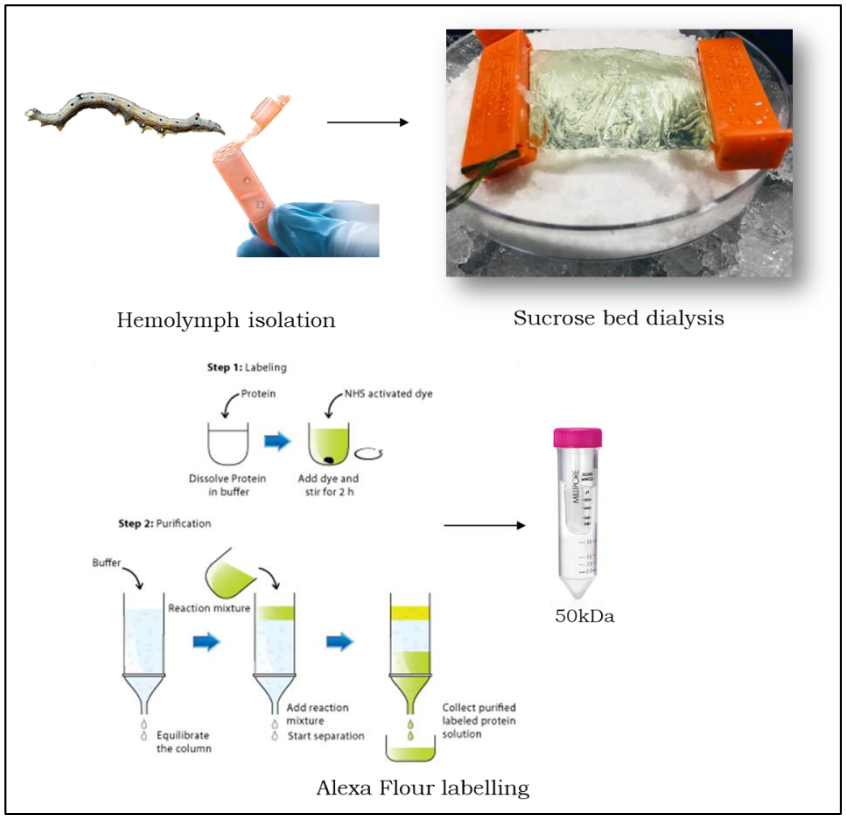

Fig. 2 Collecion of haemolymph from narcotised larvae by cutting their prolegs. The haemolymph was diluted and transferred to dialysis bag (50 kDa pore size cutoff) and concentrated using sucrose bed. The haemolymph proteins were labelled with Alexa Flour using kit based protocol.

Concentrated protein (100 µl of 1 mg/ml) was diluted in 0.1 M sodium carbonate buffer (pH 9.2), was added with Alexa Flour^{TM} 488 NHS Ester (Succinimidyl Ester) (Invitrogen, USA) activated dye provided in protein labelling kit. Reaction mixture was kept for slow stir

at 4℃ for 4 h. The labelled protein was purified using column provided in kit. Column was first thoroughly equilibrated with equilibration buffer (0.1M sodium carbonate buffer in MilliQ water). After equilibration reaction mixture was added the column (Fig. 2; this was adopted from Invitrogen manual). After separation started, purified labelled protein was collected. The total process was carried out either in dark room or the column and tube were covered with aluminium foil. Labelled protein mixture was electrophoresed using 10% SDS-PAGE for quality check. Unbound fluorescent dye was separated from labelled protein by Millipore Amicon ultra centrifugal filters with 50 kDa cut off size.

2.4 Microinjection

Labelled hexamerin protein was injected into *A. janata* 3rd instar larvae. Hamilton syringe (Hamilton™) was used for the microinjection. Before microinjection larvae were narcotised using ice based cold shock therapy. After numbing of larvae, they were blot dried using soft tissue paper, followed by injection of labelled protein between intersegmental membranes through anterior side of the larvae (Fig. 3). Prior to injection labelled protein sample was once again checked under UV illuminator for confirmation of sufficient fluorescence (Fig. 3). After injection, needle was gently pulled out and the wound was sealed with moulten paraplast to prevent leakage of haemolymph. Once again the larvae were placed back on ice for 30 min. Later they were transferred to fresh castor leaves and maintained for different time period.

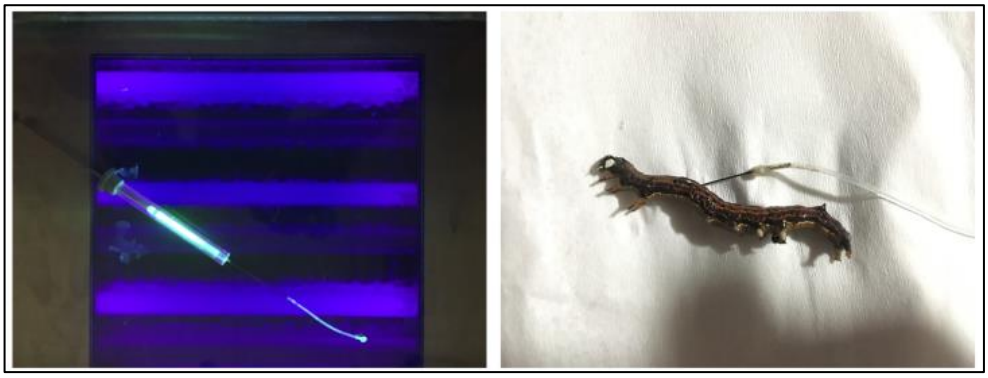

Fig**.** 3 Haemocoelic injection of Alexa Flour labelled hexamerin (arylphorin) into 3rd instar larval haemocoel using Hamilton microsyringe.

2.5 Sequestration analysis of labelled arylphorin using confocal microscopy

For this study, the larva injected with labelled hexamerin protein (Fig. 3) was dissected carefully under moderately dark condition and various tissues were collected. For the fluorescence observation confocal laser scanning ZEISS LSM 900 microscope (CLSM) was used. Fluorescent image capturing was done using microscope integrated Axiocam cameras enabled with low-noise electronic and cooled image sensing. Captured images were further processed using microscope integrated ZEN Imaging core software. Image acquisition and processing was performed using setting up image processing speed time. Image data acquisition was optimized by frame acquisition at multiple positions. For final image capturing, region of interest (ROI) was defined and the ROI was captured with scanning field of 6144 x 6144 pixels. Few tissue sample were also analysed along z-axis, optical serial sectioning was carried out by suitably modified plane and ROI followed by the production of clear images of fairly thick midgut samples. Excitation/emission spectra of individual flour component was used for setting up the wavelength.

Arylphorin incorporation was also analysed during sublethal Cry toxin exposure. Prior to sublethal exposure larvae were injected with labelled arylphorin using microinjection. As discussed in previous section, 3rd instar larva were fed with Cry toxin and they were collected at 12 h, 24 h, 36 h, 48 h, 60 h and 72 h time frame after Cry toxin exposure. The larvae were narcotized by keeping them for 15-20 min on ice, and the tissues were dissected as mentioned in earlier section.

2.6 Cell proliferation analysis using BrdU incorporation

Midgut cell proliferation analysis was carried using BrdU incorporation (Invitrogen Corporation, USA) following the manufacture's protocol with small alteration. For the current experiment, prior to tissue isolation, larvae were injected with BrdU labelling reagent (10 µl/g

body weight). Microinjection was carried out similar to afore mentioned method in section (2.4). After different time points, the midgut tissue was dissected and fixed in 4% PFA for 12-14 h. Embedding and sectioning was done in similar pattern as mentioned in General Materials and Methods section. After removing paraplast from the embedded midgut sections, quenching was performed using peroxidase with 30% H_2O_2 in absolute methanol (1:9) and the flouro-immunocytochemistry of injected BrdU was carried out. Firstly slide was washed twice with PBS (pH 7.4) for 10 min then tissue blocking was done using 5% BSA dissolved in PBST (0.1% Tween 20). After blocking slide was over flowed with primary antibody solution, mouse monoclonal BrdU Antibody [MoBU-1 (B35128, Invitrogen)] in 1:500 ratio, diluted with 2% BSA-PBST solution and incubated for 12-14 hr at 4°C. Slide was re-washed using PBS and antibody detection was carried out using anti-mouse IgG secondary antibody (tagged with Alexa Flour 555). Visualization of stained section was carried out using confocal microscope at specific wavelength (mentioned in section 2.4). For colocalization of labelled arylphorin and BrdU proliferative cells, prior to sublethal exposure larvae were injected with labelled arylphorin using microinjection.

2.7 cDNA synthesis and qRT-PCR validation

Gene specific primers for midgut specific arylphorin, Cyclin B, Cyclin E, Cyclin J and CDK2 were designed for qPCR analysis. After manually designing the primers, they were analysed using Oligo analyzer tool 3 (Table 1). Each primer was individually checked for oligonucleotide properties such as melting temperature, hairpins, dimers and mismatches etc. and commercially procured (Integrated DNA Technologies Inc, USA). Before proceeding to the qPCR each primer set was checked using regular PCR followed by detection of amplicon using agarose gel electrophoresis. After primer confirmation qPCR reaction was carried out, in each 10 µl reaction mixture 1 µl of each primer (10 µM), 1 µl of sample cDNA, 10 µl of master mix (SYBR® Green) was added. Reaction was programmed in qRT-PCR system (Step-One

Plus, Thermo Fisher Scientific). The qPCR theromocycling parameters: 95 °C for 10 min, 40 cycles of 95 °C for 30 s and 60 °C for 30 s, were programmed and followed by melting curve generation (59 to 68 °C). Each qPCR reactions were performed thrice for obtaining biological replicate and each time three technical replicates were used in the reaction. Cycle threshold was obtained for each reaction and comparative Ct was calculated using Schmittgen and Livak, (2008) mehtod. Calculation of change ($2^{-\Delta\Delta CT}$) in Ct value with respect control was carried out using Microsoft Excel and obtained value was statistically analyzed by Sigma Plot software (v14.0, Systat Software Inc., USA). To check the significance of $2^{-\Delta\Delta CT}$ value One-Way ANOVA analysis was carried out, followed by SNK test (Student-Newman-Keuls). Comparison between each set of experiment was performed and plotted as P value for each set of experiments.

S.No.	Sequence Name	Sequence (5'-3')
1	Aryl FP	GTCATGTGCTTGGCGCAAGT
2	Aryl RP	CGAAACTTTCGGGCTGTTGCTG
3	Aryl T7 FP	TAATACGACTCACTATAGGGGTCATGTGC TTGGCGCAAGT
4	Aryl SP6 RP	ATTTAGGTGACACTATAGAACGAAACTTT CGGGCTGTTGCTG
5	Cyclin B FP	GCCCTTTGGAGAATGTGGCAA
6	Cyclin B RP	CATCACAGTCACACATGCTGTTCC
7	Cyclin J FP	CCCATCGCCAGGTTACTGCAG
8	Cyclin J RP	CTACGTTGAGTTGGCTGCGGG
9	Cyclin E FP	GCCCTTTGGAGAATGTGGCAA
10	Cyclin E RP	CATCACAGTCACACATGCTGTTCC
11	CDK2 FP	CCACGATTGCTGTGAGTGTGC
12	CDK2 RP	GCCTGGCTGTTATTGCCATGG
13	APN2 FP	CGCTCCACCACAGTACAATGTTGTC
14	APN2 RP	CTCTGAAGGGAATGTTGAAGATGGGA
15	APN4 FP	CACCCGTGACATCAATCTTAGCCCT
16	APN4 RP	CGTGGGTAAGATCTTCAGCGATCG

Table 1. List of primers used for PCR expression analysis of control and toxin exposed larval RNA samples and RNAi as well as dsRNA RNA preparations.

2.8 Western blot and immunohistochemical analysis for the detection of Cyclin B

A. janata Cyclin B antibody was not available so the NCBI database was checked for sequence similarity. Interestingly, human Cyclin B showed resemblance with *A, janata*

sequence, using this information Cyclin B sequences were pooled out from transcriptomic sequence data, mentioned in Chapter 2. These sequences were checked using Basic Alignment Search Tool based algorithm. Homology of *A. janata* Cyclin B with Human Cyclin B sequence was checked using CLUSTAL format alignment by MAFFT (v7.427) and MAFFT based L-INS-I result was obtained. For antibody assisted analysis human antibody (monoclonal antibody; Sc7393, Santa Cruz Biotechnology) was used. Before proceeding for immunohistochemical analysis, cross reactivity of Cyclin B human sequence based monoclonal antibody with *A. janata* tissue protein was checked using western blot analysis. Laval midgut proteins/peptides were electrophoresed and transferred to nitrocellulose membrane (details mentioned in General Materials and Methods). The membrane was washed thrice for 15 min and then submerged in blocking solution (5% BSA solution with 0.1% Tween-20 containing TBS) to avoid non-specific binding. After 3 h of blocking the blot was washed with TBS-TBST-TBS, 15 min each, followed by incubation with Cyclin B (Sc7393) primary antibody with 1:1000 dilution (diluted in 2% BSA) at 4℃ for 12-14 h. Further, primary antibody was collected in 50 ml tube and blot was washed again with TBS-TBST-TBS, 15 min each to remove excess antibody. Incubation of blot was carried out with secondary mouse IgG conjugated with alkaline phosphatase. The secondary antibody was diluted with 2% BSA (1:4000) and blot was soaked for 3-4 h. The excess unbound antibody was removed from blot by washing with TBS-TBST-TBS and processed for blot development with BCIP/NBT (G-Biosciences, USA). Developed blot was immediately documented with Kodak Photo Imager.

For immunocytochemical detection of Cyclin B, midgut transverse sections were p`repared using cryotome and fixed on clean glass slide. They were rinsed twice with PBS (pH 7.4) for 10 min. Tissue blocking was done using 5% BSA dissolved in PBST containing 0.1% Tween 20. After blocking, the slide was over flowed with primary antibody of Cyclin B (1:500, dissolved in 2% BSA) and incubated for 12-14 h at 4°C. Then it was washed using PBST

solution (3 times, 5 min each) and antibody detection was carried out using anti-mouse IgG secondary antibody (tagged with Alexa Flour 555 and Alexa Flour 633). Visualization of stained slide was carried out using confocal microscope at specific wavelength.

2.9 Detection of various mRNA using fluorescence *in situ* hybridization

Larval midgut was dissected and fixed in 0.1 M PBS containing 4% PFA (pH 7.4) (Sigma-Aldrich, USA) and 5 µm transverse sections were obtained as discussed in General Materials and Methods section. *A. janata* arylphorin, aminopeptidase-2 and aminopeptidase-4 cRNA probes were prepared and midgut specific arylphorin gene fragment (289 bp) was prepared. T7 promoter sequence (5'-TAATACGACTCACTATAGGGAGA-3') based primer was used for synthesis of the antisense probe (positive), while Sp6 based promoter sequence (5´-ATTTAGGTGACACTATAG -3´) was used for sense probe (negative). *In vitro* transcription of DNA template was carried out using thermocycler followed by RNA probe synthesis using DIG RNA labelling kit using manufactures protocol (Roche Diagnostics, Germany). DIG labelled mRNA was synthesized and analysed using sequencing and agarose gel electrophoresis.

Cryotome cut midgut transverse section was fixed on the clean glass slide and washed with PBST buffer. Then it was permeabilized using proteinase K (1 µg/ml) and fixed again with 4% PFA. After fixation the slides were incubated with 200 µl hybridization buffer (50% formamide, 5X SSC, 1% SDS, 5 mM EDTA, 0.1% CHAPS, and 50 µg/ml heparin) for 1 h at 50°C. Laboratory prepared DIG labelled cRNA (added with 200 µl of hybridization buffer) probe was used and heat denatured by incubating it for 5 min at 80°C. While incubating the slides were covered with parafilm and kept in sterile incubator. After cRNA hybridisation, the slides were washed using wash buffer (SSC, 50% formamide, 0.1% Tween 20), five times for 5 min at 50°C. Each time SSC concentration was gradually decreased followed by incubation

of slides with solution A (10 mM Tris-HCl pH 8.0, 0.5 M NaCl, 5 mM EDTA, containing 0.1% Tween 20,) at RT for 5 min. To avoid any irrelevant contamination reaction was supplemented with RNase A (20 µg/ml) and incubated for 20 min at RT. After RNase treatment the probed sections slides were rewashed twice for 5 min with solution A. Followed by washing with maleic acid buffer (150 mM NaCl, 100 mM maleic acid, 0.1% Tween 20, pH 7.5) for enhanced antibody reaction at RT for 5 min, incubated with 5% BSA blocking solution at RT for 1.5 h followed by incubation with Anti-Digoxigenin-FITC antibody [21H8] (FITC) (ab119349) (1: 500) at 4ºC for overnight. These slides were washed four times for 15 min with DIG wash buffer (Roche Diagnostics, Germany). Visualization of fluorescent labelled section was carried out using confocal microscope at 480 nm wavelength as mentioned in Chapter 2 Section 2.5.

2.10 Double stranded RNAi preparation

A. janata arylphorin dsRNA as well as midgut specific arylphorin gene fragment (289 bp) were generated for this protocol. T7 promoter sequence added (5'-AATACGACTCACTATAGGGAGA-3') forward and reverse primers were used for the synthesis of dsRNA synthesis. Further *in vitro* transcription, based on midgut arylphorin cDNA template was carried out using Ambion® MEGAscript™ RNAi Kit (Invitrogen™, USA). Prior to final transcription T7 sequence attached cDNA template was prepared. PCR reaction was carried out with three different set of primers i.e. i) T7 sequence attached forward primer + gene specific reverse primer, ii) gene specific forward primer + T7 sequence attached reverse primer and iii) T7 sequence attached forward primer + T7 sequence attached reverse primer. PCR product of first and second reactions was used as template for third set of reaction. Finally the amplicon obtained was used for dsRNA synthesis. Final *in vitro* transcription reaction mixture consisted of 2 µg linear cDNA template, 8 µl nucleotide mixture (2 µl of ATP, CTP, GTP and UTP each), 2 µl 10X T7 reaction buffer, and 2 µl of T7 RNA polymerase enzyme and then the final volume made up to 20 µl using nuclease free water. The reaction mixture

was incubated at 37ºC for 6 h followed by short incubation (5 min) at 75ºC. Afore mentioned steps lead to formation of dsRNA complex, which was used for knock down experiments. For arylphorin transcript knockdown analysis, 4-5 µl of 100 ng dsRNA was microinjected into haemocoel Hamilton micro-syringe. Subsequently microinjected larvae were sacrificed for transcript analysis. For confirmation of appropriate nucleotide delivery larvae were microinjected with fluorescent nucleotide probe (ChromaTide™ Texas Red™-12-dUTP). As discussed in section 2.6 cDNA synthesis was carried out and efficacy of dsRNA was checked using qRT-PCR validation.

2.10 Brush border labelling

High affinity F-actin conjugated antibody probe was used for the detection of epithelial brush border. For immunocytochemical analysis of brush border, midgut transverse section fixed on clean glass slide was rinsed twice with PBS (pH 7.4) for 10 min. Tissue blocking was done using 5% BSA dissolved in PBST (0.1% Tween 20). After blocking slide was over flowed with primary antibody of Alexa Fluor® 647 phalloidin (1:500, dissolved in 2% BSA) and kept for 12-14 h at 4°C. Slide was re-washed with PBST solution and visualization of fluorescent stained section was carried out using confocal microscope at specific wavelength.

3. Results

3.1 Sequencing analysis for exogenous and endogenous arylphorin

Endogenous arylphorin sequences were pooled out from transcriptomic sequence data and sequence homology was checked by comparing it with exogenous arylphorin (Chauhan, 2017). CLUSTAL format alignment result is presented in figure 4. NCBI-BLAST based Sequence similarity analysis confirmed that both the sequence resemble with silkworm storage

protein, hemocyanin and others. Interestingly, endogenous arylphorin sequence resembled with *Bombyx mori* Sp3 transcription factor (sp3) sequence. Protein prediction for the sequence was done using PredictProtein© 1992-2019 Rostlab software, and result revealed endogenous arylphorin deduced amino acid sequence, showed a polynucleotide binding region, which was absent in exogenous arylphorin sequence (Fig. 5).

Fig. 4 CLUSTAL format based sequence alignment of endogenous arylphorin (gut) and exogenous arylphorin (fat body).

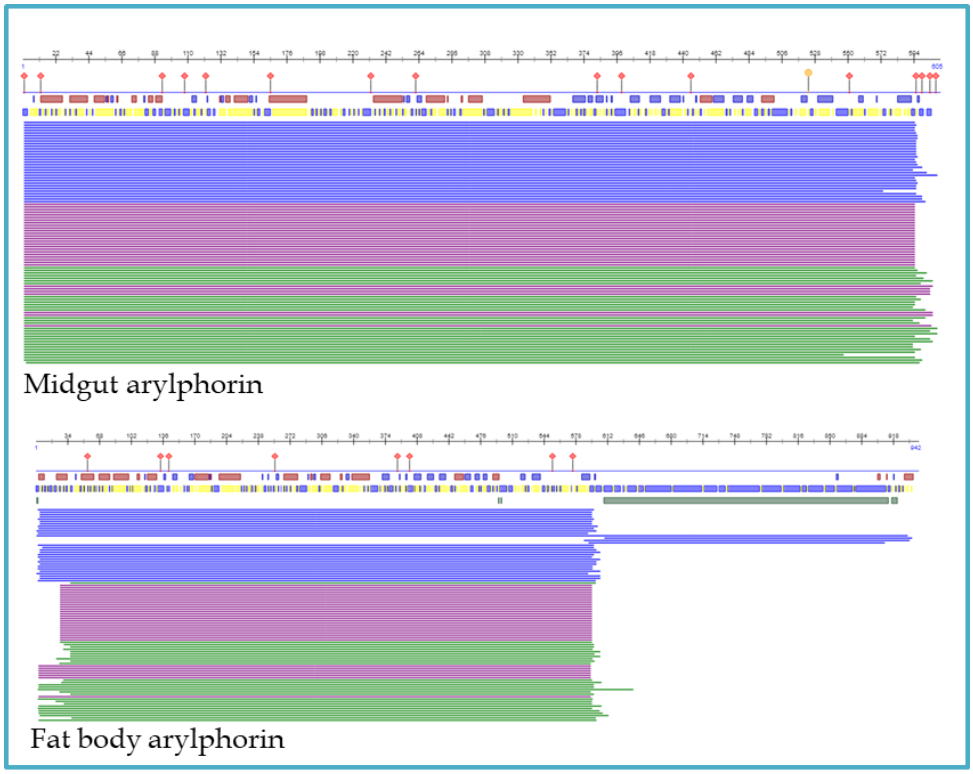

Fig. 5 Protein prediction analysis using deduced amino acid sequence, thr query is available online in Rostlab database (https://www.predictprotein.org/text_results?req_id=672366).

3.2 Analysis of Alexa Flour 488 labelled protein

Labelled protein mixture was electrophoresed using 10% SDS-PAGE in light protected chamber. The labelled fluorescent proteins obtained from *A. janata* larval haemolymph clearly show the presence of two fluorescent proteins in the expected molecular weight region of arylphorin (~75 kDa) (Fig. 6).

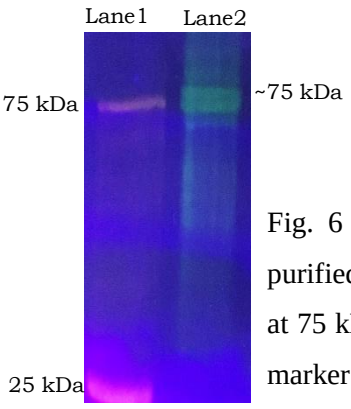

Fig. 6 Visualization of Alexa Flour labelled proteins- labelled protein was purified with kit based column separation. The intense thick band seen in lane 2 at 75 kDa size represents arylphorin protein. Lane 1 repersents molecular mass marker in kDa.

3.3 Sequestration of labelled arylphorin (exogenous) by larval midgut

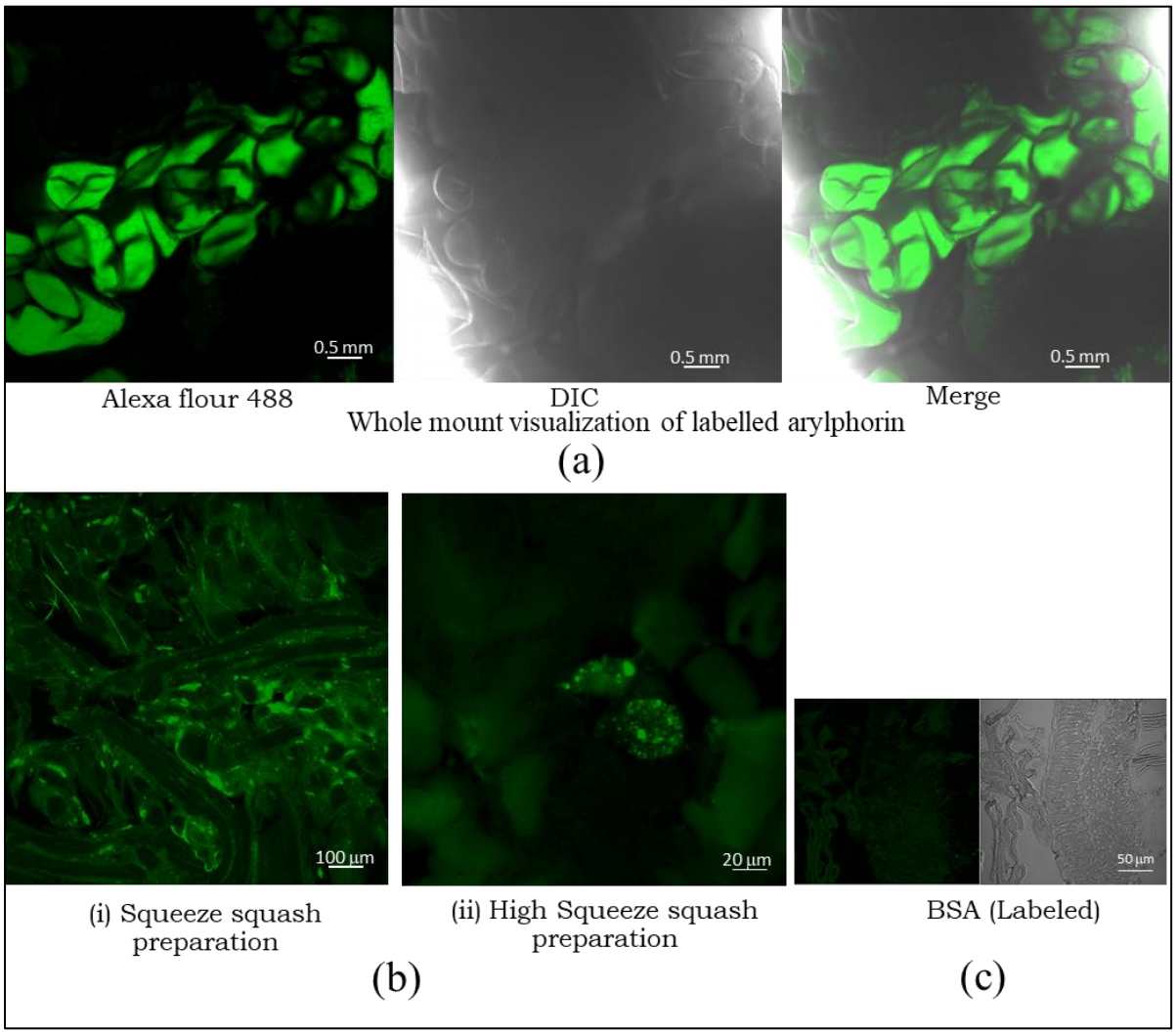

Fig. 7 Shows the sequestration of labelled arylphorin (exogenous) by midgut, a) Fluorescent green colour indicates the presence of labelled exogenous arylphorin which is present in midgut tissue (whole mount). b) Squeeze squash prepared from midgut tissue also confirmed the result as seen in whole mount, however high squeeze squash prepared sample clearly revealed presence of exogenous arylphorin in specific midgut cell. c) Please note that sequestration was not seen in midgut tissue isolated from larvae, injected with flour labelled BSA solution. Scale bar, in (a) 0.5 mm, (b) (i) 100 µm, (ii) 20 µm and 50 µm in (c).

Larva injected with labelled protein was dissected and whole mount of larval midgut tissue was visualized under confocal microscope. Results obtained clearly show that exogenous arylphorin gets sequestrated into midgut tissue dissected after 12 h of incubation period. High intensity of labelled protein was observed in whole midgut mount (Fig. 7a). This was followed by midgut visualization, using squeeze squash and high squeeze squash prepration (Fig. 7b)

and both of them showed presence of labelled arylphorin in cells. Labelled BSA was injected as positive control but there it did not sequestered (Fig. 7c)

3.4 Sequestration of labelled arylphorin by other visceral tissues

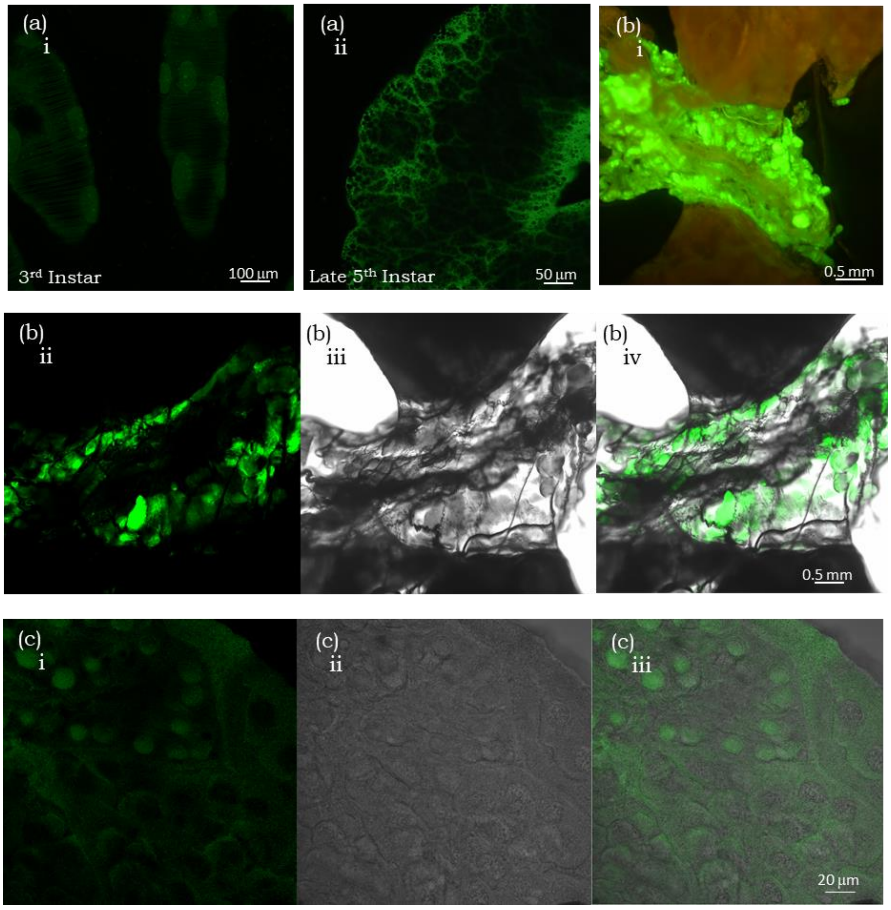

Fig. 8 Sequestration of labelled arylphorin (exogenous) after haemocoelic injection by other visceral tissues, a) Fluorescent green colour indicates the presence of labelled exogenous arylphorin, please note the sequestration of this protein and its presence (i) 3rd instar larval fat body (whole mount), ii) in transerverse section of fat body (late 5th instar larva). b) The sequestration was also seen in whole mount of vas deferens (i, ii) and MARG (iii, iv) as well as c) in transverse section of testis. Scale bar, in (a) (i) 100 µm, (a) (ii) 50 µm, (b) 0.5 mm and 20 µm in (c).

Larvae injected with labelled protein was dissected and different visceral tissues (fat body, vas deferens/ MARG and testis) were collected. They were visualized under confocal microscope and documented. Results obtained clearly show that exogenous arylphorin gets sequestered into other visceral tissues too after 12 h of incubation period. High intensity of labelled protein was observed in whole mount as well as transverse sections (Fig. 8) showing

its localization in various visceral tissues including testis. Further, labelled BSA experiment was carried out as positive control and it did not get sequestered.

3.5 Detection of presence of exogenous arylphorin in midgut muscle cells

For finding out the route of arylphorin entry in midgut, larva injected with labelled protein was dissected after 2 h of injection. Optical serial sectioning of whole mount of larval midgut tissue was carried out using confocal microscope. Presence of green fluorescence indicated the presence of labelled exogenous arylphorin at specific site. Results obtained clearly demonstrated the presence of exogenous arylphorin in outer layer of midgut which was selectively localized in midgut muscle cell (Fig. 9) suggesting that arylphorin molecules were sequestered through these cells.

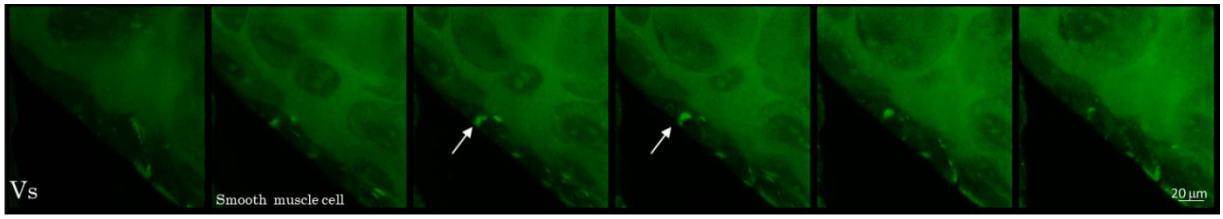

Fig. 9 Optical serial sectioning (0.5 mm) carried out after labelled protein microinjection for 2 h, figure shows localization of fluorescence green colour protein in midgut muscle (→) cells suggesting that the sequestration of labelled arylphorin (exogenous) is most like mediated by them. Scale bar, 20 µm.

3.6 Sequestration of exogenous arylphorin by midgut during Cry toxin exposure

Arylphorin sequestration was also analysed during Cry toxin exposure. Fluorescent labelled arylphorin was microinjected into larval haemocoel prior to sublethal Cry toxin exposure and kept for 72 h. Transverse section of larval midgut showed the presence of fluorescent labelled protein (Fig. 10). Intensity of green fluorescent colour was more towards the basal epithelium of both control and toxin exposed 24 h midgut tissue sample. In addition, significant number of labelled cells were visualised during 24 h and 36 h time point. Interestingly, during 60 h and 72 h time points these cells were present towards lumen side.

Studies using whole mount (Fig. 7) as well as transverse section (Fig. 10) parallely confirmed that exogenous arylphorin gets sequestered in midgut tissue even during sublethal toxin exposure.

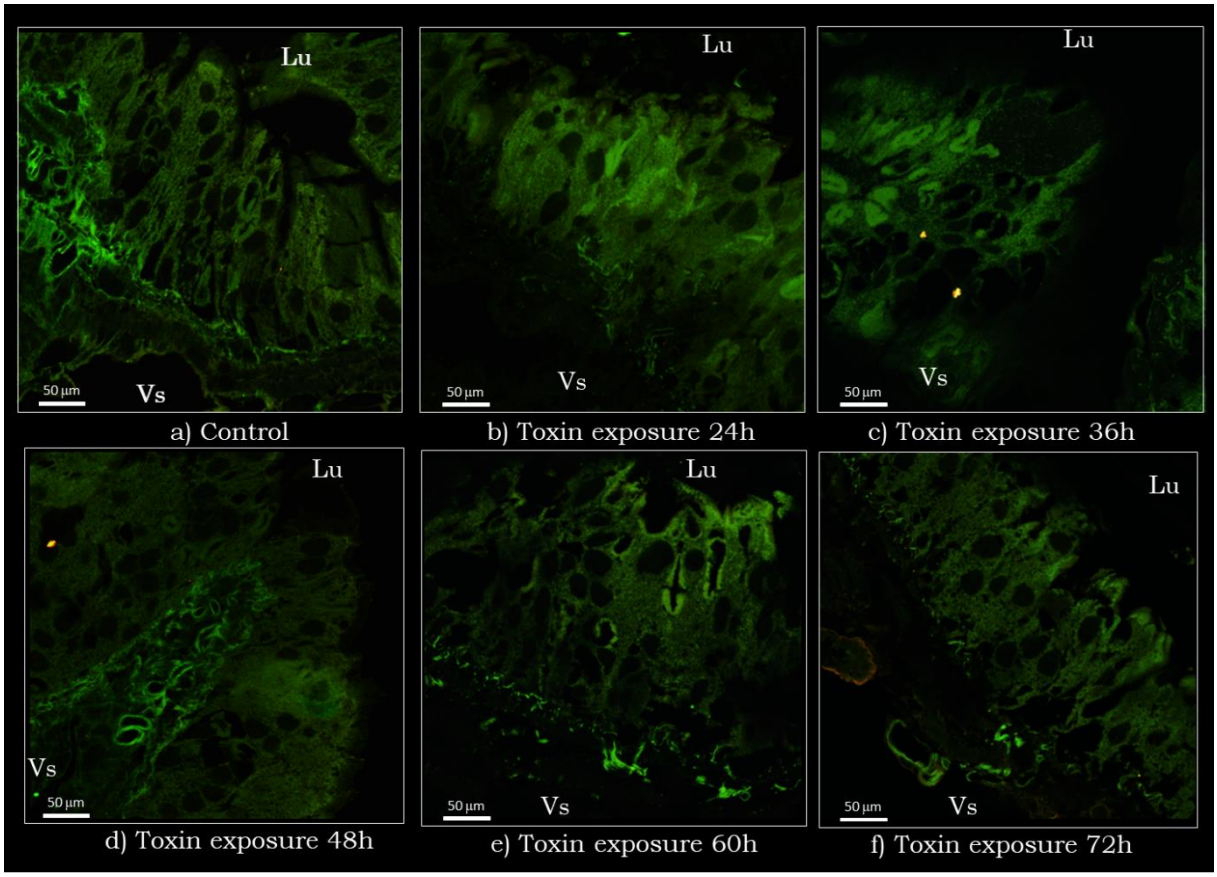

Fig. 10 Shows the transverse section of midgut during Cry toxin exposure (24 – 72 h). Please note the presence of exogenous arylphorin in the midgut epithelium. Scale bar, 50 µm.

3.7 Colocalization of proliferative cells and labelled exogenous arylphorin

Proliferative cells during Cry toxin exposure were labelled using BrdU labelling kit. At the start of sublethal toxin exposure, the larvae were injected with BrdU labelling reagent as well as fluorescent labelled exogenous arylphorin. After various time points BrdU detection was carried out using anti-BrdU mouse monoclonal antibody. Results present in figure 11 show the presence of few pockets of red fluorescent stained cell (Fig. 11a, b, c). During cell division BrdU gets incorporated and found in the nucleus of the dividing cells. The BrdU positive cells were only present in the midgut towards the basal epithelium in control as well as toxin exposed

larvae at 24 h time point. However, interestingly in 72 h toxin exposed midgut sample BrdU labelled nuclei/cells were also seen towards the luminal side of the epithelium (Fig. 11d inset, 11c). Figure 10b shows the presence of localization of green fluorescence labelled exogenous arylphorin in BrdU positive cells. Presence of exogenous arylphorin was significantly high in midgut regenerative cells when compared with other epithelial cell suggesting that it might play important role in cell proliferation. Further, the exogenous arylphorin might support, precursor supply for macromolecules synthesis as well as provide energy to proliferative, migratory and differentiating cells.

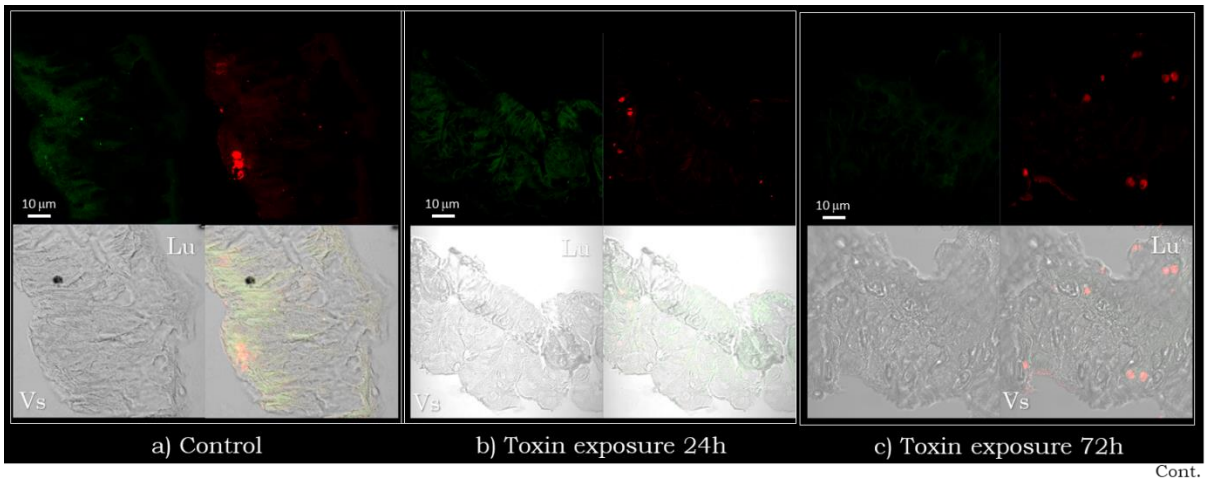

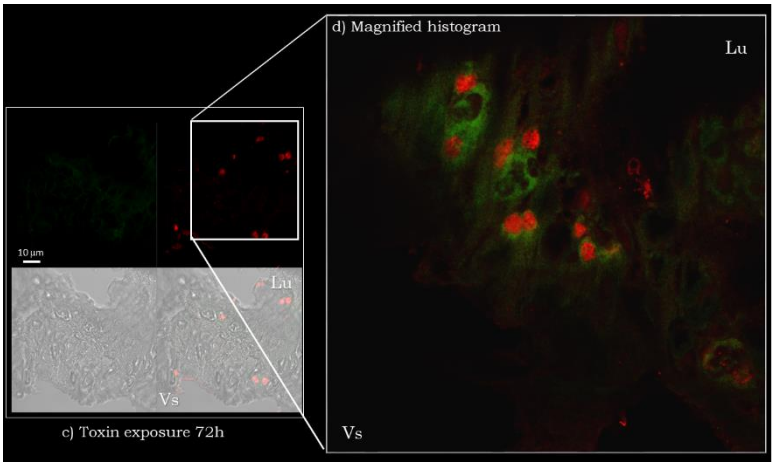

Fig. 11 Transverse section of midgut with dual staining showing the presence of exogenous arylphorin (green flourescence) during Cry toxin exposure and BrdU positive cells with red fluorescence. a) Basal midgut epithelial cells were labelled with BrdU in control larvae while upon toxin exposure- (b) at 24 h time point and (c) 72 h time point sample and their distribution was different. d) Magnified image of

midgut epithelium (T.S.) showing dual fluorescent stained cell, the red fluorescent (BrdU) positive nuclei and green cytosolic flourescenc with labelled arylphorin. Scale bar, 10 μm.

3.8 Endogenous arylphorin gene expression during Cry toxin exposure

Endogenous arylphorin transcript level in midgut tissue was monitored using real time PCR analysis. Larval midgut tissue of non-exposed and sublethal toxin exposed was used for current experiment. Compared to control, arylphorin transcript expression was more in toxin exposed larval midgut samples (Fig. 12).

From 12 h to 36 h time point mRNA level gradually increased in toxin exposed midgut sample, followed by a decline at later time points of 48 h and 60 h (Fig. 11). Interestingly, there was a significant increase at 72 h in control larval sample (Fig. 11). This period basically coincided with the moulting of the larvae to next instar.

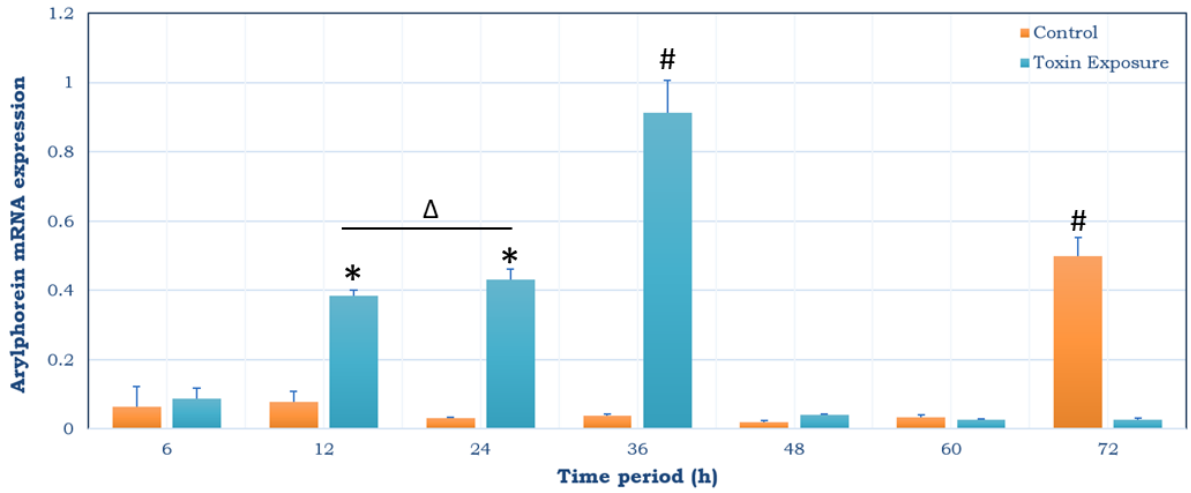

Fig. 12 Showing the expression of midgut arylphorin (endogenous) mRNA during toxin exposure, A gradual increase was observed from 6 to 36 h of Cry toxication which declined later to a basal level. Note the higher expression of arylphorin transcript in 72 h control larvae, a period which coincides with molting (from 3rd to 4th larval instar). *$p < 0.05$ indicates significance between experimental groups, #$p < 0.005$ significant among control groups and Δ, the values are non-significant.

3.9 Analysis of Cyclin mRNA during Cry toxin exposure

In our previous publication we have reported that midgut cells undergo proliferation during Cry toxin exposure between the time points of 24 h to 48 h (Chauhan et al., 2017). In current study we have checked cell cycle associated Cyclin mRNA expression using real time PCR analysis. Cyclin B, Cyclin E, Cyclin J and CDK2 mRNA expression was monitored (Fig. 13). mRNA isolated from larval midgut tissue of non-exposed and sublethal toxin exposed was used for the analysis. Cyclin B expression was relatively more as compared to other Cyclins in toxin exposed midgut sample. Cyclin E mRNA expression was also relatively higher at 36 h time point of Cry toxin exposure. Cyclin J and CDK2 mRNA expression at all time point was at basal level except at 72 h toxin exposure where it was slightly high. Interestingly, Cyclin B expression was relatively higher during 36 h of toxin exposure, when cell proliferation was seen in our earlier study (Chauhan et al., 2017).

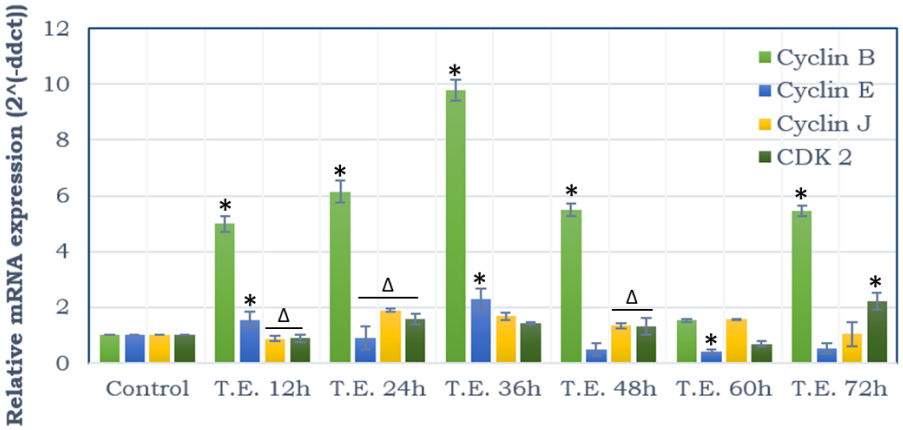

Fig. 13 Expression of midgut Cyclin mRNAs during Cry toxin exposure- Cyclin B mRNA expression was relatively higher at 36 h of Cry intoxication as compared to other time points. Further compared to Cyclin E, Cyclin J and CDK; Cyclin B mRNA expression was significantly altered during all time points. Symbol *$p < 0.05$ indicates significance between experimental groups and Δ, the values are non-significant.

3.10 Characterisation of Cyclin B as midgut stem cell marker

A. janata is a non model organism so availability of antibodies against its protein is very difficult. However, Cyclin B annotated sequences of *A. janata* align well with human

Cyclin B1 sequence. Sequence similarity of human Cyclin B1 and *A. janata* Cyclin B was analysed using CLUSTAL format alignment with MAFFT (v7.427) software. MAFFT-L-INS-i result was obtained, revealed ~70% similarity with ~50% query coverage of a small human sequence against which monoclonal antibody is commercially available (Fig. 14a). NCBI BLAST®» blastp suite based obtained results showed the maximum similarity of *A. janata* Cyclin B with *Spodoptera litura*, *Manduca sexta*, *Heliothis virescens* and *Helicoverpa armigera* (Fig. 14b).

Fig. 14a Sequence alignment of human Cyclin B domain against which monoclonal antibody was commercialy procured (Sc7393, Santa Cruz). As this antibody was used for the detection a comparision was made with Castor semilooper Cyclin B using Cluistal Omega (MAFFT-L-INS-i algorithm).

Description	Max Score	Total Score	Query Cover	E value	Per. Ident	Accession
G2/mitotic-specific cyclin-B1 [Spodoptera litura]	280	280	95%	5e-90	93.53%	XP_022822124.1
G2/mitotic-specific cyclin-B isoform X2 [Manduca sexta]	270	270	95%	2e-86	89.21%	XP_030029391.1
G2/mitotic-specific cyclin-B2 isoform X1 [Manduca sexta]	271	271	95%	2e-86	89.21%	XP_030029390.1
hypothetical protein B5V51_8832 [Heliothis virescens]	270	270	94%	2e-86	89.78%	PCG65687.1
hypothetical protein B5V51_8832 [Heliothis virescens]	270	270	94%	2e-86	89.78%	PCG65686.1
G2/mitotic-specific cyclin-B isoform X1 [Helicoverpa armigera]	268	268	94%	2e-85	88.32%	XP_021187350.1
G2/mitotic-specific cyclin-B isoform X2 [Helicoverpa armigera]	268	268	94%	2e-85	88.32%	XP_021187351.1
G2/mitotic-specific cyclin-B isoform X3 [Helicoverpa armigera]	268	268	94%	2e-85	88.32%	XP_021187352.1
G2/mitotic-specific cyclin-B [Ostrinia furnacalis]	266	266	95%	1e-84	87.77%	XP_028156235.1
hypothetical protein evm_004850 [Chilo suppressalis]	265	265	95%	4e-84	87.77%	RVE50521.1
G2/mitotic-specific cyclin-B2 [Bombyx mandarina]	263	263	95%	2e-83	86.33%	XP_028028961.1
cyclin B homolog [Bombyx mori]	262	262	95%	7e-83	85.61%	NP_001037343.1
PREDICTED: G2/mitotic-specific cyclin-B [Amyelois transitella]	256	256	95%	9e-81	85.61%	XP_013191183.1
G2/mitotic-specific cyclin-B1 [Trichoplusia ni]	256	256	95%	1e-80	83.45%	XP_026731829.1
G2/mitotic-specific cyclin-B2-like [Galleria mellonella]	252	252	95%	4e-79	82.01%	XP_026759014.1
G2/mitotic-specific cyclin-B [Vanessa tameamea]	249	249	98%	2e-78	80.42%	XP_026501045.1
G2/mitotic-specific cyclin-B1-like [Galleria mellonella]	249	249	98%	3e-78	78.32%	XP_026755615.1
PREDICTED: G2/mitotic-specific cyclin-B-like [Plutella xylostella]	239	239	92%	7e-76	79.85%	XP_011566029.1
PREDICTED: G2/mitotic-specific cyclin-B-like [Plutella xylostella]	240	240	92%	1e-74	79.85%	XP_011556113.1
cyclin B protein [Danaus plexippus plexippus]	236	236	98%	2e-73	82.52%	OWR48918.1
cyclin B protein [Danaus plexippus plexippus]	235	235	97%	6e-73	83.10%	OWR48917.1
G2/mitotic-specific cyclin-B2 [Pieris rapae]	232	232	100%	1e-71	71.72%	XP_022117536.1
unnamed protein product [Leptidea sinapis]	228	228	97%	4e-70	71.13%	VUZ04230.1
PREDICTED: G2/mitotic-specific cyclin-B1 [Papilio polytes]	225	225	95%	5e-69	74.82%	XP_013134762.1
G2/mitotic-specific cyclin-B2 [Hyposmocoma kahamanoa]	224	224	95%	2e-68	76.98%	XP_026319766.1
PREDICTED: G2/mitotic-specific cyclin-B-like isoform X2 [Papilio xuthus]	218	218	96%	3e-66	78.17%	XP_013177422.1
G2/mitotic-specific cyclin-B [Papilio xuthus]	218	218	96%	4e-66	78.17%	KPI94796.1

Fig. 14b Shows NCBI BLAST® blastp suite based sequence similarity search of castor semilooper Cyclin B deduced amino acid sequence.

Prior to immunohistochemical analysis of midgut stem cell, human monoclonal Cyclin B1 antibody was checked for its cross reactivity using western blot analysis. Western blot analysis confirmed a selective cross reactivity of a midgut protein of *A. janata* having the size of ~ 32 kDa (Fig. 15). For immunohistochemical analysis toxin exposed 24 h midgut transverse section was used. The results obtained clearly revealed the cross reactivity in the basal stem cells suggesting the presence of Cyclin B in these cells of midgut (Fig. 16).

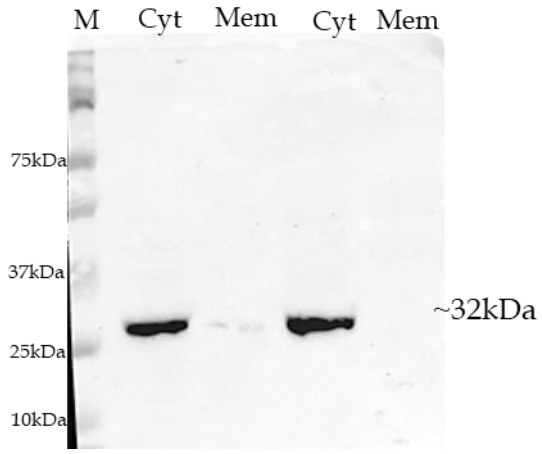

Fig. 15 Western blot analysis of midgut cytosolic and membrane proteins, showing its cross reactivity with Cyclin B antibody (human monoclonal). The band at ~32 kDa size represents *A. janata* CyclinB protein. (M, Molecular Mass Marker in kDa; Cyt, cytosolic protein; Mem, membrane protein)

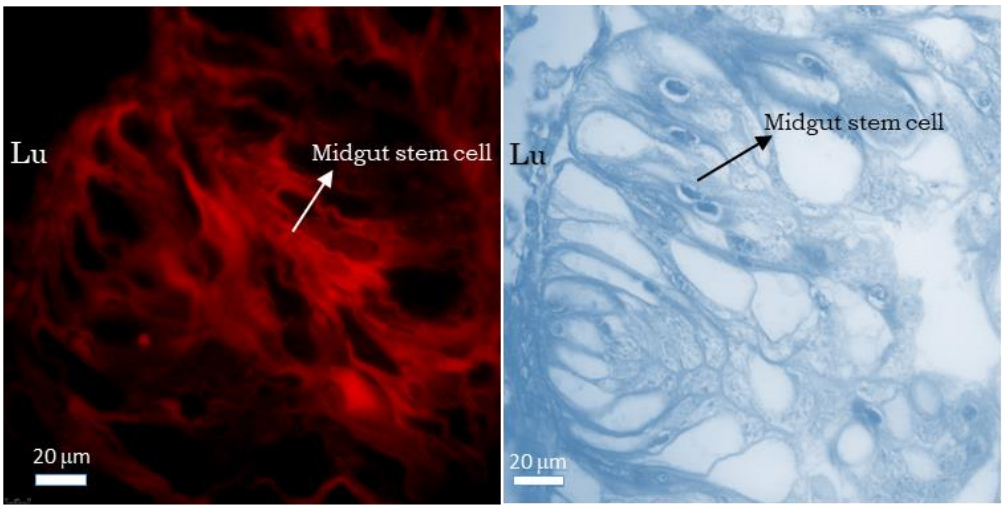

Fig. 16 Cross section of midgut- (a) Cyclin B labelled midgut stem cells toward basal epithelium (→). (b) Methylene blue stained section shows the similar stem cells during toxin exposure 24 h time point. For this study secondary Alexa Flour 555 tagged mouse antibody was used for the detection of primary human monoclonal Cyclin B1 anitbody (Sc7393). Scale bar, 20 µm.

3.11 Detection of endogenous arylphorin mRNA in larval midgut using *in situ* hybridization

DIG labelled probe was generated for endogenous arylphorin mRNA detection, and DIGmRNA (289 bp) obtained by *in vitro* transcription was confirmed using agarose gel electrophoresis (Fig. 17a). Sense and antisense probe was checked for their usage as positive and negative controls (Fig. 17b). DIG labelled arylphorin probe was detected using anti-digoxigenin, FITC labelled antibody. Green fluorescence indicated the presence of endogenous arylphorin mRNA in the cells (Fig. 17b).

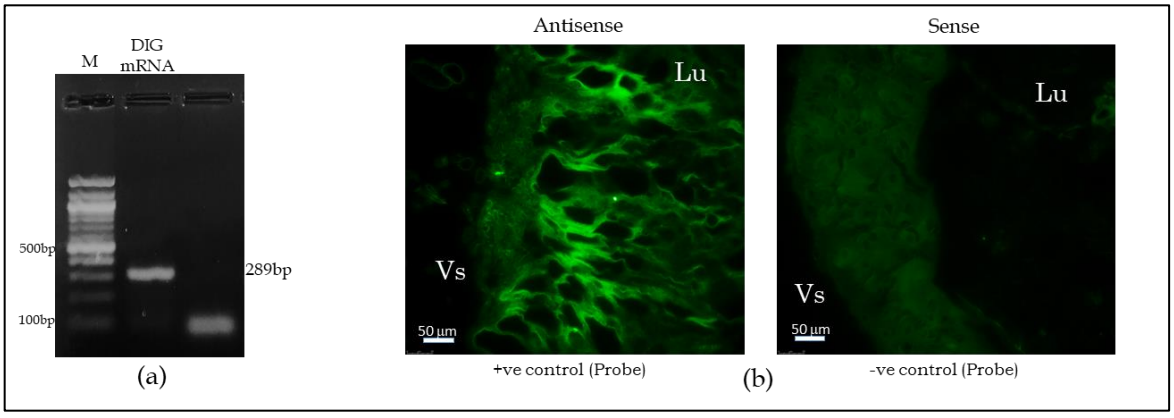

Fig. 17 For *in situ* hybridisation study endogenous arylphorin mRNA was *in vitro* transcribed and DIG

labelled cRNA was generated (a) agrose gel showing the size and quality of generated cRNA (DIG labelled) of ~289 bp. (b) *In situ* hybridization using midgut cross section showing the localization of endogenous arylphorin mRNA (green fluorescent). Scale bar, 50 µm.

In situ hybridization based arylphorin mRNA expression was also analysed during Cry toxin exposure. Presence of DIG labelled arylphorin cRNA was confirmed in transverse section of larval midgut (Fig. 17). The results presented in figure 18 show anti-DIG-FITC tagged based intensity of green fluorescent colour was more prominent in epithelial cells of toxin exposed 24 h and 36 h midgut sample (Fig. 18b, c). In addition, a small number of labelled basal epithelium cells were seen in control, toxin exposed 60 h and 72 h midgut sample. Precise cytological localization of arylphorin mRNA transcript was carried out using toxin exposed 24 h sample at higher magnification. Results obtained revealed that arylphorin transcripts are primarily located in the stem cell (Fig. 19). These result corroborate well with Cyclin B analysis and both were found to be localized in same epithelial cell type (Fig. 16, 19).

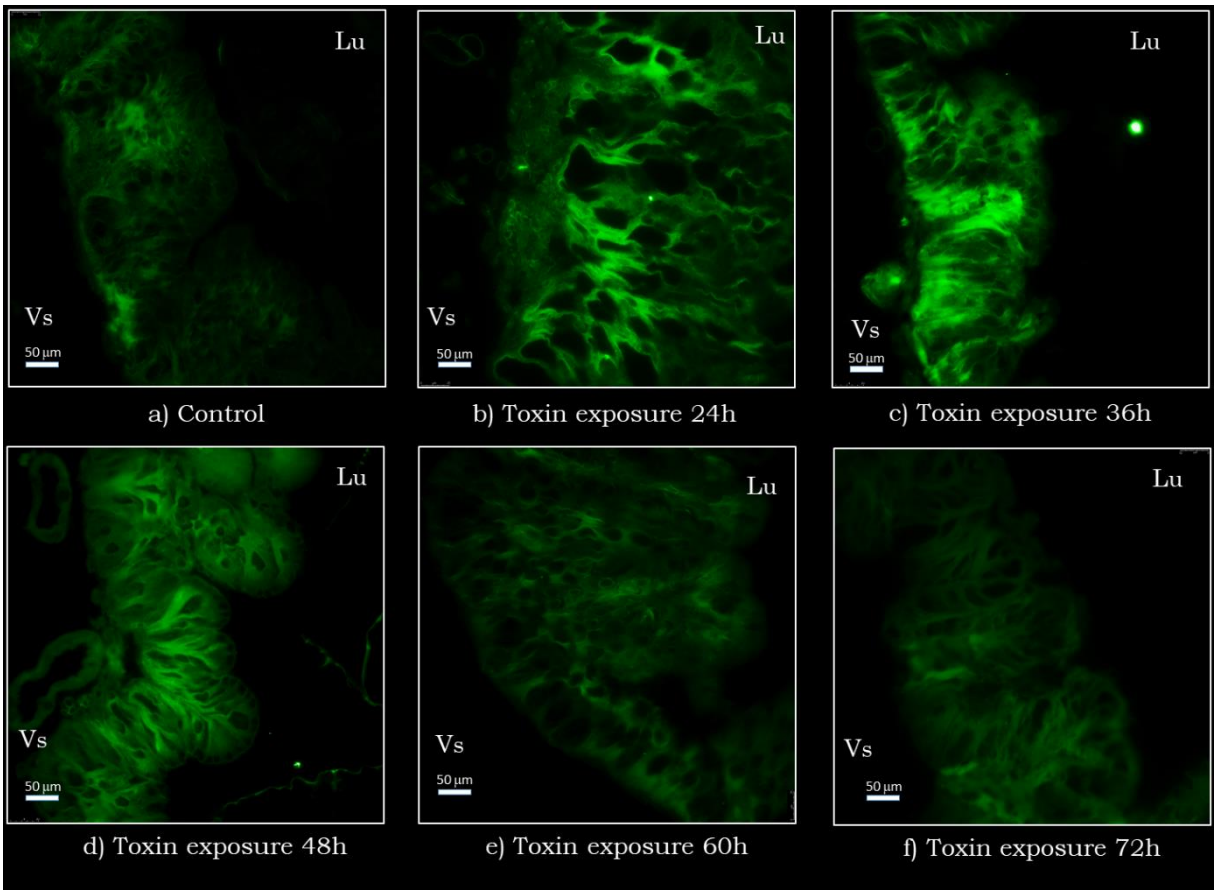

Fig. 18 Midgut transverse section from Cry toxin exposed larvae showing the presence of endogenous

arylphorin mRNA. Fluorescent green stain in cells represent the presence of DIG labelled cRNA. Please note that samples obtained after 24 h and 36 h time point of Cry toxin exposure show relatively higher labelling as compared to other time points. Fluorescent stained cells are observed in basal part of epithelium in control as well as 60 h and 72 h Cry toxin exposed midgut samples.

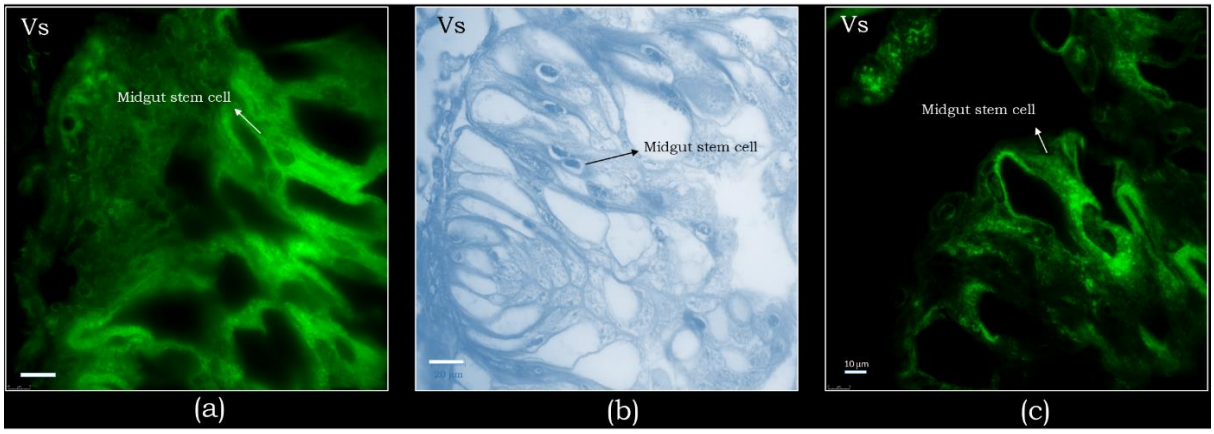

Fig. 19 Cross section of midgut from 24 h toxin exposed larve. a) *In situ* hybridization showing distribution of endogenous arylphorin. b) Methylene blue stained section showing intact midgut stem cells during toxin exposure. c) Please note the clear distribiution of endogenous arylphorin in cytosol of midgut stem cell upon *in situ* hybridization. Scale bar, in (a) (b) 20 µm and 10 µm in (c).

3.12 Endogenous arylphorin mRNA knockdown study

In vitro transcription of midgut specific arylphorin dsRNA (289 bp) was carried out using MEGSscript RNAi kit (Fig. 20a). Further, the delivery of dsRNA was also checked using midgut cross section labelling with fluorescence nucleotide tag (ChromaTide™ Texas Red™-12-dUTP tagged dsRNA) (Fig. 20b). Efficacy of dsRNA was verified using qRT-PCR anlaysis. The results obtained clearly shows a decline of midgut arylphorin mRNA (Fig. 20c). However, with a single micro injection successful knockdown was seen only till 24 h of dsRNA injection, and subsequently the values were comparable with respective control.

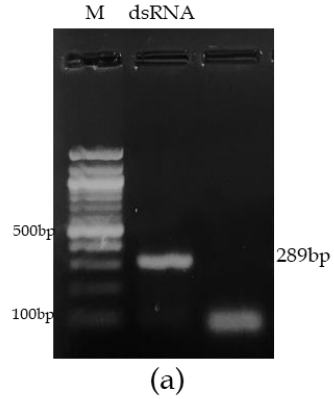

Fig. 20. Cont.

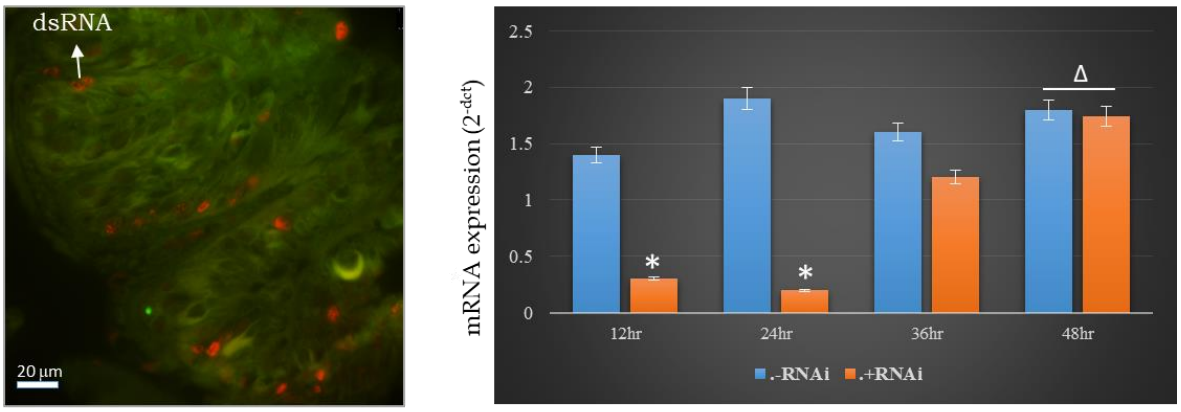

(b) (c)

Fig. 20 *In vitro* transcription of arylphorin dsRNA prepared for knock down analysis, a) Agarose gel electrophoresis of arylphorin dsRNA, the band seen at ~289 bp marker represents the *in vitro* transcribed dsRNA. b) Proper delivery of microinjected fluorescent tagged dsRNA was confirmed using microinjection followed by midgut histological analysis. c) Efficacy of dsRNA delivery was checked using qRT-PCR analysis. A significant decline in endogenous arylphorin mRNA is observed in 12 h and 24 h time points after the injection. *p < 0.05 indicates significance between experimental groups, Δ the values are non-significant. Scale bar, 20 µm.

3.13 Cyclin B mRNA expression upon dsRNA arylphorin microinjection

For this study dsRNA was injected in 3rd instar larvae and maintained for Cry toxin exposure upto 72 h. Cyclin B mRNA expression was checked using real time PCR analysis upon dsRNA injection. Results obtained in arylphorin knockdown experiment showed relatively lower Cyclin B mRNA expression in RNAi(+) sample as compared to RNAi(-) sample (Fig. 21). Intriguingly, Cyclin B mRNA expression was higher in Cry toxin exposed larval midgut sample of 36 h time point but it reduced significantly when subjected to arylphorin dsRNA based RNAi (Fig 21). In qRT-PCR analysis it was noticed that after 48 h of dsRNA injection, Cyclin B expression got restored to its original level.

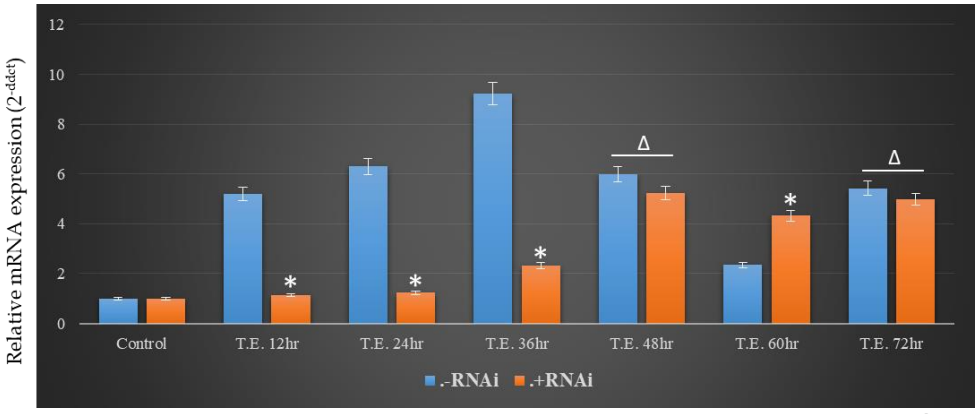

Cont.

Fig. 21 Cyclin B mRNA expression upon arylphorin dsRNA microinjection during continuous sublethal Cry toxin exposure. Cyclin B mRNA expression was significantly lower in 12 h to 36 h time point and the expression restorted back gradually after 48 h of RNAi injection. *p < 0.05 indicates significance among experimental sets, Δ the values are non-significant.

3.14 Midgut epithelial regeneration associated with development of new brush border

Development of renewed brush border during regeneration of apical border of midgut epithelium was analysed using phalloidin based immunohistochemical analysis. Cry toxin exposed 24 h–72 h midgut transverse sections were carefully examined at higher magnification (Fig. 22). Results obtained revealed specific F-actin fluorescent staining (Fig. 22). In control midgut sections continuous line of brush border was observed (Fig. 22a) which was absent in toxin exposed 24 h–48 h samples (Fig. 22b-d). However, in 72 h Cry toxin exposed midgut sample, repaired/regenerated brush border was clearly visualized with Alexa Fluor® 647 tagged phalloidin fluorescence (Fig. 22f).

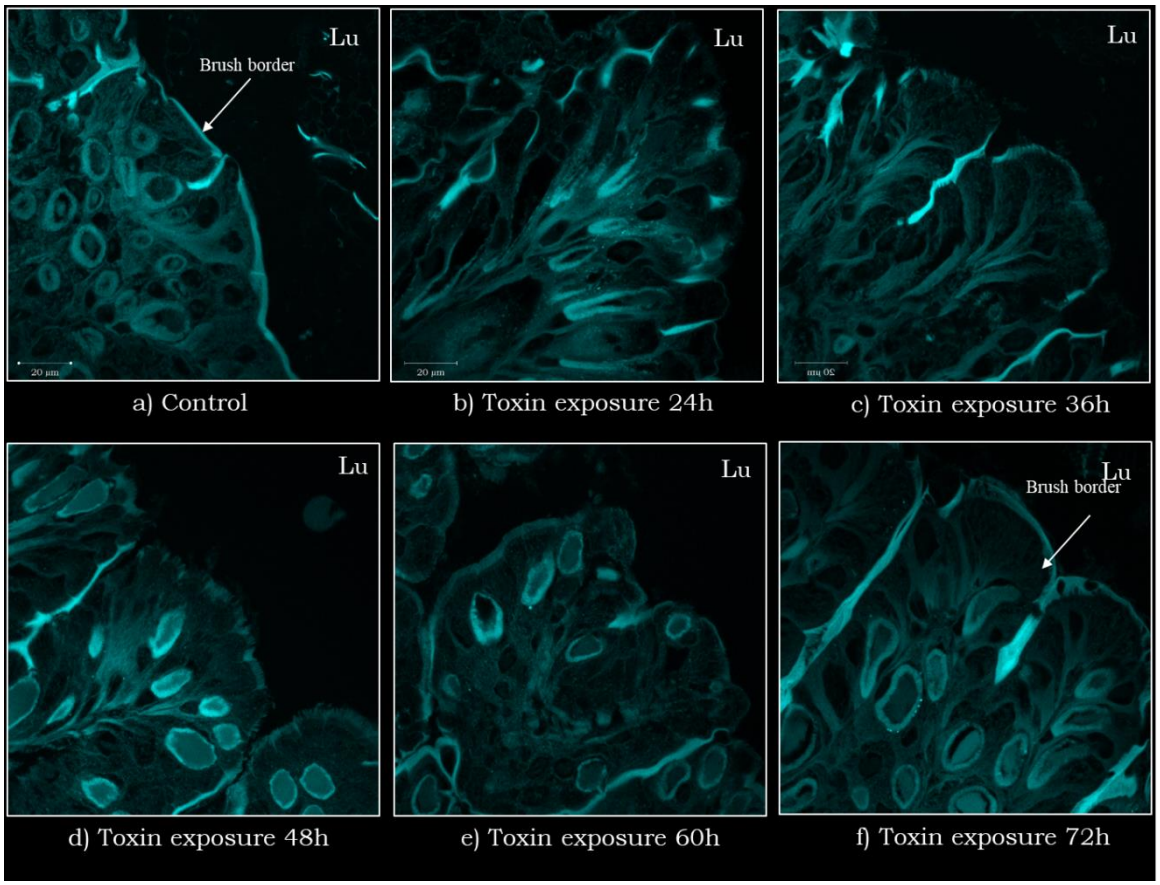

Fig. 22 Shows T.S. of midgut during continuous sublethal Cry toxin exposure undergoes regeneration and new brush border is formed. Blue green fluorescens in micrograph selectively represents F-actin.

Uninterrupted F-actin labelling is selectively observed in control and 72 h toxin exposed midgut samples. Whereas intruded brush border staining is seen in all other afore mentioned time points, suggesting its damage.

3.15 AminopeptidaseN-2 mRNA expression in susceptible and tolerant *A. janata* larvae

As discussed in Chapter 2 that Cry toxin tolerant larval population was maintained in laboratory condition. APN2 (Cry toxin receptor) mRNA expression was checked using real time PCR analysis in susceptible and tolerant larval population. Results obtained revealed that APN2 mRNA expression was significantly low in Cry toxin tolerant population when compared with susceptible population (Fig. 23a).

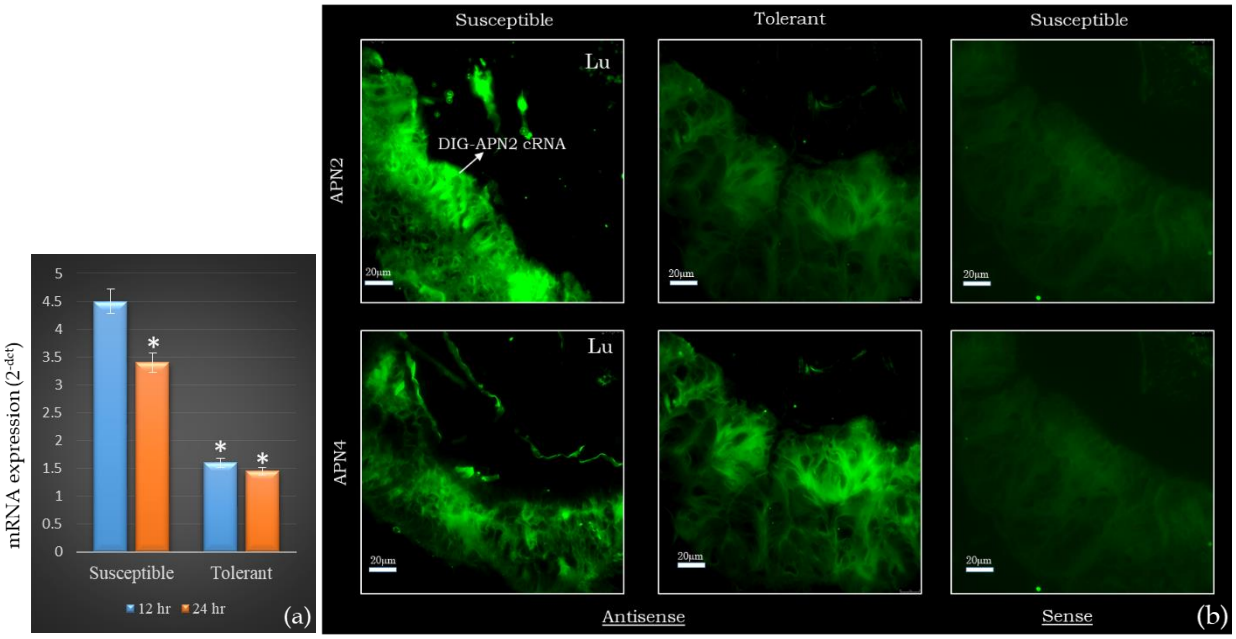

Fig. 23 APN mRNA expression analysis in Cry toxin susceptible and tolerant *A. janata* larvae. a) Upon continuous sublethal Cry toxin exposure for fifteen generations APN2 mRNA expression is significantly lower in tolerant larval midgut sample when compared with susceptible controls. *$p < 0.05$ indicates significance between experimental groups. b) Green fluorescence represents the presence APN2 and APN4 mRNA tagged with DIG labelled cRNA (→). Micrograph clearly shows that APN mRNAs are primarily located in differentiated cells of midgut and towards apical brush border side.

In situ hybridisation based aminopeptidaseN-2 (Cry toxin receptor) and aminopeptidaseN-4 (control) mRNA expression was also analysed Cry toxin tolerant and susceptible larvae. Presewnce of DIG labelled APN2 and APN4 cRNA was confirmed in transverse section of larval midgut (Fig. 23b). Anti-DIG-FITC tagged based intensity of green

fluorescent seen for APN2 was more prominent in epithelium cell of Cry toxin susceptible larvae (Fig. 23b). APN2 and APN4 mRNA were primarily localized in differentiated epithelial cells present towards lumen side (Fig 23b). Further, decreased fluorescent visualized for APN2 cRNA in tolerant larvae midgut sample suggested significant decline in APN2 mRNA expression upon generation wise continuous Cry toxin exposure.

4. Discussion

The results obtained in present study clearly show that *A. janata* larval midgut epithelial cells undergo structural as well as functional reorganisation during Cry toxication. In general, cellular alteration in midgut epithelium is known to be affected by food intake and growth habitats (Wu et al., 2009; Roel et al., 2010). Appropriate distribution of various cell types in gut epithelial is responsible for its unique function. However this may vary from insect to insect during moulting, metamorphosis, intoxication etc., where larval epithelium was shown to undergo significant cellular rearrangement (Judy and Gilbert, 1969; Baldwin and Hakim, 1991). Though several changes take place during these cellular process but the overall integrity of larval gut is always retained. During Cry toxication, the larval midgut of lepidopteran insect faces lots of challenges which include peritrophic membrane alteration (Rees et al., 2009), altered enzyme secretion (González-Cabrera et al., 2013) and food digestion (Mohan and Gujar, 2003), brush border impairment (Tiewsiri and Wang, 2011), epithelial cell damage (Chauhan et al., 2017) etc. However the larvae try to cope up with the altered physiology and the structural damage of midgut via stem cell mediated repair mechanism (Huang et al., 2015). Insect gut stem cells play a key role in all regenerative/restoration responses. Similar to other lepidopteran and dipteran insects, in the present study we have identified midgut stem cells in the *A. janata* larva, which are primarily located at the base of midgut epithelium and are quite distinctive from other mature epithelial cells (Fig. 11). In Lepidoptera and Diptera, stem cells

are normally present in small clusters in addition to regenerative nidi cell, whereas in Orthoptera and Odonata they are arranged in regenerative crypts or pouches (Wigglesworth 1972). Lehane and Billingsley, (1996) microscopically characterised these stem cells and showed that their morphology, cytoplasmic content, and few other organelles are dissimilar to all differentiated/mature cells present in gut eithelium. In *A. janata*, the stem cells are primarily localized in the basal part of midgut, aligned adjacent to basal epithelial muscle layer which is in direct contact with haemolymph present in the open circulatory system (Figs. 11, 15). Various lepidopteran and dipteran midgut stem cells were shown to be rich in glycogen granules and lipid droplets in its cytoplasm (Tettamanti et al. 2007; Marianes and Spradling 2013; Franzetti et al. 2015). Exact role of these storage granules are yet to be deciphered, in our current study, optical serial sectioning confirmed the presence as well as sequestration of fluorescent labelled arylphorin by muscle cells lining the visceral side of the midgut after 2 h of haemocoelic microinjection (Fig. 9). Further, the midgut transverse sections prepared from Cry toxin exposed larvae also confirmed the presence of arylphorin. Detailed analysis revealed that stem cells were labelled in both control and toxin exposed larvae after 24 h (Fig. 11). Interestingly BrdU labelled midgut stem also displayed, relatively higher presence of fluorescent labelled arylphorin (Fig. 11d). The above findings clearly suggested that sequestered exogenous arylphorin, which was present in significantly higher quantity played a crucial role in cell proliferation and most likely facilitated the cell migration from basal to apical luminal side of the epithelium. As hexamerin including arylphorin are known to supply precursors as well as energy for macromolecular synthesis during moulting and metamorphosis (Pan and Tefler, 1996). The sequestered exogenous arylphorin in *A. janata* larva might act as a building block for proliferative migratory cells which undergo differentiation during epithelial repair seen in the present study. As discussed before presence of glycogen granules and lipid droplets present in midgut stem cell cytoplasm, this study shows the presence of

storage proteins primarily arylphorin in the stem cell of midgut. We also suggest that exogenous arylphorin (well-established insect storage molecule) might enter into midgut through basal muscle cells in glycogen and/or lipid covered droplets and then gets incorporated into stem cell as well as other epithelial cells. However, further studies need to be carried out to ascertain this.

Like other organism in insect stem cells undergo division and during the process few proliferative cell divide and undergo differentiation to ensure the maintenance of gut epithelium. Literature survey reveals that our knowledge of insect stem cell is primarily based on holometaolus insect particularly *D. melanogaster* and few lepidopterans like *Bombyx mori, Helicoverpa armigera* and *Manduca sexta* (Loeb and Hakim, 1996; Dubreuil et al., 1998; Loeb et al., 1999; Loeb et al., 2001, 2003; Smagghe et al. 2005; Ohlstein and Spradling 2006; Lin et al., 2008; Hakim et al., 2007, 2010; Lucchetta and Ohlstein 2012; Buchon and Osman 2015; Nászai et al., 2015; Guo et al. 2016; Li et al., 2016; Gervais and Bardin 2017). The well reported remarkable proliferative capacity of stem cell and describes its fundamental character to ensure not only growth but also repair epithelium during larval development. A 200 fold increase in midgut stem cell number was reported in *M. sexta* during larval development (Baldwin and Hakim 1991), which was established as episodic behaviour during each moult. Ecdysteroid peak which occur prior to moult was shown to trigger the division and the stem cells continued to divide to increase in number during early moulting (Baldwin and Hakim 1991). Contrasting to above result Franzetti et al., (2016) proved that in stem cell proliferation activity is basically limited to first half of the moult period. Biphasic pattern of stem cell division was also reported in silkworm when the two ecdysone peaks were observed, first at spinning stage when the larva starts to spin cocoon and second when cell division resumed at pupal stage (Franzetti et al. 2015). However, in both lepidopteran species moulting process lead to differentiation of stem cell into mature cell types. In addition to the tissue remodeling,

which occured during metamorphosis it also facilitated larvae to reach its final size. Further, these studies revealed that epithelial cells originated from the previous one via proliferation and differentiation of stem cells (Tettamanti et al. 2007; Franzetti et al. 2015).

The insects undergoes exposure to variety of pathogenes and xenobiotics which cause physical, chemical, or pathogen-induced midgut epithelial damages and the homeostatic stem cell renewal facilitates repair. Recent studies revealed high plasticity of the midgut stem cell, even during alteration of nutritional condition and starvation (Shim et al., 2013; Hudry et al. 2016; Mattila et al. 2018; Obniski et al. 2018). However, very less is known about their regulatory factors which mediate the proliferation, based on the information available in *Drosophila* or primary cell culture of lepidopteran larval midgut, few mitogenic proteins have been identified. Using *in vitro* study Baines et al., (1994) and Sadrud-Din et al., (1994) demonstrated that *M. sexta* midgut stem cell actively proliferated and differentiated by supplementing fat body extract in the media culture, suggesting that midgut stem cell respond to fat body signals/molecules. *H. virescens* based immunohistological studies demonstrated that four peptides isolated from haemolymph, MDF 1-4 (midgut differentiation factors), promoted differentiation of stem cells (Loeb et al. 2004). Further, *in vitro* proliferation and differentiation of midgut stem cell was also promoted by 20-hydroxyecdysone (20E; ecdysteroids derivatives) (Smagghe et al. 2005). Blackburn et al., (2004) presented evidence that α-arylphorin (pupal fat body extract) promoted stem cell proliferation in *M. sexta* larval midgut primary cultures. Followed by Hakim et al., (2007), who demonstrated that α-arylphorin induced *in vitro* as well as *in vivo* stem cell proliferation in *H. virescens* larvae. In addition, Bombyxin (insulin family peptide) was shown to stimulate stem cell proliferation in *H. virescens, M. sexta* and *Mamestra brassicae* larvae (Goto et al. 2005; Nijhout et al. 2007).

As cited earlier in Introduction, arylphorins are high molecular weight proteins which are subunits of storage protein hexamerins. This protein is synthesised by fat body and released

into the haemolymph followed by sequestration/uptake in various tissues during late larval, pre-pupal and the early pupal stages (Bumester, 1999; Arif et al., 2003, 2008; Martins et al., 2008, 2010, 2011; Damara et al., 2010; Manohar et al., 2010). Interestingly in present study, next generation sequencing, real time PCR and *in situ* hybridization results confirmed the presence of an additional arylphorin transcript in midgut named as endogenous arylphorin. To the best of our knowledge till now no one has reported expression of arylphorin gene in midgut of insects in any literature. Present transcriptomic data from *A. janata* larval midgut showed not only the presence of endogenous arylphorin transcript but also showed its similarity with exogenous fat body origin arylphorin transcript. Further, this study clearly showed presence of endogenous arylphorin mRNA in midgut stem cell which increased at 24 h and 36 h Cry toxin exposure (Fig. 18). Magnified view of *in situ* hybridised micrographs clearly revealed localization of endogenous arylphorin in midgut stem cells (Fig. 19). These result suggested that endogenous arylphorin expressed by midgut stem cells, might play role in stem cell proliferation. Further, localization of large quantity of Cyclin B protein in midgut stem cell prompts us to propose that endogenous arylphorin might act as mitogen and promotes Cyclin B expression which is well proven cell cycle regulatory molecule.

Interestingly endogenous arylphorin knockdown lead to decline of Cyclin B transcript level (Fig. 21) once again supported the concept. Hence, the findings of the present study suggest that endogenous arylphorin in *A. janata* larval midgut functions as mitogenic factor and this is different from that of exogenous arylphorin mentioned in earlier reported *in vitro* studies. Overall the findings of regenerative analysis in the present study show that a small number of undifferentiated cells remain as midgut stem cell, these midgut stem cells of *A. janata* larvae are subjected to a significant turnover during Cry toxin exposure which caused damage. Midgut stem cells proliferated, differentiated and migrated towards the apical border and repaired the damaged area. Further, the exogenous arylphorin most likely acted as a

building block and provide precursors for molecular synthesis as well as energy for the cell proliferation and has altogether a different function from endogenous arylphorin which functioned as mitogenic factor.

In addition, midgut stem cells located at the base of midgut epithelium proliferate, differentiate and migrate to ensure the renewal and repair of damaged midgut during Cry intoxication. In current study we have analysed epithelial alteration in APN profile of Cry toxin susceptible and tolerant larvae. AminopeptidaseN's are well known Cry toxin receptors and there are several reports which suggest that reduced and differential expression of various APN isoforms is related with toxin tolerance (Ma et al., 2005; Herrero et al., 2005; 52. Heckel et al., 2007; Hernandez-Martinez et al., 2010; Tiewsiri and Wang, 2011, Guo et al., 2015). Mutation of Cry toxin receptor, well correlated with toxin resistance (Ferre et al., 1991; Gahan et al., 2001, 2010; Bravo et al., 2013; Jin et al., 2014; Wang et al., 2018; Fritz et al., 2019; Guo et al., 2019; Yang et al., 2019). In present study we demonstrated that midgut stem cell migrate and diferentiated to ensure the renewal and repair of damaged midgut and each time whenever it happened it repaired the damaged brush border (Fig. 22). Every time the larvae try to cope up the toxic effect and for their survival they try to alter cell surface toxin receptor profile. Altered expression of APN2 (Cry toxin receptor) during sublethal toxin exposure might be one of them. In our laboratory we have maintained fifteen generations of insect on sublethal dosage of DOR Bt-1 formulation, which became fairly tolerant to this formulation. Findings from the present study suggest that long term generation causes a significant decline of APN2 transcript expression. Current study further supports the view that *A. janata* larvae like many other lepidopteran larvae (Tabashnik et al., 2013; Tabashnik and Carriere, 2019) adopt receptor alteration strategy to avoid Cry toxin based deleterious effects of Cry intoxication and become tolerant against Bt formulations.

Summary and Conclusion

The present study was carried out to evaluate the Cry toxin induced cellular changes in the larval midgut of *Achaea janata*. For this study the major focus was on the usage of sublethal dosage of toxin, which is frequently seen in field based application. Further to understand the epithelial regeneration- i) Role of various arylphorins was evaluated in regeneration and repair of midgut epithelium and ii) Analysis of APN profile in Cry toxin susceptible and tolerant larvae was carried out. The above study revealed following interesting findings:

1. There was early damage of gut epithelial cells including brush border upon Cry toxin feeding (24 h). The gut epithelial cells were swollen and vacuolized during Cry intoxication.
2. With longer period of 36-48 h toxin exposure of the midgut, proliferation of cells towards basal border of epithelium was seen.
3. Several changes were noticed with longer duration of toxin exposure which included division, migration and differentiation of midgut proliferative cells in the epithelium that supported the regeneration and repair of the apical border of epithelium.
4. The transcriptomic study revealed a large repertoire of differentially expressed genes involved in modulating Cry toxin responses in *A. janata* midgut. The RNA-seq analysis provided an initial step towards unraveling the molecular mechanisms in the organism that potentially aid to understanding the toxin induced tolerance/resistance in Cry exposed *A. janata* larvae.
5. Detailed DEG analysis revealed the group of genes associated with Cry toxication in *A. janata* larvae.
6. The transcriptome analysis once again confirmed altered profile of expression of various gene which further supported that histological alteration seen in the midgut was associated with the molecular alteration during sublethal Cry toxin exposure.

7. The present study revealed transcript level variation in susceptible and tolerant larvae exposed for fifteen generation.
8. Sequestration of exogenous arylphorin by the midgut and localization of this exogenous arylphorin was primarily found in proliferative cells.
9. Interestingly for the first time we found the presence of endogenous arylphorin transcript in midgut stem cells. It was also observed that endogenous arylphorin knockdown was associated with CyclinB decline.
10. The formation of brush border is a proof of regeneration of midgut cell and it was associated with alteration in its protein profile. The detailed study revealed downregulation of Cry toxin receptor APN2 in tolerant larval midgut as compared to susceptible insect once again suggested it to be a Cry toxin receptor in *A. janata*.

Finally the present study clearly demonstrated that the Cry toxin sublethal toxicity is associated with damage as well as stem cell proliferation in midgut epithelium. Endogenous and exogenous arylphorin support and promote midgut stem cell proliferation. Proliferative, differentiated migratory cells help in the regeneration of new epithelium. Generation wise toxin exposure leads to the alteration in Cry toxin receptor profile.

References

Adang, M. J., Crickmore, N., & Jurat-Fuentes, J. L. (2014). Diversity of *Bacillus thuringiensis* crystal toxins and mechanism. *Insect Midgut Insect Proteins*, 47: 39-87.

Agrawal, N., Malhotra, P., & Bhatnagar, R. K. (2002). Interaction of gene-cloned and insect cell-expressed aminopeptidase N of *Spodoptera litura* with insecticidal crystal protein Cry1C. *Applied and Environmental Microbiology*, 68: 4583-4592.

Ahmedani, M. S., Haque, M. I., Afzal, S. N., Iqbal, U. M. E. R., & Naz, S. (2008). Scope of commercial formulations of *Bacillus thuringiensis berliner* as an alternative to methyl bromide against *Tribolium castaneum* adults. *Pakistan Journal of Botany*, 40: 2149-2156.

Ali, S., Huang, Z., & Ren, S. (2010). Production of cuticle degrading enzymes by *Isaria fumosorosea* and their evaluation as a biocontrol agent against diamondback moth. *Journal of Pest Science*, 83: 361-370.

Alvarado, A. S., & Tsonis, P. A. (2006). Bridging the regeneration gap: genetic insights from diverse animal models. *Nature Reviews Genetics*, *7*(11): 873.

Ambriz, X., de Lanerolle, P., & Ambrosio, J. R. (2018). The mechanobiology of the actin cytoskeleton in stem cells during differentiation and interaction with biomaterials. *Stem Cells International*, e2891957, 1-11.

Amcheslavsky, A., Song, W., Li, Q., Nie, Y., Bragatto, I., Ferrandon, D., ... & Ip, Y. T. (2014). Enteroendocrine cells support intestinal stem-cell-mediated homeostasis in *Drosophila*. *Cell Reports*, 9(1): 32-39.

Anders, S., & Huber, W. (2010). Differential expression analysis for sequence count data. *Genome Biology*, 11(10): R106.

Angelucci, C., Barrett-Wilt, G. A., Hunt, D. F., Akhurst, R. J., East, P. D., Gordon, K. H., & Campbell, P. M. (2008). Diversity of aminopeptidases, derived from four lepidopteran gene duplications, and polycalins expressed in the midgut of *Helicoverpa armigera*: Identification of proteins binding the δ-endotoxin, Cry1Ac of *Bacillus thuringiensis*. *Insect Biochemistry and Molecular Biology*, 38: 685-696.

Arif, A., Manohar, D., Gullipalli, D., & Dutta-Gupta, A. (2008). Regulation of hexamerin receptor phosphorylation by hemolymph protein HP19 and 20-hydroxyecdysone directs hexamerin uptake in the rice moth *Corcyra cephalonica*. *Insect Biochemistry and Molecular Biology*, 38: 307-319.

Arrese, E. L., & Soulages, J. L. (2010). Insect fat body: energy, metabolism, and regulation. *Annual Review of Entomology*, 55: 207-225.

Badran, A. H., Guzov, V. M., Huai, Q., Kemp, M. M., Vishwanath, P., Kain, W., ... & Wang, P. (2016). Continuous evolution of *Bacillus thuringiensis* toxins overcomes insect resistance. *Nature*, 533(7601): 58.

Bagla, P. (2010). Hardy cotton-munching pests are latest blow to GM crops. *Science*, 19(327): 1439-1439

Baines, D., Schwartz, J. L., Sohi, S., Dedes, J., & Pang, A. (1997). Comparison of the response of midgut epithelial cells and cell lines from lepidopteran larvae to CryIA toxins from *Bacillus thuringiensis*. *Journal of Insect Physiology*, 43(9): 823-831.

Baldwin, K. M., & Hakim, R. S. (1991). Growth and differentiation of the larval midgut epithelium during molting in the moth, *Manduca sexta*. *Tissue and Cell*, 23: 411-422.

Baton, L. A., & Ranford-Cartwright, L. C. (2007). Morphological evidence for proliferative regeneration of the *Anopheles stephensi* midgut epithelium following *Plasmodium falciparum* ookinete invasion. *Journal of Invertebrate Pathology*, 96(3): 244-254.

Baxter, S. W., Badenes-Pérez, F. R., Morrison, A., Vogel, H., Crickmore, N., Kain, W., ... & Jiggins, C. D. (2011). Parallel evolution of *Bacillus thuringiensis* toxin resistance in Lepidoptera. *Genetics*, 189: 675-679.

Baxter, S. W., Zhao, J. Z., Shelton, A. M., Vogel, H., & Heckel, D. G. (2008). Genetic mapping of *Bt*-toxin binding proteins in a Cry1A-toxin resistant strain of diamondback moth *Plutella xylostella*. *Insect Biochemistry and Molecular Biology*, 38: 125-135.

Beckwith, R. C., & Stelzer, M. J. (1987). Persistence of *Bacillus thuringiensis* in two formulations applied by helicopter against the western spruce budworm (Lepidoptera: Tortricidae) in north central Oregon. *Journal of Economic Entomology*, 80: 204-207.

Bely, A. E., & Nyberg, K. G. (2010). Evolution of animal regeneration: re-emergence of a field. *Trends in Ecology & Evolution*, 25(3): 161-170.

Blackburn, M. B., Loeb, M. J., Clark, E., & Jaffe, H. (2004). Stimulation of midgut stem cell proliferation by *Manduca sexta* α-arylphorin. *Archives of Insect Biochemistry and Physiology*, 55: 26-32.

Blum, H., Beier, H., & Gross, H. J. (1987). Improved silver staining of plant proteins, RNA and DNA in polyacrylamide gels. *Electrophoresis*, 8: 93-99.

Bolger, A. M., Lohse, M., & Usadel, B. (2014). Trimmomatic: a flexible trimmer for Illumina sequence data. *Bioinformatics*, 30(15): 2114-2120.

Bonfini, A., Liu, X., & Buchon, N. (2016). From pathogens to microbiota: how *Drosophila* intestinal stem cells react to gut microbes. *Developmental & Comparative Immunology*, 64: 22-38.

Boudjelida, H., Bouaziz, A., Soin, T., Smagghe, G., & Soltani, N. (2005). Effects of ecdysone agonist halofenozide against *Culex pipiens*. *Pesticide Biochemistry and Physiology*, 83(2-3): 115-123.

Bradford, M. M. (1976). A rapid and sensitive method for the quantitation of microgram quantities of protein utilizing the principle of protein-dye binding. *Analytical Biochemistry*, 72: 248-254.

Bravo, A., Gill, S. S., & Soberón, M. (2007). Mode of action of *Bacillus thuringiensis* Cry and Cyt toxins and their potential for insect control. *Toxicon*, 49: 423-435.

Bravo, A., Gomez, I., Conde, J., Munoz-Garay, C., Sánchez, J., Miranda, R., ... & Soberon, M. (2004). Oligomerization triggers binding of a *Bacillus thuringiensis* Cry1Ab pore-forming toxin to aminopeptidase N receptor leading to insertion into membrane microdomains. *Biochimica et Biophysica Acta (BBA)-Biomembranes*, 1667: 38-46.

Bravo, A., Gómez, I., Porta, H., García-Gómez, B. I., Rodriguez-Almazan, C., Pardo, L., & Soberón, M. (2013). Evolution of *Bacillus thuringiensis* Cry toxins insecticidal activity. *Microbial Biotechnology*, 6(1): 17-26.

Bravo, A., Jansens, S., & Peferoen, M. (1992). Immunocytochemical localization of *Bacillus thuringiensis* insecticidal crystal proteins in intoxicated insects. *Journal of Invertebrate Pathology*, 60: 237-246.

Bretschneider, A., Heckel, D. G., & Pauchet, Y. (2016). Three toxins, two receptors, one mechanism: Mode of action of Cry1A toxins from *Bacillus thuringiensis* in *Heliothis virescens*. *Insect Biochemistry and Molecular Biology*, 76: 109-117.

Broderick, N. A., Buchon, N., & Lemaitre, B. (2014). Microbiota-induced changes in *Drosophila melanogaster* host gene expression and gut morphology. *MBio*, 5(3): e01117-14, 1-13.

Bruce, M. J., Gatsi, R., Crickmore, N., & Sayyed, A. H. (2007). Mechanisms of resistance to *Bacillus thuringiensis* in the Diamondback Moth. *Biopesticides International*, 3: 1-12.

Bruno, D., Bonelli, M., De Filippis, F., Di Lelio, I., Tettamanti, G., Casartelli, M., ... & Caccia, S. (2019). The intestinal microbiota of Hermetia illucens larvae is affected by diet and shows a diverse composition in the different midgut regions. *Applied Environmental Microbiology*, 85(2): e01864-18, 1-14.

Buchon, N., & Osman, D. (2015). All for one and one for all: regionalization of the *Drosophila* intestine. *Insect Biochemistry and Molecular Biology*, 67: 2-8.

Buchon, N., Broderick, N. A., & Lemaitre, B. (2013). Gut homeostasis in a microbial world: insights from *Drosophila melanogaster*. *Nature Reviews Microbiology*, 11(9): 615-626.

Budatha, M., Meur, G., & Dutta-Gupta, A. (2007). A novel aminopeptidase in the fat body of the moth *Achaea janata* as a receptor for *Bacillus thuringiensis* Cry toxins and its comparison with midgut aminopeptidase. *Biochemical Journal*, 405: 287-297.

Budatha, M., Meur, G., & Dutta-Gupta, A. (2008). Identification and characterization of midgut proteases in *Achaea janata* and their implications. *Biotechnology Letters*, 30(2): 305-310.

Budatha, M., Ningshen, T. J., & Dutta-Gupta, A. (2011). Is hexamerin receptor a GPI-anchored protein in *Achaea janata* (Lepidoptera: Noctuidae)? *Journal of Biosciences*, 36(3): 545-553.

Burmester, T. (2015). Expression and evolution of hexamerins from the tobacco hornworm, *Manduca sexta*, and other Lepidoptera. *Insect Biochemistry and Molecular Biology*, 62: 226-234.

Burmester, T., & Schellen, K. (1996). Common origin of arthropod tyrosinase, arthropod hemocyanin, insect hexamerin, and dipteran arylphorin receptor. *Journal of Molecular Evolution*, 42: 713-728.

Burmester, T., & Scheller, K. (1999). Ligands and receptors: common theme in insect storage protein transport. *Naturwissenschaften*, 86(10): 468-474.

Burmester, T., Massey Jr, H. C., Zakharkin, S. O., & Benes, H. (1998). The evolution of hexamerins and the phylogeny of insects. *Journal of Molecular Evolution*, 47: 93-108.

Burmester. (1999). Evolution and function of the insect hexamerins. *European Journal of Entomology*, 96: 213-226.

Caccia, S., Casartelli, M., & Tettamanti, G. (2019). The amazing complexity of insect midgut cells: types, peculiarities, and functions. *Cell and Tissue Research*, 352(2): 1-21.

Campbell, E. M., Ball, A., Hoppler, S., & Bowman, A. S. (2008). Invertebrate aquaporins: a review. *Journal of Comparative Physiology B*, 178(8), 935-955.

Candas, M., Loseva, O., Oppert, B., Kosaraju, P., & Bulla, L. A. (2003). Insect resistance to *Bacillus thuringiensis*: alterations in the indianmeal moth larval gut proteome. *Molecular & Cellular Proteomics*, 2(1): 19-28.

Carmona, D., Rodríguez-Almazán, C., Muñoz-Garay, C., Portugal, L., Pérez, C., De Maagd, R. A., ... & Bravo, A. (2011). Dominant negative phenotype of *Bacillus thuringiensis* Cry1Ab, Cry11Aa and Cry4Ba mutants suggest hetero-oligomer formation among different Cry toxins. *PLoS One*, 6(5): e19952, 1-6.

Carriere, Y., Crowder, D. W., & Tabashnik, B. E. (2010). Evolutionary ecology of insect adaptation to Bt crops. *Evolutionary Applications*, *3*(5-6): 561-573.

Cary, G. A., Wolff, A., Zueva, O., Pattinato, J., & Hinman, V. F. (2019). Analysis of sea star larval regeneration reveals conserved processes of whole-body regeneration across the metazoa. *BMC Biology*, 17(1): 16, 1-19.

Casartelli, M., Bonelli, M., Bruno, D., Caccia, S., Sgambetterra, G., Cappellozza, S., & Tettamanti, G. (2019). Structural and functional characterization of *Hermetia illucens* larval midgut. *Frontiers in Physiology*, 10: 204, 1-16.

Castagnola, A., & Jurat-Fuentes, J. L. (2009). Resistance to Cry toxins and epithelial healing. *IOBC/WPRS Bulletin*, 45, 27-32.

Castagnola, A., & Jurat-Fuentes, J. L. (2016). Intestinal regeneration as an insect resistance mechanism to entomopathogenic bacteria. *Current Opinion in Insect Science*, 15: 104-110.

Castagnola, A., Eda, S., & Jurat-Fuentes, J. L. (2011). Monitoring stem cell proliferation and differentiation in primary midgut cell cultures from *Heliothis virescens* larvae using flow cytometry. *Differentiation*, 81(3): 192-198.

Castagnola, A., Jackson, J., Perera, O. P., Oppert, C., Eda, S., & Jurat-Fuentes, J. L. (2017). Alpha-arylphorin is a mitogen in the *Heliothis virescens* midgut cell secretome upon Cry1Ac intoxication. *PeerJ*, 5, e3886, 1-21.

Cavalcante V M, Cruz-Landim C (1999) Types of cells present in the midgut of the insects: a review. *Naturalia,* 24: 19-39.

Chajec, Ł., Rost-Roszkowska, M. M., Vilimova, J., & Sosinka, A. (2012). Ultrastructure and regeneration of midgut epithelial cells in *Lithobius forficatus* (Chilopoda, Lithobiidae). *Invertebrate Biology*, 131(2), 119-132.

Chandrasekar, R., Sumithra, P., Jae, S. S., & Krishnan, M. (2008). Sequestration of storage protein 1 (SP1) in differentiated fat body tissues of the female groundnut pest *Amsacta albistriga* (Lepidoptera: Arctiidae). *International Journal of Tropical Insect Science*, 28(2), 78-87.

Chapman, R. F. (2013). The Insects. Structure and Function. (SJ Simpson and AE Douglas, eds).

Chauhan, V. K. (2017). Larval midgut responses against sublethal dosages of Cry toxins in Lepidopteran pest, *Achaea janata* (Doctoral dissertation). University of Hyderabad, Hyderabad, India.

Chauhan, V. K., Dhania, N. K., Chaitanya, R. K., Senthilkumaran, B., & Dutta-Gupta, A. (2017). Larval mid-gut responses to sub-lethal dose of cry toxin in lepidopteran pest *Achaea janata*. *Frontiers in Physiology*, 8: 662, 1-11.

Chiang, A. S., Yen, D. F., & Peng, W. K. (1986). Defense reaction of midgut epithelial cells in the rice moth larva (*Corcyra cephalonica*) infected with *Bacillus thuringiensis*. *Journal of Invertebrate Pathology*, 47(3): 333-339.

Cioffi, M. (1979). The morphology and fine structure of the larval midgut of a moth (*Manduca sexta*) in relation to active ion transport. *Tissue and Cell*, 11(3): 467-479.

Cohen, E. (2012). Roles of aquaporins in osmoregulation, desiccation and cold hardiness in insects. *Entomol Ornithol Herpetol S*, 1: 2161-0983, 1-17.

Colombani, J., Bianchini, L., Layalle, S., Pondeville, E., Dauphin-Villemant, C., Antoniewski, C., ... & Léopold, P. (2005). Antagonistic actions of ecdysone and insulins determine final size in *Drosophila*. *Science*, 310: 667-670.

Crava, C. M., Bel, Y., Jakubowska, A. K., Ferré, J., & Escriche, B. (2013). Midgut aminopeptidase N isoforms from *Ostrinia nubilalis*: activity characterization and differential binding to Cry1Ab and Cry1Fa proteins from *Bacillus thuringiensis*. *Insect Biochemistry and Molecular Biology*, 43: 924-935.

Crava, C. M., Bel, Y., Lee, S. F., Manachini, B., Heckel, D. G., & Escriche, B. (2010). Study of the aminopeptidase N gene family in the lepidopterans *Ostrinia nubilalis* (Hübner) and *Bombyx mori* (L.): Sequences, mapping and expression. *Insect Biochemistry and Molecular Biology*, 40: 506-515.

Crickmore, N., Baum, J., Bravo, A., Lereclus, D., Narva, K., Sampson, K., Schnepf, E., Sun, M. and Zeigler, D.R. (2016) "*Bacillus thuringiensis* toxin nomenclature" http://www.btnomenclature.info/.

Crickmore, N., Zeigler, D. R., & Feitelson, J. (2008). *B. thuringiensis* toxin nomenclature. 1092: 2172, 1-20.

Cristofoletti, P. T., Ribeiro, A. F., & Terra, W. R. (2001). Apocrine secretion of amylase and exocytosis of trypsin along the midgut of *Tenebrio molitor* larvae. *Journal of Insect Physiology*, 47(2): 143-155.

Damara, M., Gullipalli, D., & Dutta-Gupta, A. (2010). Cloning and expression of fat body hexamerin receptor and its identification in other hexamerin sequestering tissue of rice moth, *Corcyra cephalonica*. *Journal of Insect Physiology*, 56(9): 1071-1077.

das Dores Teixeira, A., Fialho, M. D. C. Q., Zanuncio, J. C., de Souza Ramalho, F., & Serrão, J. E. (2013). Degeneration and cell regeneration in the midgut of *Podisus nigrispinus* (Heteroptera: Pentatomidae) during post-embryonic development. *Arthropod Structure & Development*, 42(3): 237-246.

de Maagd, R. A., Bravo, A., & Crickmore, N. (2001). How *Bacillus thuringiensis* has evolved specific toxins to colonize the insect world. *TRENDS in Genetics*, 17: 193-199.

de Maagd, R. A., Bravo, A., Berry, C., Crickmore, N., & Schnepf, H. E. (2003). Structure, diversity, and evolution of protein toxins from spore-forming entomopathogenic bacteria. *Annual Review of Genetics*, *37*: 409-433.

Desai, A., & Mitchison, T. J. (1997). Microtubule polymerization dynamics. *Annual Review of Cell and Developmental Biology*, 13(1): 83-117.

Dhania, N. K., Chauhan, V. K., Chaitanya, R. K., & Dutta-Gupta, A. (2019a). Midgut *de novo* transcriptome analysis and gene expression profiling of *Achaea janata* larvae exposed with *Bacillus thuringiensis* (Bt)-based biopesticide formulation. *Comparative Biochemistry and Physiology Part D: Genomics and Proteomics*, 30: 81-90.

Dhania, N. K., Chauhan, V. K., Chaitanya, R. K., & Dutta-Gupta, A. (2019b). RNA-Seq analysis and de novo transcriptome assembly of Cry toxin susceptible and tolerant *Achaea janata* larvae. *Scientific Data*, 6(1): 1-6.

Dhurua, S., & Gujar, G. T. (2011). Field-evolved resistance to Bt toxin Cry1Ac in the pink bollworm, *Pectinophora gossypiella* (Saunders) (Lepidoptera: Gelechiidae), from India. *Pest Management Science*, 67: 898-903.

Dieffenbach, C. W., & Dveksler, G. S. (2003). PCR primer: a laboratory manual (No. Ed. 2). *Cold Spring Harbor Laboratory Press*.

Dow, J. A. (1987). Insect midgut function. *Advances in Insect Physiology*, 19: 187-328.

Drake, L. L., Rodriguez, S. D., & Hansen, I. A. (2015). Functional characterization of aquaporins and aquaglyceroporins of the yellow fever mosquito, *Aedes aegypti*. *Scientific Reports*, 5: 7795, 1-7.

Dulmage, H. T., & Martinez, E. (1973). The effects of continuous exposure to low concentrations of the δ-endotoxin of *Bacillus thuringiensis* on the development of the tobacco budworm, *Heliothis virescens*. *Journal of Invertebrate Pathology*, 22(1): 14-22.

Dulmage, H. T., Graham, H. M., & Martinez, E. (1978). Interactions between the tobacco budworm, *Heliothis virescens*, and the δ-endotoxin produced by the HD-1 isolate of *Bacillus thuringiensis var. kurstaki:* relationship between length of exposure to the toxin and survival. *Journal of Invertebrate Pathology*, 32: 40-50.

Eizaguirre, M., Tort, S., Lopez, C., & Albajes, R. (2005). Effects of sublethal concentrations of *Bacillus thuringiensis* on larval development of *Sesamia nonagrioides*. *Journal of Economic Entomology*, 98(2): 464-470.

Endo, H., Tanaka, S., Imamura, K., Adegawa, S., Kikuta, S., & Sato, R. (2017). Cry toxin specificities of insect ABCC transporters closely related to lepidopteran ABCC2 transporters. *Peptides*, 98: 86-92.

Fabrick JA, Jech LF, Henneberry TJ (2009) Novel pink bollworm resistance to the *Bt* toxin Cry- 1Ac: effects on mating, oviposition, larval development and survival. *Journal of Insect Science* 9: 1–8

Feil, S. C., Polekhina, G., Gorman, M. A., & Parker, M. W. (2010). Proteins: membrane binding and pore formation. *Advances in Experimental Medicine and Biology*, 677: 1-13.

Ferré, J., & Van Rie, J. (2002). Biochemistry and genetics of insect resistance to *Bacillus thuringiensis*. *Annual Review of Entomology*, 47: 501-533.

Ferré, J., Real, M. D., Van Rie, J., Jansens, S., & Peferoen, M. (1991). Resistance to the *Bacillus thuringiensis* bioinsecticide in a field population of *Plutella xylostella* is due to a change in a midgut membrane receptor. *Proceedings of the National Academy of Sciences*, 88: 5119-5123.

Feyereisen, R. (2006). Evolution of insect P450. *Biochemical Society Transactions*, 34(6): 1252-1255.

Finney, D. J., & Tattersfield, F. (1978). Probit analysis. Cambridge University Press; Cambridge.

Fletcher, D. A., & Mullins, R. D. (2010). Cell mechanics and the cytoskeleton. *Nature*, 463(7280): 485-92.

Forcada C, Alcacer E, Garcera MD, Tato A, Martinez R (1999) Resistance to *Bacillus thuringiensis* Cry1Ac toxin in three strains of *Heliothis virescens*: proteolytic and SEM study of the larval midgut. *Archives of Insect Biochemistry Physiology,* 42: 51-63.

Frank, U., Plickert, G., & Müller, W. A. (2009). Cnidarian interstitial cells: the dawn of stem cell research. In *Stem cells in marine organisms* (pp. 33-59). Springer, Dordrecht.

Franzetti, E., Casartelli, M., D'Antona, P., Montali, A., Romanelli, D., Cappellozza, S., ... & Tettamanti, G. (2016). Midgut epithelium in molting silkworm: a fine balance among cell growth, differentiation, and survival. *Arthropod Structure & Development*, 45(4): 368-379.

Franzetti, E., Romanelli, D., Caccia, S., Cappellozza, S., Congiu, T., Rajagopalan, M., ... & Tettamanti, G. (2015). The midgut of the silkmoth *Bombyx mori* is able to recycle molecules derived from degeneration of the larval midgut epithelium. *Cell and Tissue Research*, 361(2): 509-528.

Friedman, R. (2011). Genomic organization of the glutathione S-transferase family in insects. *Molecular Phylogenetics and Evolution*, 61(3): 924-932.

Fritz, M., Nunziata, S., Guo, R., Tabashnik, B., & Carrière, Y. (2019). Mutations in a novel cadherin gene associated with Bt resistance in *Helicoverpa zea*. *bioRxiv*, 698530: 1-37.

Fu, L., Niu, B., Zhu, Z., Wu, S., & Li, W. (2012). CD-HIT: accelerated for clustering the next-generation sequencing data. *Bioinformatics*, *28*(23): 3150-3152.

Gahan, L. J., Gould, F., & Heckel, D. G. (2001). Identification of a gene associated with *Bt* resistance in *Heliothis virescens*. *Science*, 293: 857-860.

Gahan, L. J., Pauchet, Y., Vogel, H., & Heckel, D. G. (2010). An ABC transporter mutation is correlated with insect resistance to *Bacillus thuringiensis* Cry1Ac toxin. *PLoS Genetics*, 6: e1001248, 1-11.

Gaikwad, B. B., & Bilapate, G. G. (1992). Parasitization of *Achaea janata* and estimation of losses on castor. *Journal of Maharashtra Agricultural Universities*, 0378(2395): 243-256.

Gervais, L., & Bardin, A. J. (2017). Tissue homeostasis and aging: new insight from the fly intestine. *Current Opinion in Cell Biology*, 48: 97-105.

Gold, D. A., & Jacobs, D. K. (2013). Stem cell dynamics in Cnidaria: are there unifying principles? *Development Genes and Evolution*, 223(1-2): 53-66.

Gomes, F. M., Carvalho, D. B., Machado, E. A., & Miranda, K. (2013). Ultrastructural and functional analysis of secretory goblet cells in the midgut of the lepidopteran *Anticarsia gemmatalis*. *Cell and Tissue Research*, 352(2): 313-326.

Gomez, I., Oltean, D. I., Gill, S. S., Bravo, A., & Soberón, M. (2001). Mapping the epitope in Cadherin-like receptors involved in *Bacillus thuringiensis* Cry1A toxin interaction using phage display. *Journal of Biological Chemistry*, 276(31): 28906-28912.

Gomez, I., Sánchez, J., Miranda, R., Bravo, A., & Soberón, M. (2002). Cadherin-like receptor binding facilitates proteolytic cleavage of helix α-1 in domain I and oligomer pre-pore formation of *Bacillus thuringiensis* Cry1Ab toxin. *FEBS Letters*, 513: 242-246.

Gonzalez, M. R., Bischofberger, M., Pernot, L., Van Der Goot, F. G., & Freche, B. (2008). Bacterial pore-forming toxins: the whole story? *Cellular and Molecular Life Sciences*, 65: 493-507.

González-Cabrera, J., García, M., Hernández-Crespo, P., Farinós, G. P., Ortego, F., & Castañera, P. (2013). Resistance to Bt maize in *Mythimna unipuncta* (Lepidoptera: Noctuidae) is mediated by alteration in Cry1Ab protein activation. *Insect Biochemistry and Molecular Biology*, 43(8): 635-643.

Goto, S., Loeb, M. J., & Takeda, M. (2005). Bombyxin stimulates proliferation of cultured stem cells derived from *Heliothis virescens* and *Mamestra brassicae* larvae. *In Vitro Cellular & Developmental Biology-Animal*, 41(1-2): 38-42.

Grabherr, M. G., Haas, B. J., Yassour, M., Levin, J. Z., Thompson, D. A., Amit, I., ... & Chen, Z. (2011). Full-length transcriptome assembly from RNA-Seq data without a reference genome. *Nature Biotechnology*, 29(7): 644.

Grant, J. B. (2006). Diversification of gut morphology in caterpillars is associated with defensive behavior. *Journal of Experimental Biology*, 209(15): 3018-3024.

Griego, V. M., Fancher, L. J., & Spence, K. D. (1980). Scanning electron microscopy of the disruption of tobacco hornworm, *Manduca sexta*, midgut by *Bacillus thuringiensis* endotoxin. *Journal of Invertebrate Pathology*, 35(2): 186-189.

Gullipalli, D., Arif, A., Aparoy, P., Svenson, G. J., Whiting, M. F., Reddanna, P., & Dutta-Gupta, A. (2010). Identification of a developmentally and hormonally regulated Delta-Class glutathione S-transferase in rice moth *Corcyra cephalonica*. *Comparative Biochemistry and Physiology Part B: Biochemistry and Molecular Biology*, 156(1): 33-39.

Guo, W., Kain, W., & Wang, P. (2019). Effects of disruption of the peritrophic membrane on larval susceptibility to Bt toxin Cry1Ac in cabbage loopers. *Journal of Insect Physiology*, 117: e103897, 1-19.

Guo, Z., Kang, S., Chen, D., Wu, Q., Wang, S., Xie, W., ... & Zhang, Y. (2015). MAPK signaling pathway alters expression of midgut ALP and ABCC genes and causes resistance to *Bacillus thuringiensis* Cry1Ac toxin in diamondback moth. *PLoS Genetics*, 11: e1005124, 1-32.

Guo, Z., Sun, D., Kang, S., Zhou, J., Gong, L., Qin, J., ... & Zhang, Y. (2019). CRISPR/Cas9-mediated knockout of both the PxABCC2 and PxABCC3 genes confers high-level resistance to *Bacillus thuringiensis* Cry1Ac toxin in the diamondback moth, *Plutella xylostella* (L.). *Insect Biochemistry and Molecular Biology*, 107: 31-38.

Hakim, R. S., Baldwin, K., & Smagghe, G. (2010). Regulation of midgut growth, development, and metamorphosis. *Annual Review of Entomology*, 55: 593-608.

Hakim, R. S., Blackburn, M. B., Corti, P., Gelman, D. B., Goodman, C., Elsen, K., ... & Smagghe, G. (2007). Growth and mitogenic effects of arylphorin *in vivo* and *in vitro*. *Archives of Insect Biochemistry and Physiology*, 64: 63-73.

Hathaway, M., Hatle, J., Li, S., Ding, X., Barry, T., Hong, F., ... & Borst, D. (2009). Characterization of hexamerin proteins and their mRNAs in the adult lubber grasshopper: the effects of nutrition and juvenile hormone on their levels. *Comparative Biochemistry and Physiology Part A: Molecular & Integrative Physiology*, 154(3): 323-332.

Heckel, D. G., Gahan, L. J., Baxter, S. W., Zhao, J. Z., Shelton, A. M., Gould, F., & Tabashnik, B. E. (2007). The diversity of *Bt* resistance genes in species of Lepidoptera. *Journal of Invertebrate Pathology*, 95: 192-197.

Hernández-Martínez, P., Navarro-Cerrillo, G., Caccia, S., de Maagd, R. A., Moar, W. J., Ferré, J., ... & Herrero, S. (2010). Constitutive activation of the midgut response to *Bacillus thuringiensis* in Bt-resistant *Spodoptera exigua*. *PLoS One*, 5(9): e12795, 1-10.

Herrero, S., Combes, E., Van Oers, M. M., Vlak, J. M., de Maagd, R. A., & Beekwilder, J. (2005). Identification and recombinant expression of a novel chymotrypsin from *Spodoptera exigua*. *Insect Biochemistry and Molecular Biology*, 35(10): 1073-1082.

Hillyer, J. F. (2010). Mosquito immunity. In *Invertebrate Immunity* (pp. 218-238). Springer, Boston, MA.

Huang, J. H., Jing, X., & Douglas, A. E. (2015). The multi-tasking gut epithelium of insects. *Insect Biochemistry and Molecular Biology*, 67: 15-20.

Huang, W., Zhang, J., Yang, B., Beerntsen, B. T., Song, H., & Ling, E. (2016). DNA duplication is essential for the repair of gastrointestinal perforation in the insect midgut. *Scientific Reports*, 6: 19142, 1-10.

Hubert, W. A., & Rhodes, H. A. (1989). Food selection by brook trout in a subalpine stream. *Hydrobiologia*, 178(3): 225-231.

Hudry, B., Khadayate, S., & Miguel-Aliaga, I. (2016). The sexual identity of adult intestinal stem cells controls organ size and plasticity. *Nature*, 530(7590): 344-348.

Hussein, H. M., Habuštová, O., Turanli, F., & Sehnal, F. (2006). Potato expressing beetle-specific *Bacillus thuringiensis* Cry3Aa toxin reduces performance of a moth. *Journal of Chemical Ecology*, 32(1): 1-13.

Inaba, M., & Yamashita, Y. M. (2012). Asymmetric stem cell division: precision for robustness. *Cell Stem Cell*, 11(4): 461-469.

Ishibashi, K., Morishita, Y., & Tanaka, Y. (2017). The evolutionary aspects of aquaporin family. In *Aquaporins* (pp. 35-50). Springer, Dordrecht.

Ismail, F., & Wright, D. J. (1991). Cross-resistance between acylurea insect growth regulators in a strain of *Plutella xylostella* L.(Lepidoptera: Yponomeutidae) from Malaysia. *Pesticide Science*, 33(3): 359-370.

Ismail, P. M., Ismail, S. M., & Ray, A. D. G. (1993). Ecdysteroid mediated uptake and secretion of larval haemolymph proteins by the male accessory reproductive glands of *Chilo partellus*. *Journal of Insect Physiology*, 39: 811-815.

Jakka, S. R., Gong, L., Hasler, J., Banerjee, R., Sheets, J. J., Narva, K., ... & Jurat-Fuentes, J. L. (2015). Field-evolved Mode 1 fall armyworm resistance to Bt corn associated with reduced Cry1Fa toxin binding and midgut alkaline phosphatase expression. *Applied and Environmental Microbiology*, 82(4): 1023-1034.

Janeh, M., Osman, D., & Kambris, Z. (2017). Damage-induced cell regeneration in the midgut of *Aedes albopictus* mosquitoes. *Scientific Reports*, 7: 44594, 1-10.

Janmey, P. A. (1998). The cytoskeleton and cell signaling: component localization and mechanical coupling. *Physiological Reviews*, 78(3): 763-781.

Jiang, H., Tian, A., & Jiang, J. (2016). Intestinal stem cell response to injury: lessons from Drosophila. *Cellular and Molecular Life Sciences*, 73(17): 3337-3349.

Jin, T., Chang, X., Gatehouse, A., Wang, Z., Edwards, M., & He, K. (2014). Downregulation and mutation of a cadherin gene associated with Cry1Ac resistance in the Asian corn borer, *Ostrinia furnacalis* (Guenée). *Toxins*, 6(9): 2676-2693.

Judy, K. J., & Gilbert, L. I. (1969). Morphology of the alimentary canal during the metamorphosis of *Hyalophora cecropia* (Lepidoptera: Saturniidae). *Annals of the Entomological Society of America*, 62(6): 1438-1446.

Jurat-Fuentes, J. L., & Adang, M. J. (2004). Characterization of a Cry1Ac-receptor alkaline phosphatase in susceptible and resistant *Heliothis virescens* larvae. *The FEBS Journal*, 271: 3127-3135.

Jurat-Fuentes, J. L., & Crickmore, N. (2017). Specificity determinants for Cry insecticidal proteins: Insights from their mode of action. *Journal of Invertebrate Pathology*, 142: 5-10.

Just, D. R. (2006). Behavioral economics, food assistance, and obesity. *Agricultural and resource economics review*, 35(2), 209-220.

Just, D. R., Wang, S., & Pinstrup-Andersen, P. (2006). Tarnishing silver bullets: Bt technology adoption, bounded rationality and the outbreak of secondary pest infestations in China. *AgEcon*, 379(2016-21746): 1-35.

Karmawati, E. & Tobing, S. L. (1988). Laboratory biology of *Achaea janata* L. castor large semiloopers, *Industrial Crops Research*, 1: 37-42.

Kellogg, V. L. (1906). Physiological Regeneration in Insects. *Science*, 23(578): 149-152.

Khajuria, C., Buschman, L. L., Chen, M. S., Siegfried, B. D., & Zhu, K. Y. (2011). Identification of a novel aminopeptidase P-like gene (OnAPP) possibly involved in *Bt* toxicity and resistance in a major corn pest (*Ostrinia nubilalis*). *PLoS One*, 6: e23983, 1-10.

KiranKumar, N., Ismail, S. M., & Dutta-Gupta, A. (1997). Uptake of storage protein in the Rice Moth *Corcyra cephalonica*: Identification of storage protein binding proteins in the fat body cell membranes. *Insect Biochemistry and Molecular Biology*, 27: 671-679.

Kliot, A., & Ghanim, M. (2012). Fitness costs associated with insecticide resistance. *Pest Management Science*, 68(11): 1431-1437.

Knaak, N., & Fiuza, L. M. (2005). Histopathology of *Anticarsia gemmatalis Hübner* (Lepidoptera; Noctuidae) treated with Nucleopolyhedrovirus and *Bacillus thuringiensis serovar kurstaki*. *Brazilian Journal of Microbiology*, 36(2): 196-200.

Knaak, N., Franz, A. R., Santos, G. F., & Fiuza, L. M. (2010). Histopathology and the lethal effect of Cry proteins and strains of Bacillus thuringiensis Berliner in *Spodoptera frugiperda* JE Smith Caterpillars (Lepidoptera, Noctuidae). *Brazilian Journal of Biology*, 70(3): 677-684.

Kramer, K. J., Tager, H. S., & Childs, C. N. (1980). Insulin-like and glucagon-like peptides in insect hemolymph. *Insect Biochemistry*, 10(2): 179-182.

Kruger, M., Van Rensburg, J. B. J., & Van den Berg, J. (2011). Resistance to Bt maize in *Busseola fusca* (Lepidoptera: Noctuidae) from Vaalharts, South Africa. *Environmental Entomology*, 40(2): 477-483.

Laemmli, U. K. (1970). Denaturing (SDS) discontinuous gel electrophoresis. *Nature*, 277: 680-685.

Lakshminarayana, M., & Raoof, M. A. (2005). Insect pests and diseases of castor and their management. *Directorate of Oilseeds Research, Hyderabad*, 78: 2-28.

Langmead, B., & Salzberg, S. L. (2012). Fast gapped-read alignment with Bowtie 2. *Nature Methods*, 9(4): 357.

Law, J. H. & Wells, M. A. (1989). Insects as biochemical models. *Journal of Biological Chemistry*, 264: 16335-16338.

Le Caherec, F., Guillam, M. T., Beuron, F., Cavalier, A., Thomas, D., Gouranton, J., & Hubert, J. F. (1997). Aquaporin-related proteins in the filter chamber of homopteran insects. *Cell and Tissue Research*, 290(1): 143-151.

Lee, H. O., Davidson, J. M., & Duronio, R. J. (2009). Endoreplication: polyploidy with purpose. *Genes & Development*, 23(21): 2461-2477.

Leenaars, M., & Hendriksen, C. F. (2005). Critical steps in the production of polyclonal and monoclonal antibodies: evaluation and recommendations. *Ilar Journal*, 46(3): 269-279.

Lehane, M. J., & Billingsley, P. F. (1996). *Biology of the insect midgut*. Chapman and Hall.

Lei, Y., Zhu, X., Xie, W., Wu, Q., Wang, S., Guo, Z., ... & Zhang, Y. (2014). Midgut transcriptome response to a Cry toxin in the diamondback moth, *Plutella xylostella* (Lepidoptera: Plutellidae). *Gene*, 533(1): 180-187.

Lemos, F. J., & Terra, W. R. (1991). Digestion of bacteria and the role of midgut lysozyme in some insect larvae. *Comparative Biochemistry and Physiology. B, Comparative Biochemistry*, 100(2): 265-268.

Leong, K. L. H., Cano, R. J., & Kubinski, A. M. (1980). Factors affecting *Bacillus thuringiensis* total field persistence. *Environmental Entomology*, 9: 593-599.

Li H, Oppert B, Higgins RA, Huang F, Zhu KY & Bushman L.L (2004). Comparative analysis of proteases activites of *Bacillus thuringiensis* resistant and susceptoble *Ostrinia nubilalis* (Lepidoptera: Crambiae). *Insect Biochemistry and Molecular Biology*, 34: 753-762.

Li, H., Jiang, W., Zhang, Z., Xing, Y., & Li, F. (2013). Transcriptome analysis and screening for potential target genes for RNAi-mediated pest control of the beet armyworm, *Spodoptera exigua*. *PLoS One*, 8(6): e65931, 1-10.

Li, H., Qi, Y., & Jasper, H. (2016). Ubx dynamically regulates Dpp signaling by repressing Dad expression during copper cell regeneration in the adult *Drosophila* midgut. *Developmental Biology*, 419(2): 373-381.

Li, Q., Yang, H., & Zhong, T. P. (2015). Regeneration across metazoan phylogeny: lessons from model organisms. *Journal of Genetics and Genomics*, 42(2): 57-70.

Li, W., & Godzik, A. (2006). Cd-hit: a fast program for clustering and comparing large sets of protein or nucleotide sequences. *Bioinformatics*, 22(13): 1658-1659.

Likitvivatanavong, S., Chen, J., Evans, A. M., Bravo, A., Soberon, M., & Gill, S. S. (2011). Multiple receptors as targets of Cry toxins in mosquitoes. *Journal of Agricultural and Food Chemistry*, 59: 2829-2838.

Lin, G., Xu, N., & Xi, R. (2008). Paracrine Wingless signalling controls self-renewal of *Drosophila* intestinal stem cells. *Nature*, 455(7216): 1119-1123.

Lin, P., Cheng, T., Jin, S., Jiang, L., Wang, C., & Xia, Q. (2014). Structural, evolutionary and functional analysis of APN genes in the Lepidoptera *Bombyx mori*. *Gene*, 535: 303-311.

Liu, L., Chen, Z., Yang, Y., Xiao, Y., Liu, C., Ma, Y., ... & Liu, K. (2018). A single amino acid polymorphism in ABCC2 loop 1 is responsible for differential toxicity of *Bacillus thuringiensis* Cry1Ac toxin in different Spodoptera (Noctuidae) species. *Insect Biochemistry and Molecular Biology*, 100: 59-65.

Livak, K. J., & Schmittgen, T. D. (2001). Analysis of relative gene expression data using real-time quantitative PCR and the $2^{-\Delta\Delta CT}$ method. *Methods*, 25: 402-408.

Loeb, M. J. (2010). Factors affecting proliferation and differentiation of lepidopteran midgut stem cells. *Archives of Insect Biochemistry and Physiology*, 74: 1-16.

Loeb, M. J., & Jaffe, H. (2002). Peptides that elicit midgut stem cell differentiation isolated from chymotryptic digests of hemolymph from *Lymantria dispar* pupae. *Archives of Insect Biochemistry and Physiology*, 50(2): 85-96.

Loeb, M. J., Clark, E. A., Blackburn, M., Hakim, R. S., Elsen, K., & Smagghe, G. (2003). Stem cells from midguts of Lepidopteran larvae: clues to the regulation of stem cell fate. *Archives of Insect Biochemistry and Physiology*, 53(4): 186-198.

Loeb, M. J., Coronel, N., Natsukawa, D., & Takeda, M. (2004). Implications for the functions of the four known midgut differentiation factors: an immunohistologic study of *Heliothis virescens* midgut. *Archives of Insect Biochemistry and Physiology*, 56(1): 7-20.

Loeb, M. J., Jaffe, H., Gelman, D. B., & Hakim, R. S. (1999). Two polypeptide factors that promote differentiation of insect midgut stem cells in vitro. *Archives of Insect Biochemistry and Physiology,* 40(3): 129-140.

Loeb, M. J., Martin, P. A., Hakim, R. S., Goto, S., & Takeda, M. (2001). Regeneration of cultured midgut cells after exposure to sub-lethal doses of toxin from two strains of *Bacillus thuringiensis*. *Journal of Insect Physiology,* 47: 599-606.

Lomate, P. R., & Hivrale, V. K. (2013). Effect of *Bacillus thuringiensis* (Bt) Cry1Ac toxin and protease inhibitor on growth and development of *Helicoverpa armigera* (Hübner). *Pesticide biochemistry and physiology*, 105(2): 77-83.

Lu, Y., & Li, Z. (2015). No intestinal stem cell regeneration after complete progenitor ablation in *Drosophila* adult midgut. *Journal of Genetics and Genomics,* 42(2): 83.

Lu, Y., Wu, K., Jiang, Y., Xia, B., Li, P., Feng, H., ... & Guo, Y. (2010). Mirid bug outbreaks in multiple crops correlated with wide-scale adoption of Bt cotton in China. *Science*, 328(5982): 1151-1154.

Lucchetta, E. M., & Ohlstein, B. (2012). The *Drosophila* midgut: a model for stem cell driven tissue regeneration. *Wiley Interdisciplinary Reviews: Developmental Biology,* 1(5): 781-788.

Ma, G., Roberts, H., Sarjan, M., Featherstone, N., Lahnstein, J., Akhurst, R., & Schmidt, O. (2005). Is the mature endotoxin Cry1Ac from *Bacillus thuringiensis* inactivated by a coagulation reaction in the gut lumen of resistant *Helicoverpa armigera* larvae? *Insect Biochemistry and Molecular Biology*, 35: 729-739.

Manohar, D., Gullipalli, D., & Dutta-Gupta, A. (2010). Ecdysteroid-mediated expression of hexamerin (arylphorin) in the rice moth, *Corcyra cephalonica*. *Journal of Insect Physiology*, 56: 1224-1231.

Marianes, A., & Spradling, A. C. (2013). Physiological and stem cell compartmentalization within the Drosophila midgut. *elife*, 2: e00886, 1-19.

Martinez-Ramirez AC, Gould F, Ferre J (1999) Histopathological effects and growth reduction in a susceptible and a resistant strain of *Heliothis virescens* (Lepidoptera: Noctuidae) caused by sub-lethal doses of pure Cry1A crystal proteins from *Bacillus thuringiensis*. *Biocontrol Science and Techecnology,* 9: 239-246.

Martínez-Solís, M., Pinos, D., Endo, H., Portugal, L., Sato, R., Ferré, J., ... & Hernández-Martínez, P. (2018). Role of *Bacillus thuringiensis* Cry1A toxins domains in the binding to the ABCC2 receptor from *Spodoptera exigua*. *Insect Biochemistry and Molecular Biology*, 101: 47-56.

Martins, J. R., Anhezini, L., Dallacqua, R. P., Simões, Z. L., & Bitondi, M. M. (2011). A honey bee hexamerin, HEX 70a, is likely to play an intranuclear role in developing and mature ovarioles and testioles. *PLoS One*, 6(12): e29006, 1-11.

Martins, J. R., Nunes, F. M. F., Simões, Z. L. P., & Bitondi, M. M. G. (2008). A honeybee storage protein gene, hex 70a, expressed in developing gonads and nutritionally regulated in adult fat body. *Journal of Insect Physiology*, 54: 867-877.

Martins, J. R., Nunes, F. M., Cristino, A. S., Simões, Z. L., & Bitondi, M. M. (2010). The four hexamerin genes in the honey bee: structure, molecular evolution and function deduced from expression patterns in queens, workers and drones. *BMC Molecular Biology*, 11: 1-20.

Mathavan, S., Sudha, P. M., & Pechimuthu, S. M. (1989). Effect of *Bacillus thuringiensis israelensis* on the midgut cells of *Bombyx mori* larvae: a histopathological and histochemical study. *Journal of Invertebrate Pathology*, 53(2): 217-227.

Mattila, J., Kokki, K., Hietakangas, V., & Boutros, M. (2018). Stem cell intrinsic hexosamine metabolism regulates intestinal adaptation to nutrient content. *Developmental Cell*, 47(1): 112-121.

Mattila, P. K., & Lappalainen, P. (2008). Filopodia: molecular architecture and cellular functions. *Nature reviews Molecular Cell Biology*, 9(6): 446.

McNall, R. J., & Adang, M. J. (2003). Identification of novel *Bacillus thuringiensis* Cry1Ac binding proteins in *Manduca sexta* midgut through proteomic analysis. *Insect Biochemistry and Molecular Biology*, 33: 999-1010.

Melo, A. L. D. A., Soccol, V. T., & Soccol, C. R. (2016). *Bacillus thuringiensis*: mechanism of action, resistance, and new applications: a review. *Critical Reviews in Biotechnology*, 36(2), 317-326.

Micchelli, C. A., & Perrimon, N. (2006). Evidence that stem cells reside in the adult *Drosophila* midgut epithelium. *Nature*, 439(7075): 475.

Mohan, M., & Gujar, G. T. (2003). Characterization and comparison of midgut proteases of *Bacillus thuringiensis* susceptible and resistant diamondback moth (Plutellidae: Lepidoptera). *Journal of Invertebrate Pathology*, 82(1): 1-11.

Morgan, T. H., (1901) *Regeneration*. The Macmillan Company, New York, pp 19-25.

Morin, S., Biggs, R. W., Sisterson, M. S., Shriver, L., Ellers-Kirk, C., Higginson, D., ... & Dennehy, T. J. (2003). Three cadherin alleles associated with resistance to *Bacillus thuringiensis* in pink bollworm. *Proceedings of the National Academy of Sciences*, 100(9): 5004-5009.

Moriya, Y., Itoh, M., Okuda, S., Yoshizawa, A. C., & Kanehisa, M. (2007). KAAS: an automatic genome annotation and pathway reconstruction server. *Nucleic Acids Research*, 35: 182-185.

Nagamatsu, Y., Koike, T., Sasaki, K., Yoshimoto, A., & Furukawa, Y. (1999). The cadherin-like protein is essential to specificity determination and cytotoxic action of the *Bacillus thuringiensis* insecticidal CryIAa toxin. *FEBS Letters*, 460: 85-390.

Nakaishi, Y., Sato, M., Bando, H., & Asano, S. I. (2018). A mutation in *Plutella xylostella* ABCC2 causes resistance to *Bacillus thuringiensis* Cry1Ac by interfering with its receptor function. *Journal of Insect Biotechnology and Sericology*, 87(2): 2045-2051.

Nakanishi, K., Yaoi, K., Nagino, Y., Hara, H., Kitami, M., Atsumi, S., ... & Sato, R. (2002). Aminopeptidase N isoforms from the midgut of *Bombyx mori* and *Plutella xylostella*–their classification and the factors that determine their binding specificity to *Bacillus thuringiensis* Cry1A toxin. *FEBS Letters*, 519: 215-220.

Nardi, J. B., Bee, C. M., Miller, L. A., Mathur, D., & Ohlstein, B. (2011). Cell renewal in adjoining intestinal and tracheal epithelia of *Manduca*. *Journal of Insect Physiology*, 57(4): 487-493.

Nászai, M., Carroll, L. R., & Cordero, J. B. (2015). Intestinal stem cell proliferation and epithelial homeostasis in the adult *Drosophila* midgut. *Insect Biochemistry and Molecular Biology*, 67: 9-14.

Nation Sr, J. L. (2015). *Insect Physiology and Biochemistry*. CRC press.

Navarro-Cerrillo, G., Hernández-Martínez, P., Vogel, H., Ferré, J., & Herrero, S. (2013). A new gene superfamily of pathogen-response (repat) genes in Lepidoptera: Classification and expression analysis. *Comparative Biochemistry and Physiology Part B: Biochemistry and Molecular Biology*, 164(1): 10-17.

Nie, Z. E. T. A. N. (1992). Fetuin: its enigmatic property of growth promotion. *American Journal of Physiology-Cell Physiology*, 263(3): C551-C562.

Nijhout, H. F., Smith, W. A., Schachar, I., Subramanian, S., Tobler, A., & Grunert, L. W. (2007). The control of growth and differentiation of the wing imaginal disks of *Manduca sexta*. *Developmental Biology*, 302(2): 569-576.

Ningshen, T. J., Chaitanya, R. K., Hari, P. P., Devi, P. V., & Dutta-Gupta, A. (2013). Characterization and regulation of *Bacillus thuringiensis* Cry toxin binding aminopeptidases N (APNs) from non-gut visceral tissues, Malpighian tubule and salivary gland: Comparison with midgut-specific APN in the moth *Achaea janata*. *Comparative Biochemistry and Physiology Part B: Biochemistry and Molecular Biology*, 166: 194-202.

Ningshen, T. J., Chauhan, V. K., Dhania, N. K., & Dutta-Gupta, A. (2017). Insecticidal effects of hemocoelic delivery of *Bacillus thuringiensis* Cry toxins in *Achaea janata* larvae. *Frontiers in Physiology*, 8: 289.

Obniski, R., Sieber, M., & Spradling, A. C. (2018). Dietary lipids modulate Notch signaling and influence adult intestinal development and metabolism in *Drosophila*. *Developmental Cell*, 47(1): 98-111.

O'Brien, L. E., Soliman, S. S., Li, X., & Bilder, D. (2011). Altered modes of stem cell division drive adaptive intestinal growth. *Cell*, 147(3): 603-614.

Ohlstein, B., & Spradling, A. (2006). The adult *Drosophila* posterior midgut is maintained by pluripotent stem cells. *Nature*, 439(7075): 470.

Okuda, K., de Almeida, F., Mortara, R. A., Krieger, H., Marinotti, O., & Bijovsky, A. T. (2007). Cell death and regeneration in the midgut of the mosquito, *Culex quinquefasciatus*. *Journal of Insect Physiology*, 53(12): 1307-1315.

Oppert, B., Kramer, K. J., Beeman, R. W., Johnson, D., & McGaughey, W. H. (1997). Proteinase-mediated insect resistance to *Bacillus thuringiensis* toxins. *Journal of Biological Chemistry*, 272: 23473-23476.

Pacheco, S., Gómez, I., Arenas, I., Saab-Rincon, G., Rodríguez-Almazán, C., Gill, S. S., ... & Soberón, M. (2009). Domain II loop 3 of *Bacillus thuringiensis* Cry1Ab toxin is involved in a "ping pong" binding mechanism with *Manduca sexta* aminopeptidase-N and cadherin receptors. *Journal of Biological Chemistry*, 284: 32750-32757.

Palma, L., Muñoz, D., Berry, C., Murillo, J., & Caballero, P. (2014). *Bacillus thuringiensis* toxins: an overview of their biocidal activity. *Toxins*, 6(12): 3296-3325.

Pan, M. L., & Telfer, W. H. (1996). Methionine-rich hexamerin and arylphorin as precursor reservoirs for reproduction and metamorphosis in female luna moths. *Archives of Insect Biochemistry and Physiology*, 33: 149-162.

Pan, M. L., & Telfer, W. H. (2001). Storage hexamer utilization in two lepidopterans: differences correlated with the timing of egg formation. *Journal of Insect Science*, 1(2): 1-8.

Pardo-Lopez, L., Soberon, M., & Bravo, A. (2012). *Bacillus thuringiensis* insecticidal three-domain Cry toxins: mode of action, insect resistance and consequences for crop protection. *FEMS Microbiology Reviews*, 37: 3-22.

Pardo-Lopez, L., Soberon, M., & Bravo, A. (2013). *Bacillus thuringiensis* insecticidal three-domain Cry toxins: mode of action, insect resistance and consequences for crop protection. *FEMS microbiology reviews*, 37(1): 3-22.

Paris, M., Melodelima, C., Coissac, E., Tetreau, G., Reynaud, S., David, J. P., & Despres, L. (2012). Transcription profiling of resistance to Bti toxins in the mosquito *Aedes aegypti* using next-generation sequencing. *Journal of Invertebrate Pathology*, 109(2): 201-208.

Patel, H. K., Jani, J. J., & Vyas, H. G. (2009). Isolation and characterization of lepidopteran specific *Bacillus thuringiensis*. *IJIB*, 6(3): 121-126.

Pavani, A., Chaitanya, R. K., Chauhan, V. K., Dasgupta, A., & Dutta-Gupta, A. (2015). Differential oxidative stress responses in castor semilooper, *Achaea janata. Journal of Invertebrate Pathology*, 132: 157-164.

Pavlidi, N., Vontas, J., & Van Leeuwen, T. (2018). The role of glutathione S-transferases (GSTs) in insecticide resistance in crop pests and disease vectors. *Current Opinion in Insect Science*, 27: 97-102.

Peng, D., Xu, X., Ye, W., Yu, Z., & Sun, M. (2010). *Helicoverpa armigera* cadherin fragment enhances Cry1Ac insecticidal activity by facilitating toxin-oligomer formation. *Applied Microbiology and Biotechnology*, 85: 1033-1040.

Pereira, A. E., Wang, H., Zukoff, S. N., Meinke, L. J., French, B. W., & Siegfried, B. D. (2015). Evidence of field-evolved resistance to bifenthrin in western corn rootworm (*Diabrotica virgifera virgifera LeConte*) populations in western Nebraska and Kansas. *PloS One*, 10: e0142299, 1-16.

Perera, O. P., Shelby, K. S., Popham, H. J., Gould, F., Adang, M. J., & Jurat-Fuentes, J. L. (2015). Generation of a transcriptome in a model lepidopteran pest, *Heliothis virescens*, using multiple sequencing strategies for profiling midgut gene expression. *PloS One*, 10: e0128563, 1-28.

Peyronnet, O., Vachon, V., Brousseau, R., Baines, D., Schwartz, J. L., & Laprade, R. (1997). Effect of *Bacillus thuringiensis* toxins on the membrane potential of lepidopteran insect midgut cells. *Appl. Environ. Microbiol.*, 63(5), 1679-1684.

Pigott, C. R., & Ellar, D. J. (2007). Role of receptors in *Bacillus thuringiensis* crystal toxin activity. *Microbiology and Molecular Biology Reviews*, 71: 255-281.

Pimentel, A. C., Barroso, I. G., Ferreira, J. M., Dias, R. O., Ferreira, C., & Terra, W. R. (2018). Molecular machinery of starch digestion and glucose absorption along the midgut of *Musca domestica*. *Journal of Insect Physiology*, 109: 11-20.

Pinheiro, D. O., Quagio-Grassiotto, I., & Gregório, E. A. (2008). Morphological regional differences of epithelial cells along the midgut in *Diatraea saccharalis fabricius* (Lepidoptera: Crambidae) larvae. *Neotropical Entomology*, 37: 413-419.

Pinnock, D. E., Brand, R. J., Milstead, J. E., & Jackson, K. L. (1975). Effect of tree species on the coverage and field persistence of *Bacillus thuringiensis* spores. *Journal of Invertebrate Pathology*, 25(2): 209-214.

Pinos, D., Martínez-Solís, M., Herrero, S., Ferré, J., & Hernández-Martínez, P. (2019). The Spodoptera exigua ABCC2 Acts as a Cry1A Receptor Independently of its Nucleotide Binding Domain II. *Toxins*, 11(3): 172, 1-13.

Qiu, L., Fan, J., Zhang, B., Liu, L., Wang, X., Lei, C., ... & Ma, W. (2017). RNA interference knockdown of aminopeptidase N genes decrease the susceptibility of *Chilo suppressalis* larvae to Cry1Ab/Cry1Ac and Cry1Ca-expressing transgenic rice. *Journal of Invertebrate Pathology*, 145: 9-12.

Rajamohan, F., Lee, M. K., & Dean, D. H. (1998). *Bacillus thuringiensis* insecticidal proteins: molecular mode of action. *Progress in Nucleic acid Research and Molecular Biology*, 60: 1-27.

Rausell, C., De Decker, N., Garcıa-Robles, I., Escriche, B., Van Kerkhove, E., Real, M. D., & Martınez-Ramırez, A. C. (2000). Effect of *Bacillus thuringiensis* toxins on the midgut of the nun moth *Lymantria monacha*. *Journal of Invertebrate Pathology*, 75(4): 288-291.

Reddy, V. P., Rao, N. N., Devi, P. V., Narasu, M. L., & Kumar, V. D. (2012). PCR-based detection of *cry* genes in local *Bacillus thuringiensis* DOR *Bt*-1 Isolate. *Pest Technology*, 6: 79-82.

Rees, J. S., Jarrett, P., & Ellar, D. J. (2009). Peritrophic membrane contribution to Bt Cry δ-endotoxin susceptibility in Lepidoptera and the effect of Calcofluor. *Journal of Invertebrate Pathology*, 100(3): 139-146.

Riddiford, L. M., Hiruma, K., Lan, Q., & Zhou, B. (1999). Regulation and role of nuclear receptors during larval molting and metamorphosis of Lepidoptera. *American Zoologist*, 39(4):, 736-746.

Rodríguez-Cabrera, L., Trujillo-Bacallao, D., Borrás-Hidalgo, O., Wright, D. J., & Ayra-Pardo, C. (2008). Molecular characterization of *Spodoptera frugiperda–Bacillus thuringiensis* Cry1Ca toxin interaction. *Toxicon*, *51*(4), 681-692.

Roel, A. R., Dourado, D. M., Matias, R., Porto, K. R., Bednaski, A. V., & Costa, R. B. D. (2010). The effect of sub-lethal doses of *Azadirachta indica* (Meliaceae) oil on the midgut of *Spodoptera frugiperda* (Lepidoptera, Noctuidae). *Revista Brasileira de Entomologia*, 54(3): 505-510.

Romanelli, D., Casartelli, M., Cappellozza, S., De Eguileor, M., & Tettamanti, G. (2016). Roles and regulation of autophagy and apoptosis in the remodelling of the lepidopteran midgut epithelium during metamorphosis. *Scientific Reports*, 6: 32939, 1-15.

Rost-Roszkowska, M. M., Poprawa, I., Klag, J., Migula, P., Mesjasz-Przybyłowicz, J., & Przybyłowicz, W. (2010). Differentiation of regenerative cells in the midgut epithelium of *Epilachna cf. nylanderi* (Mulsant 1850) (Insecta, Coleoptera, Coccinellidae). *Folia biologica*, 58(3-4): 209-216.

Ryu, J. H., Ha, E. M., & Lee, W. J. (2010). Innate immunity and gut–microbe mutualism in *Drosophila*. *Developmental & Comparative Immunology*, *34*(4): 369-376.

Sadrud-Din, S. Y., Hakim, R. S., & Loeb, M. (1994). Proliferation and differentiation of midgut epithelial cells from *Manduca sexta*, *in vitro*. *Invertebrate Reproduction & Development*, 26(3): 197-204.

Sambrook, J., Fritsch, E. F., & Maniatis, T. (1989). *Molecular cloning: a laboratory manual* (No. Ed. 2). *Cold spring harbor laboratory press.*

Sanahuja, G., Banakar, R., Twyman, R. M., Capell, T., & Christou, P. (2011). *Bacillus thuringiensis*: a century of research, development and commercial applications. *Plant Biotechnology Journal*, 9: 283-300.

Santos, C. D., Ribeiro, A. F., Ferreira, C., & Terra, W. R. (1984). The larval midgut of the cassava hornworm (*Erinnyis ello*). *Cell and Tissue Research*, 237(3): 565-574.

Sayyed, A. H., Raymond, B., Ibiza-Palacios, M. S., Escriche, B., & Wright, D. J. (2004). Genetic and biochemical characterization of field-evolved resistance to *Bacillus thuringiensis* toxin Cry1Ac in the diamondback moth, *Plutella xylostella*. *Applied and Environmental Microbiology*, 70: 7010-7017.

Schmittgen, T. D., & Livak, K. J. (2008). Analyzing real-time PCR data by the comparative C $_T$ method. *Nature Protocols*, 3(6): 1101-1108.

Schnepf, E., Crickmore, N. V., Van Rie, J., Lereclus, D., Baum, J., Feitelson, J., ... & Dean, D. H. (1998). *Bacillus thuringiensis* and its pesticidal crystal proteins. *Microbiology and Molecular Biology Reviews*, 62: 775-806.

Sen, B., Uzer, G., Samsonraj, R. M., Xie, Z., McGrath, C., Styner, M., ... & Rubin, J. (2017). Intranuclear actin structure modulates mesenchymal stem cell differentiation. *Stem Cells*, 35(6): 1624-1635.

Sen, B., Xie, Z., Uzer, G., Thompson, W. R., Styner, M., Wu, X., & Rubin, J. (2015). Intranuclear actin regulates osteogenesis. *Stem Cells*, 33(10): 3065-3076.

Shabbir, M. Z., Quan, Y., Wang, Z., Bravo, A., Soberón, M., & He, K. (2018). Characterization of the Cry1Ah resistance in Asian corn borer and its cross-resistance to other *Bacillus thuringiensis* toxins. *Scientific Reports*, 8(1): 234, 1-19.

Shanbhag, S., & Tripathi, S. (2009). Epithelial ultrastructure and cellular mechanisms of acid and base transport in the *Drosophila* midgut. *Journal of Experimental Biology*, 212(11): 1731-1744.

Shim, J., Gururaja-Rao, S., & Banerjee, U. (2013). Nutritional regulation of stem and progenitor cells in *Drosophila*. *Development*, 140(23): 4647-4656.

Sim, S., Jupatanakul, N., & Dimopoulos, G. (2014). Mosquito immunity against arboviruses. *Viruses*, 6(11): 4479-4504.

Smagghe, G. J., Elsen, K., Loeb, M. J., Gelman, D. B., & Blackburn, M. (2003). Effects of a fat body extract on larval midgut cells and growth of lepidoptera. *In Vitro Cellular & Developmental Biology-Animal*, 39(1-2): 8-12.

Smagghe, G., Vanhassel, W., Moeremans, C., De Wilde, D., Goto, S., Loeb, M. J., ... & Hakim, R. S. (2005). Stimulation of midgut stem cell proliferation and differentiation by insect hormones and peptides. *Annals of the New York Academy of Sciences*, 1040(1): 472-475.

Soberón, M., Gill, S. S., & Bravo, A. (2009). Signaling versus punching hole: How do *Bacillus thuringiensis* toxins kill insect midgut cells?. *Cellular and Molecular Life Sciences*, 66: 1337-1349.

Song, W., Veenstra, J. A., & Perrimon, N. (2014). Control of lipid metabolism by tachykinin in *Drosophila*. *Cell Reports*, 9(1): 40-47.

Spies, A. G., & Spence, K. D. (1985). Effect of sub-lethal *Bacillus thuringiensis* crystal endotoxin treatment on the larval midgut of a moth, *Manduca*: SEM study. *Tissue and Cell*, 17: 379-394.

Spring, J. H., Robichaux, S. R., & Hamlin, J. A. (2009). The role of aquaporins in excretion in insects. *Journal of Experimental Biology*, 212(3): 358-362.

Storer, N. P., Babcock, J. M., Schlenz, M., Meade, T., Thompson, G. D., Bing, J. W., & Huckaba, R. M. (2010). Discovery and characterization of field resistance to Bt maize: *Spodoptera frugiperda* (Lepidoptera: Noctuidae) in Puerto Rico. *Journal of Economic Entomology*, 103(4): 1031-1038.

Tabashnik, B. E., & Carrière, Y. (2019). Global Patterns of Resistance to Bt Crops Highlighting Pink Bollworm in the United States, China, and India. *Journal of Economic Entomology*, toz173.

Tabashnik, B. E., Brévault, T., & Carrière, Y. (2013). Insect resistance to *Bt* crops: lessons from the first billion acres. *Nature Biotechnology*, 31: 510-521.

Tanaka, S., Endo, H., Adegawa, S., Kikuta, S., & Sato, R. (2016). Functional characterization of Bacillus thuringiensis Cry toxin receptors explains resistance in insects. *The FEBS Journal*, 283(24): 4474-4490.

Tanaka, S., Miyamoto, K., Noda, H., Jurat-Fuentes, J. L., Yoshizawa, Y., Endo, H., & Sato, R. (2013). The ATP-binding cassette transporter subfamily C member 2 in *Bombyx mori* larvae is a functional receptor for Cry toxins from *Bacillus thuringiensis*. *The FEBS Journal*, 280: 1782-1794.

Tanaka, S., Yoshizawa, Y., & Sato, R. (2012). Response of midgut epithelial cells to Cry1Aa is toxin-dependent and depends on the interplay between toxic action and the host apoptotic response. *The FEBS journal*, 279(6): 1071-1079.

Tassone, E. E., Zastrow-Hayes, G., Mathis, J., Nelson, M. E., Wu, G., Flexner, J. L., ... & Fabrick, J. A. (2016). Sequencing, *de novo* assembly and annotation of a pink bollworm larval midgut transcriptome. *GigaScience*, 5(1): 28, 1-5.

Telfer, W. H., & Kunkel, J. G. (1991). The function and evolution of insect storage hexamers. *Annual Review of Entomology*, 36: 205-228.

Terra, W. R., & Ferreira, C. (1994). Insect digestive enzymes: properties, compartmentalization and function. *Comparative Biochemistry and Physiology Part B: Comparative Biochemistry*, 109: 1-62.

Terra, W. R., Ferreira, C., & Baker, J. E. (1996). Compartmentalization of digestion. In *Biology of the insect midgut* (pp. 206-235). Springer, Dordrecht.

Tettamanti, G., & Casartelli, M. (2019). Cell death during complete metamorphosis. *Philosophical Transactions of the Royal Society B*, 374(1783): 0065, 1-11.

Tettamanti, G., Carata, E., Montali, A., Dini, L., & Fimia, G. M. (2019). Autophagy in development and regeneration: role in tissue remodelling and cell survival. *The European Zoological Journal*, 86(1): 113-131.

Tettamanti, G., Grimaldi, A., Casartelli, M., Ambrosetti, E., Ponti, B., Congiu, T., ... & De Eguileor, M. (2007). Programmed cell death and stem cell differentiation are responsible for midgut replacement in *Heliothis virescens* during prepupal instar. *Cell and Tissue Research*, 330(2): 345-359.

Tiewsiri, K., & Wang, P. (2011). Differential alteration of two aminopeptidases N associated with resistance to *Bacillus thuringiensis* toxin Cry1Ac in cabbage looper. *Proceedings of the National Academy of Sciences*, 108: 14037-14042.

Towbin, H., Staehelin, T., & Gordon, J. (1979). Electrophoretic transfer of proteins from polyacrylamide gels to nitrocellulose sheets: procedure and some applications. *Proceedings of the National Academy of Sciences*, 76: 4350-4354.

Vacher, C., Bourguet, D., Rousset, F., Chevillon, C., & Hochberg, M. E. (2003). Modelling the spatial configuration of refuges for a sustainable control of pests: a case study of Bt cotton. *Journal of Evolutionary Biology*, 16(3): 378-387.

Vadlamudi, R. K., Ji, T. H., & Bulla, L. A. (1993). A specific binding protein from for the insecticidal toxin of *Bacillus thuringiensis subsp*. berliner. *Journal of Biological Chemistry*, 268: 12334-12340.

VanFrankenhuyzen, K., & Nystrom, C. (1989). Residual toxicity of a high-potency formulation of *Bacillus thuringiensis* to spruce budworm (Lepidoptera: Tortricidae). *Journal of Economic Entomology*, 82: 868-872.

Vimala Devi, P. S., & Sudhakar, R. (2006). Effectiveness of a local strain of *Bacillus thuringiensis* in the management of castor semilooper, *Achaea janata* on castor (*Ricinus communis*). *Indian Journal of Agricultural Science*, 76: 447-449.

Wang, L., Ma, Y., Wan, P., Liu, K., Xiao, Y., Wang, J., ... & Li, X. (2018). Resistance to *Bacillus thuringiensis* linked with a cadherin transmembrane mutation affecting cellular trafficking in pink bollworm from China. *Insect Biochemistry and Molecular Biology*, 94: 28-35.

Wang, P., Zhang, X., & Zhang, J. (2005). Molecular characterization of four midgut aminopeptidase N isozymes from the cabbage looper, *Trichoplusia ni*. *Insect Biochemistry and Molecular Biology*, 35: 611-620.

Wehrle-Haller, B., & Imhof, B. A. (2003). Actin, microtubules and focal adhesion dynamics during cell migration. *The International Journal of Biochemistry & Cell Biology*, 35(1): 39-50.

Whalon, M. E., & Wingerd, B. A. (2003). Bt: mode of action and use. *Archives of Insect Biochemistry and Physiology: Published in Collaboration with the Entomological Society of America*, 54(4): 200-211.

Wheeler, D. E., Tuchinskaya, I., Buck, N. A., & Tabashnik, B. E. (2000). Hexameric storage proteins during metamorphosis and egg production in the diamondback moth, *Plutella xylostella* (Lepidoptera). *Journal of Insect Physiology*, 46: 951-958.

Wigglesworth, V. B. (1972). Digestion and nutrition. In *The Principles of Insect Physiology* (pp. 476-552). Springer, Dordrecht.

Willott, E., Bew, L. K., Nagle, R. B., & Wells, M. A. (1988). Sequential structural changes in the fat body of the tobacco hornworm, *Manduca sexta*, during the fifth larval stadium. *Tissue and Cell*, 20(4): 635-643.

Wilson, C. M. (1979). Studies and critique of Amido Black 10B, Coomassie Blue R, and Fast Green FCF as stains for proteins after polyacrylamide gel electrophoresis. *Analytical Biochemistry*, 96: 263-278.

Wolf, J. B. (2013). Principles of transcriptome analysis and gene expression quantification: an RNA-seq tutorial. *Molecular Ecology Resources*, 13(4): 559-572.

Wu, G. X., Gao, X., Ye, G. Y., Li, K., Hu, C., & Cheng, J. A. (2009). Ultrastructural alterations in midgut and Malpighian tubules of *Boettcherisca peregrina* exposure to cadmium and copper. *Ecotoxicology and Environmental Safety*, 72(4): 1137-1147.

Xie, R., Zhuang, M., Ross, L. S., Gomez, I., Oltean, D. I., Bravo, A., ... & Gill, S. S. (2005). Single amino acid mutations in the cadherin receptor from *Heliothis virescens* affect its toxin binding ability to Cry1A toxins. *Journal of Biological Chemistry*, 280(9): 8416-8425.

Xie, Y., Wu, G., Tang, J., Luo, R., Patterson, J., Liu, S., ... & Zhou, X. (2014). SOAPdenovo-Trans: *de novo* transcriptome assembly with short RNA-Seq reads. *Bioinformatics*, 30(12): 1660-1666.

Xu, L. N., Ling, Y. H., Wang, Y. Q., Wang, Z. Y., Hu, B. J., Zhou, Z. Y., ... & He, K. L. (2015). Identification of differentially expressed microRNAs between *Bacillus thuringiensis* Cry1Ab-resistant and-susceptible strains of *Ostrinia furnacalis*. *Scientific Reports*, 5: 15461, 1-15.

Xu, X., Yu, L., & Wu, Y. (2005) Disruption of a cadherin gene associated with resistance to Cry1Ac δ-endotoxin of *Bacillus thuringiensis* in *Helicoverpa armigera*. *Applied and Environmental Microbiology*, 71: 948-954.

Yang, X., Chen, W., Song, X., Ma, X., Cotto-Rivera, R. O., Kain, W., ... & Wang, P. (2019). Mutation of ABC transporter ABCA2 confers resistance to Bt toxin Cry2Ab in *Trichoplusia ni*. *Insect Biochemistry and Molecular Biology*, 112: 103209, 1-15.

Yao, J., Zhu, Y. C., Lu, N., Buschman, L., & Zhu, K. (2017). Comparisons of transcriptional profiles of gut genes between Cry1Ab-resistant and susceptible strains of *Ostrinia nubilalis* revealed genes possibly related to the adaptation of resistant larvae to transgenic Cry1Ab corn. *International Journal of Molecular Sciences*, 18(2): 301, 1-17.

Yin, C., Liu, Y., Liu, J., Xiao, H., Huang, S., Lin, Y., ... & Li, F. (2014). ChiloDB: a genomic and transcriptome database for an important rice insect pest *Chilo suppressalis*. *Database*, 65: 1-7.

Yinghua, S., Yan, D., Jin, C., Jiaxi, W., & Jianwu, W. (2017). Responses of the cutworm Spodoptera litura (Lepidoptera: Noctuidae) to two Bt corn hybrids expressing Cry1Ab. *Scientific Reports*, 7: 41577, 1-13.

Yu, T., Li, X., Coates, B. S., Zhang, Q., Siegfried, B. D., & Zhou, X. (2018). microRNA profiling between *Bacillus thuringiensis* Cry1Ab-susceptible and-resistant European corn borer, *Ostrinia nubilalis* (Hübner). *Insect Molecular Biology*, 27(3): 279-294.

Zhang, F., Peng, D., Cheng, C., Zhou, W., Ju, S., Wan, D., ... & Ye, X. (2016). *Bacillus thuringiensis* crystal protein Cry6Aa triggers *Caenorhabditis elegans* necrosis pathway mediated by aspartic protease (ASP-1). *PLoS Pathogens*, 12: e1005389, 1-25.

Zhang, H., Tian, W., Zhao, J., Jin, L., Yang, J., Liu, C., ... & Tabashnik, B. E. (2012). Diverse genetic basis of field-evolved resistance to *Bt* cotton in cotton bollworm from China. *Proceedings of the National Academy of Sciences*, 109: 10275-10280.

Zhang, H., Yin, W., Zhao, J., Jin, L., Yang, Y., Wu, S., ... & Wu, Y. (2011). Early warning of cotton bollworm resistance associated with intensive planting of Bt cotton in China. *PLoS One*, 6(8): e22874, 1-8.

Zhang, X., Candas, M., Griko, N. B., Taussig, R., & Bulla, L. A. (2006). A mechanism of cell death involving an adenylyl cyclase/PKA signaling pathway is induced by the Cry1Ab toxin of *Bacillus thuringiensis*. *Proceedings of the National Academy of Sciences*, 103(26): 9897-9902.

Zhang, X., Griko, N. B., Corona, S. K., & Bulla, L. A. (2008). Enhanced exocytosis of the receptor BT-R 1 induced by the Cry1Ab toxin of *Bacillus thuringiensis* directly correlates to the execution of cell death. *Comparative Biochemistry and Physiology Part B: Biochemistry and Molecular Biology*, 149: 581-588.

Zhao, J., Jin, L., Yang, Y., & Wu, Y. (2010). Diverse cadherin mutations conferring resistance to Bacillus thuringiensis toxin Cry1Ac in Helicoverpa armigera. *Insect Biochemistry and Molecular Biology*, 40(2): 113-118.

Zhao, L., & Kanost, M. R. (1996). In search of a function for hemolin, a hemolymph protein from the immunoglobulin superfamily. *Journal of Insect Physiology*, 42: 73-79.

Zhou, C., Yang, H., Wang, Z., Long, G. Y., & Jin, D. C. (2018). Comparative transcriptome analysis of Sogatella furcifera (Horváth) exposed to different insecticides. *Scientific Reports*, 8(1): 8773, 1-12.

Zhou, Z., Wang, Z., Liu, Y., Liang, G., Shu, C., Song, F., ... & Zhang, J. (2016). Identification of ABCC2 as a binding protein of Cry1Ac on brush border membrane vesicles from *Helicoverpa armigera* by an improved pull-down assay. *Microbiology Open*, 5: 659-669.

Zhu, Y. C., Guo, Z., Chen, M. S., Zhu, K. Y., Liu, X. F., & Scheffler, B. (2011). Major putative pesticide receptors, detoxification enzymes, and transcriptional profile of the midgut of the tobacco budworm, *Heliothis virescens* (Lepidoptera: Noctuidae). *Journal of Invertebrate Pathology*, 106(2): 296-307.

Zhu-Salzman, K., & Zeng, R. (2015). Insect response to plant defensive protease inhibitors. *Annual Review of Entomology*, 60: 233-252.

Publications

SCIENTIFIC DATA

OPEN

DATA DESCRIPTOR

Received: 28 March 2019
Accepted: 17 July 2019
Published online: 22 August 2019

RNA-Seq analysis and *de novo* transcriptome assembly of Cry toxin susceptible and tolerant *Achaea janata* larvae

Narender K. Dhania[1], Vinod K. Chauhan[1], R. K. Chaitanya[2] & Aparna Dutta-Gupta[1]

Larvae of most lepidopteran insect species are known to be voracious feeders and important agricultural pests throughout the world. *Achaea janata* larvae cause serious damage to *Ricinus communis* (Castor) in India resulting in significant economic losses. Microbial insecticides based on crystalline (Cry) toxins of *Bacillus thuringiensis* (Bt) have been effective against the pest. Excessive and indiscriminate use of Bt-based biopesticides could be counter-productive and allow susceptible larvae to eventually develop resistance. Further, lack of adequate genome and transcriptome information for the pest limit our ability to determine the molecular mechanisms of altered physiological responses in Bt-exposed susceptible and tolerant insect strains. In order to facilitate biological, biochemical and molecular research of the pest species that would enable more efficient biocontrol, we report the midgut *de novo* transcriptome assembly and clustering of susceptible Cry toxin-exposed and Cry toxin tolerant *Achaea janata* larvae with appropriate age-matched and starvation controls.

Background & Summary

Bacillus thuringiensis (Bt) insecticidal proteins used in sprayable formulations and transgenic crops are the most promising alternatives to synthetic insecticides. However, the evolution of resistance in the field, as well as laboratory insect populations is a serious roadblock to this technology. *Achaea janata*, a major castor crop pest in India, is controlled using Bt-based formulation[1] comprising of *Cry1* (*Cry1Aa*, *Cry1Ab*, and *Cry1Ac*) and *Cry2* (*Cry2Aa* and *Cry2Ab*) genes[2]. Recent studies from our group reported extensive changes at the cellular and molecular level in the midgut of *A. janata* exposed to a sublethal dose of the *Bt* formulation[3–5]. Since a decade, reports of resistance against Bt toxins and their mechanisms have been emerging[6,7]. Long term exposure to Cry toxin formulations promotes tolerance in larvae which eventually leads to resistance[6–8]. Development of Bt resistance could be due to alterations in proteolytic cleavage of the Cry toxin, altered receptor binding or enhanced midgut regeneration responses[9–11]. With the advent of next generation sequencing technology it is now possible to characterize the entire repertoire of transcripts under different conditions and predict pathways involved in various molecular mechanisms. The RNA sequencing study presented here generated the first *de novo* transcriptome assembly of castor semilooper, *Achaea janata* (Noctuidae: Lepidoptera), and compared gene expression signatures between toxin-exposed susceptible and tolerant larvae. This article, is a first step in determining the primary basis for Cry tolerance in the pest, which could facilitate new long term management strategies.

Methods

Toxin administration and sample preparation. Wild population of *A. janata* larvae, unexposed to pesticides, was field collected from the Indian Institute of Oil Seed Research, Hyderabad, India. Further, the larvae were reared and maintained on castor leaves at 27 ± 2 °C, 14:10 h (light: dark) photoperiod and 60–70% relative humidity for three generations at the insectary of School of Life Sciences, University of Hyderabad, India. In the present *de novo* transcriptome analysis for the sublethal toxin exposure, 1/10 of LD_{50} was used (Group ii) (Fig. 1),

[1]Department of Animal Biology, School of Life Sciences, University of Hyderabad, Hyderabad, 500046, India. [2]Department of Animal Sciences, School of Basic and Applied Sciences, Central University of Punjab, Bathinda, 151001, India. Correspondence and requests for materials should be addressed to A.D.-G. (email: aparnaduttagupta@gmail.com) or R.K.C. (email: chaitanyark@cup.ac.in)

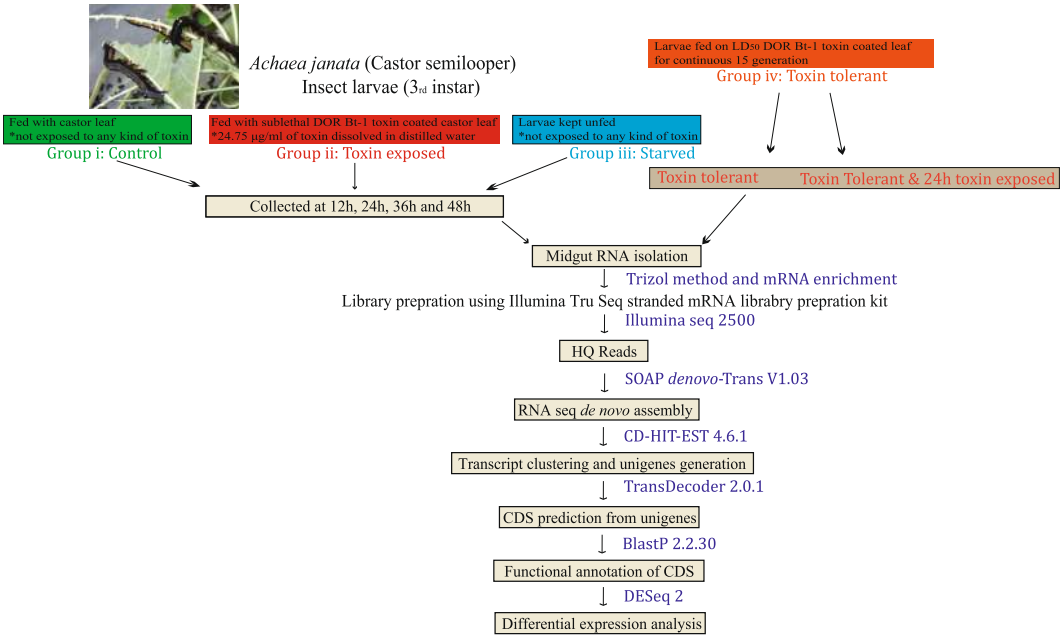

Fig. 1 Flow chart showing the methodology used for the present study.

while for the generation of a tolerant population (Group iv) (Fig. 1) an LD_{50} dose of DOR Bt-1 formulation was administered[1]. Larval batches (n = 100) designated as Cry-susceptible larvae and control larvae were exposed to toxin-coated and distilled water coated leaves respectively. The midgut was isolated from 15 randomly selected surviving larvae from each batch after every 12 h till 48 h. In earlier study we noticed that larvae probably sense the toxin and avoid feeding on toxin coated leaves after a short exposure. Hence, to eliminate any effect induced by starvation, an additional batch (Group iv) of 3rd instar larvae was maintained on moist filter paper and collected for the midgut isolation every 12 h till 48 h. All the midgut dissections were carried out in ice-cold insect Ringer solution (130 mM NaCl, 0.5 mM KCl, and 0.1 mM $CaCl_2$). The experiment was performed in duplicates. For the Cry tolerant larval population, larvae (n = 100) in each generation were exposed to LD_{50} dose and the surviving insects were maintained for larval development, pupal molting, adult emergence and egg laying. The larvae hatched from the eggs were collected and reared till 3rd larval instar larvae and exposed to LD_{50} Bt dose once again. This schedule was carried out for fifteen generations. The batch (n = 100) of Cry tolerant larvae thus generated were exposed to toxin-coated leaves and the midguts were isolated from randomly selected fifteen larvae after 24 h. Total RNA was isolated from the midgut samples using Trizol-based method. The RNA was quantified using NanoDrop™ 8000 spectrophotometer and the quality was assessed using 1% formaldehyde denaturing agarose gel.

Library preparation. Illumina 2 × 150 pair end libraries were prepared as follows. Briefly, mRNA was enriched from isolated total RNA and fragmented. The fragmented mRNA was used for first-strand cDNA synthesis, followed by second-strand generation, A-tailing and adapter ligation. Adapter ligated products were purified and PCR amplification was carried out. PCR amplified cDNA libraries were assessed for quality and quantity using DNA High Sensitivity Assay Kit (Agilent Technologies).

Quality assessment prior to cluster generation and sequencing. The amplified libraries were analyzed using Bioanalyzer 2100 and High Sensitivity DNA chip (Agilent Technologies). After obtaining the Qubit concentration for each of the libraries, it was loaded on Illumina platform (2 × 150 bp chemistry) for cluster generation and sequencing. Data was generated on Illumina HiSeq. 2500 system and paired-end sequencing allowed the template fragments to be sequenced in both the forward and reverse directions. The library molecules bind to complementary adapter oligos on paired-end flow cell. The adapters were designed to allow selective cleavage of the forward strands after re-synthesis of the reverse strand during sequencing. The copied reverse strand was then used to sequence from the opposite end of the fragment. Total RNA was subjected to pair-end library preparation with Illumina TruSeq Stranded Total RNA Library Preparation Kit. The mean size of the libraries was between 357 bp to 567 bp for the 28 samples. The libraries were sequenced and high quality data was generated for ~ 3.05 GB data per sample (Online-only Table 1).

Sequence analysis. Illumina 2 × 150 pair end libraries were prepared using the Illumina TruSeq stranded mRNA Library Preparation Kit and as per the firm's protocol (Illumina Inc.). The amplified libraries were analyzed on the Bioanalyzer 2100 with a High Sensitivity DNA chip (Agilent Technologies). The *de novo* master assembly was generated using "SOAP-denovo-Trans (v1.03)" assembler (Short Oligonucleotide Analysis Package)[12]. For each data set, raw quality was assessed and filtered with Trimmomatic (v.0.36)[13]. Transcripts were clustered using the CD-HIT (Cluster Database at High Identity with Tolerance) package[14]. The predicted proteins

Description	Master Assembly
Total number of transcripts	1,74,066
Total transcriptome length in bps	100,247,510
Average transcript length in bps	575
N50	421
Maximum transcript length in bps	25,338
Minimum transcript length in bps	200
Metrics	**Master Assembly**
Length >=200 & <=300	85429
Length >300 & <=400	32056
Length >400 & <=500	13439
Length >500 & <=600	8124
Length >600 & <=700	5796
Length >700 & <=800	4098
Length >800 & <=900	3028
Length >900 & <=1000	2444
Length >1000 & <=5000	18383
Length >5000	1269

Table 1. Statistics of assembled transcripts and transcript length distribution.

Description	Unigenes
Total number of unigenes	1,36,618
Total size of all unigenes in bps	86,577,226
Average unigene length in bps	633
N50	458
Maximum unigene length in bps	25,338
Minimum unigene length in bps	200
Metrics	**Unigenes**
Length >=200 & <=300	56403
Length >300 & <=400	26874
Length >400 & <=500	12354
Length >500 & <=600	7740
Length >600 & <=700	5647
Length >700 & <=800	3980
Length >800 & <=900	2941
Length >900 & <=1000	2366
Length >1000 & <=5000	17193
Length >5000	1120

Table 2. Statistics of unigenes and length distribution.

of CDS (Coding sequence) were subjected to similarity search against NCBI's non-redundant (nr) database using the BLASTP (Basic Local Alignment Search Tool) algorithm.

Data Records

The total raw sequencing data from 28 samples (14 biological replicates, where the sequencing experiment was performed twice and the replicates are derived from different pool of larvae and they are biologically independent samples) was used for assembly in the present study. They have been deposited in the NCBI SRA database, with identifier SRP18670[15] and accession numbers SRR8617834, SRR8617835, SRR8617836, SRR8617837, SRR8617838, SRR8617839, SRR8617840, SRR8617841, SRR8617842, SRR8617843, SRR8617844, SRR8617845, SRR8617846, SRR8617847, SRR8617848, SRR8617849, SRR8617850, SRR8617851, SRR8617852, SRR8617853, SRR8617854, SRR8617855, SRR8617856, SRR8617857, SRR8617858, SRR8617859, SRR8617860 and SRR8617861, under BioProject PRJNA523326 and BioSample SAMN09241884. This Transcriptome Shotgun Assembly project has been deposited at DDBJ/ENA/GenBank under the accession GHGZ00000000[16]. The version described in this paper is the first version, GHGZ01000000.

Description	Metrics
Total number of cds	35,559
Total size of all cds in bps	25,527,927
Average cds length in bps	717
Maximum cds length in bps	8,595
Metrics	**CDS**
Length >200 & <=300	761
Length >300 & <=400	9515
Length >400 & <=500	5643
Length >500 & <=600	4127
Length >600 & <=700	3003
Length >700 & <=800	2275
Length >800 & <=900	1867
Length >900 & <=1000	1652
Length >1000 & <=5000	6684
Length >5000	32

Table 3. Statistics and length distribution of the predicted CDS.

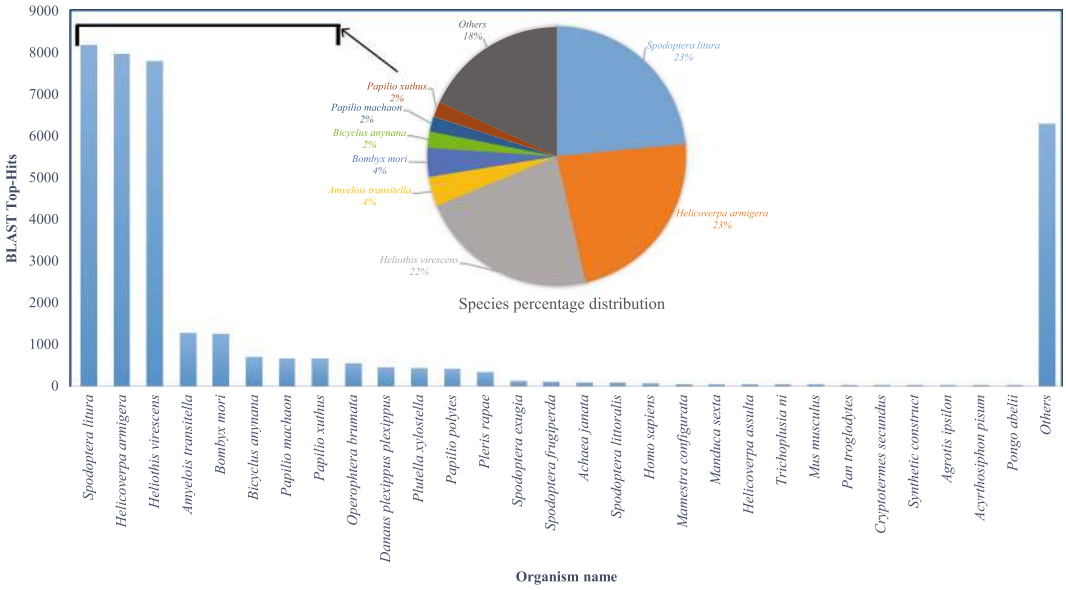

Fig. 2 Top-hit species distribution of most closely related insect species demonstrated using a horizontal bar graph.

Technical Validation

SOAPdenovo-Trans assembler was used to generate *de novo* transcriptome assembly from four experimental sets of midgut samples viz. Group (i) susceptible larvae exposed to medium (water), Group (ii) susceptible larvae exposed to 1/10 of LD_{50} dosage of DOR Bt-1 formulation, Group (iii) susceptible larvae subjected to starvation and Group (iv) tolerant larvae exposed to LD_{50} dosage of DOR Bt-1 formulation (reared for 15 generations) (Fig. 1). A total of 1,74,066 transcripts were generated for master assembly with a transcriptome length of 10,02,47,510 bps (base pairs). A total of 1,36,818 unigenes were reported using CD-HIT and 35,559 coding sequences were predicted by Transdecoder. The top-hit species distribution revealed that majority (23%) of the CDS aligned with *Spodoptera litura* followed by *Helicoverpa armigera* and *Heliothis virescens* all of which belong to family Noctuidae in the Lepidoptera order.

Transcriptome assembly. The *de novo* master assembly of high quality reads of 28 processed samples was accomplished using "SOAP-denovo-Trans (v1.03)" assembler[12]. For each data set, raw quality (phred40) was assessed and filtered with Trimmomatic (v.0.36) using the parameters ILLUMINACLIP:adapter.fasta:2:30:8 MINLEN:40 to remove adaptor sequence and filter by quality score[13]. An average of 19 million clean reads were obtained. Statistics of high quality reads with total reads, base count and data size are summarized in Online-only Table 1 and statistics of assembled transcripts as well as length distribution is presented in Table 1.

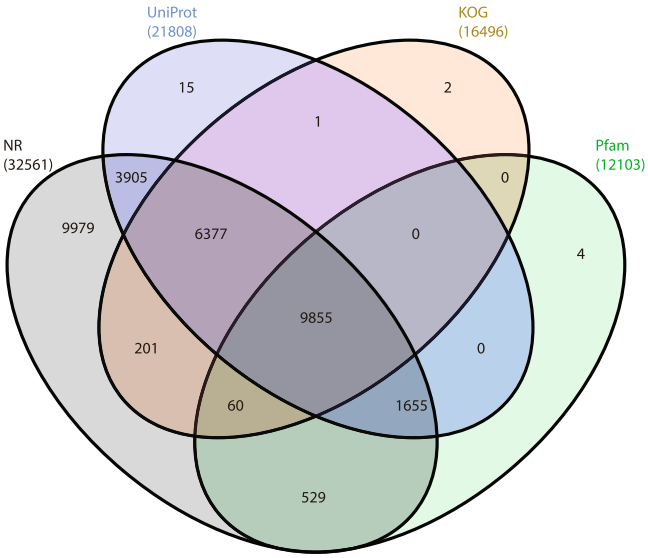

Fig. 3 Venn diagram representation of annotated protein in different databases.

Clustering. To filter the redundancy or the noise, it was required to select one representative transcript for transcripts clusters. Transcripts were clustered using CD-HIT (Cluster Database at High Identity with Tolerance) package[14]. CD-HIT-EST v4.6.1 was used to remove the shorter redundant transcripts when they were 100% covered by other transcripts with more than 90% identity. The non-redundant clustered transcripts were then designated as unigenes (Table 2). CDS were predicted from the unigene sequences with Transdecoder at default parameters which resulted in the identification of 35,559 CDS (Table 3).

Annotation. The predicted proteins of CDS were subjected to similarity search against NCBI's non-redundant (nr) database using the BLASTP algorithm. Out of total 35,559 proteins, 32,561 proteins were captured with hits and 2,998 with no hits (Annotation of each transcript of the assembled transcriptome)[17]. The top-hit species distribution revealed that majority of the hits were found to be against the species *Spodoptera litura* followed by *Helicoverpa armigera* and *Heliothis virescens* (Fig. 2). Simultaneously, all protein sequences were searched for similarity against NR, UniProt (Universal Protein Resources), KOG (EuKaryotic Orthologous Groups) and Pfam database using BLASTP with an e-value threshold of $1e^{-5}$. The BLAST result of four databases has resulted in Fig. 3.

Differential expression. In this work we compared the control and Cry toxin tolerant larval transcript map reads for the differential expression analysis. Analysis of count data was done using DESeq. 2 in RStudio platform[18]. Differential expression analysis shows significant differences in the tolerant larval population as compared to the susceptible population (Differential expression analysis)[17]. Out of 35,559 CDS analysed, 320 CDS show significant variation (padj < 0.05). Few of these genes like (i) gi|1131919362| Ca^{2+}-binding protein, RTX toxin-related, (ii) gi|1199381583| superoxide dismutase [Cu-Zn] 2-like, (iii) gi|315139350| serine protease 63, (iv) gi|1274141826| trypsin, alkaline C-like and (v) gi|1274136486| apolipophorins isoform X2 were shown to be upregulated, while (i) gi|123995301| ribosomal protein SA, (ii) gi|744619941| predicted: 60 S ribosomal protein L8, (iii) gi|45219787| ribosomal protein S3A, (iv) gi|1344818460| alanine aminotransferase 1-like and (v) gi|501300966| ubiquitin were downregulated.

Code Availability

The following software version/script were used in the current manuscript. The RStudio software packages are available open-source from the repository at https://www.rstudio.com/. SOAPdenovo-Trans (v.1.03)[12]. Trimmomatic (v.0.36)[13]. CD-HIT-EST (v.4.6.1)[14]. BlastP (v.2.2.30). The DESeq. 2 scripts were used for plotting the differential expression data. https://bioconductor.org/packages/release/bioc/vignettes/DESeq. 2/inst/doc/DESeq. 2.html. As an input we have used- (1) a table having RAW read counts and (2) metadata, that is, each line contains description of one of the samples. See example below: #SampleName Condition. C1_raw_read_count control. D1_raw_read_count tolerant.

References

1. Vimala Devi, P. S. & Sudhakar, R. Effectiveness of a local strain of *Bacillus thuringiensis* in the management of castor semilooper, *Achaea janata* on castor (*Ricinus communis*). *Indian J Agr Sci* **156**, 447–449 (2006).
2. Reddy, V. P., Rao, N. N., Devi, P. V., Narasu, M. L. & Kumar, V. D. PCR-based detection of cry genes in local *Bacillus thuringiensis* DOR Bt-1 isolate. *Pest Technol.* **6**, 79–82 (2012).
3. Ningshen, T. J., Chauhan, V. K., Dhania, N. K. & Dutta-Gupta, A. Insecticidal effects of hemocoelic delivery of Bacillus *thuringiensis* Cry toxins in *Achaea janata* larvae. *Front Physiol.* **8**(289), 1–10 (2017).
4. Chauhan, V. K., Dhania, N. K., Chaitanya, R. K., Senthilkumaran, B. & Dutta-Gupta, A. Larval mid-gut responses to sub-lethal dose of cry toxin in lepidopteran pest *Achaea janata*. *Front Physiol.* **8**(662), 1–11 (2017).

5. Dhania, N. K., Chauhan, V. K., Chaitanya, R. K. & Dutta-Gupta, A. Midgut *de novo* transcriptome analysis and gene expression profiling of *Achaea janata* larvae exposed with *Bacillus thuringiensis* (Bt)-based biopesticide formulation. *Comp Biochem Physiol Part D Genomics Proteomics* **30**, 81–90 (2019).
6. Tabashnik, B. E., Mota-Sanchez, D., Whalon, M. E., Hollingworth, R. M. & Carrière, Y. Defining terms for proactive management of resistance to Bt crops and pesticides. *J Econ Entomol* **107**, 496–507 (2014).
7. Badran, A. H. *et al*. Continuous evolution of *Bacillus thuringiensis* toxins overcomes insect resistance. *Nature* **533**(7601), 58 (2016).
8. Melo, A. L. D. A., Soccol, V. T. & Soccol, C. R. *Bacillus thuringiensis*: mechanism of action, resistance, and new applications: a review. *Crit Rev Biotechnol* **36**, 317–326 (2016).
9. Bretschneider, A., Heckel, D. G. & Pauchet, Y. Three toxins, two receptors, one mechanism: Mode of action of Cry1A toxins from *Bacillus thuringiensis* in *Heliothis virescens*. *Insect Biochem Mol Bio* **76**, 109–117 (2016).
10. Jurat-Fuentes, J. L. & Crickmore, N. Specificity determinants for Cry insecticidal proteins: Insights from their mode of action. *J Invert Path* **142**, 5–10 (2017).
11. Carrière, Y., Fabrick, J. A. & Tabashnik, B. E. Can pyramids and seed mixtures delay resistance to Bt crops? *Trends Biotechnol.* **34**, 291–302 (2016).
12. Xie, Y. *et al*. SOAPdenovo-Trans: *de novo* transcriptome assembly with short RNA-Seq reads. *Bioinformatics* **30**, 1660–1666 (2014).
13. Bolger, A. M., Lohse, M. & Usadel, B. Trimmomatic: a flexible trimmer for Illumina sequence data. *Bioinformatics* **30**, 2114–2120 (2014).
14. Fu, L., Niu, B., Zhu, Z., Wu, S. & Li, W. CD-HIT: accelerated for clustering the next-generation sequencing data. *Bioinformatics* **28**, 3150–3152 (2012).
15. *NCBI Sequence Read Archive*, https://identifiers.org/insdc.sra:SRP186750 (2019).
16. *GenBank*, https://identifiers.org/ncbi/insdc:GHGZ00000000.1 (2019).
17. Dhania, N. K., Chauhan, V. K., Chaitanya, R. K. & Dutta-Gupta, A. RNA-Seq analysis and de novo transcriptome assembly of Cry toxin susceptible and tolerant Achaea janata larvae. *figshare*, https://doi.org/10.6084/m9.figshare.c.4436612 (2019).
18. Love, M. I., Huber, W. & Anders, S. Moderated estimation of fold change and dispersion for RNA-seq data with DESeq2. *Genome Biol.* **15**(12), 550 (2014).

Acknowledgements

This research was supported by the grant from the Council of Scientific and Industrial Research (Grant No. 37(1709)/18/EMR-11), UGC-BSR Faculty Fellowship to ADG and UGC research grant to RKC. Financial support in form of senior research fellowship to NKD by UGC and VC by DBT, India are acknowledged. Special thanks to Dr. Vivek, Department of System & Computational Biology, School of Life Sciences in the help provided in DESeq analysis.

Author Contributions

N.K.D., V.K.C. and R.K.C. designed the study and A.D.G. contributed to the project coordination. N.K.D. and V.K.C. performed the experiments and collected sample; N.K.D. and RKC analyzed the data and evaluated; N.K.D. wrote the paper which was critically evaluated and edited by R.K.C. and A.D.G. The research funding was procured by R.K.C. and A.D.G. All authors read and approved the manuscript.

Additional Information

Competing Interests: The authors declare no competing interests.

Publisher's note: Springer Nature remains neutral with regard to jurisdictional claims in published maps and institutional affiliations.

Comparative Biochemistry and Physiology - Part D 30 (2019) 81–90

Contents lists available at ScienceDirect

Comparative Biochemistry and Physiology - Part D

journal homepage: www.elsevier.com/locate/cbpd

Midgut *de novo* transcriptome analysis and gene expression profiling of *Achaea janata* larvae exposed with *Bacillus thuringiensis* (Bt)-based biopesticide formulation

Narender K. Dhania[a], Vinod K. Chauhan[a], R.K. Chaitanya[b], Aparna Dutta-Gupta[a,*]

[a] Department of Animal Biology, School of Life Sciences, University of Hyderabad, Hyderabad 500046, India
[b] Department of Animal Sciences, School of Basic and Applied Sciences, Central University of Punjab, Bathinda 151001, India

ARTICLE INFO

Keywords:
Bacillus thuringiensis
Castor semilooper
Larval midgut
de novo transcriptome
Microarray

ABSTRACT

India is the major producer and exporter of castor oil in the world. Castor semilooper, *Achaea janata* is one of the main castor crop pests, which causes serious economic loss of crop, hence management and control of the pest are important. Currently, *Bacillus thuringiensis* (Bt) based biopesticides are being used for their control. However, the insects are known to develop resistance not only against chemical pesticides but also to Bt based biopesticides. In the present study, *de novo* transcriptome analysis was conducted to monitor the expression pattern of larval midgut genes in *Achaea janata* exposed to sublethal dose of Bt formulation. A total of 34,612 and 41,109 transcripts were identified in control and toxin-exposed larval midgut samples out of which 18,836 in control and 21,046 in toxin-exposed samples are annotated. Microarray data analysis employed to monitor the gene expression upon Cry toxin exposure revealed that 375 genes were upregulated and 579 genes were downregulated during all the time points (12–60 h) of toxin exposure. The differentially expressed transcripts include *i.e.* Cry toxin receptors, gut proteases, arylphorin, REPATs, detoxification enzymes and aquaporins. Validation of microarray data was performed by real-time quantitative PCR using few randomly selected genes and the results obtained were in corroboration. This is the first study on transcriptome data from the castor semilooper and the results would provide valuable resources for the characterization of Bt toxin response in the pest.

1. Introduction

Castor (*Riccinus communis*) is a non-edible oilseed crop cultivated in various parts of India, Mozambique, China and Brazil, produce 1.7 million, 68.9, 40.0 and 37.5 thousand tons, respectively (**http://www.fao.org/faostat**). Castor bean oil is known to have high viscosity due to the presence of ricinoleic acid and extensively used in paints and varnishes, lubricants in aviation, cosmetics, nylon type synthetic polymers, textile dyeing, resins, leather industry *etc.* India exports (90%) of castor oil (Kallamadi et al., 2015), the major state which grow castor are Gujarat, followed by Andhra Pradesh and Rajasthan (Patel et al., 2016). Its potential as a 'biofuel crop' is hindered by a number of biotic factors, particularly pests which destroy the crop and productivity.

The main defoliator of castor crop is castor semilooper, *Achaea janata*, which occasionally feeds on other important crops (Sujatha et al., 2011). In Indian subcontinent *A. janata* L. (Noctuidae: Lepidoptera) infestation occurs during July–October during which larvae defoliate the castor plantation causing serious loss of crop. The pest is highly susceptible to *Bacillus thuringiensis* (Bt)-based biopesticides, which are both economical and environment-friendly (Chauhan et al., 2017). However, pest larvae are known to become tolerant as well as develop resistance to Bt biopesticides which would become a serious threat in long run for the application of Bt based formulation/Cry transgenics. Instances of field evolved resistance to Bt crops have already been reported in various insect species including *Spodoptera frugiperda* (Storer et al., 2010; Jakka et al., 2016), *Pectinophora gossypiella* (Dhurua and Gujar, 2011), *Busseola fusca* (Kruger et al., 2011), *Helicoverpa armigera* (Zhang et al., 2011), *Diabrotica virgifera* (Pereira et al., 2015), *Chilo suppressalis* (Shabbir et al., 2018), *Tribolium castaneum* (Kliot and Ghanim, 2012), *Ostrinia nubilalis* (Yu et al., 2018), *and Ostrinia furnacalis* (Xu et al., 2015) *etc*.

Well characterized and widely accepted resistance mechanisms to Bt toxin include alterations in proteolytic cleavage of Cry toxins and reduction in toxin binding to their specific receptors due to mutations (Ferré and Van Rie, 2002; Tabashnik et al., 2013). Recent reports on non-receptor related resistance mechanisms suggest involvement of

* Corresponding author.
E-mail address: apdgsl@uohyd.ernet.in (A. Dutta-Gupta).

https://doi.org/10.1016/j.cbd.2019.02.005
Received 9 October 2018; Received in revised form 19 December 2018; Accepted 14 February 2019
Available online 15 February 2019
1744-117X/

stem cell-mediated regeneration of midgut epithelium as well as differential expression of pathogen-response (REPAT) and arylphorin genes which might pose an additional threat to Bt crops as they affect steps common to all Cry toxins resulting in cross-resistance (Herrero et al., 2007; Navarro-Cerrillo et al., 2012; Bel et al., 2013; Park et al., 2014; Burmester, 2015; Castagnola and Jurat-Fuentes, 2016, Chauhan et al., 2017).

Transcriptome analysis through RNA-seq provides novel opportunities to characterize the expression profile of unique genes and their temporal patterns in non-model organisms of agricultural importance lacking genome or transcriptome sequence information (Wolf, 2013). RNA-seq data in insect pests would further serve as a useful resource to study aspects of pest control (Li et al., 2013, Perera et al., 2015; Song et al., 2016; Zhou et al., 2018; Pavlidi et al., 2018).

The larval stage is an important developmental stage in *A. janata* being responsible for economic damage. The larval midgut is the primary target tissue for Bt toxins (Abrol and Shankar, 2016). Hence, in the present study RNA sequencing was performed on the Illumina platform to produce a midgut *de novo* transcriptome from the 3rd instar *A. janata* larvae. *De novo* assembled unigenes were annotated and analyzed, generating the first deep-sequencing gene catalogues for this pest species. Microarray and Quantitative Real Time-PCR (qRT-PCR) analysis further validate the gene expression in both control and toxin-exposed larval insect groups at different time points. This study would not only form a basis to investigate the molecular mechanisms underlying host responses to Bt toxins but also contribute towards the elucidation of survival mechanism(s) of the pest against sub-lethal dose of the Cry formulation.

2. Materials and methods

2.1. Insect collection and rearing

A. janata larvae were collected from the castor field of Indian Institute of Oil Seed Research, Hyderabad, India without any exposure to Bt pesticides. Before experimentation, the insects were reared and maintained on castor leaves at 27 ± 2 °C, 14:10 h (light:dark) photoperiod and 60–70% relative humidity for three generations at the insectary facility of University of Hyderabad, India for obtaining a homogeneous population (Ningshen et al., 2017).

2.2. Bioassay and sample preparation

A. janata 3rd instar larvae were fed with uniform toxin-coated castor leaves. For the present analysis, one tenth of LC_{50} value (24.75 μg/ml of toxin dissolved in distilled water) of a local DOR *Bt*-1 formulation was used. Reddy et al. (2012) demonstrated the presence of *Cry1* (*Cry1Aa*, *Cry1Ab*, and *Cry1Ac*) and *Cry2* (*Cry2Aa* and *Cry2Ab*) genes in the isolate. For *de novo* transcriptome analysis, two groups of 30 insects each were separated from a homogenous batch. One group of insects was exposed to distilled water coated leaves (control larvae) and the other group was exposed to the toxin coated leaves (toxin-exposed larvae). After 24 h, fifteen surviving larvae from each set were randomly collected for subsequent midgut isolation. For microarray and qRT-PCR analysis, control and experimental insect groups were collected for tissue isolation after every 12 h exposure till 60 h. Larval midgut tissue was dissected in ice-cold insect Ringer solution (130 mM NaCl, 0.5 mM KCl, and 0.1 mM $CaCl_2$) and RNA was isolated quickly using TRIzol® method (Thermo Fischer Scientific, USA). The purity and quantity of the obtained RNA samples was assessed using NanoDrop™ 2000 spectrophotometer (Thermo Fischer Scientific, USA). The quality of the RNA was assessed on the Bioanalyzer 2100 (Agilent Technologies, USA). The RNA integrity number (RIN) threshold was found to be ~7.5.

2.3. cDNA library construction and Illumina sequencing

Control and toxin-exposed midgut libraries were prepared using the Sure Select Strand-Specific RNA Library Prep Kit (Agilent Technologies, USA, Cat # 5500-0116; # 5190-6410). Briefly, poly(A) + mRNA from the total RNA was isolated using oligo (dT) magnetic beads. The purified mRNA was chemically fragmented to 150 bp at elevated temperature (94 °C for 8 min) using RNA-Seq fragmentation mix. First strand cDNA was synthesized using RNA Seq First Strand Master Mix (Actinomycin D (120 ng/μl) was added to maintain specificity) and cleaned up using AMPure XP beads. Second strand cDNA was synthesized using RNA-Seq Second Strand Mix. The cDNA was cleaned up using AMPure XP beads followed by end repair, addition of poly A and adaptor ligation using RNA-Seq dA Tailing Master Mix. The adaptor ligated cDNA was purified and indexed. Further amplification and enrichment was carried out using 12 cycles of PCR with adapter ligated fragments. Agilent 2100 Bioanalyzer system was used for quality check of final cDNA library (Supplementary Fig. 1), and was sequenced by using Illumina NextSeq500 (Illumina, San Diego, CA, USA).

2.4. De novo assembly and annotation

Before assembly, the raw reads were processed for quality based trimming towards 5′- and 3′-ends using an in-house script. Quality check was performed by FASTA QC software. Clean reads from both the samples were pooled and *de novo* assembled into transcripts using Trinity software (Grabherr et al., 2011). CD-HIT (http://www.bioinformatics.org/cd-hit/) fast program was used for clustering, comparing sets of nucleotide sequences and avoiding the redundancy in the final assembly at 95% threshold identity (Li and Godzik, 2006). Alignment of reads (control and treated samples) were done using Bowtie2 paired end alignment mode (http://bowtie-bio.sourceforge.net/bowtie2/index.shtml) (Langmead and Salzberg, 2012). Transcripts > 300 bp were annotated using BLASTx uniprot (http://www.uniprot.org/) and the high sequence similarity proteins were identified and assigned with putative functional annotation. Homology search and transcription factor identification were carried out using NCBI BLAST 2.2.29 and animal TFDB (http://www.bioguo.org/AnimalTFDB/) databases. Simple sequence reads (SSRs) were identified in each transcript using MIcroSAtellite (MISA) Perl script (http://pgrc.ipk-gatersleben.de/misa/). Pathway analysis was carried out using KAAS server (http://www.genome.jp/tools/kaas/) (Moriya et al., 2007) (Supplementary Fig. 2a). *Nasonia vitripennis* (jewel wasp), *Apis mellifera* (honey bee), *Anopheles gambiae* (mosquito), *Drosophila melanogaster* (fruit fly) and *Acyrthosiphon pisum* (pea aphid) were used as reference organisms for pathway analysis. Differential gene expression analysis in control *vs* experimental samples was monitored using DESeq software (Anders and Huber, 2010).

2.5. Microarray hybridization and analysis

The robustness and specificity of RNA-Seq reads was corroborated by one-color microarray based gene expression analysis of midgut RNA in toxin-exposed insects at different time points (12, 24, 36, 48 and 60 h). Cyanine-3 (Cy3) labeled complementary RNA was prepared from the midgut tissue of both control and toxin-exposed larvae using Agilent's Quick-Amp labelling Kit as per manufacturer's protocol. Cy3-labeled cRNA was purified using RNeasy mini kit column purification (Qiagen, USA). Dye incorporation and cRNA yield was checked with the NanoDrop ND-1000 Spectrophotometer (Supplementary Fig. 3a). Cy3-labeled cRNA with a specific activity > 10 pmol of Cy3/μg cRNA was fragmented at 60 °C for 30 min in 1 × Agilent fragmentation buffer and 2 × Agilent blocking agent as per manufacturer's instructions. Hybridization to Agilent Castor semilooper 8 × 60 K chip was carried out at 65 °C in a rotating oven for 17–18 h using Agilent's hybridization buffer. Post hybridization, the slides were washed with Gene Expression

wash buffers 1 and 2 and dried. The hybridized slides were scanned and the images were manually verified for uneven hybridization, streaks blobs and other artifacts. The array data normalization was carried out using Gene Spring GX Software (https://www.agilent.com/en/products/software-informatics/life-sciences-informatics/genespring-gx). Normalization of each column in the experiment was done independently and the computed value was derived from the percentile of expression values for a given array across all the spots (where n has a range from 0 to 100 and n = 75 was the median) (Supplementary Fig. 3b). Post intra-array normalization, the processed signal was log transferred and 75th percentile value for each of the array was calculated separately. The expression values were obtained by subtracting 75th percentile value of the respective array from the log transformed intensity value for each probe.

2.6. qRT-PCR validation

The NGS and microarray data was further validated by monitoring the expression of selected genes by qRT-PCR with 40S ribosomal gene, S7 as an internal control (Chauhan et al., 2017). RNA was isolated by TRIzol method® and was dissolved in diethyl pyro carbonate (DEPC)-treated H_2O (1 µg/µl). cDNA synthesis was carried out using manufacturer's protocol (Invitrogen, Life Technologies, USA). Specific primer pairs (Table 1) for each gene were designed using Oligo analyzer tool 3.1 (Integrated DNA Technologies Inc., USA). Each reaction of 20 µl mixture containing 1 µl of sample cDNA, 1 µl of each primer (10 µM), 10 µl of SYBR® Green Master Mix was set up in Step-One Plus qRT-PCR system (Thermo Fisher Scientific, USA). The qPCR cycling parameters were programmed as follows: 95 °C for 10 min, followed by 40 cycles of 95 °C for 30 s and 60 °C for 30 s, and melting curve generation was performed from 59 to 68 °C. The qPCR for each sample was performed in three technical and biological replicates for reproducibility. Relative expression of the genes was calculated using comparative $2^{-\Delta\Delta CT}$ method (Livak and Schmittgen, 2001). Data analysis was performed using Sigma Plot v12.3 software (Systat Software Inc., USA). One-Way ANOVA analysis followed by Student-Newman-Keuls test was conducted to check significance between groups. P value was calculated for pair wise multiple comparison between each set of experiments.

Table 1
List of primers used in Real time PCR for the expression analysis in control and toxin-exposed larval sample for the validation of DESeq and microarray analysis.

S. no.	Sequence name	Sequence
1	DUF233 FP	TCTTAGCAGTCGGCATTCCTGA
2	DUF 233 RP	TATGATCACCACCTGCTTCGCT
3	SERINE PROTIASE I FP	ACAGCGAGAATCACGACCTTGA
4	SERINE PROTIASE I RP	TAGAGCGACGTCAACCTCTGTG
5	Unknown +8.0 FP	GGACACGGGCACTATGAAGTGG
6	Unknown +8.0 RP	TCCAGTATACTTATCACGGAAAGGCC
7	GST EPSILON FP	CCACGGAGAAGAACATCGAGGA
8	GST EPSILON RP	CGTGAGACCCACTCAGTGGTAC
9	Cocoonae 8.0 FP	TTGCAAGGGAGATTATGGAGGTCC
10	Cocoonae 8.0 RP	GGGCTAAAGCTAGTCGTGGATCA
11	Unknown −10.25 FP	CGTGCCAATATGCGAAAGGACTTG
12	Unknown −10.25 RP	ACGTCACTAGGAACACACCTTCCA
13	Chymotrypsin FP	GGCCGACAAGATACGTAAGGCT
14	Chymotrypsin RP	GAACTTCTCCGTCGAACCAGCA
15	Niemann FP	ACTACGCTGGACCTCTTCCAAC
16	Niemann RP	GGACTTTTCGCCCAAGTTGTAGG
17	Trypsin FP	AGCTTGCCGTCATCATCTCGTA
18	Trypsin RP	GTAGGTCCACCCTGCAAAACAGT
19	Unknown −9.0 FP	CAACGCATGTAGCAATAGCCAGC
20	Unknown −9.0 RP	CGCAGTCACCTTGTCATCAACG
21	Cytochrome P450 FP	CGGGAACGTTTACCAACAGTCGA
22	Cytochrome P450 RP	GCAGTTGATGAGCGGGATGACT
23	Defense protein FP	GGCAGAAATGCTGTGCAGACTG
24	Defense protein RP	ATCACAGTCGAAGGCTCAGGTAAC
25	60S ribosomal FP	CAGGAAAGTTAGGCGTACCGAAGT
26	60S ribosomal RP	ACGAGTGGGCTTCTTCATGTGG
27	Apoptosis linked FP	AGAGACAACTCGGGCAACATTGA
28	Apoptosis linked RP	GCCGGAATGCAGAAGTCAGAGTA
29	Cecropin FP	CCGCTTCAGGTTGAATACTCGCTT
30	Cecropin RP	CGAATGTTGCGACCCACTTTCTC
31	rS7 FP	ACGTGGACGGTTCACAACTCATCA
32	rS7 RP	TTCGCGGCCTGTTAGCTTCTTGTA

2.7. Data records

The *de novo* transcriptome data was deposited into the NCBI SRA database (SRX4119388) (https://www.ncbi.nlm.nih.gov/sra/SRX4119388[accn]). The microarray data was deposited on GEO-NCBI (Gene expression omnibus) with the series number GSE114934 (https://www.ncbi.nlm.nih.gov/geo/query/acc.cgi?acc=GSE114934) on NCBI database.

3. Results

3.1. Sequencing analysis and de novo assembly

As *A. janata* reference genome is not available we carried out *de novo* transcriptome assembly using a Trinity assembler. Data was verified for integrity during the data transfer from Illumina sequencer system to lab using MD5 checksums. The details of technical validation of data obtained in the present study along with the results are presented below. Midgut sequencing of control and toxin-exposed larvae yielded a total of over 37 million reads (1,68,50,105 and 2,05,01,613, respectively). After trimming, a total of 1,57,10,416 and 1,90,81,749 clean reads were obtained from control and toxin-exposed larvae respectively. A GC-content of 44% was calculated from the clean reads obtained in both the samples. High quality reads were assembled into 34,612 and 41,109 transcripts with a total length of 39.55 and 49.11 Mb and N50 length of 1772 and 1922 nucleotides, respectively. Transcripts with a length between 200 and 500 bp represented the highest proportion in both control and treated samples (Table 2).

3.2. Functional annotation

The transcripts were annotated with BLASTx against NCBI nr database. Out of the 34,612 and 41,109 transcripts obtained, a total of 18,836 and 21,046 transcripts were successfully annotated in control and toxin-exposed samples, respectively. A high percentage of *A. janata* sequences closely matched with *Bombyx mori* (35.66%) followed by *Danaus plexippus* (32.63%), *Parargea egeria* (10.22%), *Helicoverpa armigera* (2.15%), *Papilio xuthus* (2.05%) and *Acyrthosiphon pisum* (1.91%) (Fig. 1a). Based on Gene Ontology (GO), *A. janata* transcripts obtained

Table 2
Reads and assembly statistics from *de novo* transcriptome of control and toxin-exposed larval midgut of *A. janata*.

Sample	Control	Toxin-exposed
Raw reads	1,68,50,105	2,05,01,613
Clean reads	1,57,10,416	1,90,81,749
Transcripts generated	34,612	41,109
Total transcripts length	3,95,54,452	4,91,15,238
Maximum transcripts length	17,216	26,151
Minimum transcripts length	301	301
Average transcript length	1142.8	1194.76
Sequences ≥ 300–500 bp	12,085	14,524
Sequences ≥ 500–1 Kbp	9876	11,085
Sequences ≥ 1–5 Kbp	12,141	14,696
Sequences ≥ 5–10 Kbp	491	779
Sequences ≥ 10 Kb-1 Mbp	19	25
N-50 value	1772	1922
CD-HIT clustering identity	95%	95%
GC %	44	44

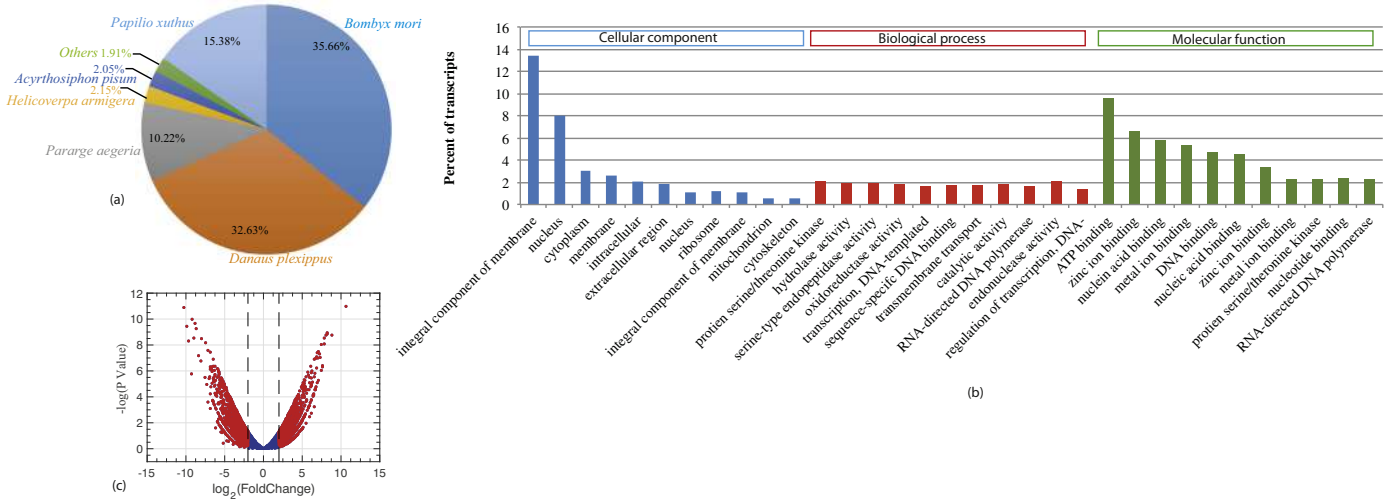

Fig. 1. *De novo* transcriptome analysis of control and toxin-exposed larvae. (a) Pie chart showing species percentage distribution of most closely related insect species resulted from annotation. (b) Gene Ontology classification analysis showing distribution based on cellular component, biological process, and molecular function, Y-axis indicates the percentage of transcript in each category. (c) Volcano plot analysis of differentially regulated genes in control and toxin-exposed sample. DeSeq was used for determining upregulation and downregulation of genes based upon relative FPKM counts (x-axis: $\log_2$fold change; y-axis: $-\log$ (P value)) plot was generated using RStudio Version 1.1.453–© 2009–2018.

were classified into three major groups: cellular component (11 subcategories), molecular function (11 subcategories) and biological processes (11 subcategories). In both control and treated samples, maximum transcripts were attributed to serine/threonine kinase activity under the biological process category. For the cellular component category, maximum number of transcripts was associated with integral membrane components followed by nucleus. For the molecular function category, maximum number of transcripts was associated with ATP and zinc-ion binding (Fig. 1b).

3.3. Differential gene expression (DGE) analysis

To ascertain differential gene expression in control *vs* toxin-exposed samples a volcano plot was constructed with a $\log_2$ fold-change > 1 for upregulated genes and < -1 for downregulated genes (Fig. 1c). Out of the 41,244 transcripts that were expressed in both control and treated samples, a total of 16,670 transcripts were differentially expressed including 8033 and 8637 commonly upregulated and downregulated transcripts respectively. A total of 24,574 transcripts were neutrally regulated in both the samples. Further, a total of 1701 and 5002 transcripts were exclusively expressed in the control and toxin-exposed samples, respectively (Table 3).

3.4. Prediction of transcription factor (TF) family

A total of 1052 transcription factors in control and 1221 in toxin-exposed samples were annotated with TFDB (http://www.bioguo.org/AnimalTFDB/), using *D. melanogaster* as reference. Transcription factors from zinc-finger family-Cys2His2, ZBTB and homeobox showed 401, 69 and 64 hits in control compared to 475, 66 and 63 hits in toxin-exposed samples (Supplementary Fig. 2b).

Table 3
Differential gene expression statistics from *de novo* transcriptome of control and toxin-exposed larval midgut of *A. janata*.

DGE statistics				
Total unigene available	47,959			
No. of transcript in each category	Total	Up	Down	Neutral
No. of transcript expressed in both samples	41,244	8033	8637	24,574
No. of transcript expressed only in control	1707	–	–	–
No. of transcript expressed only in treated	5002	–	–	–
No. of P-significant transcript	1611	701	910	–
No. of Q-significant transcript	280	115	165	–
Software used for carrying out DGE	DeSeq			

3.5. Single sequence repeats (SSR) identification

SSR mining using MISA Perl script identified a total of 3947 and 5043 transcripts that harboured SSR motifs in control and treated samples respectively. Total SSRs predicted in control and toxin-exposed samples were 4770 and 6115 respectively. In control samples, mono-nucleotide repeats were the most represented (72.41%) followed by di-nucleotide (13.12%) and tri-nucleotide repeats (12.64%) whereas in treated samples maximum representation of mono-nucleotide repeats (72.51%) was followed by tri-nucleotide (13.01%) and di-nucleotide repeats (12.72%) (Supplementary Fig. 2c).

3.6. Microarray analysis

Heat maps generated from the microarray data reflects differential gene expression values of toxin-exposed time-series samples (12, 24, 36, 48 and 60 h) compared to control (Fig. 2a). Spectrophotometric analysis of labeled cRNA showed ratio (260/280) of the samples > 2.29 and a specific activity ranging from 6.71 to 9.61. Microarray data analysis revealed that overall 954 genes were differentially regulated (375 upregulated and 579 downregulated) in all the analyzed samples. In 12, 24, 36, 48 and 60 h toxin-exposed samples, 192, 111, 187, 156 and 106 mRNAs were uniquely upregulated (Fig. 2b, i) whereas 97, 85, 108, 104 and 69 were uniquely downregulated (Fig. 2b, ii) respectively (Transcript details provided in Supplementary Files 1, 2).

3.7. qRT-PCR validation

To confirm the results of microarray analysis, qRT-PCR was performed on randomly selected differentially expressed genes. Gene expression corresponding to DUFF233, Serine protease inhibitor, Serpin 1a, GST-epsilon, Cocoonase, Chymotrypsin, Niemann-Pick type C2 protein, Trypsin-like proteinase T23, Cytochrome P450, Defense protein 1, 60S ribosomal protein L18, Apoptosis-linked protein 2, Cecropin and three uncharacterized proteins were monitored (Fig. 2c). The qRT-

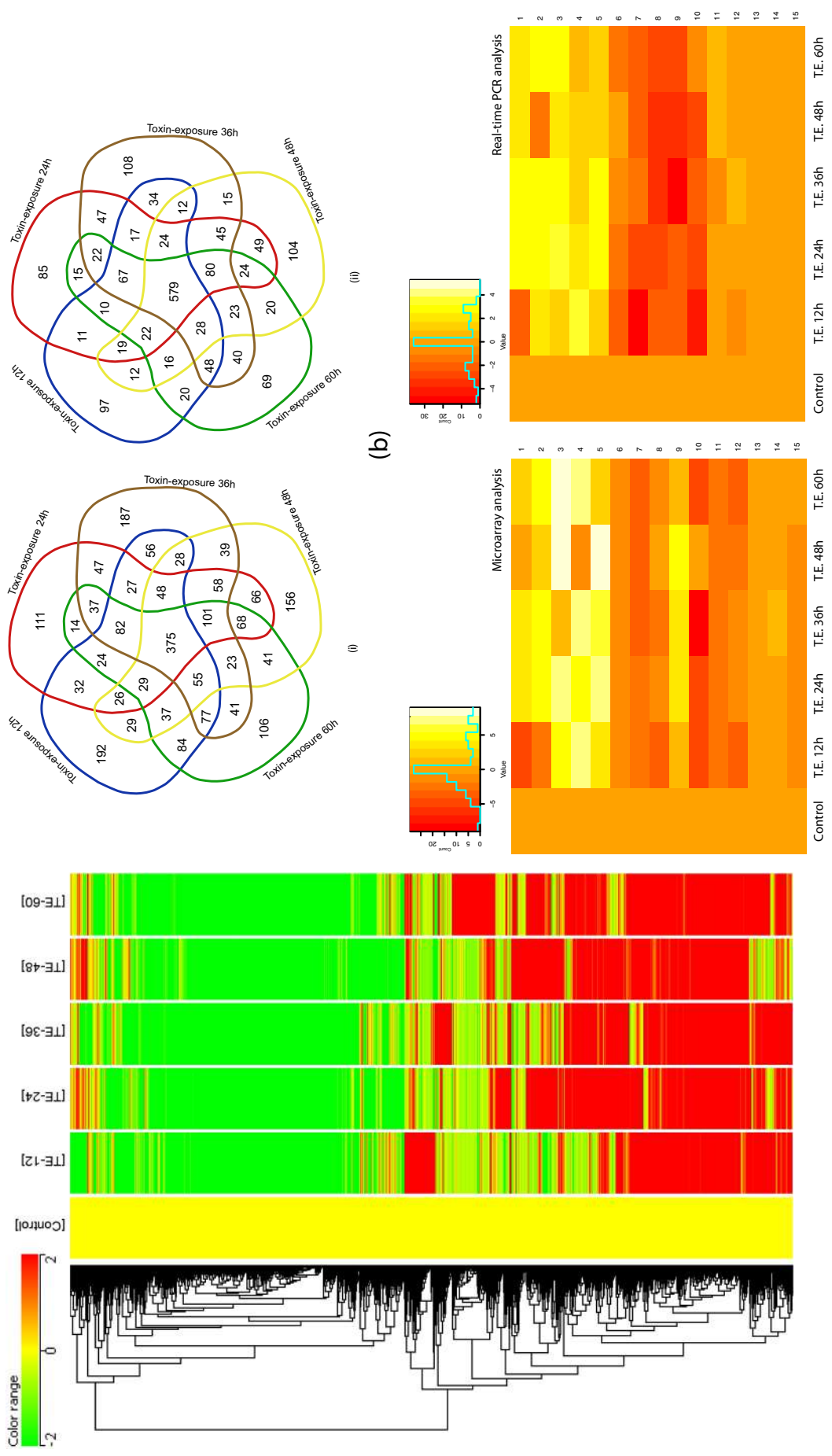

Fig. 2. Differential gene expression analysis upon continuous toxin-exposure using microarray. (a) Overall cluster of differentially regulated genes obtained through microarray analysis. The red colour indicates high, green indicate low and yellow indicate neutral gene expression levels (fold change expression was provided as $\log_2$). (b) Venn diagram depicting the number of larval midgut transcripts in various toxin exposure time point. (i) Commonly upregulated transcripts at various time point of toxin exposure, (ii) commonly downregulated transcripts at various time point of toxin exposure. (c) Validation of the RNA-seq and microarray data using qRT-PCR analysis, data was normalised with rS7 as reference gene. The transcripts validated 1. DUFF233, 2. Serine protease inhibitor, Serpin 1a, 3. Unknown + 8 fold upregulated, 4. Glutathione S-transferase epsilon, 5.Cocoonase, 6. Unknown −10 fold downregulated, 7. Chymotrypsin, 8. Niemann-Pick type C2 protein, 9.Trypsin-like proteinase T23, 10. Unknown −9 fold downregulated, 11. Cytochrome P450, 12. Defense protein, 13. 60S ribosomal protein L18, 14. Apoptosis-linked protein 2 and 15. Cecropin. (a) Heat plot were generated using value obtained from RNA-seq and microarray data, (b) Heat plot were generated using value obtained from qRT-PCR analysis. Plot was generated from RStudio Version 1.1.453—© 2009–2018. Statistical significance for qRT-PCR data was calculated using Sigma plot ($P < 0.005$, between experimental groups ($n = 3$)). Pearson's correlation coefficient was 0.5866864 between microarray data and qRT-PCR analysis calculated from RStudio.

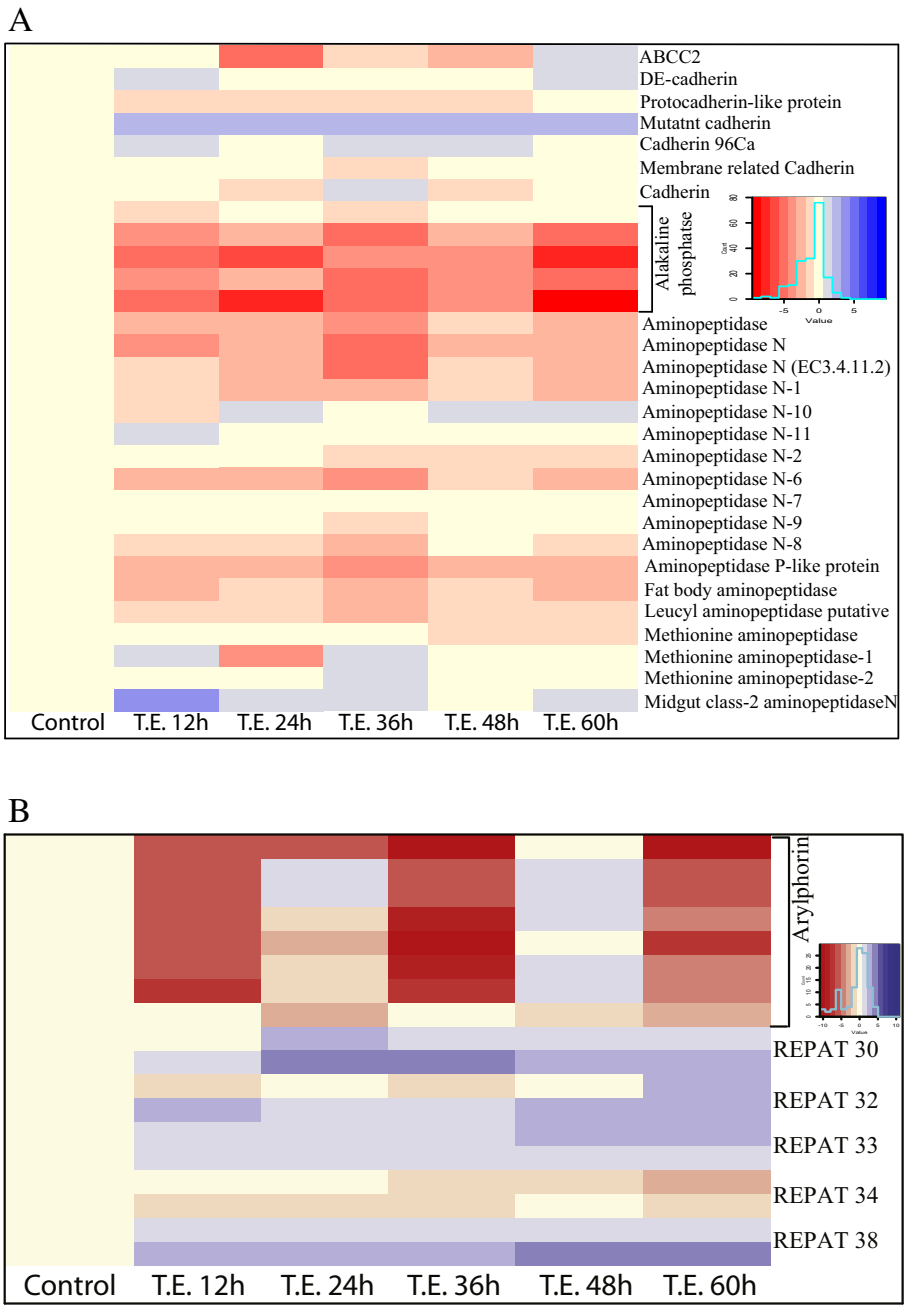

Fig. 3. Differential expression of widely reported and characterized genes at various time point of toxin exposure. (a) Cry toxin receptors transcript. (b) Arylphorin and REPATs transcript expression. (c) Transcripts analysis of gut proteases. (d) Expression analysis of detoxification enzyme transcripts at various time point of toxin exposure. (e) Aquaporin and aqua glyceroporin transcripts expression.

PCR patterns of the selected DEGs were in agreement with the results microarray analysis. Pearson's correlation coefficient between the microarray and qRT-PCR data results was 0.5866864, which indicated good correlation.

3.8. Expression of cry toxin receptors

We monitored the expression of the reported Cry toxin receptors (Pigott and Ellar, 2007; Tabashnik et al., 2013). Cry exposure resulted in downregulation of protocadherin-like protein, DE-cadherin, cadherin, alkaline phosphatases 1, 2, and 3, aminopeptidases N (*APN1*, *APN6*, *APN7*, *APN9*, *APN8*, *APN11*), fat body APN and amino peptidase P-like protein. On the other hand, mRNAs of mutant cadherin and midgut class 2 aminopeptidase N showed significant upregulation (Fig. 3a).

3.9. Arylphorin and REPATs expression

Arylphorins and REPATs are candidate molecules suggested to be involved in the non-receptor mediated midgut response to Bt toxins (Burmester, 2015; Castagnola and Jurat-Fuentes, 2016; Chauhan et al., 2017). Arylphorin was initially downregulated in Cry-exposed insects, which were upregulated later during 36–48 h time period. REPATs showed differential response to Cry toxin. REPAT 32 and REPAT 38 showed upregulation while REPAT 30 and REPAT 34 transcripts were downregulated (Fig. 3b).

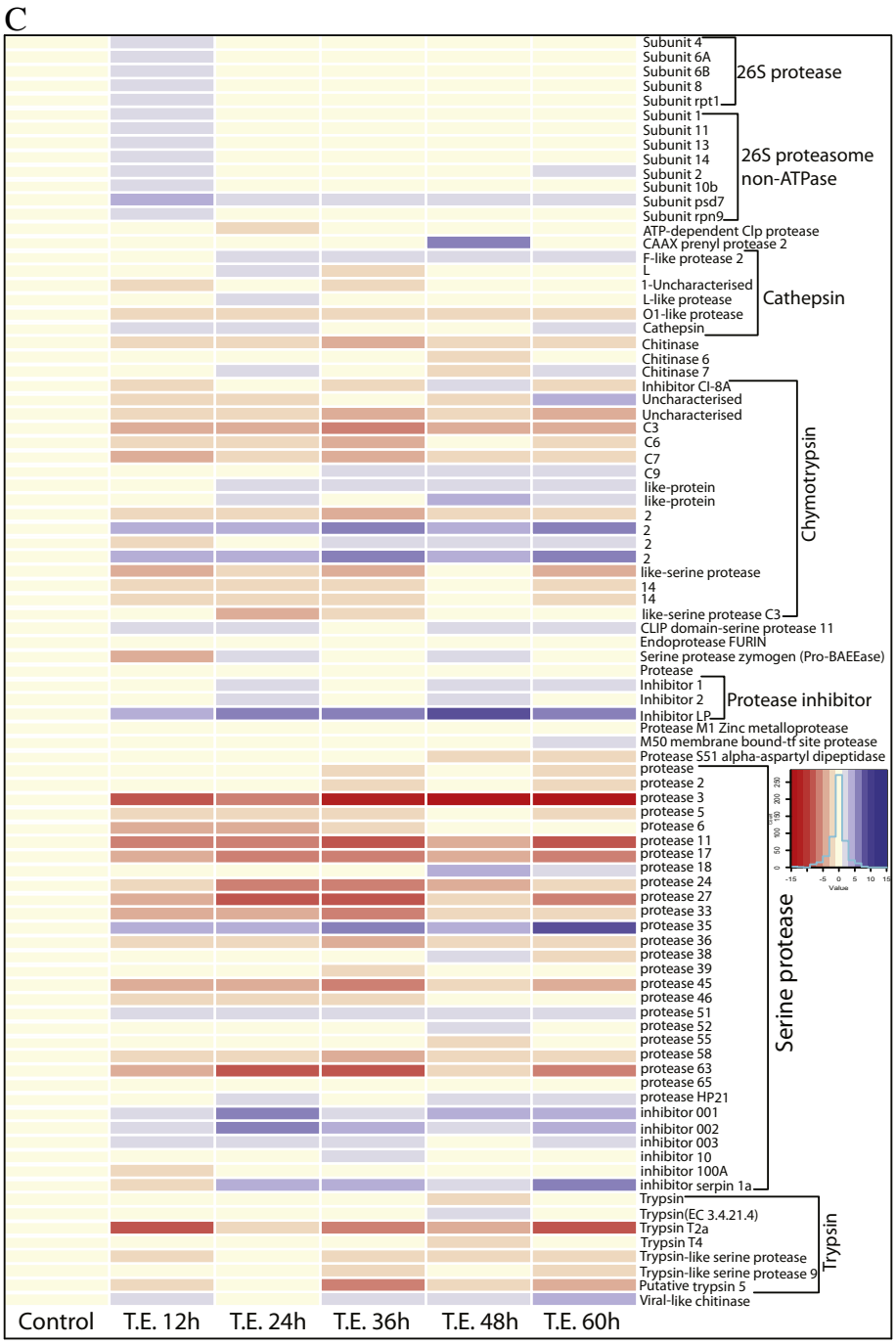

Fig. 3. (*continued*)

3.10. Expression of gut proteases

Activation of *Bt* protoxin is the initial step determining its toxicity after ingestion. Predominantly, serine proteases constitute the differentially expressed group of transcripts in toxin-exposed *A. janata* larvae. Transcripts encoding trypsin, trypsin-like proteins, chymotrypsin and chymotrypsin-like proteins were downregulated during Cry toxin exposure. On the contrary, mRNA expression of protease inhibitors including serine protease inhibitor 1, 2 & 3 and serpin 1a were upregulated. Expression of 26 s protease, endoproteases, ATP-dependent Clp proteases, protease M1, zinc metalloprotease and endopeptidases was unaffected (Fig. 3c).

3.11. Expression of detoxification enzymes

Insect cells are susceptible to toxin-induced oxidative damage that is counter balanced by detoxifying enzyme-mediated endogenous antioxidative activity (Rodríguez-Cabrera et al., 2008; Lei et al., 2014; Pavani et al., 2015). *A. janata* transcriptome analysis identified numerous Glutathione S-transferases (GSTs) belonging to various superfamilies. In the present study, GST-delta 4, GST-epsilon, Cytochrome p450 and Cu-Zn superoxide dismutase expression was significantly upregulated during Cry toxin exposure. Expression of most GSTs including GST-omega,-sigma, -zeta and -theta was marginally downregulated or unaffected (Fig. 3d).

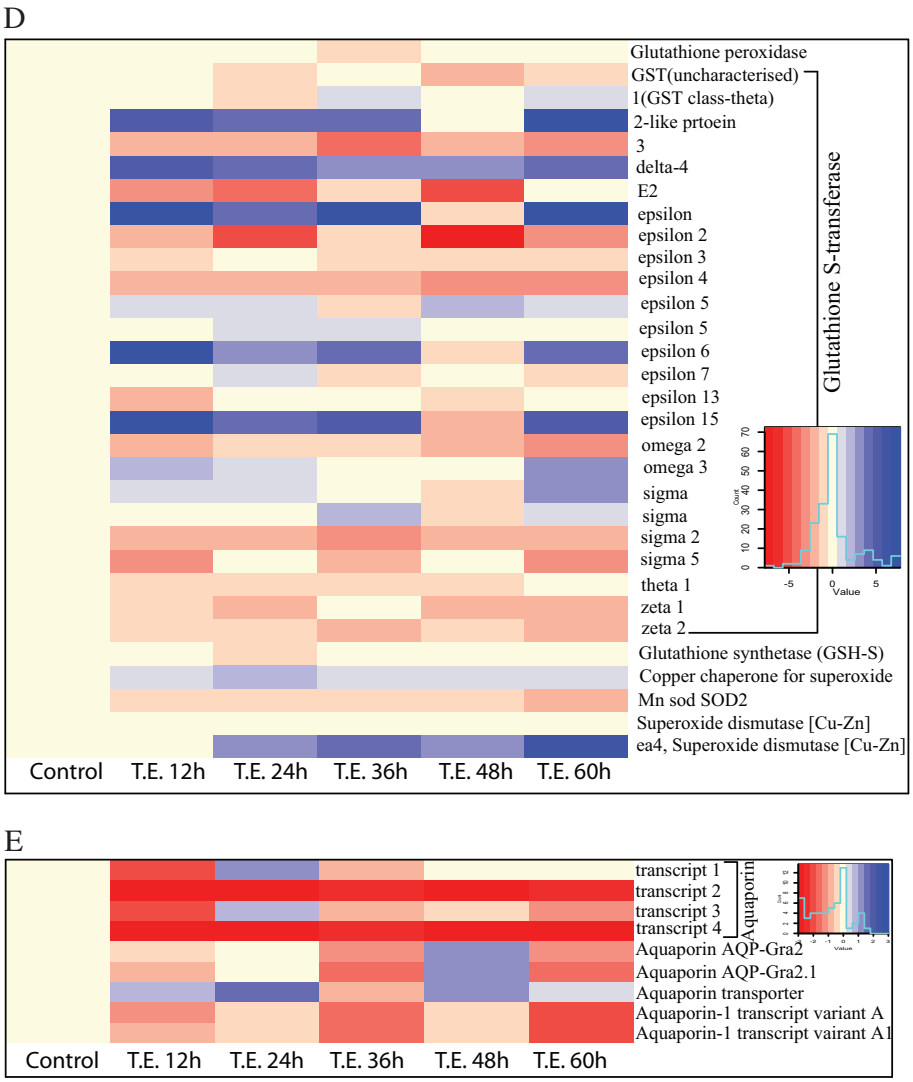

Fig. 3. (*continued*)

3.12. Expression of aquaporins

Both aquaporin and aqua-glyceroporin transcripts (Aquaporin-1 and Aquaporin-Gra2) were identified in the midgut transcriptome of *A. janata*. Expression of these two integral gut membrane water-transport proteins was downregulated in toxin-exposed insects (Fig. 3e).

4. Discussion

RNA sequencing using Illumina platform accounts for large data size, precision and ease. Trinity is an efficient tool for robust *de novo* assembly of transcriptomes particularly of species without a reference genome. Trinity was successfully used in *de novo* assembly of other insect pest's *viz.*, *Chilo suppressalis* (Yin et al., 2014) and *Spodoptera litura* (Song et al., 2016). In present report, the transcripts associated with five important classes' *viz.*, Cry toxin receptors, gut proteases, arylphorins and REPATs, detoxification enzymes, and aquaporins were detailed.

Elucidation of *Bt* insecticidal proteins interaction with their hosts is crucial to explain the molecular bases of *Bt* specificity and insecticidal activity. Previous reports demonstrated that APNs and cadherins are the functional Cry toxin receptors (Pigott and Ellar, 2007). At least eight different classes of APNs have been identified in lepidopteran insects so far (Crava et al., 2010). Differential expression and subsequent binding of APNs to Cry proteins was shown to determine insect's susceptibility or tolerance to the toxin (Tiewsiri and Wang, 2011; Qiu et al., 2017). The “ping-pong” binding mechanism is proposed by Pacheco et al. (2009) shows that in APNs initially binds to the Cry toxin facilitating concentration of the toxin at the brush border membrane and subsequent binding to cadherin. Subsequently, the toxin binds to the aminopeptidases with a higher affinity post oligomerization. Further, mutations in cadherin gene were also associated with generation of Cry toxin resistance (Pardo-Lopez et al., 2013). The upregulation of APN2 and mutant cadherin observed in the present study implicates their role in Cry intoxication.

The lepidopteran larvae require a repertoire of proteolytic enzymes including trypsins, chymotrypsins, aminopeptidases, carboxypeptidases, elastases and cathepsin-like proteases, for protein digestion. Protein-digestion in lepidopteran larvae primarily depends on trypsin- and chymotrypsin-like serine protease activities. Multiple isoforms of trypsin and chymotrypsin reported in *A. janata* and in other known lepidopteran insect species could be due to insects' acquaintance to naturally occurring antagonistic biomolecules and/or adaptation to their different food sources (Zhu-Salzman and Zeng, 2015). Activation of protoxin is mediated by midgut proteases, particularly trypsin and chymotrypsin (Bravo et al., 2007). In the present study, sub-lethal dose of *Bt* toxin resulted in the reduced transcript levels of trypsin and chymotrypsin and elevated levels of serine protease inhibitors. A

correlation of reduced activities of trypsin and chymotrypsin to the reduced conversion of protoxin to activated Cry toxin was established earlier (Pardo-Lopez et al., 2013; Adang et al., 2014; Tabashnik, 2015). Also relation of trypsin, chymotrypsin and proteinase/protease has been shown in the context of *Bt* resistance (Zhu et al., 2011). In a recent study, it was demonstrated that downregulation of trypsin gene is associated with development of *Bt* resistance (Yao et al., 2017). On the other hand, high expression of serine protease inhibitor transcripts might subsequently reduce gut protease activities and thereby prevent further gut tissue damage.

In the present study, arylphorin expression was upregulated from log2 value of −7 fold to 1.6 fold during 36–48 h time span which coincides with the active cell proliferation phase demonstrated by BrdU labeling and histological studies previously (Chauhan et al., 2017). The mitogenic effect of arylphorin might play a role in midgut restoration of Cry induced damage (Castagnola and Jurat-Fuentes, 2016; Castagnola et al., 2017). REPAT genes encode low-molecular weight proteins and their expression is restricted to the midgut cells. So far, 46 REPAT proteins were identified using data mining, which fall under the αREPAT and βREPAT groups. Variation in expression pattern of REPAT genes was earlier demonstrated in *Spodoptera* larvae exposed to Cry toxin. High level of expression of REPATs 4, 21, 32, and 42 was observed in midgut stem cells relative to whole midgut in Cry1Ca treated *Spodoptera* larvae. Further, REPAT genes 39 to 44 were downregulated (Navarro-Cerrillo et al., 2013). The differential response of REPATs to Cry toxin as observed in the present and previous studies indicate that the regulation of these genes is specific to the insect species and the type of Cry toxin exposure.

Insecticide detoxification occurs in two phases. Phase I enzymes, include cytochrome P450 proteins (P450s) which directly participate in metabolism of xenobiotics. These enzymes are divided in four groups; CYP2, CYP3, CYP4, and mitochondrial (Feyereisen, 2006). Phase II enzymes; include GSTs, which transform allelo-chemicals into water-soluble compounds for excretion. In insect's GSTs are grouped into seven major classes: sigma, zeta, omega, theta, microsomal, delta, and epsilon (Friedman, 2011). In this study, unigenes that putatively encode GST sigma, omega, delta, and epsilon classes of genes in *A. janata* were found. Among these, only GST-delta 4 was found upregulated under Cry exposure. In addition, Cu-Zn superoxide dismutase was also upregulated. In corroboration, superoxide dismutase levels showed significantly higher activities in *S. litura* larvae fed with Cry1Ab expressed leaves (Yinghua et al., 2017).

The osmotic balance like other animals in insect is also regulated by aquaporins, which also play a vital role in cold tolerance as well as in resistance against desiccation. A recent report demonstrated altered transcript levels of aquaporin in white-backed planthopper, *Sogatella furcifera* (Hemiptera: Delphacidae) exposed to an insecticide (Zhou et al., 2018). Down regulation of AQPs in *Aedes aegypti* enhanced mosquito desiccation resistance (Drake et al., 2015). The present study reported the downregulation of an aquaporins and aqua-glyceroporin. Till date, only few aqua-glyceroporins have been identified in insects (Campbell et al., 2008; Ishibashi et al., 2017).

To further validate the differential expression of genes, qRT-PCR analysis of 15 randomly selected genes was carried out. The expression pattern of the genes was in agreement with the results of the transcriptome and microarray analyses. The present study revealed a large repertoire of differentially expressed genes involved in Cry toxin responses of *A. janata*. In conclusion, RNA-seq analysis provided an initial step towards unraveling the molecular mechanisms, at the transcriptome level, that potentially aid toxin resistance in Bt-exposed *A. janata* larvae. Our ongoing/future study will be testifying that whether DEGs reported in this paper is truly associated with Cry intoxication in *A. janata* larvae, and check if they have any functional role in the Bt toxin tolerance/resistance.

Supplementary data to this article can be found online at https://doi.org/10.1016/j.cbd.2019.02.005.

Acknowledgments

The work was carried out with financial support of Council of Scientific and Industrial Research, India grant (Grant No. 37(1709)/18/EMR-11), and UGC-BSR Faculty Fellowship to ADG. Authors would like to thank Dr. Kota Arun Kumar for critical suggestion. Financial support in form of research fellowship to ND by UGC and VC by DBT and India are acknowledged. The common central facilities and instruments generated with support of DST-FIST (Level-II), DBT- CREBB, UPE-II and DST-PURSE were used for the present study.

Author contributions

N.D. and V.C. conceived, designed and performed all experimental work. N.D. has done data analysis. The work was carried out under the overall supervision of A.D. and the manuscript was drafted by N.D. and V.C. and corrected by A.D. R.C. supported in result analysis, drafting and editing of the manuscript. All authors have read and approved the final manuscript.

Competing interests

The author(s) declare no competing interests.

References

Abrol, D.P., Shankar, U., 2016. Integrated pest management. In: Breeding Oilseed Crops for Sustainable Production, pp. 523–549.
Adang, M.J., Crickmore, N., Jurat-Fuentes, J.L., 2014. Diversity of *Bacillus thuringiensis* crystal toxins and mechanism of action. In: Advances in Insect Physiology. Vol. 47. Academic Press, pp. 39–87.
Anders, S., Huber, W., 2010. Differential expression analysis for sequence count data. Genome Biol. 11 (10), R106.
Bel, Y., Jakubowska, A.K., Costa, J., Herrero, S., Escriche, B., 2013. Comprehensive analysis of gene expression profiles of the beet armyworm *Spodoptera exigua* larvae challenged with *Bacillus thuringiensis* Vip3Aa toxin. PLoS One 8 (12), e81927.
Bravo, A., Gill, S.S., Soberon, M., 2007. Mode of action of *Bacillus thuringiensis* Cry and Cyt toxins and their potential for insect control. Toxicon 49 (4), 423–435.
Burmester, T., 2015. Expression and evolution of hexamerins from the tobacco hornworm, *Manduca sexta* and other Lepidoptera. Insect Biochem. Mol. Biol. 62, 226–234.
Campbell, E.M., Ball, A., Hoppler, S., Bowman, A.S., 2008. Invertebrate aquaporins: a review. J. Comp. Physiol. B. 178 (8), 935–955.
Castagnola, A., Jurat-Fuentes, J.L., 2016. Intestinal regeneration as an insect resistance mechanism to entomopathogenic bacteria. Curr. Opin. Insect Sci. 15, 104–110.
Castagnola, A., Jackson, J., Perera, O.P., Oppert, C., Eda, S., Jurat-Fuentes, J.L., 2017. Alpha-arylphorin is a mitogen in the *Heliothis virescens* midgut cell secretome upon Cry1Ac intoxication. PeerJ 5, e3886.
Chauhan, V.K., Dhania, N.K., Chaitanya, R.K., Senthilkumaran, B., Dutta-Gupta, A., 2017. Larval midgut responses to sub-lethal dose of Cry toxin in lepidopteran pest *Achaea janata*. Front. Physiol. 8, 662.
Crava, C.M., Bel, Y., Lee, S.F., Manachini, B., Heckel, D.G., Escriche, B., 2010. Study of the aminopeptidase N gene family in the lepidopterans *Ostrinia nubilalis* (Hübner) and *Bombyx mori* (L.): sequences, mapping and expression. Insect Biochem. Mol. Biol. 40 (7), 506–515.
Dhurua, S., Gujar, G.T., 2011. Field-evolved resistance to Bt toxin Cry1Ac in the pink bollworm, *Pectinophora gossypiella* (Saunders) (Lepidoptera: Gelechiidae), from India. Pest Manag. Sci. 67 (8), 898–903.
Drake, L.L., Rodriguez, S.D., Hansen, I.A., 2015. Functional characterization of aquaporins and aquaglyceroporins of the yellow fever mosquito, *Aedes aegypti*. Sci. Rep. 5, 7795.
Ferré, J., Van Rie, J., 2002. Biochemistry and genetics of insect resistance to *Bacillus thuringiensis*. Annu. Rev. Entomol. 47 (1), 501–533.
Feyereisen, R., 2006. Evolution of insect P450. Biochem. Soc. Trans. 1252–1255.
Friedman, R., 2011. Genomic organization of the glutathione S-transferase family in insects. Mol. Phylogenet. Evol. 61 (3), 924–932.
Grabherr, M.G., Haas, B.J., Yassour, M., Levin, J.Z., Thompson, D.A., Amit, I., ... Chen, Z., 2011. Full-length transcriptome assembly from RNA-Seq data without a reference genome. Nat. Biotechnol. 29 (7), 644.
Herrero, S., Ansems, M., Van Oers, M.M., Viak, J.M., Bakker, P.L., de Maagd, R.A., 2007. REPAT, a new family of proteins induced by bacterial toxins and baculovirus infection in *Spodoptera exigua*. Insect Biochem. Mol. Biol. 37 (11), 1109–1118.
Ishibashi, K., Morishita, Y., Tanaka, Y., 2017. The evolutionary aspects of aquaporin family. In: Aquaporins. Springer, Dordrecht, pp. 35–50.
Jakka, S.R., Gong, L., Hasler, J., Banerjee, R., Sheets, J.J., Narva, K., ... Jurat-Fuentes, J.L., 2016. Field-evolved mode 1 resistance of the fall armyworm to transgenic Cry1Fa-expressing corn associated with reduced Cry1Fa toxin binding and midgut alkaline phosphatase expression. Appl. Environ. Microbiol. 82 (4), 1023–1034.
Kallamadi, P.R., Nadigatla, V.G.R., Mulpuri, S., 2015. Molecular diversity in castor

(*Ricinus communis* L.). Ind. Crop. Prod. 66, 271–281.
Kliot, A., Ghanim, M., 2012. Fitness costs associated with insecticide resistance. Pest Manag. Sci. 68 (11), 1431–1437.
Kruger, M., Van Rensburg, J.B.J., Van den Berg, J., 2011. Resistance to Bt maize in *Busseola fusca* (Lepidoptera: Noctuidae) from Vaalharts, South Africa. Environ. Entomol. 40 (2), 477–483.
Langmead, B., Salzberg, S.L., 2012. Fast gapped-read alignment with bowtie 2. Nat. Methods 9 (4), 357.
Lei, Y., Zhu, X., Xie, W., Wu, Q., Wang, S., Guo, Z., ... Zhang, Y., 2014. Midgut transcriptome response to a Cry toxin in the diamondback moth, *Plutella xylostella* (Lepidoptera: Plutellidae). Gene 533 (1), 180–187.
Li, W., Godzik, A., 2006. Cd-hit: a fast program for clustering and comparing large sets of protein or nucleotide sequences. Bioinformatics 22 (13), 1658–1659.
Li, H., Jiang, W., Zhang, Z., Xing, Y., Li, F., 2013. Transcriptome analysis and screening for potential target genes for RNAi-mediated pest control of the beet armyworm, *Spodoptera exigua*. PLoS One 8 (6), e65931.
Livak, K.J., Schmittgen, T.D., 2001. Analysis of relative gene expression data using real-time quantitative PCR and the $2^{-\Delta\Delta CT}$ method. Methods 25 (4), 402–408.
Moriya, Y., Itoh, M., Okuda, S., Yoshizawa, A.C., Kanehisa, M., 2007. KAAS: an automatic genome annotation and pathway reconstruction server. Nucleic Acids Res. 35 (suppl_2) (W182-W185).
Navarro-Cerrillo, G., Ferré, J., de Maagd, R.A., Herrero, S., 2012. Functional interactions between members of the REPAT family of insect pathogen-induced proteins. Insect Mol. Biol. 21 (3), 335–342.
Navarro-Cerrillo, G., Hernández-Martínez, P., Vogel, H., Ferré, J., Herrero, S., 2013. A new gene superfamily of pathogen-response (repat) genes in Lepidoptera: classification and expression analysis. Comp. Biochem. Physiol. B: Biochem. Mol. Biol. 164 (1), 10–17.
Ningshen, T.J., Chauhan, V.K., Dhania, N.K., Dutta-Gupta, A., 2017. Insecticidal effects of hemocoelic delivery of *Bacillus thuringiensis* Cry toxins in *Achaea janata* larvae. Front. Physiol. 8, 289.
Pacheco, S., Gómez, I., Arenas, I., Saab-Rincon, G., Rodríguez-Almazán, C., Gill, S.S., ... Soberón, M., 2009. Domain II loop 3 of *Bacillus thuringiensis* Cry1Ab toxin is involved in a "ping-pong" binding mechanism with *Manduca sexta* aminopetidase-N and cadherin receptors. J. Biol. Chem. 284, 32750–32757.
Pardo-Lopez, L., Soberon, M., Bravo, A., 2013. Bacillus thuringiensis insecticidal three-domain Cry toxins: mode of action, insect resistance and consequences for crop protection. FEMS Microbiol. Rev. 37 (1), 3–22.
Park, Y., González-Martínez, R.M., Navarro-Cerrillo, G., Chakroun, M., Kim, Y., Ziarsolo, P., ... Herrero, S., 2014. ABCC transporters mediate insect resistance to multiple Bt toxins revealed by bulk segregant analysis. BMC Biol. 12 (1), 46.
Patel, V.R., Dumancas, G.G., Viswanath, L.C.K., Maples, R., Subong, B.J.J., 2016. Castor oil: properties, uses, and optimization of processing parameters in commercial production. Lipid Insights 9 (LPI-S40233).
Pavani, A., Chaitanya, R.K., Chauhan, V.K., Dasgupta, A., Dutta-Gupta, A., 2015. Differential oxidative stress responses in castor semilooper, *Achaea janata*. J. Invertebr. Pathol. 132, 157–164.
Pavlidi, N., Vontas, J., Van Leeuwen, T., 2018. The role of glutathione S-transferases (GSTs) in insecticide resistance in crop pests and disease vectors. Curr. Opin. Insect Sci. 27, 97–102.
Pereira, A.E., Wang, H., Zukoff, S.N., Meinke, L.J., French, B.W., Siegfried, B.D., 2015. Evidence of field-evolved resistance to bifenthrin in western corn rootworm (*Diabrotica virgifera virgifera LeConte*) populations in western Nebraska and Kansas. PLoS One 10 (11), e0142299.
Perera, O.P., Shelby, K.S., Popham, H.J., Gould, F., Adang, M.J., Jurat-Fuentes, J.L., 2015. Generation of a transcriptome in a model lepidopteran pest, *Heliothis virescens*, using multiple sequencing strategies for profiling midgut gene expression. PLoS One 10 (6), e0128563.
Pigott, C.R., Ellar, D.J., 2007. Role of receptors in *Bacillus thuringiensis* crystal toxin activity. Microbiol. Mol. Biol. Rev. 71 (2), 255–281.
Qiu, L., Fan, J., Zhang, B., Liu, L., Wang, X., Lei, C., ... Ma, W., 2017. RNA interference knockdown of aminopeptidase N genes decrease the susceptibility of *Chilo suppressalis* larvae to Cry1Ab/Cry1Ac and Cry1Ca-expressing transgenic rice. J. Invertebr. Pathol. 145, 9–12.
Reddy, V.P., Rao, N.N., Devi, P.V., Narasu, M.L., Kumar, V.D., 2012. PCR-based detection of Cry genes in local *Bacillus thuringiensis* DOR Bt-1 isolate. Pest Technol. 6, 79–82.
Rodríguez-Cabrera, L., Trujillo-Bacallao, D., Borrás-Hidalgo, O., Wright, D.J., Ayra-Pardo, C., 2008. Molecular characterization of *Spodoptera frugiperda–Bacillus thuringiensis* Cry1Ca toxin interaction. Toxicon 51 (4), 681–692.
Shabbir, M.Z., Quan, Y., Wang, Z., Bravo, A., Soberón, M., He, K., 2018. Characterization of the Cry1Ah resistance in Asian corn Borer and its cross-resistance to other *Bacillus thuringiensis* toxins. Sci. Rep. 8 (1), 234.
Song, F., Chen, C., Wu, S., Shao, E., Li, M., Guan, X., Huang, Z., 2016. Transcriptional profiling analysis of *Spodoptera litura* larvae challenged with Vip3Aa toxin and possible involvement of trypsin in the toxin activation. Sci. Rep. 6, 23861.
Storer, N.P., Babcock, J.M., Schlenz, M., Meade, T., Thompson, G.D., Bing, J.W., Huckaba, R.M., 2010. Discovery and characterization of field resistance to Bt maize: *Spodoptera frugiperda* (Lepidoptera: Noctuidae) in Puerto Rico. J. Econ. Entomol. 103 (4), 1031–1038.
Sujatha, M., Devi, P.V., Reddy, T.P., 2011. Insect Pests of Castor (*Ricinus communis* L) and their Management Strategies. BS Publications, CRC Press.
Tabashnik, B.E., 2015. ABCs of insect resistance to Bt. PLoS Genet. 11 (11), e1005646.
Tabashnik, B.E., Brévault, T., Carrière, Y., 2013. Insect resistance to Bt crops: lessons from the first billion acres. Nat. Biotechnol. 31 (6), 510.
Tiewsiri, K., Wang, P., 2011. Differential alteration of two aminopeptidases N associated with resistance to *Bacillus thuringiensis* toxin Cry1Ac in cabbage looper. Proc. Natl. Acad. Sci. 108 (34), 14037–14042.
Wolf, J.B., 2013. Principles of transcriptome analysis and gene expression quantification: an RNA-seq tutorial. Mol. Ecol. Resour. 13 (4), 559–572.
Xu, L.N., Ling, Y.H., Wang, Y.Q., Wang, Z.Y., Hu, B.J., Zhou, Z.Y., ... He, K.L., 2015. Identification of differentially expressed microRNAs between Bacillus thuringiensis Cry1Ab-resistant and-susceptible strains of *Ostrinia furnacalis*. Sci. Rep. 5, 15461.
Yao, J., Zhu, Y.C., Lu, N., Buschman, L.L., Zhu, K.Y., 2017. Comparisons of transcriptional profiles of gut genes between Cry1Ab-resistant and susceptible strains of *Ostrinia nubilalis* revealed genes possibly related to the adaptation of resistant larvae to transgenic Cry1Ab corn. Int. J. Mol. Sci. 18 (2), 301.
Yin, C., Liu, Y., Liu, J., Xiao, H., Huang, S., Lin, Y., ... Li, F., 2014. ChiloDB: a genomic and transcriptome database for an important rice insect pest *Chilo suppressalis*. Database 2014. https://doi.org/10.1093/database/bau065.
Yinghua, S., Yan, D., Jin, C., Jiaxi, W., Jianwu, W., 2017. Responses of the cutworm *Spodoptera litura* (Lepidoptera: Noctuidae) to two Bt corn hybrids expressing Cry1Ab. Sci. Rep. 7, 41577.
Yu, T., Li, X., Coates, B.S., Zhang, Q., Siegfried, B.D., Zhou, X., 2018. microRNA profiling between *Bacillus thuringiensis* Cry1Ab-susceptible and-resistant European corn borer, *Ostrinia nubilalis* (Hübner). Insect Mol. Biol. 27 (3), 279–294.
Zhang, H., Yin, W., Zhao, J., Jin, L., Yang, Y., Wu, S., ... Wu, Y., 2011. Early warning of cotton bollworm resistance associated with intensive planting of Bt cotton in China. PLoS One 6 (8), e22874.
Zhou, C., Yang, H., Wang, Z., Long, G.Y., Jin, D.C., 2018. Comparative transcriptome analysis of *Sogatella furcifera* (Horváth) exposed to different insecticides. Sci. Rep. 8 (1), 8773.
Zhu, Y.C., Guo, Z., Chen, M.S., Zhu, K.Y., Liu, X.F., Scheffler, B., 2011. Major putative pesticide receptors, detoxification enzymes, and transcriptional profile of the midgut of the tobacco budworm, *Heliothis virescens* (Lepidoptera: Noctuidae). J. Invertebr. Pathol. 106 (2), 296–307.
Zhu-Salzman, K., Zeng, R., 2015. Insect response to plant defensive protease inhibitors. Annu. Rev. Entomol. 60, 233–252.

Anti-plagiarism Certificate

Analysis of midgut regeneration in lepidopteran pest, Achaea janata upon Cry toxication

by Narender .

Submission date: 22-Oct-2019 04:38PM (UTC+0530)
Submission ID: 1197950907
File name: 15laph10 PhD thesis.pdf (6.7M)
Word count: 31032
Character count: 172259

Analysis of midgut regeneration in lepidopteran pest, Achaea janata upon Cry toxication

ORIGINALITY REPORT

10%	7%	8%	8%
SIMILARITY INDEX	INTERNET SOURCES	PUBLICATIONS	STUDENT PAPERS

PRIMARY SOURCES

1	Submitted to University of Hyderabad, Hyderabad Student Paper	1%
2	www.frontiersin.org Internet Source	1%
3	Narender K. Dhania, Vinod K. Chauhan, R.K. Chaitanya, Aparna Dutta-Gupta. "Midgut de novo transcriptome analysis and gene expression profiling of Achaea janata larvae exposed with Bacillus thuringiensis (Bt)-based biopesticide formulation", Comparative Biochemistry and Physiology Part D: Genomics and Proteomics, 2019 Publication	1%
4	etheses.whiterose.ac.uk Internet Source	<1%
5	Submitted to Jawaharlal Nehru Technological University Student Paper	<1%

33	www.jmbfs.org Internet Source	<1%
34	L. Maré, L.M.T. Dicks, M.L. van der Walt. "Characterization of South African isolates of Salmonella enteritidis by phage typing, numerical analysis of RAPD-PCR banding patterns and plasmid profiles", International Journal of Food Microbiology, 2001 Publication	<1%

Exclude quotes	On	Exclude matches	< 14 words
Exclude bibliography	On		

Analysis of midgut regeneration in lepidopteran pest, Achaea janata upon Cry toxication

ORIGINALITY REPORT

15%	7%	13%	6%
SIMILARITY INDEX	INTERNET SOURCES	PUBLICATIONS	STUDENT PAPERS

PRIMARY SOURCES

1	Narender K. Dhania, Vinod K. Chauhan, R.K. Chaitanya, Aparna Dutta-Gupta. "Midgut de novo transcriptome analysis and gene expression profiling of Achaea janata larvae exposed with Bacillus thuringiensis (Bt)-based biopesticide formulation", Comparative Biochemistry and Physiology Part D: Genomics and Proteomics, 2019 Publication	6%
2	www.nature.com Internet Source	1%
3	link.springer.com Internet Source	1%
4	Narender K. Dhania, Vinod K. Chauhan, R. K. Chaitanya, Aparna Dutta-Gupta. "RNA-Seq analysis and de novo transcriptome assembly of Cry toxin susceptible and tolerant Achaea janata larvae", Scientific Data, 2019 Publication	1%

65 "Characterization of South African isolates of Salmonella enteritidis by phage typing, numerical analysis of RAPD-PCR banding patterns and plasmid profiles", International Journal of Food Microbiology, 2001 <1%

Publication

Exclude quotes	On	Exclude matches	< 14 words
Exclude bibliography	Off		